united nations educational, scientific and cultural organization

international atomic energy agency

the
abdus salam
international centre for theoretical physics

H4.SMR/1519-10

"Seventh Workshop on Non-Linear Dynamics and Earthquake Prediction"

29 September - 11 October 2003

SEISMOLOGY of
EARTHQUAKE AND VOLCANO PREDICTION

Keiiti AKI

Observatoire Volcanologique
14 Route Nationale 3
971418, La Plaine des Cafres, La Reunion
France

Introduction

This is the lecture note of Keiiti Aki to be presented at the Seventh International Workshop on Non-Linear Dynamics and Earthquake Prediction. The title of the talk is "Seismology of Earthquake and Volcano Prediction", and it is given in a series of lectures in September-October, 2003.

Since the idea presented in the talk is new and rapidly evolving, it is given in an unusual style. The first part consists of personal communications describing the latest results, the second part is a summary of a paper presented at the IUGG meeting at Sapporo, Japan in June-July, 2003, and the last part describes in detail how the idea was originated using an unpublished book, written in mid-2002, titled "An Introduction to Seismology for Earthquake Prediction."

Acknowledgement.

The work presented here has been supported in part by the Association for Development of Earthquake Prediction (ADEP) in Japan. The author gratefully acknowledges the encouragement given by Dr. Akio Takagi of ADEP and the assistance of Dr. Anshu Jin of NIED/ADEP in preparing the manuscript.

Part 1 Personal communications

This part includes my memo to V.I.Keilis-Borok dated May 15, 2003, slightly modified for public exposure, which explains how my talk fits in the workshop on non-linear dynamics and earthquake prediction, and two others to him and Anshu Jin which explain my latest view of the earthquake prediction without figures, tables or equations.

Memo to V. I. Keilis-Borok from Kei Aki dated May 15, 2003

Dear Volodya:

I finished the first-round reading of your new book co-edited by A.A.Soloviev titled "Non-linear Dynamics and Earthquake Prediction", stopping and pondering on some pages and skimming through others. This book contains both your accomplishments and intensions. In Chapter 4, you and your colleagues perfected the earthquake prediction based on the catalog data as Jeffreys and Gutenberg did with Classical Seismology. The probability gain of 3 to 10 attained in such a rigorous manner is impressive. Chapter 5 by Molochan offers a general framework for earthquake prediction and will enjoy a long life. I stopped, however, more often on pages expressing your intension going beyond the approach based on the catalog data alone in a well-balanced way between physics and geology.

I like particularly your two lines on p.34 in Chapter 1 about Geodynamics and Nonlinear Dynamics being at the opposite ends of the earthquake prediction expanse. The word "expanse" means *stretch, region, tract, breadth, extent, sweep, plain and field* according to my Oxford Thesaurus, and your statement gives me a wonderful horizon of the future of the earthquake prediction research.

The path you have chosen toward connecting with Geodynamics, namely the block and fault network described in Chapter 3 and 6, is natural and straight-forward. It reminded me a series of papers by Steven Ward of UC Santa Cruz, who, for relying too heavily on geology, has been harshly criticized by earthquake physicists. I have supported him because of his use of observable earthquake source parameters such as the nucleation-zone size and sub-event size as model parameters of his seismicity simulation. But now I feel that the loading assigned by him to each fault segment independently according to its geologic slip history may be unrealistic from the geodynamic point of view. The approach taken in Chapter 3 of your book may resolve this difficult problem.

To a geodynamicist, the earth's property is smoothly varying within bodies bounded by large-scale interfaces. Most seismologists also belong to this "smooth earth club", because once you start with an initial model of smooth earth your data usually do not require the addition of small-scale heterogeneity to your initial model. As summarized well in a recent book by Sato and Fehler (1998, Seismic wave propagation and scattering in the heterogeneous earth, Springer-Verlag, New York, 308pp), the acceptance of coda waves in the data set is needed for the acceptance of small-scale seismic heterogeneity of the lithosphere. There are an increasing number of seismologists who accept it, forming the" rough earth club". I believe that you are also a member of the rough earth club, judging from the emphasis on the hierarchical heterogeneity of the lithosphere in Chapter 2.

Thus coda waves are central in my mind in trying to connect Geodynamics with Nonlinear Dynamics. While the coda wave may originate from a fractal medium, the coda Q is a concept of continuum, as Q is such a concept. It is natural for me to consider the observed correlation between the temporal variation of coda Q^{-1} and N(Mc), the frequency of earthquakes with the lower fractal limit magnitude Mc, as something fundamental to connect Geodynamics with Nonlinear Dynamics of the lithosphere.

Let me start with the segment of the San Andreas fault from the creeping zone to the Parkfield segment, which is probably one of the faults on the earth studied in most details seismologically and geodynamically because of the proximity to Menlo Park and Stanford. The creeping segment is particularly interesting to me because it may be considered as an exhumed "brittle-ductile transition zone", where I believe the interface between Geodynamics and Nonlinear dynamics exists.

Evidence for aseismic creep there was discovered in 1956 during an investigation of damage at Cienega Winery. Continuous measurements of creep started in 1958 by Don Tocher, and the result has been summarized by Burford (1988, PAGEOPGH, 126, 499-530). A typical creep record consists of a sequence of so called "creep events", each of which appears to show a step-like slip with amplitude on the order of 1 mm, although occasional events with amplitude exceeding 10 mm also occur. Once I measured the amplitude of the step for three sites (CWC3, CWN1 and XMR1) on figures published by Burford. The distribution of the amplitude followed very well the Gaussian distribution, and clearly deviated from the power law distribution, supporting the non-fractal nature of the creep events. The good fit of the Gaussian distribution suggests the existence of a mean characteristic slip associated with them and consequently the existence of a mean size of creep fracture in the ductile part of the creeping fault zone.

As well known, there are earthquakes in this creeping zone. They are originating in the relatively high-velocity part of the zone (according to local earthquake seismic tomography) with the maximum magnitude about 5. I like to imagine here that the brittle part of the lithosphere is vertically in contact with the ductile part, in which deformation occurs more or less continuously but as discrete events. This is exactly what I imagine at the usual horizontal brittle-ductile transition zone. I imagine that the creep deformation load the brittle part to cause earthquakes. For the usual transition zone typically responsible for M=7 earthquakes, the creep fracture size may be around a few hundred meters as described in my unpublished book. Since the maximum magnitude of 5 corresponds to the size of a few km, if we scale the size of creep fracture with the size of the maximum earthquake, the size of the creep fracture in the creeping zone of the San Andreas fault may be around a few 10's of meters. The observed amplitude of 1 mm for each creep events may be consistent with this size, although we have no idea how the amplitude observed at the surface is related to the slip at its source.

The temporal change in coda Q was first discovered at Stone Canyon in the creeping zone by Chouet (1979, Geophys. Res. Lett., 6, 143-146). Unlike other regions where the greatest changes occur at a few Hz and the time constant of the change is several years, the change observed by Chouet was very rapid (within a month or so) and the greatest change occurred for the highest frequency band (24 Hz). Looking back at Chouet's PhD thesis at MIT, I found that the decrease in coda Q appears to be concurrent with the increase in the seismicity of earthquakes with magnitude around 2, indicating that the change represent the normal loading process according to my view. In fact there was no major earthquakes in the area during the period of his study. I now believe that all these observations in the creeping zone of the San Andreas fault can be considered as a scaled-down version of the loading process of the plate-driving forces taking place at the brittle-ductile transition zone of the lithosphere.

Now let us move to the Parkfield segment. The observed cyclic occurrence of the Parkfield characteristic earthquake until 1966 can be explained by the steady accumulation of stress at the Middle Mountain barrier due to the slip in the creeping segment, and we may say that the Parkfield experiment is based on the fault-specific geodynamic approach. Its apparent failure, of course, is no surprise for your robust holistic nonlinear dynamic approach. I learned, however, from my volcano study that giving up the Parkfield experiment because of this failure may result in a "double mistake". As explained in detail in Aki and Ferrazzini (2000, J. Geophys. Res., 105, 16617-16640), we found a systematic relation between the duration of the precursory seismic swarm and the elevation of eruption site from many eruptions in 1985 to 1998. This empirical relation failed spectacularly for the largest eruption in this century occurred in 1998. The relation, however, was applicable to eruptions after mid-2000 until now. I can explain all these observations by the cyclic change in the condition of magma system, which has been constrained by the waveform coherence of the so called "long-period (LP) events". If I did not have this model and did not know about the cyclic change of its condition, I must have thrown away the empirical relation because of the failure in 1998 although it became valid after 2000, thus making a double mistake. I believe that the earthquake prediction research based solely on the empirical data may be full of such double mistakes. The condition of the fault system also changes and the change may be monitored by the existing network. For example, Segall and Du (1993, J. Geophys. Res., 98, 4527-4538) found that the rupture in the 1966 Parkfield earthquake may be different from earlier ones, and broke through the barrier at the southern end of the segment which will certainly change the recurrence interval. I feel that the close coupling between modeling and monitoring (which is the subject of Chapter 3 of my unpublished book using a particularly simple magma system of a volcano in an isolate tectonic setting) may be able to rescue the simple geodynamic approach by representing the outside of a given fault system by a model whose parameters can be constrained by the continuously monitored data. Your approach so far has not included such data other than the catalog data and I see there a difference between your approach and mine.

From my experience with the volcano, I found that there are two different sets of monitored data. One of them is useful for constructing the above mentioned model, but is not useful for practical empirical prediction, while the other set is useful for practical prediction but not for constraining the model. For my volcano, the former includes the LP events which involves fluid at the source, and the latter comes from the source in the brittle part such as the precursory seismic swarm mentioned earlier. I see here a contact point between the geodynamic continuum and the nonlinear dynamic fractal as I see it in the loading process of plate-driving forces at the brittle-ductile transition zone. From this very fundamental viewpoint, the volcano and earthquake prediction science are very similar and they can benefit from each other. The volcano may be easier to study because of the shallowness of the transition zone. This is why I am particularly pleased with your statement on p. 34.

In Chapter 4 of your book, I was intrigued by the behavior of the B pattern, the burst of aftershocks. (I still remember that you asked me publicly after your talk at the Florida AGU meeting in late 1970's what is the reason for this precursor. I still do not know the answer.) The B pattern behavior is much shorter in the time scale than other patterns, and show conspicuous false alarms. This is similar to the behavior of the precursory seismic swarm of my volcano and also similar to the behavior of so called "foreshocks". I now feel that this type of phenomena may be characteristic to the brittle part. They are not useful for model construction (that is probably why I still cannot find the answer to your question about the B pattern) but useful for empirical prediction. I believe that recognition of two data sets, one useful for modeling and the other useful for practical empirical prediction, may resolve many problems we encountered in the earthquake and volcano prediction research.

As I wrote you in an e-mail earlier, I feel that the loading process of plate-driving forces in the brittle-ductile transition zone during the normal period may be more linear, more stationary and more easily predictable than the nonlinear dynamic process in the brittle part. As I discussed in Chapter 4 of my unpublished book (part of which will be given in Part 3 of this lecture note), the positive simultaneous correlation between coda Q^{-1} and N(Mc) reminded me the microscopic reversibility in the linear stationary irreversible thermodynamics used for deriving the Onsager reciprocal theorem. For example, Chapter IV of the book by Prigogine (1967, Introduction to thermodynamics of irreversible processes, third edition, Interscience Publishers, a division of John Wiley and Sons, New York-London-Sydney) derived the theorem under the assumption of linearity between the generalized flow and force starting with the microscopic reversibility of component processes expressed by equation 4.46. This equation shows that the fluctuations in the component processes have cross-correlation functions which are even-functions with respect to the time shift. This is exactly the same as observed for the temporal variations in the coda Q^{-1} and N(Mc). I used the Onsager theorem in one of my earliest papers (in Japanese) on the concentration of magma into a volcano from the upper mantle, and I always wondered how physicists extended it to nonlinear cases.

Yesterday I was reading my old diary about our dinner table conversation at the Irvine symposium on Earthquake Prediction in 1995, and was surprised to find that I was anticipating some of the ideas described in this letter. You told me then that you were interested in volcano because of its nonlinear process, and I said that I would focus on its linear part for predicting eruptions. In Aki and Ferrazzini (2001, J. Geophys. Res., 105, 16617-16640) we tried a computer simulation on such a basis for a comparative study of eruption histories at La Reunion, Kilauea and Mount Etna. I have now nearly completed the study of the eruption history of my volcano since 1972 (which includes 49 eruptions) by the model (described in Part 2 and 3 of this lecture note) which allowed me a quantitative prediction on the time, amount of lava and mode of eruptions for the next 10 years. I am now considering to proceed to a similar study of Kilauea, which involves both LP and brittle events of much greater extent in magnitude and space, and closer to the situation of earthquake prediction in its complexity.

Thank you for reading this long letter. I shall be happy if you would show it to anyone who may be interested.

Very sincerely yours,

Kei Aki,

Memo to V.I. Keilis- Borok, copy to Anshu Jin, from Kei Aki, dated 23 May, 2003

Dear Volodya:

I hope by this time you received from Anshu the figure of the cross-correlation curve between the coda Q^{-1} and N(Mc) for Central California for the period 1990-2003 calculated using the data sent from Mr. Liu. It looks quite significant. The maximum correlation coefficient is more than 0.6, and N(Mc) is delayed from coda Q^{-1} by about 3 years. In other words, the main difference from the normal period, for which the correlation is peaked at zero time-shift, is the finite time shift between the two time series. The correlation is not simultaneous now. However, I found that my visual check on the time series in Anshu's figure clearly tells me that N(Mc) precedes, rather than delays, coda Q^{-1}. With a copy of this mail, I am asking Anshu to check it out. Following your suggestion, I compared the new result with the Kern County and Loma Prieta case, and found that in all three cases, N(Mc) is preceding coda Q^{-1} change. The limited data for the Landers case appears to show the same. This is in accordance with my idea that the loading process in the ductile part is affected by some change in the brittle part. But the delay time is about 1 year for both Kern County and Loma Prieta, significantly shorter than the present case for Central California. From the self-similar point of view, it may mean a larger earthquake being prepared now in Central California. However, from the geodynamical point, it may mean a difference in mechanical property of the lithosphere involved. In fact, in the case of Misasa earthquake of 1983 studied by Tsukuda (1988, PAGEOPH, 128, 261-280), the delay time is 2-3 years although the earthquake was only M=6.2. I like to ask Anshu to compute the cross-correlation function for the Kern County and Loma Prieta cases (which is given in Part 2).

In any case, what I thought as " a loss of correlation" may be simply " delay of coda Q^{-1} from N(Mc)". *If the other cases confirm this simple observation, there must be a simple explanation. From this viewpoint, the earthquake prediction may be simpler than we thought!*

I received a formal letter of invitation to the Trieste meeting of 29 September-11 October from Prof. Giorgi yesterday. He asks me for lecture notes in advance. It naturally occurred to me if I could use some part of my unpublished book titled "An Introduction to Seismology for Earthquake Prediction" for this purpose. I thought, however, it may be too long. But in your May 21 mail you indicated that there is no problem with that. In that case I like also to include, in lecture notes, my May 15 memo to you and the paper I plan to present at the IUGG meeting in the coming July.

My only problem in following this idea is that most figures in the book need polishing, and I need help from Anshu. With a copy of this e-mail, I am checking the possibility with her.

With best regards,

Kei

Memo to Anshu Jin, copy to V. I. Keilis-Borok from Kei Aki dated 26 May, 2003

Dear Anshu:

You are amazed by my sharp eyes, but I am more amazed by your quick response to readily confirm my guess. Actually it was not my eyes that detected something wrong with your initial cross-correlation curve between coda Q^{-1} and N(Mc). First I accepted the delay of N(Mc) from coda Q^{-1} as indicated in your figure because of the causality that the loading by the ductile part should precede the phenomena in the brittle part. But I could not think of any realistic mechanism to generate such a delay before a major earthquake. Then Volodja's suggestion to compare it with the Kern County and Loma Prieta case led me to look at the original time series. It was then clear that it is the delay of coda Q^{-1} relative to N(Mc) (See Figures 6 and 7 in Part 2), that is more easily explained by the idea that this anomalous behavior is caused by something happened in the brittle part of the lithosphere.

What is really amazing is the perfect match of the two time series when you advanced N(Mc) curve (for Central California 1990-2003) by 3.5 years. I think it is difficult to produce such a simple effect by any linear system. I thought about a system with coda Q^{-1} as the input and N(Mc) as the output. When something anomalous happens in the brittle part, a feed-back circuit is activated and the input is modified. Such a system in the linear domain, however, would not easily produce the observed simple delay. The observed simplicity in your cross-correlation curve demands a simple explanation. *It appears to me that the strain energy stored in the brittle part reached a certain saturation limit and started to flow back to the ductile part.*

Whatever the cause is, I seem to find the same simple phenomena for the Kern County, Loma Prieta and very likely Landers earthquakes (awaiting for your confirmation using the data from Mr. Liu). Tsukuda's observation on the Misasa earthquake of 1983 may be regarded as another example with the delay time of 2-3 years. Comparison of Figure 5 and 8 of Hiramatsu et al. (2000, JGR 105 , 6141-6151) also shows that the minimum in N(M3.1-3.5) precedes that of coda Q^{-1} by about two years in the case of the Hyogoken-Nanbu (Kobe) earthquake of 1995. All known observations on the coda Q^{-1} vs N(Mc), including the New Zealand case (discussed in Part 3 of this lecture note) and Stone Canyon case mentioned in my May 15 memo to Volodya , may be summarized as " *the temporal variation in coda Q^{-1} is simultaneous with that in N(Mc) during the normal period, but the former becomes delayed from the latter by 1 to 4 years before a major earthquake*".

Can we include the Tangshan and Heicheng cases as examples of the above statement?

With best regards,

Kei

Memo from Anshu Jin to Kei Aki dated 26 May, 2003.

Dear Kei:

This is to answer your question about the Tangshan and Heicheng cases. I checked with what I have in hand and found that (1) for the Tangshang case, the b value estimated from events with M=2 to 4.5 showed a significant low since the beginning of 1970, and the coda Q decrease started around 1973 at the earliest. Although the starting time of the coda Q decrease is not exact, we may safely say that there was about 3 years delay of the Q decrease relative to the increase in frequency of events with M=4.5-5.0, and (2) for the Heicheng case, we do not have enough data.

Regards,

Anshu.

Part 2. A new view of earthquake and volcano precursors

Abstract

A close interplay between monitoring and modeling is needed for a quantitative prediction of volcanic eruption and earthquake occurrence. The need is demonstrated for Piton de la Fournaise, for which a relatively simple model can be constructed because of the isolate tectonic setting and can be tested in a short time because of the high rate of eruptions. Lessons learned from the volcano is applied to earthquakes in California, and I found a model of earthquake loading process by plate-driving forces that can be effectively constrained by data from the existing seismic network and can be used to identify both safe and dangerous periods from a major earthquake in a seismic region.

Introduction and summary

The traditional way of searching for earthquake precursors was uniquely empirical, relying only on the data gathered by the monitoring network. Those precursory phenomena that sometimes show correlation with the earthquake occurrence, but not consistently in a robust manner, have been discarded as unreliable. I have lived in an active volcanic island for 8 years and learned that the traditional way cannot deal with the delicate and complex interaction between the volcanic cycle determined by the deep process of magma supply and the phenomena observed at the surface by a monitoring network. It is too rigid and tends to lead to serious mistakes.

For example, I found that a predictive relation established empirically for eruptions during a certain period did not apply to eruptions in another period, simply because the condition of a magma system changed. If we apply it blindly to any eruption, it can make a wrong prediction and may be discarded as useless although it is useful for eruptions when the magma system is in the applicable condition. The purpose of this paper is to summarize lessons learned from a volcano and points out that we might have made a similar mistake by blindly applying empirical precursory relations to individual earthquakes without considering the regional condition of earthquake loading cycle. Understanding the dependence of monitored data on the regional condition requires a deterministic modeling of the earthquake loading system, and it will necessarily open up an interplay between monitoring and theoretical modeling much needed for a scientifically sound development of the earthquake prediction research.

Another message I like to convey in this paper is the great benefit one may gain for the prediction research from exchanges between studies of precursors for earthquakes and those for volcanoes. I found that not only volcano studies are useful for earthquake studies, but the opposite is also true. For example, one of the key observations I used for recognizing the cycle of the volcanic activity of the Piton de la Fournaise came from an analogy to the occurrence of a particular earthquake repeatedly observed at a certain phase of a regional earthquake cycle, such as the Odawara earthquake before the great Tokyo earthquake discussed by Ishibashi (2003).

An important outcome of such a parallel study of earthquake and volcano precursors is the need for distinguishing two different types of precursory phenomena, which I learned first from the volcano. One type is useful for constructing a deterministic model of the eruptive cycle of a volcano, but is not useful for practical prediction of individual eruptions in the traditional sense. The other is of the opposite usefulness, essential for practical prediction, but not useful for constraining the model. The latter phenomena are originating from the brittle part of the volcano such as the volcano-tectonic (VT) events, and the former from the part where the fluid magma is involved such as the long-period (LP) events. This difference is physically understandable because the fractal, self-similar nature of the phenomena in the brittle part prevents the construction of a simple deterministic model. On the other hand, the phenomena originating from the part involving fluid magma that can effectively constrain the model of magma system have unique scale lengths because of the finite structure of the magma system and show a consequent departure from the self-similarity.

Looking at earthquake precursors from this viewpoint, we expect that the phenomena useful for constructing a deterministic physical model of the regional cycle of earthquake occurrence may not be coming from the brittle part of the lithosphere, and may be originating from the brittle-ductile transition region, such as silent earthquakes, deep non-volcanic LP events, temporal change in coda Q and various phenomena showing the departure from the self-similarity. Some of these phenomena might have been discarded as useless for a practical prediction of the occurrence of individual earthquakes. More specifically, I was drawn back to the extraordinary observation made by Jin and Aki (1989,1993) about a strong positive and simultaneous correlation between the temporal change in the coda Q^{-1} and the frequency of earthquakes with a certain magnitude Mc characteristic to a seismic region, because the correlation was explained by an interaction between the brittle part and the ductile part of lithosphere. From a closer look at old observations I found that the correlation actually depended on the regional cycle, and is positive and simultaneous during the normal period of the loading of the tectonic stress, and the positive simultaneous correlation is disturbed for several years before a large earthquake of the region. This finding is in harmony with the conclusion of Zoback and Zoback (2002) from a global survey of the tectonic stress that the tectonically stable region is stable because of the low rate of deformation in its ductile part, and the active region is active because of the high rate of deformation in its ductile part.

In a recent book titled “Nonlinear dynamics of lithosphere and earthquake prediction”, Keilis-Borok(2003) put Nonlinear Dynamics and Geodynamics at the opposite ends of the earthquake prediction expanse. From this viewpoint the observed correlation between the coda Q^{-1} and the frequency of earthquakes with magnitude Mc mentioned above can be considered at the contact point of the two dynamics, because Q^{-1} is a continuum concept while Mc is a fractal concept (the lower fractal limit of magnitude distribution). From this viewpoint, our analogy between the prediction of volcanic eruption and the earthquake prediction becomes logical and inevitable, because the VT event is a brittle fractal phenomenon while the LP event involves continuum fluid. Let us begin with the volcano study..

Quantitative prediction of eruptions at Piton de la Fournaise

The volcano chosen for the present study is Piton de la Fournaise on the Reunion island in the Indian ocean. It is a basaltic island volcano originating from a hot spot in the mantle like Kilauea, Hawaii. This hot spot had a long active life and is considered to be responsible for the Decan plateau in India. It has been monitored by a permanent network of IPGP since 1980 offering an ideal experimental site for the prediction research with its high rate of eruption and simplicity of the magma system owing to its isolate tectonic setting.

This volcano has rift-zones like Kilauea as indicated in Figure 2.1, but they are not extensive and eruption sites are mostly confined within the caldera called "Enclos" with a diameter of about 10 km. All 49 eruptions since 1972 originated in one of the four areas marked in Figure 2.1, namely, Bory-west, Dolomieu-east, NE rift-zone and SE rift-zone. Only two of them erupted outside the caldera from fissures extending along the rift-zone. The classification of all eruption sites into the four areas was made unambiguously and uniquely according to the model depicted in Figure 2.2.

The model shown in Figure 2.2 was evolved from the one proposed by Aki and Ferrazzini (2000) on the basis of seismic observations made between 1980 and 1998. It was merged harmoniously with the one proposed earlier by Lenat and Bachelery (1990) in which patches of magma remaining from earlier eruptions at shallow part of the volcano played an important role. These patches were introduced in our model on the basis of the concurrent temporal change in eruption tremor amplitude with that in the chemical composition of lava attributed to mixing of old and new magma by Bachelery (1999). The dike-like magma path to the Bory-west area was included after the finding that all six active periods, as identified by the sharp rise in the cumulative curve for the erupted lava (shown in Figure 2.3) were preceded by an eruption from a narrow zone marked as Bory-west in Figure 2.1. The path is connected to the main channel of magma supply at a deep part of the volcanic edifice in our model (Figure 2.2). It plays the role of the Odawara earthquake in the earthquake cycle of the Tokyo region as proposed by Ishibashi (2003). We recognize from Figure 2.3 that there were three cycles of eruptive activity since 1972 with the period of 13 years, and each cycle had 2 active phases.

The main magma path inclined to the west is clearly recognizable in 3-D images from seismic tomography obtained by Hirn and his coworkers as a high velocity body. It is of high seismic velocity, because the fluid magma fills cracks and joints of the volcanic edifice and solidifies it. The magma conduits must be harder than the surrounding, and we may visualize a system of several such channels connected at a junction below the summit. Such a system of channels will cause stress concentration at their junction wherever the fluid flow meets barriers to overcome. That may be the reason why we observe a swarm of volcano-tectonic events (so called summit seismic crisis) originating from practically the same place beneath the summit at about the sea level wherever the fluid moves in the system

In Figure 2.3, we recognized that each of the six active phase started with an eruption in the Bory-west area was followed by a nearly flat curve indicating a quiet period. This let us distinguish 12 alternating active and quiet periods since 1972 as summarized in Table 1 which lists the starting date of each period, its duration in month and the total amount of lava output in million cubic meters for each period. The last column in Table 1 called "amount in L-B" is the amount of magma, at the beginning of each period, left in the Lenat-Bachelery magma patches (shown in Figure 2.2) from the earlier period assuming that each active period brings 60 million cubic meters from the mantle into the magma system of the volcanic edifice. It is also assumed that there was no left-over magma in the system before the period I-1A, which may be justified by the long quiescence preceding the period as well as the large eruptions in 1961 and 1964-66 which might have emptied the shallow magma system. If it is not zero, we can correct the column by simply adding the non-zero number to each number listed in the column. The assumption of the stability of the deep supply system is supported by the stationary occurrence of deep tremors observed by Aki and Koyanagi (1981) under Kilaeuea.

Table 1. List of the consecutive eruption periods since 1972 (See text above for explanation of each column)

cycle	period	starting date	duration in month	erupted lava	amount in L-B
I	1A	1972/6/9	12	17.4	0
I	1Q	1973/5/29	53	12	43
I	2A	1976/11/2	13	35.3	31
I	2Q	1977/11/17	91	34.3	56
II	1A	1985/6/14	10	43.7	22
II	1Q	1986/4/5	19	16.9	38
II	2A	1987/11/6	14	49.6	21
II	2Q	1988/12/9	110	17	31
III	1A	1998/3/9	6	60	14
III	1Q	1998/9/21	17	3.3	14
III	2A	2000/2/14	23	45.2	11
III	2Q	2002/1/16			26

We examined the details of various observations made visually and by the monitoring network for each period and interpreted them in terms of the changing condition of the magma system model shown in Figure 2.2. We found that although the supply system showed the 13-year periodicity, the shallow magma system changed without this regularity. We searched for any causal relationships between the mode of eruption and the condition of the magma system for all consecutive periods and used them as the basis for a quantitative prediction of eruptions in the future. Details of the observation, modeling and causal relationships were given in ***appendix***. The prediction for the next decade as of March, 2003 is summarized below.

The volcano is currently in the quiet period of phase 2 of cycle III, designated as III-2Q. We had already one eruption (December, 2002) in the current period. Table 1 shows the current estimate of remaining magma in the L-B patches to be 26 M cubic meters minus whatever erupted in the December, 2002 eruption, which is significantly smaller than the amount (31 M) we had in the beginning of the corresponding period of the last cycle, namely, II-2Q. With the increase of pressure in these patches we may have minor eruptions in the next several years, but the total amount of lava output during the current period, III-2Q, would be significantly smaller than that of II-2Q (17 M).

If the system of magma supply from the mantle stays in the same condition as in the past 30 years, we expect the next arrival of new magma in 2011, 13 years after 1998. We notice in Figure 2.2 the decreasing trend in the time interval between the beginning of phase 1 and that of phase 2 during the 30-year period, and the best fitting model of Cabusson (2002) using the computer program developed by Aki and Ferrazzini (2001) predicts a simultaneous arrival from the two mantle reservoirs for the next active period. This means that there will be 120 M cubic meters of magma to be supplied to the magma system in 2011. If the flow rate between the mantle reservoir and the NTR/NCR reservoirs (shown in Figure 2.2) in the edifice is the same as in 1996-98, the filling of the latter will take 15 months. The arrival of new magma of 120 M cubic meters in 15 months at depths around 5 km b.s.l. should be detectable by the satellite geodesy. The monitoring network will record an increase in regional seismicity with focal depths in the range 10 to 30 km for several years before the arrival of new magma as in 1993-98 (See Figure 10 of Aki and Ferrazzini (2000)) as well as the upward migration of VT events beneath the summit area as before the March, 1998 eruption.

The shallow magma system at the time of arrival of new magma will be the least developed of all periods for which the monitored data exist, and may be comparable to the condition preceding the period I-1A. The first eruption will be from the Bory-west area as usual, and may be followed by eruptions in the peripheral areas of the Dolomieu-east and the two rift-zones such as in the period I-1A. We cannot exclude the possibility of an eruption in the NW rift-zone as occurred in 1820. Because of the underdeveloped condition of the shallow magma system, there would be no eruption in the rift-zone outside the Enclos caldera nor the pit-crater collapse in the Dolomieu crater.

The above scenario would imply a relatively small amount of erupted magma during the next active period as in the period I-1A, leaving a large amount of magma in many L-B patches. Another possible scenario is the repeat of the 1998 eruption, in which a large amount of lava flow comes out in a single eruption in the NE rift zone. In either case, the eruption will be primarily confined within the Enclos caldera.

The monitoring network can tell us, at an early stage of the next active period, which scenario will be followed.

We like to emphasize that the above prediction was not possible from the empirical cumulative curve of the lava output shown in Figure 2.3. We needed observations from the monitoring network as well as modeling. Our prediction may be wrong if some unexpected change occurs in the magma system, but the monitored data can tell us about the change and we shall be able to quickly adjust our model. The prediction based entirely on the past data does not have this flexibility. Thus a close coupling between monitoring and modeling is essential not only for understanding the precursory phenomena but also for practicing prediction.

Now let us turn to the earthquake precursor. We shall start with a model of the loading process of plate-driving forces widely believed to be the cause of earthquakes.

Earthquake loading by plate-driving forces

After a thorough survey of the tectonic stress in the Earth's lithosphere based on observations about its brittle part, Zoback and Zoback (2002) offered a new perspective on the role of its ductile part in the earthquake loading process by plate-driving forces. Assuming that a three-layer lithosphere composed of the brittle upper crust and the ductile lower crust and upper mantle, as a whole, support plate-driving forces (Zoback and Townend, 2001), they concluded that the tectonically stable region is stable because of the low rate of deformation in its ductile part, and the active region is active because of the high rate of deformation in its ductile part. They state that because of the applied force to the lithosphere will result in steady-state creep in the lower crust and upper mantle, as long as the three-layer lithosphere is coupled, stress will build up in the upper brittle layer due to the creep deformation in the layer below.

The above view suggests a simultaneous occurrence of the higher (lower) rate of stress increase in the brittle part and the higher (lower) rate of deformation in the ductile part due to plate-driving forces. This is exactly how Jin and Aki (1989, 1993) interpreted the strong correlation between coda Q^{-1} and the relative frequency N(Mc) of earthquakes with a certain magnitude Mc (characteristic to a seismic region) observed both for Central California and Southern California. Figure 2.4 shows the 50-year records of the two time series for Central California with the cross-correlation function, and Figure 2.5 shows the same set of curves for nearly 60 years for Southern California reproduced from their papers. It is clear that the correlation between coda Q^{-1} and N(Mc) is simultaneous and positive with the correlation coefficient higher than 0.8 for both regions. They explained the observed correlation assuming the presence of ductile fractures in the brittle-ductile transition zone with a unique scale length characteristic to a seismic region. The increase in fractures in the ductile part increases coda Q^{-1} and, at the same time, generates stress concentration with the same scale length responsible for the increase in frequency of earthquakes around magnitude Mc. The scale length corresponding to the observed Mc is a few hundred meters for Southern California and roughly 1 km for Central California.

When the stress in the brittle part builds up over time to the point of failure preparing for a major earthquake, we may expect a change in its mechanical property as a whole as suggested in various laboratory experiments on rock samples. There is, however, an important difference between laboratory and nature. In the controlled experiment in laboratory, the loading is a fixed condition given externally by the experimental device. In nature, the loading is an internal process that is likely influenced by the change in the property of the material being loaded. We then expect a change in the mode of loading as the brittle part undergoes such a change preparing for a failure. We may expect the break down of the positive simultaneous correlation between coda Q^{-1} and N(Mc). That was exactly what we found for several years before the M7.1 Loma Prieta earthquake of 1989 and also for several years before the M7.3 Kern County earthquake of 1952 as shown in Figures 6 and 7, respectively, in the same format as Figures 4 and 5. These are the largest earthquakes for the respective regions for the period for which the data were available. The positive simultaneous correlation between coda Q^{-1} and N(Mc) was clearly disturbed for several years before both the Kern County and the Loma Prieta earthquake. The cross-correlation function shown in Figures 6 and 7 indicates that the correlation between the two time series is no longer simultaneous, but the coda Q^{-1} change attributed to the ductile part is delayed by about 1 year relative to that of N(Mc) attributed to the brittle part before both earthquakes. This sense of delay is consistent with the idea that the simultaneous correlation is disturbed by the change in the property of the brittle part of lithosphere as mentioned above. Except for these two periods (and possibly also the period several years before the M7.3 Landers earthquake of 1992 which is just at the data limit), the positive simultaneous correlation appears to hold well for the whole period for both regions, enabling us to make prediction for both safety and danger from a major earthquake with a time scale of a few years.

Comparison with the loading by fault slip in an earthquake

Recently much attention has been given to the triggering of earthquakes by the stress induced by the fault slip of a major earthquake in spite of its secondary nature in the loading process of plate-driving forces. It was found that, in the work of Hiramatsu et al.(2000), their effects on coda Q^{-1} and seismicity are different from what we saw as the manifestation of the loading by plate-driving forces.

The Tamba, Japan, region is adjacent to the epicentral area of the Hyogo-ken Nanbu (Kobe) earthquake of 1995 and is well covered by a high quality seismic network. The seismicity of the Tamba region and its surrounding area in Japan has been studied with special attention to the depth of the brittle-ductile transition zone inferred from the maximum focal depth by Ito (1990). More than 8000 earthquakes in the magnitude range from 1.8 to 5.3 were relocated and it was found that the frequency of occurrence of hypocenters per unit focal depth increases with depth down to about 10 km and sharply drops beyond about 12 km. There is a remarkable similarity between the observed depth distribution of hypocenters and the theoretical distribution of the shear resistance based on Byerlee's law (Byerlee, 1978; Sibson, 1982) for the brittle part and the dislocation creep law for the ductile part. Ito (1990) made a contour map of the depth of brittle-ductile transition in this region, and found a similarity with the map of the Curie point derived from aeromagnetic surveys by .Okubo et al. (1989). The comparison with the Curie point depth as well as the heat flow data gave an estimate of the temperature at which the brittle-ductile transition occurs. In the Tamba region, the brittle ductile transition occurs at depths around 14-16 km corresponding to a temperature around 300°-350° C.
The Hyogo-ken Nanbu earthquake (M7.2), on January 17, 1995 produced a significant change in the tectonic stress in the Tamba region. The sudden increase in the seismicty in the Tamba region after the earthquake was attributed to the increase in the Coulomb failure function by about 0.04 Mpa (Hashimoto et al., 1997). The average increase in shear stress at a depth of 10 km, close to the depth of brittle-ductile transition zone, on the vertical plane trending over the study area was estimated to be about 0.02 Mpa by Hiramatsu et al. (2000).
The seismicity of the Tamba region increased significantly after the Hyogo-ken Nanbu earthquake with the hypocenter distribution and focal mechanism indistinguishable from those before the earthquake according to Katao et al. (1997). However, a significant change in coda Q^{-1} was observed for the two frequency bands centered at 3 and 4 Hz. Coda Q^{-1} may change due to the change in the epicenter locations, focal depth distributions, and focal mechanisms of the earthquakes used for the analyses, and their effects were carefully examined and all rejected by Hiramatsu et al. (2000). The change in coda Q^{-1} is about 20%, and its statistical significance is confirmed by the Student's t test with a confidence level of 99 %. The above change in coda Q^{-1} combined with the estimated change in tectonic stress mentioned earlier gives the stress-sensitivity of about 10% change per 0.01 MPa (0.1 bar). Applying this sensitivity to the observed coda Q^{-1} for Central and Southern California shown in Figure 2.4 and 2.5, we find that the fluctuation of coda Q^{-1} over the 50-year period corresponds to the change in stress of the order of 0.1 MPa (1 bar).
The frequency dependence of the change in coda Q^{-1} found in the Tamba region by Hiramatsu et al. may be attributed to scattering attenuation by fractures.

According to Yomogida and Benites (1995), the scattering of seismic waves by a fracture is most effective when the wave length is comparable to twice the characteristic length of the fracture. The seismic wave length for which the change in coda Q^{-1} was significant (frequency bands centered at 3 and 4 Hz) is around 1 km corresponding to the characteristic size of the fracture of 500 m, which agrees well with the creep fracture size proposed to explain the correlation between coda Q^{-1} and N(Mc) for California.

Hiramatsu et al. (2000) suggested that the observed change in b-value might be consistent with the creep model of Jin and Aki (1989, 1993). A closer look at the observed change in the frequency of earthquakes in different magnitude ranges, however, reveal that there was no selectively higher increase in the magnitude range around Mc (a little over 3) corresponding to the size of 500 m. In fact, numerous recent studies on the triggering of seismicity by fault slip during some major earthquakes appear to show a uniform increase of the seismicity independent of magnitude. Such a uniform increase may be attributed to the mode of loading that is originated locally in the brittle part without the active participation of the ductile part envisioned earlier in the case of plate-driving forces. The fractures in the ductile part responded only passively with negligible additional contribution to the seismicity increase. The above recognition of the difference between plate-driving forces and the local source of stress in the brittle part is fundamentally important in understanding the earthquake loading processes in a seismic region.

The brittle-ductile transition: Origin of Mc.

The scale-invariance in earthquake phenomena, sometimes called the self-similarity, has been widely manifested in various seismological observations such as the magnitude-frequency relation, the aftershock decay rate, and the scaling law of seismic spectrum. The scale-invariance means that the only length scale governing earthquake phenomena is the earthquake source size, implying that a seismogenic region has no structure. Although there have been some evidence in support of a departure from the self-similarity at large scales (e.g., Shimazaki et al., 1986) as well as at small scales (e.g., Aki, 1996), it is true that the earthquake phenomena as a whole are dominated by the self-similarity.

On the other hand, there is a class of seismic events originating from volcanoes which show spectral features indicating the presence of some structure in the source region. They are long-period (LP) events and volcanic tremors associated with the pressure fluctuation in fluid magma and/or gas contained in the solid earth (See Chouet, 2003, for the latest review on volcano seismology). They have characteristic band-limited spectra independent of amplitude, clearly indicating the existence of structure in the source region, namely, structure of the magma system. Recent discovery of deep non-volcanic LP events distributed in a long narrow zone between the Eurasian plate and the down-going Philippine Sea plate in Southwest Japan by Obara (2002), however, suggests the pervasive existence of such a structure throughout the ductile region between the two plates. Their observed frequency band of 2 to 5 Hz is similar to those observed beneath volcanoes in Japan and elsewhere in the world. The fact that coda Q^{-1} showed a significant change in the Tamba region by the occurrence of the Hyogo-ken Nanbu earthquake at a similar frequency range (3-4 Hz) suggests a common origin for the ductile fracture hypothesized in the brittle-ductile transition zone and the source of deep non-volcanic LP events. It is natural to imagine that the ductile fractures responsible for the temporal change in coda Q^{-1} might generate LP events when

sufficient fluid is injected to them from the subducting plate.
The above reasoning suggests that the departure from the self-similarity may be found for earthquakes occurring in or near the brittle-ductile transition zone. In fact, some of the clearest cases of such a departure includes the Matsushiro, Japan, earthquake swarm (Sacks and Rydelek, 1995) believed to involve water in the source volume and the Mammoth Lakes, California, earthquake sequence studied by Archuleta et al. (1982) close to a volcanic area. In both cases, the corner frequency tended to remain at a constant value with decreasing magnitude below about 3 implying the influence of some structure with the scale length of a few hundred meters. If the phenomena take place primarily in the brittle part, such as the earthquakes triggered by a fault slip of a major earthquake, it may be difficult to detect the existence of such a structure, because observations will be dominated by the self-similar process within the brittle part.
A direct support for the existence of a structure with the scale length of a few hundred meters in the brittle-ductile transition zone comes from a study of the Hatagawa fault in Northeast Japan, which is believed to be an exhumed brittle-ductile transition zone. Ohtani et al. (2001) described a cataclasite zone with the width of about 100 m formed under temperature range 200° to 300° C and the appearance of mylonite with the maximum width of 1 km in the fault zone and discussed evidence for the coexistence of plastic deformation and brittle rupture in the zone.
Another support comes from a numerical simulation of deformation in the brittle-ductile transition zone by Shibazaki (2002), who found an appearance of cell-like structure with enhanced slip rate near the transition zone. He uses a fault model specified by the slip-weakening constitutive law of Ohnaka et al. (1997) with appropriate parameters chosen for various depths covering the brittle part, transition part and ductile part. The primary purpose of the simulation was to study the nucleation of earthquake rupture in the brittle part, but it may be extended to study the steady-state loading process of plate-driving forces for the three-dimensional, three-layer model of Zoback and Townend (2001) using constitutive relations applicable to each layer.

Discussions

Central to the assertion of the present paper is the temporal correlation between coda Q^{-1} and N(Mc) observed by Jin and Aki (1989, 1993) and generally disregarded by the seismological community in spite of my repeated mention of the subject The general disregard is understandable because it involves two currently most controversial issues in Earthquake Seismology, namely, the departure from the self-similarity (or the existence of Mc) and the temporal change in coda Q^{-1}. With regard to Mc, the controversy may be resolved if we can attribute its existence to the influence of ductile fracture in the manner explained in the preceding section. The controversy regarding to coda Q^{-1}, however, is deeply rooted.
In spite of many studies on the coda of local earthquakes since late 1960's as reviewed by Sato and Fehler (1998) and Fehler and Sato(2003), the seismological community in general still does not trust the results obtained from it. An example is the discovery of pervasive non-linear soil response in the strong motion records of the Loma Prieta earthquake of 1989 by Chin and Aki (1991). The discovery was based on the site amplification factor for weak motion estimated earlier from coda waves, which was the target of criticism by Wennerberg (1996). Because of the criticism, despite the defense by Chin and Aki (1996), their 1991 paper was regarded as controversial, and let Beresnev (2002) undertake a similar study 10

years later and essentially confirm the original result. I am afraid that the same thing will happen to the present paper, and I must wait for at least 50 years to get the similar result by a new method acceptable for the community but applicable only to the recent high-quality data. Nevertheless, I believe that the publication of the present paper may have some benefit, because the Chin-Aki paper promoted, at the Southern California Earthquake Center (Aki, 2002) and elsewhere, a productive cooperation between seismologists and geotechnical engineers who had believed in the non-linear site response for a long time from laboratory experiments on soil samples. This time, I hope it would promote a productive cooperation with scientists working on geomagnetism and geoelectricity, because the sharp increase in coda Q^{-1} observed in late 1980's in Southern California as shown in Figure 2.5 was concurrent with a significant change in electrical conductivity in the lower (ductile) crust detected by Madden et al. (1993). In concluding their review of coda studies over the past three decades, Fehler and Sato (2003) gave me credit for the validity of many of my old ideas and observations obtained using very little data that were poorly recorded by today's standards. I think that the credit should go to the nature of Earth's lithosphere, which is, in general, so uniformly heterogeneous in small scales that the coda possesses simple regular statistical properties as the sum of numerous little back-scattered waves, just as the simple laws of statistical mechanics apply to an ensemble of a large number of molecules. In coda formation, nature does the averaging for us, and that is why I needed very little data to obtain the valid result.

References

Aki, K., 1995, Interrelation between fault zone structures and earthquake processes, Pure Appl. Geophys., **145**, 647-676.

Aki, K., 1996, Scale dependence in earthquake phenomena and its relevance to earthquake prediction, Proc. Nat. Acad. Sci. USA, **93**, 3740-3747.

Aki, K., 2002, Synthesis of earthquake science information and its public transfer: A history of the Southern California Earthquake Center, International Handbook of Earthquake and Engineering Seismology, Academic Press, Amsterdam, 39-49.

Aki, K. and V. Ferrazzini, 2000, Seismic monitoring and modeling of an active volcano for prediction, J. Geophys. Res., 105, 16617-16640.

Aki, K. and V. Ferrazzini, 2001, Comparison of Mount Etna, Kilauea and Piton de la Fournaise by a quantitative modeling of their eruption histories, J. Geophys. Res., 105, 16617-16640.

Aki, K., and R. Koyanagi, 1981, Deep volcanic tremor and magma ascent mechanism under Kilauea, Hawaii, J. Geophys. Res., 86, 7095-7109.

Archuleta, R., J. E. Cranswick, C. Mueller and P. Spudich, 1982, Source parameters of the 1980 Mammoth Lakes, California, earthquake sequence, J. Geophys. Res., **87**, 4595-4608.

Bachelery, P., 1999, Le fonctionnement des Volcans-Boucliers, Memoire, Faculte des Sciences et Technologies, Universite de la Reunion, Saint-Denis, La Reunion, France.

Beresnev, I. A., and G. M. Atkinson, Bull. Seism. Soc. Am., **92,** 695-710 (2002).

Byerlee, J. D., 1978, Friction of rocks, Pure Appl. Geophys., **116**, 615-626.

Cabusson, S., 2002, personal communication.

Chin, B. H. and K. Aki, 1991, Simultaneous study of the source, path, and site effects on strong ground motion during the Loma Prieta earthquake: A preliminary result on pervasive nonlinear effects, Bull. Seism. Soc. Am., **81**, 1859-1884.

Chin, B. H. and K. Aki, 1996, Reply to Leif Wennerberg's comment on " Simultaneous study of the source, path, and site effects on strong ground motion during the Loma Prieta earthquake: A preliminary result on pervasive nonlinear effects", Bull. Seism. Soc. Am., **86**, 268-273.

Chouet, B. (1996). Long-period volcano seismicity: Its source and use in eruption forecasting, Nature, **380,** 309-316.

Chouet, B. (2003). Volcano Seismology, Pure Appl. Geophys., **160,** 739-788.

Fehler, M. and H. Sato, coda, Pure Appl. Geophys., **160**, 541-554.

Hiramatsu, Y., N. Hayashi, M. Furumoto and H. Katao, 2000, Temporal change in coda Q-1 and b value due to the static stress change associated with the 1995 Hyogo-ken Nanbu earthquake, J. Geophys. Res., **105**, 6141-6151.

Ishibashi, K., 2003, Seismo-tectonic modeling of the repeating M7-class disastrous earthquakes near Odawara, Japan, due to the Izu collision, presented at the Hagiwara symposium (JSS1) at the IUGG meeting at Sapporo.

Ito, K., 1990, Regional variations of the cutoff depth of seismicity in the crust and their relation to heat flow and large inland-earthquakes, J. Phys. Earth, **38**, 223-250.

Jin, A. and K. Aki, 1989, Spatial and temporal correlation between coda Q^{-1} and seismicity and its physical mechanism, J. Geophys. Res., **94**, 14041-14059.

Jin, A. and K. Aki, 1993, Temporal correlation between coda Q^{-1} and seismicity -

evidence for a structural unit in the brittle-ductile transition zone, J. Geodynamics, **17**, 95-120.

Katao, H., N. Maeda, Y. Hiramatsu, Y. Iio and S. Nakao, 1997, Detailed mapping of focal mechanisms in/around the 1995 Hyogo-ken Nanbu earthquake rupture zone, J Phys. Earth, **45**, 105-119.

Lénat, J. F.,et P. Bachèlery, 1990, Structure et fonctionnement de la zone centrale du Piton de la Fournaise, in Le Volcanisme de La Réunion. -Monographie- ed. J. F. Lénat, Centre de Recherches Volcanologiques, Observatoire de Physique du Globe de Clermont-Universté Blaise Pascal and C. N. R. S., 257-296.

Madden, T. R., G. A. LaTorraca and S.K. Park, 1993, Electrical conductivity variations around the Palmdale section of the San Andreas fault zone, J. Geophys. Res., **98**, 795-808.

Obara, K.,2002, Nonvolcanic deep tremor associated with subduction in Southwest Japan, Science, **296,** 1,679-1,681 (2002).

Ohnaka, M., M. Akatsu, H. Mochizuki, A. Odera, F. Tagashira, and Y. Yamamoto, 1997, A constitutive law for the shear failure of rock under lithospheric conditions, Tectonophysics, **277**, 1-27.

Ohtani, T, N. Shigematsu, K. Fujimoto, Y. Miyashita, T. Tomita, H. Tanaka, and K. Omura, 2001, Hatagawa fault zone: Exhumed brittle-plastic transition zone, Proceedings of International Symposium on Slip and Flow Processes in and below the Seismogenic Region, Sendai, Japan, November 5-8, 2001, 131-135.

Okubo, Y., H. Tsu and K. Ogawa, 1989, Estimation of Curie point temperature and geothermalstructure of island arcs of Japan, Tectonophysics, **159**, 279-290.

Sacks,I. S. and P. A. Rydelek, Bull. Seism. Soc. Am., **85,** 808-813 (1995).

Sato, H. and M. Fehler, 1998, Seismic wave propagation and scattering in the heterogeneous earth, Springer-Verlag, New York, 308pp.

Shibazaki, B., 2002, Nucleation of large earthquakes determined by the seismic-aseismic boundary: agreement between models and observations, Phys. Earth Planet. Int.,**134**, 129-138.

Shimazaki, 1986, Small and large earthquakes: The effects of the thickness of seismogenic layer and the free surface, in *Earthquake Source Mechanics*, AGU monograph **37**, 209-216, American Geophysical Union.

Sibson, R. H., 1982, Fault zone models, heat flow and depth distribution of earthquakes in the continental crust of the United States,Bull. Seis. Soc. Am., **72**, 151-163.

Wennerberg, L., 1996, Comment on " Simultaneous study of the source, path, and site effects on strong ground motion during the Loma Prieta earthquake: A preliminary result on pervasive nonlinear effects" by B. H. Chin and K. Aki, Bull. Seism. Soc. Am., 86, 259-267.

Yomogida, K. and R. Benites, 1995, Relation between direct wave Q and coda Q: A numerical approach, Geophys. J. Int., **123**, 471-483.

Zoback, M. D. and M. L. Zoback, 2002, State of stress in the Earth's lithosphere, in International Handbook of Earthquake and Engineering Seismology, Academic Press, Amsterdam, 559-568.

Zoback, M. D. and J. Townend, 2001, Implications of hydrostatic pore pressures and high crustal strength for the deformation of intraplate lithosphere, Tectonophysics, **336**, 19-30.

Appendix. The eruption history of the Piton de la Fournaise since 1972

In the following, I shall first describe briefly various observations for each period. Then I shall interpret them in terms of our model of the magma system shown in Figure 2.2. Finally possible causal relationships between consecutive periods are discussed. Eruptions are numbered as given in Table A1, where the starting time, duration, and amount of lava output are listed for 49 eruptions since 1972. The numbering follows Benard and Krafft.

Table A1. List of the duration (days) and amount of lava (million cubic meters) for eruptions since 1972 classified according to the eruption areas defined in Figure 2.1.

No	starting date	Duration in days	Bory-west	Dolomieu-east	NE rift-zone	SE rift-zone	To PdC
1	1972/6/9	2	0.1				
2	1972/7/25	24		3			
3	1972/9/9	19			5		
4	1972/10/10	62				9.3	
5 & 6	1975/11/4	15		0.9			
7	1975/12/18	39		1.3			
8	1976/1/12	19				3.8	
9	1976/1/29	61				6	
10	1976/11/2	2	0.3				
11	1977/4/5	12			12		
12	1977/10/24	24		23			
13	1979/7/13	1	0.3				
14	1981/2/3	18	3				
15	1981/2/26	32	4				
16	1981/4/1	35					5
17	1983/12/4	46	8				
18	1984/1/18	32	9				
19	1985/6/14	1	1				
20	1985/8/5	27			7		
21	1985/9/6	36		14			
22	1985/12/1	1		0.7			
23	1985/12/29	41		7			
24	1986/3/19	13				14	
25	1986/3/29	270		2.5			
26	1987/1/6	36					10
27	1987/6/10	20		1.5			
28	1987/7/19	2		0.8			
29	1987/11/6	3	1.6				
30	1987/11/30	33		10			
31	1988/2/7	56		8			
32	1988/5/18	76		15			
33	1988/8/31	57	7				

34	1988/12/14	16			8		
35	1990/1/18	2		0.5			
36	1990/4/18	21				8	
37	1991/7/19	2		2.8			
38	1992/8/27	28		5.5			
39	1998/3/9	196			60		
40	1998/3/12	21	1				
41	1999/7/19	13		1.8			
42	1999/9/28	26		1.5			
43	2000/2/14	19	4				
44	2000/6/23	37		6			
45	2000/10/12	32		9			
46	2001/3/27	8		4.8			
47	2001/6/11	26		9.5			
48	2002/1/5	12			12.5		
49	2002/11/16						

§ 1.1. Active period of phase 1 of cycle I (I-1A): Observations.

This is the period from which Benard and Krafft start showing photos of eruptions with detailed description. It starts with the eruption #1 on 1972/6/9 at the Bory-west area and ends with the one in the Dolomieu crater on 1973/5/10.

The eruption #1 occurred after the inactivity of 6 years on 1972/6/9 from three fissures at elevations between 2540 and 2200 m on the south side of Bory. The eruption site is close to the first eruption of cycle II (#19) and that of cycle III(#40), all of which belong to the Bory-west area. The eruption stopped during the night between June 10 and 11, with the estimated lava output of 0.12 M cubic meters.

The eruption #2 occurred around 1972/7/25 on the east side of the Dolomieu at elevations between 2200 and 1760 m from four segments of radial fissures. The lava flow front reached an elevation of 1050 m when the eruption stopped on August 17. The amount of lava erupted was estimated at 3 M cubic meters. The eruption site is at the eastern periphery of the Dolomieu-east area.

The eruption #3 occurred on 1972/9/9 on the north side of the Dolomieu cone at an elevation 2100 m, near the site of a minor eruption 2 days earlier. This site is located at the boundary of the Bory-west and the NE rift-zone area. The eruption stopped abruptly on September 27 after emitting 5 M cubic meters of lava. It accompanied some explosive activities which produced Pele's hair.

The eruption #4 started on October 10, 1972 and occurred from several sites distributed over an area south of the Dolomieu cone at elevations between 1800 and 1750 m. They are located at the periphery of the SE rift-zone. The eruption lasted for two months and produced 9.3 M cubic meters of lava.

The final eruption of this period occurred on 1973/5/10 at an elevation of 2380 m in the Dolomieu crator. It lasted until May 28 and covered a part of the floor of the Dolomieu crator with 0.6 M cubic meters of lava. This eruption was not numbered by Benard and Krafft, and was not included in Table A1.

In summary the period I-1A lasted for 12 months and produced 17.4 M cubic meters of lava. As shown in Table 1, this is the lowest output of all active periods. The three main eruption sites, #2, 3 and 4, are located in the peripheral part of the Dolomieu-east, NE rift-zone, and SE rift zone, respectively.

§ 1.2. Active period of phase 1 of cycle I (I-1A): Modeling.

This period is similar to the period III-1A in being preceded by a long period of inactivity. The mode of eruption, however, is quite different. In III-1A, the Bory-west eruption and the beginning of eruption from fissures close to the summit was nearly simultaneous, while in this period, there is an interval of 11 months between the Bory-west eruption (June, 1972) and the first summit eruption (May, 1973). Furthermore, all three eruptions between the two occurred at peripheral part of the Dolomieu-east, NE rift-zone and SE rift-zone. Combined with the fact that this period produced the lowest lava output of all active periods, we infer that the magma system of the volcanic edifice sketched in Figure 2.2 was not developed fully during this period. Because of the underdeveloped system, the new magma arrived in June, 1972 had to overcome many barriers before reaching the summit crater. If we had the monitoring network then, we could have recorded the upward migration of the volcano-tectonic (VT) events lasting for 11 months in a manner similar to those observed during the 1 1/2 day preceding the March, 1998 eruption of III-1A. We could have, then, come up with a clearer picture of how the system developed. Unfortunately, the observatory was installed in 1980, and the first eruption observed instrumentally was #14 in the period I-2Q.

When the system is well developed, magma channels may have no barriers, and there may be no VT activity associated with breaking barriers. The known absence of the upward migration of VT events associated with the new arrival of magma during II-1A, II-2A and III-2A may be attributed to the better developed magma system than during III-1A.

The end of the eruption #3 was described as abrupt (brutalement). As we shall see later the mode of ending of an eruption appears to reflect how the lava is supplied to the eruption site. When an eruption occurs from an isolated magma patch such as postulated by Lenat and Bachelery (1990) due to the pressure increase by degassing, the eruption will be ending gradually with the decrease in the pressure. On the other hand, if the eruption site is connected to a main magma channel, there is a possibility of diversion to other paths than the one connected to the current eruption site. The abrupt ending of #3 suggests that the source of lava is not the old magma in an isolated patch left over from the earlier cycle, but the new magma arrived at the time of #1. This is similar to what happened during the period III-2A as mentioned in item 3 of the March, 2002 memo and also described in detail later.

If a diversion is from the summit path to the rift-zone path, we observe a swarm of LP events when a summit eruption stops abruptly as in II-1A and III-2A during which shallow part of the magma system was well developed. As mentioned earlier the new magma has not reached the Dolomieu crater at the time of #3, and the magma system was probably not developed. If so we should not observe any LP events associated with the end of #3. If that were the case, the diversion might be due to an intrusion accompanied by a swarm of VT events. Thus the monitoring of VT and LP events is important to find the condition of the magma system.

§ 1.3. Active period of phase 1 of cycle I (I-1A): Cause and effect

This period followed the 6-year period of inactivity after May, 1966, preceded by an active period involving a major oceanite eruption of 62 M cubic meters in the NE rift zone in April, 1961. The large output in the last active period followed by the long period of inactivity are consistent with the under-developed magma system in this period. As we shall discuss in § 2.2, the shallow magma system as sketched in Figure 2.2 might be operative in the period I-1Q. If so, its development took at least a year after the arrival of new magma signaled by the eruption #1.

§ 2.1. Quiet period of phase 1 of cycle I (I-1Q): Observations.

This period starts with 29 months of inactivity preceding the eruption #5 and #6 from two separate sites in the southern floor of the Dolomieu crater. It started on

1975/11/4 and, according to Benard and Krafft, accompanied some earthquakes and minor collapses of the crater wall in the night of November 14. The lava lake formed by the eruption disappeared on November 18, marking the end of eruption with the total output of 0.9 M cubic meters.

The eruption #7 occurred on 1975/12/18 at elevations between 2115 and 2020 m in the Dolomieu-east area. It lasted until 1976/1/25 with the total lava output of 1.3 M cubic meters. While it is still active, the eruption #8 occurred on 1976/1/12 in the SE rift-zone at a low elevation of 1490 m. The lava flow from #8 reached Route Nationale 2 on January 27. The eruption stopped on January 30 with the total output of 3.8 M cubic meters.

The eruption #9 started on 1976/1/29 nearly simultaneous with the end of #8 at an elevation of 1780 in the SE rif-zone about midway between #7 and #8. It lasted until 1976/2/25 with the output of about 6M cubic meters.

§ 2.2. Quiet period of phase 1 of cycle I (I-1Q): Modeling

The occurrence of collapse on the floor of the Dolomieu crater as well as two significant eruptions from the SE rift-zone indicate that the magma system in the volcanic edifice is well developed in this period. Since there was no supply of new magma from the mantle during this period, the eruption must be due to the increase in pressure in some of the Lenat-Bachelery patches. Then we should not observe an abrupt ending of eruption. In fact, the description of Benard and Krafft on these eruptions suggests that they last long without sudden endings.

This period is similar to the early part of the period II-2Q in that both summit and rift-zone eruptions occurred. Since the initial model of the Piton de la Fournaise constructed by Aki and Ferrazzini (2000) explained various observations during the period II-2Q, we believe that the basic elements of the model sketched in Figure 2.2, namely, deep NTR and NCR reservoirs, separate path of magma to the summit and the rift-zone, and the LP source connected to the rift-zone in addition to the Lenat-Bachelery patches are operative also in this period. This could have been confirmed using observations on LP seismicity if we had a monitoring network then.

The collapse in the Dolomieu crater has been reported only three times since 1972. They are associated with eruptions #5-6 (the first eruption of I-1Q), #24 (the last eruption of II-1A) and #49(the first eruption of III-2Q). They are all in the transient period from an active period to a quiet period. In all cases, the shallow magma system in the volcanic edifice is well developed. We have some evidence that the shallow magma system was not developed well in transition periods II-2A to II-2Q, and III-1A to III-1Q. For the remaining one, from I-2A to I-2Q, we have a well developed system for its rift-zone part, but not for the part connected to the Dolomieu crater. We shall come back to this point in discussions of each period because of the important societal impact of the collapse phenomena which are sometimes accompanied by phreatic explosions.

§ 2.3. Quiet period of phase 1 of cycle I (I-1Q): Cause and effect.

The widely spread eruption sites in the NE and SE rift-zones and the Dolomieu-east area during this period shows that the shallow magma system has become well developed. It followed the active period I-1A of 1 year duration in which the newly arrived magma reached the summit crater. It is followed by the active period I-2A in which the eruption occurs along the NE rift-zone outside the Enclos caldera for the first time since 1832 (Stieltjes and Moutou, 1989), suggesting that the shallow magma system as depicted in 2.2 was developed to the extent facilitating the newly arrived magma to cross the boundary of the Enclos caldera. As we shall see later, the eruption of March, 1986 which went outside the Enclos occurred also during the period in which the shallow magma system is well developed.

§ 3.1. Active period of phase 2 of cycle I (I-2A): Observations.

The eruption #10 on 1976/11/2 in the Bory-west area marks the beginning of this period. It occurred in the northern part of the area where the events marking the beginning of the phase 2 of all three cycles cluster. It stopped next day with the estimated lava output of 0.3 M cubic meters.

On 1977/4/5 an eruption fissure opened in the NE rift-zone at an elevation of 1950 m near the Enclos boundary. The eruption stopped on April 7 with a small amount of lava output. A new fissure was opened on April 8 along the NE rift-zone outside the Enclos at an elevation of 1000 m. More eruption fissures appeared along the rift-zone toward the ocean, and the front of the lava flow reached the ocean on April 10. The whole episode of this eruption was short and the volcano became quiet on April 15. The estimate of the lava output varies greatly. Benard-Krafft's estimate is more than 100 M and Stieltjes and Moutou (1989) gives 95 M, while Bachelery (1999) gives only 12 M. We adopted the last estimate in Table A1. We shall find in the next section that this choice of estimate is compatible with our model, but the others are not.

The eruption #12 occurred on 1977/10/24 in the Dolomieu-east area at elevations between 2200 and 2050 m. It stopped abruptly on November 16 with the lava output of 23 M cubic meters.

§ 3.2. Active period of phase 2 of cycle I (I-2A): Modeling.

The most important question for this period concerns the order of magnitude difference in the estimation of the lava output for #11 among the observers. If we adopt the estimate of 12 M by Bachelery, we obtain a remarkably constant amount in the L-B patches at the beginning of all the active periods as shown in Table 1. They are, 0, 31, 22, 21, 14, and 11 in the chronological order. They are obtained under the assumptions that (1) there was no residual magma in the beginning of I-1A, and (2) each new arrival brings 60 M from the mantle. (A slight decreasing trend with time can be removed if we assume a slightly larger amount for each new arrival.) If we adopted the estimate of 100 M for the erupted lava of #11, we must make a drastic adjustment to our assumptions. The residual magma in the beginning of I-1A must be at least 60 M or the supply from the mantle in cycle I-2A was at least 120 M instead of 60 M. In fact, Lenat and Bachelery (1990) hypothesize that all the eruptions after 1977 to the early part of the 1998 eruption were from the magma stored in 1977. This means that the amount of magma arrived in the period I-2A was more than 200 M and there were no new magma arrival in cycle II. If this variable supply were true, a long term prediction of the future eruption for Piton de la Fournaise would be impossible. On the other hand if our model of regularly repeated supply is valid, we have a great potential for predicting the future activity. In any case Bachelery's estimate of 12 M output for the eruption #11 permits our model with an exactly constant (60M each) supply and roughly constant amount of residual magma at the beginning of all the active periods. The lack of significant long-term deformations before the eruption was one of the reasons for the Lenat-Bachelery model. The steady supply of relatively small amount of magma and nearly constant residual magma may be an alternate way to explain the observed lack of the precursory deformation. In fact, there was no detectable deformation even before the 1998 eruption, which clearly involved a supply of new magma (See Aki and Ferrazzini, 2001). On the other hand, I am unable to explain the observed systematic change in geochemistry of magma (Bachelery, 1999) in a simple manner with my current model.

An interesting characteristic of the eruption #12 is its sudden ending. In general the ending of eruptions from an isolated patch may be gradual as discussed in §

1.2, and the abrupt ending may mean a connection to the main magma system in which a sudden diversion of flow can take place. The abrupt ending may also be caused by blocking of flow due to some sudden collapse along its path. In § 2.2, we attributed the lack of collapse in the Dolomieu crater after this active period to the under-developed magma system for the part connected to the crater.

§ 3.3. Active period of phase 2 of cycle I (I-2A): Cause and effect.

An important aspect of this period is the eruption outside Enclos. The rapid manner in which magma proceeded to the ocean along the NE rift-zone suggests that the subsurface channel was more or less in place when the new magma arrived. This is consistent with the well-developed shallow magma system in the preceding period described in § 2.2.

§ 4.1. Quiet period of phase 2 of cycle I (I-2Q): Observations.

This 91-month period produced the largest lava output of all the quiet periods as shown in Table 1. The mode of eruption was also unique. All the eruptions except #16 are from the Bory-west area. The eruption #16 is from a fissure 700 m long oriented N70E at a location eastward from Dolomieu toward the Piton de Crac at elevations between 1930 and 1650 m. This location is shared by the eruption #26 in the period II-1Q, but is isolated from other eruptions either in the Dolomieu-east or NE rift-zone. We shall call this site "To Piton de Crac" as listed in Table A1.

The second eruption in this period, #14 on 1981/2/3, is the first eruption after the establishment of the monitoring network at Piton de la Fournaise by the IPGP. Starting on January 23, VT earthquakes originating at depths 1-3 km below the Bory crater were observed and the total number reached 73 by February 2 (Benard and Krafft). The seismicity increased one hour before the eruption (250 events recorded), marking the first observation of the "seismic crisis". All eruptions occurred in this volcano since then showed similar precursory seismic crises. A systematic relation was found later by A-F-00 between the duration of the seismic crisis and the elevation of the eruption site from observations on eruptions #22 through #38 in cycle II. The observed relation for some eruptions in this period fit well the empirical relation for cycle II as for #17 and #18, but there is some significant difference for others. For example, the observed duration of 2 hours reported by Benard and Krafft for #16 would predict the elevation in the range 2300 to 2000 m while the actual elevation was 1930-1650 m.

The eruption #14 is also the first eruption in which the concurrence of the beginning of eruption and the beginning of strong continuous tremor with dominant frequency 2 to 3 Hz was recognized. Since then all eruptions observed in the field confirmed this concurrence and the tremor has been called the eruption tremor. The origin of tremor determined from its amplitude distribution agrees well with the eruption site (e.g., Battaglia, 2000).

Thus both the precursory swarm of VT events and the eruption tremor appear consistently for all eruptions at this volcano, but the occurrence of LP events does not. This is the reason why no emphasis was placed on the LP events in early seismological studies of this volcano, but is also the reason why it has become an important indicator of the changing condition of the magma system. As far as the records left on the shelves of the observatory are concerned, we could not find any LP events clearly associated with eruptions until #20 in the period II-1A.

None of the eruptions in this period was described as ending abruptly.

§ 4.2. Quiet period of phase 2 of cycle I (I-2Q): Modeling.

One of the basic assumptions underlying our model is that there is no supply of magma from the mantle during any quiet period. Thus the lava flow coming from the Bory-west area in this period must be supplied from the residual magma in the L-B patches. The shallow magma system consisting of the Dolomieu-east and the two rift-zone must be closed for some reason. This is consistent with the gradual ending of the eruption as well as the apparent lack of LP events. Furthermore according to Benard and Krafft, the two eruptions #17 and #18 overlap, the former ending on 1985/1/23 and the latter starting on 1985/1/18 suggesting separate sources for them. This leads us to infer that the site of the eruption #16, the only one outside the Bory-west area during this period, is not connected to the LP source and cannot be from the rift-zone path as defined in our model depicted in Figure 2.2. The location of #16 is isolated form other eruptions, justifying such an idea, which is also supported by the situation of only one other eruption sharing the same site, namely, #26 as discussed in sections related to the period II-1Q.

The above sequence of 5 eruptions from the Bory-west produced the total output of 24 M cubic meters, and is followed by the June 14, 1985 eruption identified as the beginning of cycle II, and then by an exceptional seismic crisis called "east flank crisis" on July 10-11, 1985. This crisis was not followed by an immediate eruption and did not occur below the central cone as usual. It was unusual also in the range of their focal depths covering from 1 km b.s.l. down to 6 km b.s.l.. Lenat et al (1989) attributed this crisis to the stress induced by intrusion of magma into the fracture system associated with the preceding series of eruptions in the Bory-west area. A similar explanation was given by Zlotnicki et al (1990) for the displacement vectors obtained by photogrammetric areal surveys made in 1981 and 1983 in the middle of the period I-2Q. These explanations are consistent with our model of residual magma, in which the pressure is increasing by degassing, seeking a way out through the Bory-west path because of the closure of the shallow part of the magma system.

§ 4.3. Quiet period of phase 2 of cycle I (I-2Q): Cause and effect.

What is the cause of the long closure of the shallow magma system hypothesized above? In § 3.2 we defined the closure period as starting with the end of eruption #5 and #6 in November, 1975, but the actual beginning could be the end of the eruption #12 in November, 1977, which produced a large amount (23M) of lava flow and stopped suddenly. We have so far associated the sudden ending to the diversion of flow to another path which is suddenly opened, but we may also associate it with a sudden closure of the path supplying the lava blocked perhaps by some collapse along the path. Unfortunately, there was no monitoring network operating at this time to confirm this possibility.

As described in the following sections, the shallow magma system reopened with the NE rift-zone eruption (#20) on 1985/8/5, which included a swarm of LP events during the precursory seismic crisis.

§ 5.1. Active period of phase 1 of cycle II (II-1A): Observations.

This period starts with the Bory-west eruption (#19) on 1985/6/14 and ends with the SE rift-zone eruption (#24) outside Enclos accompanied by a pit crater formation in the floor of the Dolomieu crater on 1986/3/29. It lasted for 10 months and produced 43.7 M cubic meters of lava as shown in Table 1.

The eruption #19 was from a fissure on WSW of the Bory crater at elevations between 2540 and 2250, lasted only for one day and stopped gradually as is usually the case for an eruption from the Bory-west area. It was preceded by a seismic crisis of less than 1 hour duration consisting of shallow VT events beneath the summit. There were no LP events associated with this eruption.

There was a swarm of shallow VT events beneath the summit on 1985/7/9 with no accompanying eruption. This is the first seismic crisis without eruption observed here since the establishment of the monitoring network and was interpreted as a dynamic intrusion of magma without reaching the surface. On the next day a vigorous swarm of VT events called "east flank crisis" started ENE of the summit at depths of 1 to 6 km b.s.l. as mentioned in § 4.2. This crisis

surpassed the previous crises beneath the summit by two orders of magnitude in the number of earthquakes as well as the energy released.
The eruption #20 occurred on 1985/8/5 in the NE rift zone. A swarm of 13 unmistakable LP events with dominant frequencies around 1 Hz was found during its precursory seismic crisis. The eruption lasted for 26 days with the lava output of 7 M cubic meters. The duration of the precursor crisis measured on the Sefram record was 2 hour 37 min. which, together with the elevation of the eruption site (2100-2000 m) contributed to the empirical systematic relation between the elevation and the duration of seismic crisis obtained for 13 eruptions occurred from 1985 through 1992 as shown in Figure 8 of Aki and Ferrazzini (2000). The ending of #20 was not abrupt.
The eruption #21 occurred on 1985/9/6 from three fissures including one running within the Dolomieu crater. After September 7, the eruptive activity was limited to the fissure on the east flank. The eruption stopped on October 10 with the total output of 17 M cubic meters. LP events with a dominant frequency of about 1 Hz were recorded during the first few days of the eruption.
The eruption #22 occurred on 1985/12/2 from a 2 km long fissure on the south flank. It was short lasting for 28 hours with the lava output of about 1 M. It was immediately followed by a swarm of 20 LP events with a dominant frequency of about 1 Hz.. We classify this eruption to the Dolomieu-east although it is at the boundary with the Bory-west area, because the southern end of the eruption fissure is located closer to the Dolomieu-east area. The choice of the Bory-west path would contradict our interpretation of LP events following the end of eruption.
The eruption #23 started on 1985/12/29 from a fissure in the Dolomieu crater and covered 95% of the crater floor by the time when the eruption stopped on 1986/2/2 with the total lava output of 7 M cubic meters.
The eruption #24 was preceded by a seismic crisis of 9 hour 24 min. duration which included a swarm of LP events with dominant frequency around 1 Hz. The eruption started on 1986/3/19 in the SE rift-zone at an elevation of 1750 m but lasted only for 9 hours with the lava output of 0.5 M. Next day, a new fissure opened at Takamaka in the same rift-zone outside the Enclos caldera producing lava flow which reached 200 m from the coast. On 1986/3/23, an eruption started near the Pointe de la Table further along the same rift-zone preceded by a swarm of LP events with a dominant frequency of about 1 Hz originating beneath the summit. The effusive activity at Pointe de la Table stopped on 1986/4/1 with the output estimated at 3-5 M cubic meters. In the meantime, the seismicity at the summit became exceptionally intense on 1986/3/28 which culminated as a pit crater formation in the Dolomieu crater on the next day accompanied by phreatic explosions. The pit crater was 150 m in diameter and 80 m deep.
§ 5.2. Active period of phase 1 of cycle II (II-1A): Modeling.
The abundant LP events directly associated with individual eruptions during this period show that the shallow magma system is well developed. We find eruptions from the Dolomieu-east as well as both rift-zones. The path to the Dolomieu crater is open and 95 % of the crater floor was covered by the lava erupted during this period. The rapid manner the eruption #24 extended outside the Enclos along the SE rift-zone suggests that the magma path was already in place at the time of its occurrence just as in the case of #11 in the NE rift zone in 1977. The formation of a pit crater in the Dolomieu floor near the end of #24 implies that the summit path is connected to the SE rift-zone during this period.

The occurrence of LP events with the dominant frequency of 1 Hz during the precursory crisis of #20 (NE rift-zone) and #24 (SE rift-zone) indicates that the connection to the rift-zone was through the source of 1 Hz LP events. Their absence before #22 (DOlomieu-east) but their occurrence immediately following it shows that the stopping of the eruption #22 is caused by the diversion of magma flow from the summit path to the rift zone path. The absence of LP events associated with #19 (Bory-west) shows that the LP source is not connected to the Bory-west path. The eruptions during this period offered part of observations from which the separate paths for the summit and rift-zone eruptions and the location of LP source in the rift-zone path were recognized by Aki and Ferrazzini (2000) as shown in Figure 2.2..

§ 5.3. Active period of phase 1 of cycle II (II-1A): Cause and effect.

This period follows the 8-10 year closure of the path to the Dolomieu crater discussed in § 4.2 and 4.3. With the new arrival of magma concurrent with #19, the pressure and temperature were increased, and the closed path was opened. Then a seismic crisis beneath the summit occurred on 1985/7/9 without eruption and was followed by the vigorous east-flank crisis which has been the only such crisis observed since the establishment of monitoring network till now. We agree with the interpretation by Bachelery et al.. that this crisis represents the release of compressional stress accumulated in the central area of the volcano during the repeated intrusions occurred over several preceding years. This crisis may also be related to the opening of the path to the shallow magma system closed for 8-10 years, because it was followed immediately by #20 (1985/8/5) in the NE rift zone and #21 (1985/9/6) in the Dolomieu-east area with the first lava flow within the Dolomieu crater since November, 1975. Both eruptions are accompanied by a swarm of LP events, indicating that the LP source was also quickly established.

Thus we see here a quick development of the shallow magma system within a few months once a blocking barrier in the flow path is removed. The arrival of new magma into the well-developed shallow magma system resulted in the lava flow outside the Enclos during the eruption #24 in the SE rift-zone.

§ 6.1. Quiet period of phase 1 of cycle II (II-1Q): Observations.

This period follows the pit crater formation on 1986/3/29 and ends with the arrival of new magma signaled by the eruption #29 on 1987/11/6 in the Bory-west area. It lasted for 19 months and produced lava output of 16.9 M cubic meters. After the formation of the pit crater, the lava remaining from the eruption #23 which filled 95% of the Dolomieu floor fell into the pit crater as a 5 m wide cascade until April 5. Several minor eruptions from fissures in and near the pit crater occurred until 1987/1/6 with the total lava output of 2.5 M cubic meters. As soon as the eruption in the Dolomieu crater stopped, the eruption #26 began on the same day from the site we called "To Piton de Crac" in § 4.1, where the eruption #16 from the same site is attributed to a magma path not connected to the NE rift zone. The concurrence of the stopping of the eruption in the Dolomieu crater and the beginning of #26 as well as the absence of LP events associated with #26 further supports that this site does not belong to the NE rift-zone path. This eruption ended gradually sometime between 6 and 10 February, 1987 with the lava output of 10.5 M cubic meters.

The eruption #27 on 1987/6/10 was again from the floor of the Dolomieu crater. It lasted for 20 days with the lava output of 1.5 M cubic meters. The last eruption (#28) in this period occurred at two separate sites in the Dolomieu-east area at about the same elevation around 2000 m. It lasted 2-3 days with the lava output of 0.8 M cubic meters.

We observed a swarm of large LP events with dominant frequencies 1 to 1.5 Hz between mid-February and mid-March, 1987 with no direct relation with the eruptive activity. Otherwise the LP seismicity beneath the summit was relatively low as compared with the preceding period (II-1A). The low LP seismicity persisted through 1988 nearly to the end of the next active period (II-2A) when the eruption

#34 occurred on 1988/12/14 in the NE rift-zone preceded by a swarm of LP events.
As described in A-F-00, we observed numerous LP events with a dominant frequency of 3.5 Hz recorded only at station NCR (now moved nearby NSR) in 1987, particularly frequently from June to September. Their sharply peaked spectra suggested a seismic source of an isolated magma pocket with high impedance contrast. Their occurrences also had no direct relation with the eruptive activity.
§ 6.2. Quiet period of phase 1 of cycle II (II-1Q): Modeling.
The above observations suggest an intermediate development of the shallow magma system in this period. The absence of rift-zone eruption and the low level of LP seismicity indicate that the rift-zone part of the system was not as well developed as in the preceding period (II-1A). The magma path along the rift zone may be not continuous but broken into segments.
The occurrence of LP events unrelated with eruptions appears to be common during the quiet period as we shall find more examples in the period II-2Q. If the rift-zone path is segmented, we can explain LP events unrelated with eruptions as magma movements between segments. We did not observe any LP during the period I-2Q because the shallow magma system was closed at that time.
§ 6.3. Quiet period of phase 1 of cycle II (II-1Q): Cause and effect.
This period follows the spectacularly active period with eruptions outside the Enclos and a pit crater formation in the Dolomieu crater, attributed to a well-developed shallow magma system. It is followed by an active period in which there was no rift-zone eruption until its end, nor any collapse in the Dolomieu crater and the two largest eruptions ended gradually as described in § 7.1, making a strong contrast to the other active periods (I-2A and II-1A) in which the new magma arrived when the shallow magma system is well developed. The difference may be attributed to the intermediate degree of development of the shallow magma system with segmented path during this period. The segmented system may also explain the gradual ending of some eruptions in the next period.
§ 7.1. Active period of phase 2 of cycle II (II-2A): Observations.
This period starts with the eruption #29 on 198711/16 in the Bory-west area and ends with the eruption #34 on 1988/12/14, producing the total lava output of about 50 M cubic meters. The eruption #29 occurred at two sites separated by 1.5 km near the north end of the Bory-west area where the other two eruptions (#10 and #43) marking the beginning of phase 2 also occurred. It lasted for three days and produced the lava output of 1.6 M cubic meters.
The eruption #30 occurred on 1987/11/30 in the Dolomieu-east area starting with a fissure at elevation 2240 - 2080 m on the south side of Dolomieu followed by those at elevations around 1900 m. It lasted for 33 days and produced 10 M cubic meters. The ending of this eruption was very gradual with intermittent tremors sometimes interrupted for 30 minutes. The low tremor amplitude lasted for 7 days before the end of eruption. The eruption was preceded by the usual seismic crisis composed of shallow VT events beneath the summit, but there were no concurrent LP events before, during or following it.
The eruption #31 occurred on 1988/2/7 near the site of #30 and lasted for 56 days with the lava output of 8 M cubic meters. The ending of eruption was again extremely gradual, characterized by rhythmic amplitude fluctuation of the eruption tremor and a very low amplitude persisting for more than 10 days before the end of eruption. The duration of precursory seismic crisis was 2 hour 5 min. Again, we found no LP events associated with this eruption.
The eruption #32 occurred on 1988/5/18 in the Dolomieu-east area on the north side of Dolomieu. It lasted for 76 days with the lava output of 15 M cubic meters.

The ending of this eruption is again extremely gradual. The duration of the precursory seismic crisis was 31 min. and there were no LP events associated with this eruption.
The above three eruptions are similar in their characteristic and produced the total amount of lava estimated at 33 M cubic meters in 7 months. The elevation of the eruption site and the duration of the precursory seismic crisis from these eruptions contributed to the empirical relation between them shown in Figure 8 of Aki and Ferrazzini (2000).
The eruption #33 following the above sequence occurred on 1988/8/31 in the Bory-west area. It lasted for 57 days producing the lava output of 7 M cubic meters. This is the only one in the Bory-west area since 1972 occurred in the middle of an active period. All others are either at the beginning of an active period or in the quiet period I-2Q during the 8-10 year period of the closure of the shallow magma system discussed earlier. We observed a sequence of gas piston events on 1988/10/26 when the eruption was ended. The precursory crisis lasted for 2 hour 25 min., and again there were no LP events associated with the eruption.
The eruption #34 occurred on 1988/12/14 in the NE rift zone from fissures at elevations 2100-2000 m. A swarm of LP events with dominant frequencies around 2 Hz appeared during the precursory seismic crisis which lasted for 4 hour 31 min.. Unlike the usual summit eruption in which eruption fissures propagate downward, A new fissure opened above the older one during this rift-zone eruption. Unlike all the preceding eruptions of this period, this eruption stopped suddenly on 1988/12/29 followed by a swarm of LP events with a dominant frequency of 1 Hz lasting for a few days. The eruption lasted for 15 days with the lava output of 8 M cubic meters.
There were no collapse in the floor of the Dolomieu crater during the transition to the quiet period following this active period. All the eruptions in this period were confined within the Enclos caldera.
§ 7.2. Active period of phase 2 of cycle II (II-2A): Modeling.
The three major eruptions of this period are all in the Dolomieu-east area with gradual endings, which suggest an isolated magma reservoir supplying each eruption. The absence of LP events following these eruptions indicates the absence of connection between the eruption site and the rift zone. The occurrence of a Bory-west eruption following the above sequence must be due to a temporary closure of the shallow magma system, although there were no observed seismic events that might be associated with such a change in the system. After the Bory-west eruption, the rift zone part of the shallow magma system becomes suddenly well developed as indicated by the swarm of LP events in the precursory crisis of #34 and its abrupt ending. Again there were no significant seismic events which might be associated with the system change, except for an increase of shallow VT seismicity after a swarm of duration 25 min. on 1988/11/12 a month before #34..
The above observations suggest a magma system with segmented path in an unstable condition. Thus major eruptions come from isolated patches and the magma path can be closed and opened suddenly without observable effects. Apparently under this condition of the magma system, there is no violent energetic phenomena such as the collapse in the Dolomieu crater or an eruption outside the Enclos.
Aki and Ferrazzini (2000) attributed the difference in dominant frequency of LP events before and after #34 to two separate sources for 1Hz and 2 Hz LP events. The magma was supplied to the eruption site of #34 through the 2 Hz LP source, but the eruption was stopped because the connection was made between the 1 Hz

LP source and the eruption site and the magma was drained back to the 1 Hz source from the eruption site. The assumed two separate sources for 1 Hz and 2 Hz LP events are also consistent with the difference in long-term change of their activities as discussed in § 8.1.

§ 7.3. Active period of phase 2 of cycle II (II-2A): Cause and effect.

Let us compare the present period with the other active period of phase 2. In the period I-2A, the 1977 eruption outside the Enclos occurred and we attributed it to the shallow magma system well developed already before the arrival of new magma. In the period III-2A which included a lava flow from the NE rift-zone reaching the ocean , we shall see that the development of the shallow magma system as indicated by the reactivation of LP activity is nearly simultaneous as the arrival of new magma. On the other hand, the shallow magma system in the present period at the time of arrival of new magma was in an intermediate state of development as indicated by generally low LP seismicity and occasional LP swarms unrelated to eruptions in the preceding period.

Following this period, we shall enter a period with an abundant occurrence of LP events both related and unrelated to eruptions. The revival of the 1 Hz LP source following the eruption #34 indicates the reappearance of the well developed shallow magma system which will persist through the period II-2Q until LP events gradually disappear as we enter the 6-year period without eruption.

§ 8.1. Quiet period of phase 2 of cycle II (II-2Q): Observations.

We note the similarity of eruption sites during this period with those in periods I-1Q and II-1A. In all three cases an SE rift-zone eruption was preceded by an eruption inside the Dolomieu crater.

This period starts with the eruption #35 which occurred on 1990/1/18 from a fissure in the Dolomieu crater which propagated southward outside the crater. The eruption was short and stopped next day with the lava output of 0.5 M cubic meters, covering 20 % of the Dolomieu crater floor. It was preceded by a swarm of VT events with a duration of 47 min..

The LP seismicity showed a remarkable increase in 1989 (76 events with dominant frequency 1 to 3 Hz) although there was no eruption during the year. We observed a swarm of 10 small LP events in 4 days preceding #35 and a large one with the dominant frequency of 1 Hz immediately following it.

The eruption #36 occurred on 1990/4/18 in the SE rift zone at an elevation of 1800 m. The long duration of the seismic crisis (6 hour 45 min.) for this low elevation contributed to the systematic relation between the two parameters mentioned earlier. A swarm of LP events was observed during the crisis. It lasted for 21 days with the lava output of 8 M cubic meters. Its ending was gradual.

There was a major swarm of LP events during March-April, 1991 with no direct relation

to any eruption. They are characterized by the dominant frequency of 1.4 Hz, and their total number reached 110 when it was suddenly stopped concurrent with the arrival of seismic waves from a M=5.8 earthquake in Madagascar 800 km away from La Reunion.

The eruption #37 occurred on 1991/7/19 from a fissure at an elevation 2510 m along the southern edge of the Dolomieu crater, which extended toward the east flank of the volcano to an elevation of 2400 m. It lasted for 2 days and produced the lava output of 2.8 M cubic meters. The duration of its precursory seismic crisis was 52 min. and there were no LP events associated with this eruption.

A major seismic crisis without a following eruption but with numerous LP events occurred on 1991/12/7 as described in detail by Aki and Ferrazzini (2000). A vigorous LP seismicity lasted for three weeks amounting to the total number of 320 events with dominant frequencies between 1 and 3 Hz.

Last eruption of cycle II, #38, occurred on 1992/8/27 starting from a fissure within the Dolomieu crater, which propagated rapidly southward outside the crater. Four additional vents opened on the south side of the summit down to the elevation 2100 m. It lasted till 1992/9/23 with the lava output of 5.5 M cubic meters. The duration of its precursory crisis was 57 min. There was a swarm of LP events with dominant frequencies 1.1 to 1.5 Hz near the end of this eruption. After that, we have observed no LP events with dominant frequencies lower than 1.5 Hz till 5 hours before the major eruption on 1998/3/9.

The history of LP events originating beneath the summit of Piton de la Fournaise from 1985 to 1996 was summarized in a histogram of annual number of LP events with a given dominant frequency for the range between 0.8 to 3.0 Hz in Figure 2.5 of Aki and Ferrazzini (2000). The most outstanding trend in the figure is the systematic disappearance of LP events after the eruption #38. LP events with the lowest frequency disappeared first. Those with dominant frequencies around 2 Hz become dominant in 1993, decreased gradually and practically vanished in 1996. A 2 Hz LP event located beneath the summit reappeared on 1997/6/4. In the same figure we recognized a similar frequency-dependent disappearance of LP events from 1985-86 to 1987-88, when the LP seismicity declined from the period II-1A to the periods II-1Q and II-2A as described earlier.

The VT seismicity also decreased gradually after #38, but the rate of their occurrence did not become zero like the LP seismicity. The rate for 1995 is about one half of that for 1993, and there was an indication of revival already in 1996. The first seismic crisis after #38 occurred on 1996/11/26 without eruption.

§ 8.2. Quiet period of phase 2 of cycle II (II-2Q): Modeling.

The well developed shallow magma system was maintained without any supply of new magma from the end of #34 to the end of #38, spanning 45 months, in which 4 eruptions with total output of 17 M cubic meters occurred in the Dolomieu-east and SE rift-zone area. This period is characterized by abundant LP events unrelated to individual eruptions. The vigorous seismic crisis of 1991/12/7 involving numerous LP events was not followed by an eruption, but must mean a significant magma movement through the rift-zone path. According to Battaglia, the GEOSCOPE record of this crisis indicates an inflation of the summit area similar to what was observed in the beginning of the March, 1998 eruption (#39), while eruptions #38, #41 and #42 showed a deflation followed by inflation, as might be expected for eruptions from an isolated magma patch. My tentative explanation of the crisis of 1991/12/7 is that it was the last attempt of magma going into the rift-zone path during cycle II. It did not succeed and stayed in the volcano to come out as part of lava output of the March 1998 eruption.

At the time of writing of Aki and Ferrazzini (2000), we did not know about the concurrent change in the characteristics of eruption tremor and those of lava geochemistry two months after the beginning of the eruption #39, which will require the presence of the old magma remaining in the shallow part of volcanic edifice as hypothesized by Lenat-Bachelery (1990). We estimate the amount of the remaining magma at the time of the beginning of the period III-1A as 14 M cubic meters as shown in Table 1.

Thus the disappearance of LP events following the last eruption of the period II-2Q does not necessarily mean the disappearance of magma. We must conclude that magma can stay at the shallow part of a volcano (at about sea level) in an isolated patch without generating observable LP events for several years.

§ 8.3. Quiet period of phase 2 of cycle II (II-2Q): Cause and effect.

It is interesting to compare the condition of the magma system between this period and the corresponding period of cycle I, namely, I-2Q during which the path to the shallow part of the magma system was blocked from its beginning until the new arrival of magma in II-1A, after which the shallow magma system was immediately well developed. In the present period the shallow magma system was well developed at its beginning, and gradually became segmented and finally inactive with some magma remaining quietly in isolated patches. It took more than 2 years after the arrival of new magma in the period III-1A before the shallow magma system become well developed as described in § 11.1.

§ 9.1. Active period of phase 1 of cycle III (III-1A): Observations.

This period consists of two simultaneous eruptions #39 and #40. The eruption #40 is from a vent named "Fred Hudson" in the southern part of the Bory-west area where the first events in cycle I and II are also originated. It started three days after #39, lasted 21 days with the lava output of 1 M cubic meters. The eruption #39 was preceded by a seismic crisis of 1 1/2 day duration in which the focal depth of VT events migrated from about 5 km below sea level to the surface near the summit. The eruption started on 1998/3/9 from a fissure on the north flank of the central cone at an elevation of 2450 m, which propagated downward in an en echelon pattern, and became concentrated at two vents, named "Piton Kapor" and "Maurice and Katia Krafft", at an elevation of 2150 and 2080 m, respectively. The eruption lasted for 6 months with the lava output of 60 M cubic meters.

The vigorous seismic crisis of 1 1/2 day duration was preceded by an increased VT seismcity beneath the summit at about sea level for about 7 months. As mentioned in § 8.1 there was an indication of revival of VT events in 1996. Their focal depths ranged 10 to 30 km, and the largest one with M=2.5 occurred on 1996/3/2 at a depth of 15 km b. s. l. a few kilometers east of the central cone. It was followed by a cluster of seven events with M=1.6 to 1.8 occurring at depths 16 to 18 km about 5 km northwest of the central cone in September, 1996 and by an M=2.3 event under station CHR (located also northwest of the central cone, now moved to nearby TCR) at a depth of 2 km b.s.l.. Then we had the first seismic crisis since the eruption of August, 1992 occurred on 1996/11/26. This crisis consisted of 138 VT events located at about sea level beneath the central cone. The largest magnitude was 2.4, and the crisis lasted for 104 min. It was not followed by any eruption.

All the LP events originating beneath the summit before September, 1993 showed identical arrival times and very similar waveforms at the three summit stations (BOR, SFR and DSR), which we call "coherent". After September, 1993, we began to observe LP waves which did not show this coherence. All LP events in cycle II after January, 1994 showed different arrival times and incoherent waveforms at the three summit stations. The last LP event of the cycle II activity confirmed to originate from beneath the summit area occurred on 1995/4/1. It was incoherent and the dominant frequency was 2.6 Hz. The first LP event of the cycle III activity confirmed to originate from beneath the summit was also incoherent and its dominant frequency was 2 Hz. Thus the last disappearing is similar to the first reappearing. The 1 Hz LP event which disappeared after the eruption of August-September, 1992 reappeared about 5 hours before the eruption of March 9, 1998. Their waveforms at the three summit stations were incoherent. As we shall find later in the period III-2A,, the first coherent LP event in cycle III appeared on 2000/2/8 with the dominant frequency of 4 Hz, and the first large coherent LP events with the dominant frequency of 1 Hz appeared in November, 2000, 42 hours after the end of the eruption #45 that stopped suddenly.

As reported by A-F-00, the amplitude of the eruption tremor of #39 showed a large fluctuation in the first two months and become nearly constant and smooth till the end. This temporal behavior was found to be very similar to that of chemical compositions of lava found by Semet et al.(200?).

§ 9.2. Active period of phase 1 of cycle III (III-1A): Modeling.
The crisis of 1996/11/26 was interpreted by Aki and Ferrazzini (2000) as the beginning of the filling of a reservoir named “NTR” in Figure 2.2, located in the southern part of the Enclos caldera at the bottom of the volcanic edifice based on the observed spacial and temporal change in the coda localization. The 7 month period of increased VT seismicity preceding the eruption #39 was interpreted by them as the period for filling the other deep reservoir named “NCR” beneath the northern part of the Enclos caldera. It took 15 months for the newly arrived magma to fill the two deep reservoirs with 60 M cubic meters according to their interpretation. The corresponding flow rate is 8.5 times higher than that of the steady supply to each of the two mantle reservoirs (655 cubic meters per hour) assumed by Cabusson (2002) for explaining the observed two phases of each cycle . The lava output of 60 M for the eruption #34 and its duration of 6 months give the average flow rate during the eruption 21 times that of the steady mantle supply.
The temporal regularity in the disappearance and appearance of different types of LP events let Aki and Ferrazzini (2000) postulate the source of coherent 1 Hz LP event at the shallowest depth beneath the summit underlain by that of the coherent 2 Hz LP event. The source of the incoherent LP event was placed not directly beneath the summit and probably deeper than those of the coherent ones. LP events during this period were “incoherent” and scarce as in the following period III-1Q. We attribute them to the under-developed condition of the shallow magma system.
The similarity in the temporal behavior between the eruption tremor and the chemistry of lava during the eruption #39 enabled a merging of two radically different earlier models of this volcano, namely the one by A-F-00 and the other by Lenat and Bachelery (1990). The former assumes the existence of large magma reservoirs near the bottom of the volcanic edifice which supplied lava for the 1998 eruption, while the latter model consists of numerous small shallow reservoirs of magma filled in 1977 or earlier, which supplied lava for all eruptions after 1977 without any additional supply from below.
The observed irregular variation in chemical composition of lava in the first two months followed by a smooth systematic variation till the end of the eruption was interpreted by Bachelery (Memoire, Universite de la Reunion, 1999) as due to a mixing of old magma remaining since 1977 with the newly arrived one represented by the lava erupted from the “Fred Hudson” vent. Aki and Ferrazzini (2000) interpreted a similar temporal variation in the amplitude of seismic tremor as the change due to opening of connection between the eruption site and a reservoir of larger capacity. Thus it appears that the main part of the erupted lava came first from the old magma patches of Lenat and Bachelery (1990) somehow stimulated by the arrival of new magma at the summit, and it took two months before the mixing of new and old magma started and the eruption site was connected hydro-dynamically to large reservoirs located near the bottom of the volcanic edifice.
§ 9.3. Active period of phase 1 of cycle III (III-1A): Cause and effect.
In § 8.3 we compared periods I-2Q and II-2Q, and found a great difference between them in the manner in which the shallow magma system was developed. This difference is reflected in the different mode of eruption in the succeeding active period. The LP source beneath the summit was developed immediately with the new arrival in II-1A, but was not developed at all during III-1A and took two more years after the end of III-1A for its full development. We attributed the eruption outside the Enclos and the formation of pit crater collapse in the Dolomieu crater during II-1A to the well developed shallow magma system. Both are absent during III-1A, even though the total lava output was greater in III-1A

than in II-1A (60 M vs 44M).
§ 10.1. Quiet period of phase 1 of cycle III (III-1Q): Observations.
This quiet period generated the least lava output of all the quiet periods. The output was only 3.3 M as compared to 12-34 M for the others. It also had the least estimate of the residual magma at its beginning, namely, 14 M as compared to 31-56 M for the others as shown in Table 1. The two eruptions #41 and #42 in this period are both in the Dolomieu-east area and both stopped gradually. They were preceded by the seismic crisis of VT events beneath the summit as usual. There were no LP events associated with them. There was no collapse in the floor of the Dolomieu crater in the transition period from the preceding active period..
§ 10.2 Quiet period of phase 1 of cycle III (III-1Q): Modeling..
All the observations mentioned above indicates a poorly developed shallow magma system during this period. We note that the precursory swarm of VT events occurs more of less in the same way independent of the condition of the shallow magma system. This means that they are useful for a practical short-term prediction, but not for determining the condition of the magma system.
§ 10.3 Quiet period of phase 1 of cycle III (III-1Q): Cause and effect.
The activity of this period is probably due to the small amount of magma left in the shallow part of the volcano because of the large amount of lava erupted during the preceding period. The amount of residual magma, however, was enough for developing the shallow magma system quickly after the arrival of new magma in the following period.
§ 11.1 Active period of phase 2 of cycle III (III-2A): Observations.
This period starts with the eruption #43 located in the northern part of the Bory-west area where the first eruption occurred also for phase 2 of both cycle I and II. Its singular location among others in this period attracted my attention and lead to the identification of the 13-year cycle of eruption history since 1972 as mentioned in the introduction. It occurred on 2000/2/14 and lasted for 19 days with the lava output of 4 M cubic meters. Details of observations about this and the following eruptions were given by Staudacher et al. (200?).
The eruption #43 was preceded by 6 weeks of slightly enhanced seismicity of VT events beneath the summit with a mean of 5 events per day. The duration of the precursory seismic crisis was 64 min. in which 261 events occurred with magnitude up to 1.9.
The eruption #44 occurred on 2000/6/23 from several fissures on the ESE flank at elevations between 2080 and 1820 m. It lasted for 37 days with the lava output of 6 M cubic meters. It was preceded by a dramatic increase of shallow VT seismicity starting in mid-June including a minor seismic crisis on June 22. The precursory seismic crisis included 270 events with magnitude up to 2.5. This eruption stopped gradually with no associated LP events.
The next three eruptions #45, #46 and #47 all occurred from vents near #44 in the Dolomieu-east area with the total lava output of 23.3 M cubic meters. They are preceded by swarms of shallow VT events beneath the summit. These events were small in magnitude but showed unusually long durations for this volcano. All three eruptions stopped abruptly followed by swarms of LP events.
The eruption #45 which started on 2000/10/12 was preceded by 3 weeks of high VT seismicity at a rate of 10-20 events per day. The largest magnitude was 1.7. The seismic crisis immediately before the eruption had 201 events with the largest magnitude of 1.6 and a duration of 64 min. The eruption lasted for 37 days with the lava output of 9 M cubic meters. The eruption tremor increased from October 29 to November 9 continuously and stayed constant for five days before disappearing suddenly on November 13 within 25 min.
The eruption #46, which started on 2001/3/27, was preceded by three swarms of

small shallow VT events beneath the summit starting January 20, February 25 and early March. The precursory crisis had 120 VT events and a duration of 25 min. The eruption lasted for 8 days with the lava output of 4.8 M cubic meters. The eruption tremor showed a slight increase before the end of eruption.
The eruption #47 started on 2001/6/11 and lasted for 26 days with the lava output of 9.5 M cubic meters. A swarm of small shallow VT events beneath the summit started on May 23 at a rate of 6 to 36 events per day. There was a minor seismic crisis of 17 events with a duration of 10 min. on May 30, and the high rate of VT events continued for 10 days up to 35 per day with the largest magnitude 1.8. The precursory crisis had 125 VT events and lasted for 32 min. The VT seismicity continued after the beginning of eruption for 8 days with magnitude up to 2.0. Within the first 11 days, the eruption tremor showed strong variations in amplitude by a factor up to 10. From June 21, the tremor amplitude increased significantly and stayed constant at that value. The tremor amplitude reached the highest level on July 7, and simultaneously the seismicity of VT events was intensified with magnitude up to 2.8. The tiltmeter and extensometer records indicated deflation of the summit during this period. The eruption ended on July 7, with the tremor amplitude increasing first and then decreasing to less than 5 % of its highest level and disappearing completely within a few hours. A swarm of LP events followed the sudden ending of eruption.
Two months after the end of eruption #47, the seismicity of shallow VT events beneath the summit started a gradual increase in 3 months up to 50 events per day in November. Two seismic crises occurred on November 5 and 29 without eruption. The precursory crisis of the eruption #48 started on 2002/1/5 with 370 VT events lasting for 6 hour 21 min. It included LP events whose source migrated toward the eruption site in the NE rift zone. The eruption started from four vents located at elevations around 1900 m. A new vent opened on January 12, 3 km east from the first ones with a large lava flow that reached the ocean on January 14, 2002. The eruption ended on January 16 with the lava output of 12.5 M cubic meters. There was a swarm of shallow VT events beneath the summit near the end of the eruption.
As mentioned in § 9.1 a large 1 Hz LP event occurred following #45 with the characteristic observed during 1980's, namely, the identical arrival times and wave forms at the three summit stations (BOR, SFR and DSR) attributed by A-F-00 to a laterally extended magma body beneath the summit generating these events. The last time we observed an LP event with this characteristic was on October 11, 1992. For example the LP events associated with the 1998 eruption were originated from a more localized source on the north side of the central cone, and showed different waveforms and arrival times at the three stations.
The LP events observed during the period III-2A occurred always as swarms close to the ends of eruptions.
§ 11.2 Active period of phase 2 of cycle III (III-2A): Modeling.
The above occurrence of LP events directly related to individual eruptions is very similar to that observed during the active period II-1A as described in § 5.1. The first swarm in that period occurred during the precursory crisis of the eruption #20 in the NE rift zone. The second one occurred during a complex episode of eruptions from three different vents in the summit area. The third LP swarm followed a short summit eruption and the forth one occurred shortly after the summit eruption #23 which filled 95% of the Dolomieu crater. Finally the last swarm in that period began shortly before the eruption #24 in the SE rift-zone outside Enclos.
The above comparison suggests that the shallow magma system in this period has become similar to the one working during the period II-1A. In this system, magma

can move more easily in the lateral direction, with eruptions in the Dolomieu-east and both rift-zones, and even into the rift zone outside Enclos.

Ferrazzini (personal communication) attributed the high VT seismicity near the end of eruptions #45, 46 and 47 to a process of collapse under the Dolomieu crater. The lack of LP events in minor seismic crises without eruption in this period also suggested the magma movement along the vertical summit path. As described in § 5.1, the high eruptive activity including the pit-crater collapse was observed also during the period II-1A supporting the similarity in the condition of the magma system.

The observed relation between the duration of the precursory crisis and the elevation of the eruption site for #48 precisely agreed the empirical relation obtained by Aki and Ferrazzini (2000) for eruptions in the period with a well-developed shallow magma system.

§ 11.3 Active period of phase 2 of cycle III (III-2A): Cause and effect.

The above similarities between this period and the period II-1A raised a serious concern about the possibility of an eruption outside the Enclos caldera as well as the explosive eruptions inside the Dolomieu crater associated with a pit-crater collapse. The eruption #48 was threatening enough to issue an evacuation order to some villages along the NE rift-zone, but did not go outside Enclos. The vigorous seismicity near the end of the eruption #49 (which belongs to the next quiet period according to our classification in Table 1) resulted in a collapse in the floor of the Dolomieu crater, but did not generate any eruptive activity. Why the difference? The answer may be found in Table 1.

We notice in Table 1 that the magma remaining in the L-B patches were much greater during periods preceding II-1A as compared to those preceding III-2A. In other words, we had all the conditions of the magma system needed for the eruption outside the Enclos as well as the explosive pit-crater collapse, but we did not have enough magma to generate them. We had necessary conditions but not sufficient.

Swarms of LP events occurred after the eruption #48, but disappeared in April, 2002. Their occurrence in 2002 had no relation with any eruption, suggesting the beginning of the segmented magma path as seen in the period II-2Q. while the LP activity before #48 was directly related to individual eruptions similar to the active period II-1A.

On the other hand the VT seismicity became vigorous showing a similarity in the temporal behavior of the daily frequency of summit events to that before the eruption #48, although the cumulative moment curve showed that the accumulated amount of seismic moment of the summit events is 10 times smaller than the corresponding period preceding #48.

In retrospect, the high VT seismicity was related to the magma movement in the vertical path to the Dolomieu crater where a collapse occurs at the end of the eruption #49, while the horizontal path to the rift-zone was showing the signs of segmentation as indicated in the behavior of LP events.

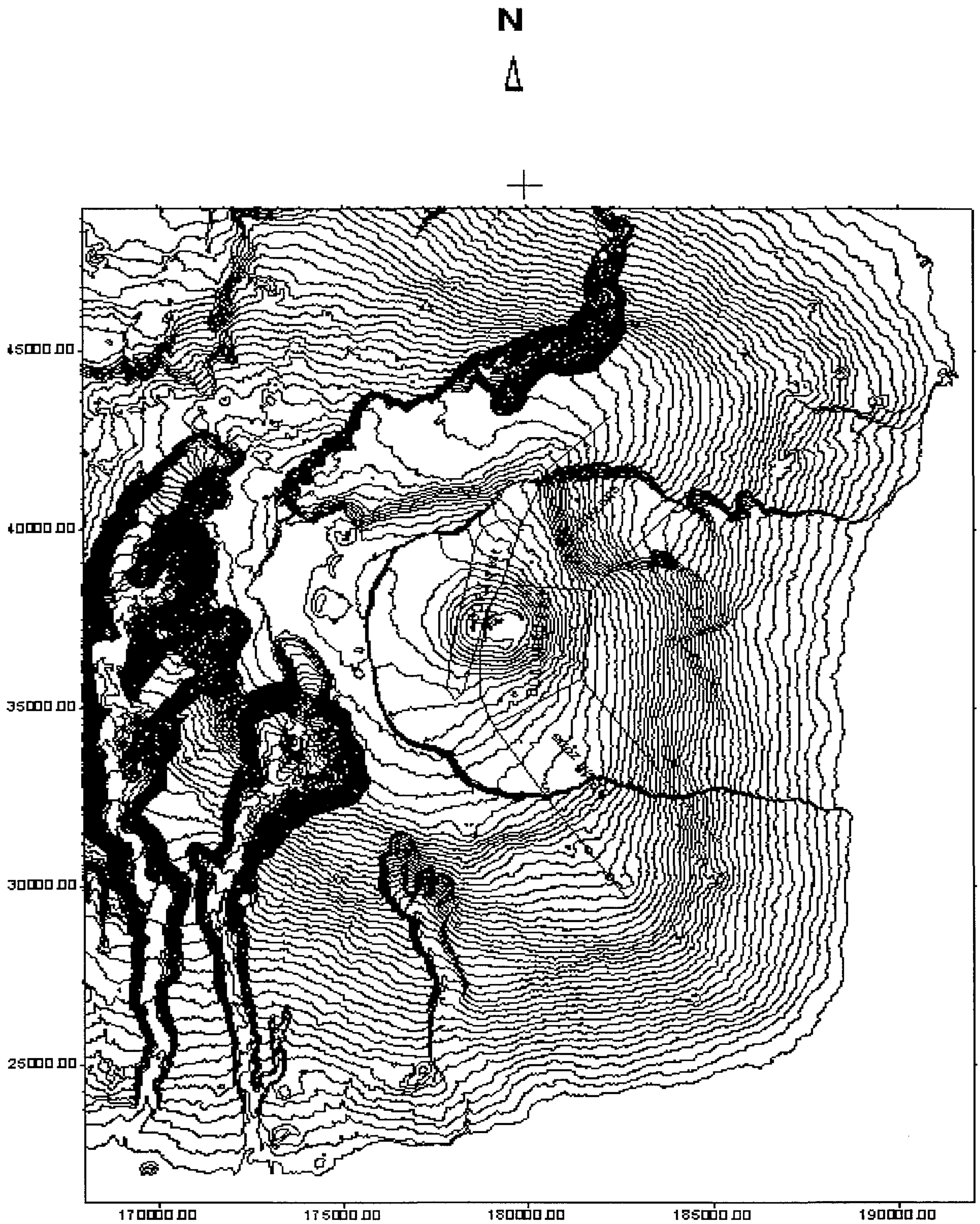

Figure 2.1. Boundaries of four areas of eruption sites at Piton de la Fournaise.

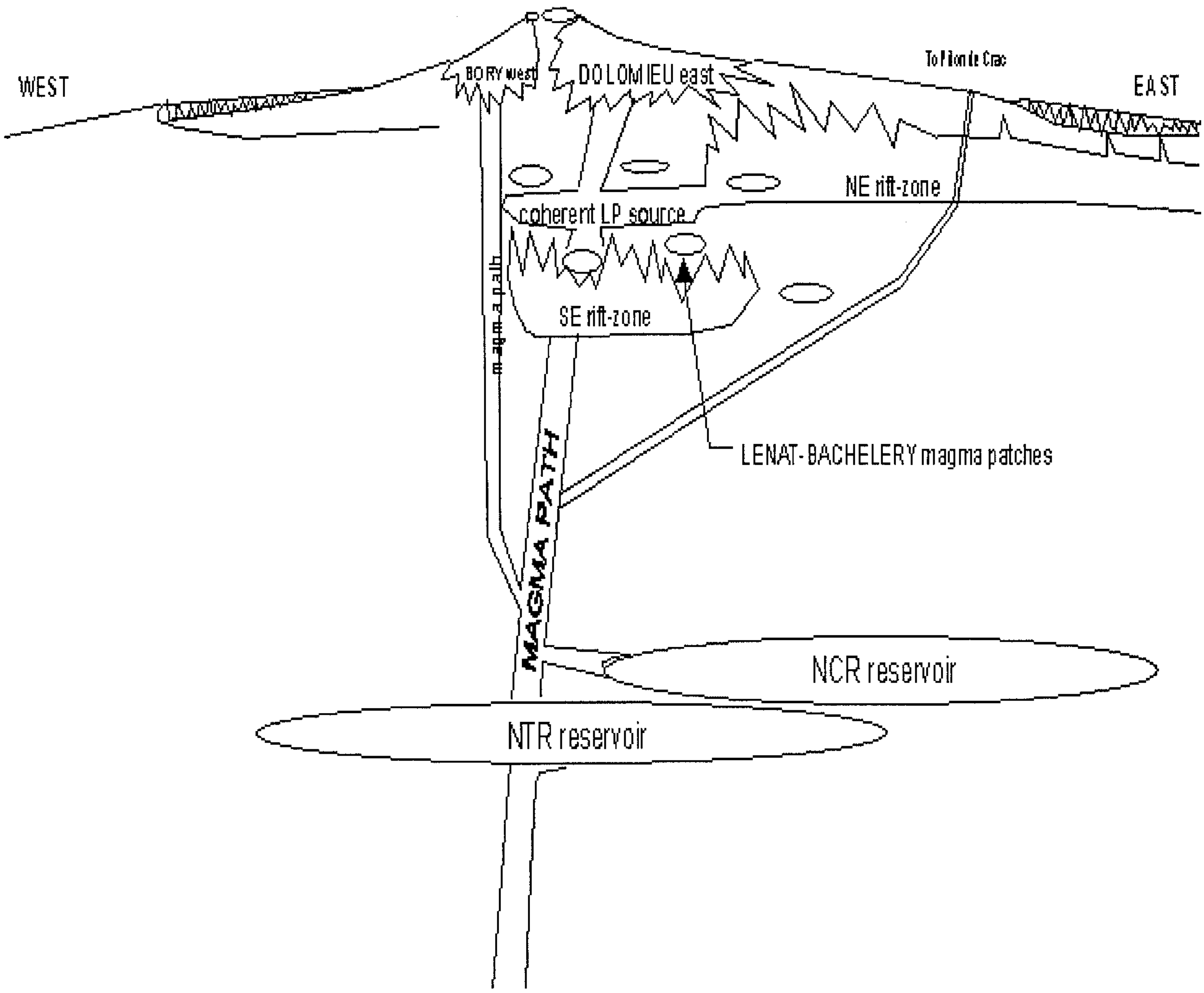

Figure 2.2. A model of magma system under Piton de la Fournaise.

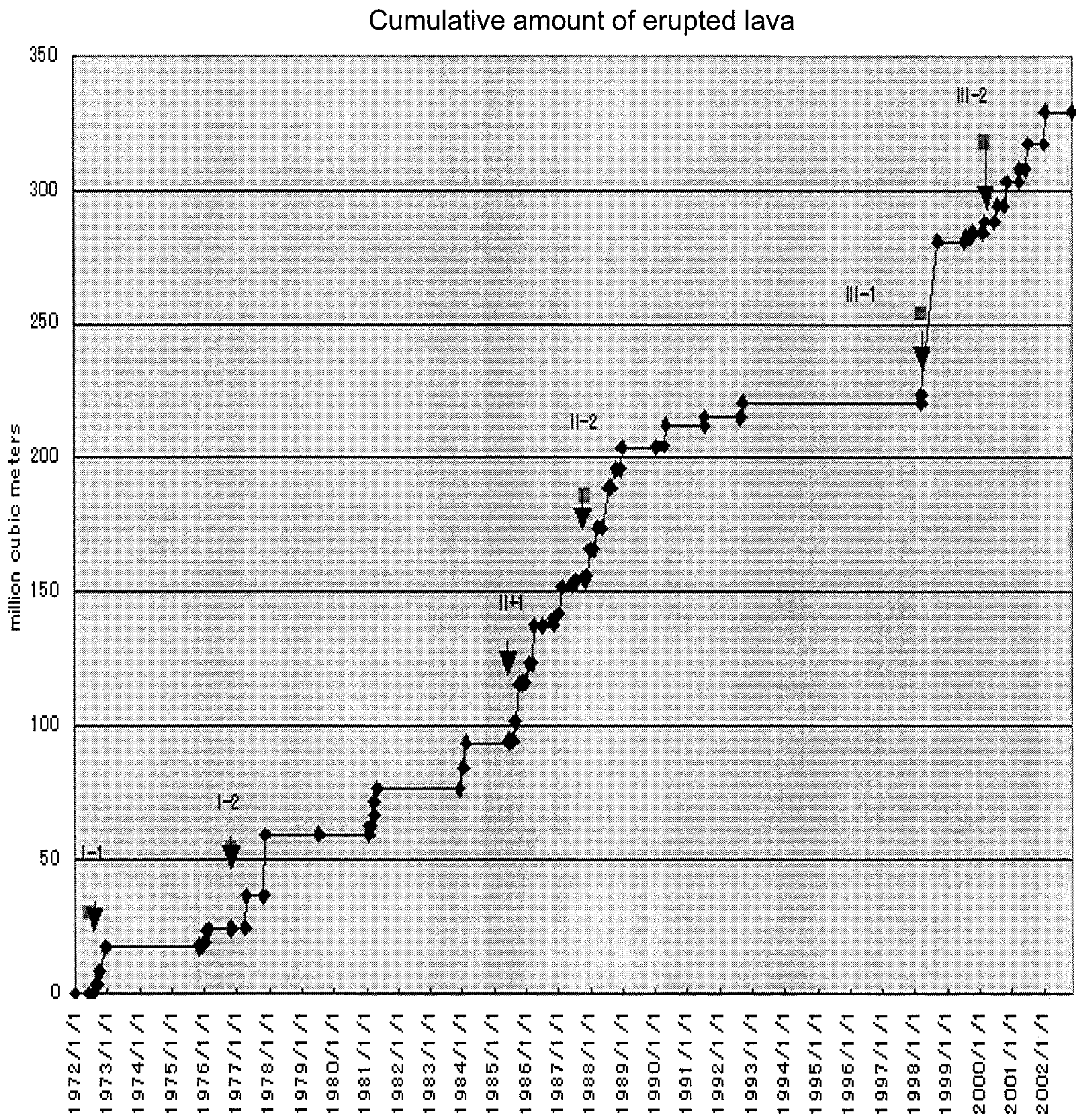

Figure 2.3. Cumulative lava output from Piton de la Fournaise in M cubic meters. The Starting dates of eruption in the Bory west area identified as the arrival of new magma are also indicated.

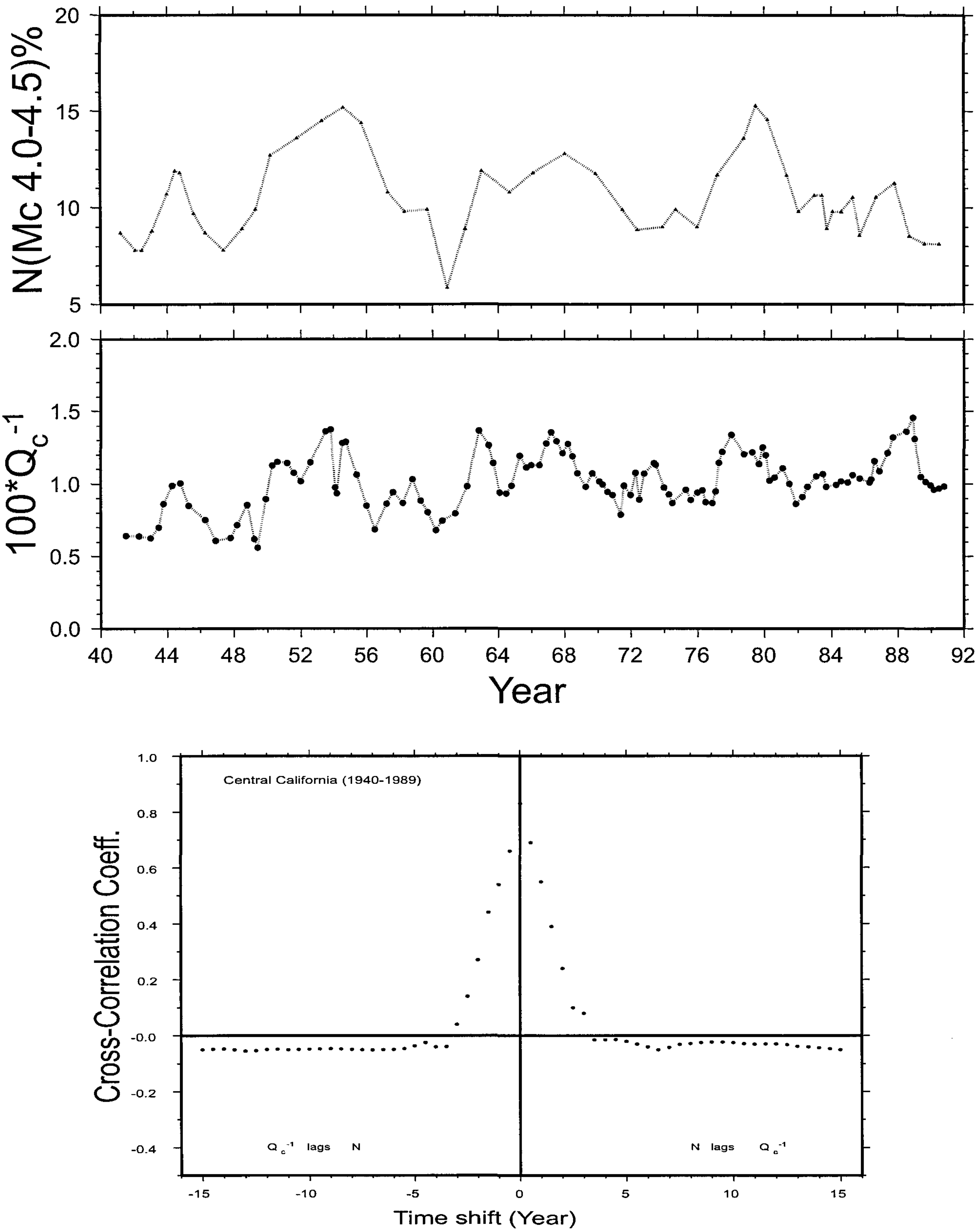

Figure 2.4. Comparison of coda Q^{-1} and the relative frequency N(Mc) of earthquakes with a certain characteristic magnitude Mc observed for central California for the 50-year period since 1941(top); and the cross-correlation between coda Q^{-1} and N(Mc=4.0-4.5)% (bottom). [Reproduced from Jin and Aki, 1993].

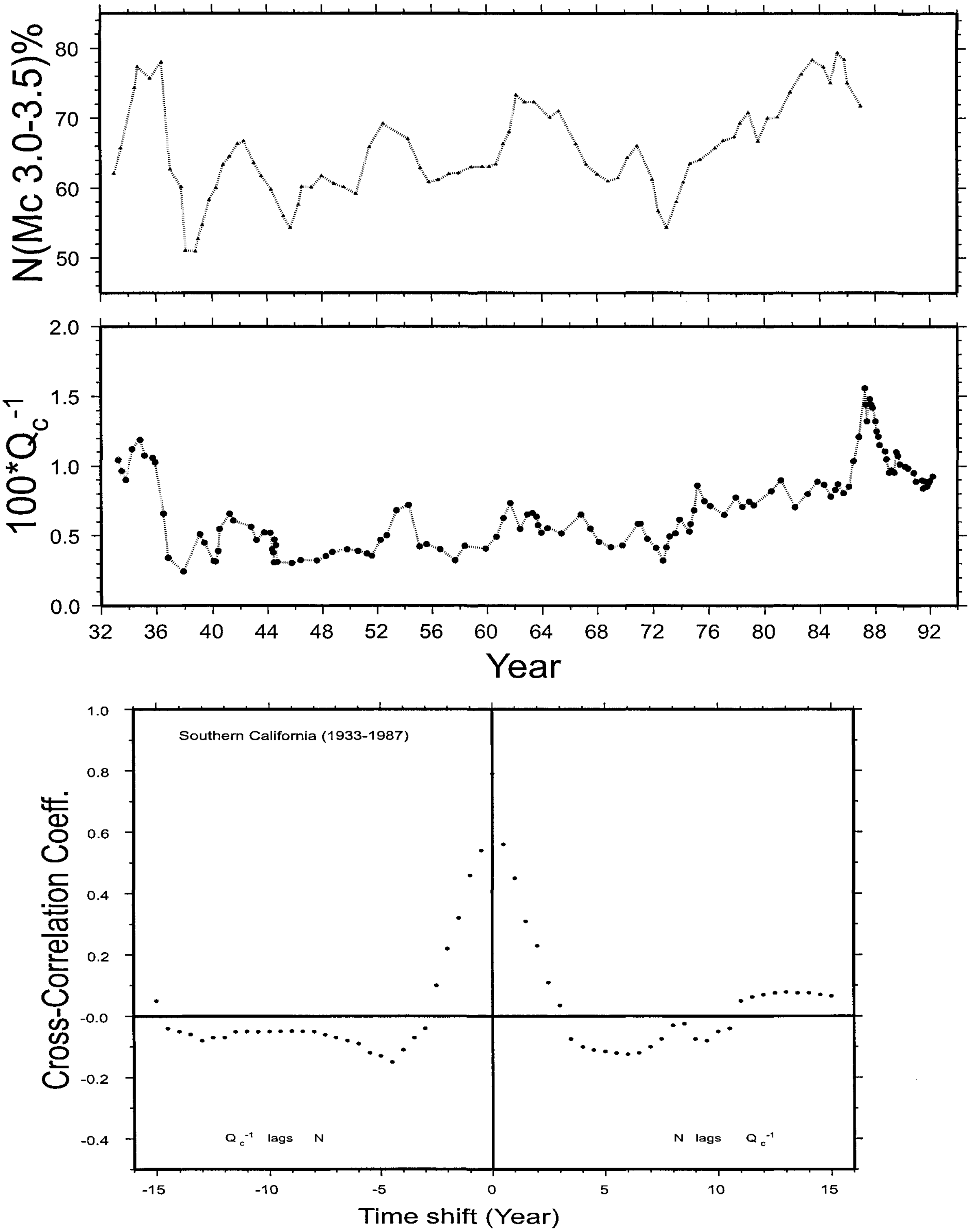

Figure 2.5. The same comparison as Figure 2.4 for Southern California for 55-year period since 1933(top); cross-correlation function between coda Q^{-1} and N(Mc=3.0-3.5)% from 1933-1987 (bottom). [Reproduced from Jin and Aki,1989].

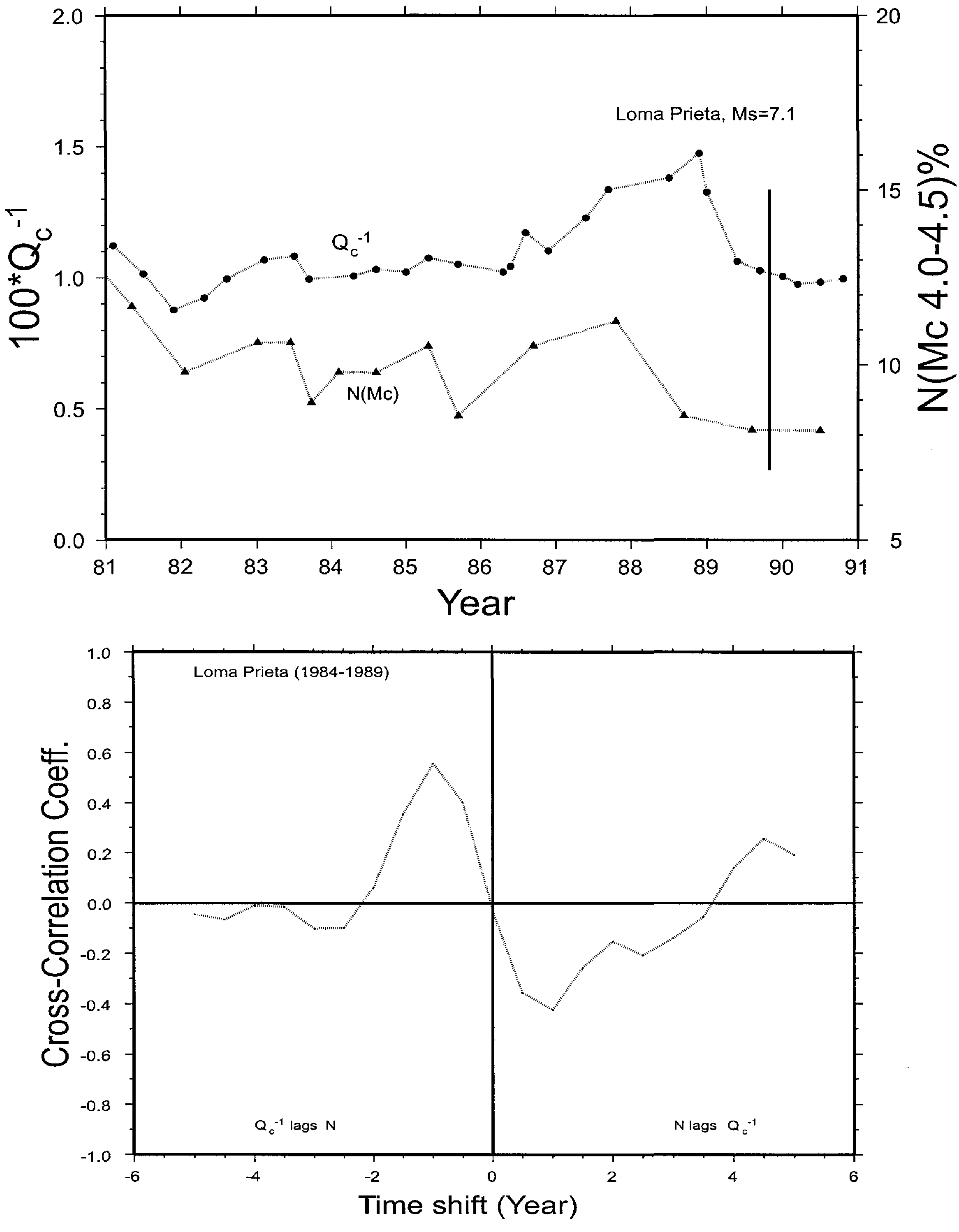

Figure 2.6. A close look at the relation between coda Q^{-1} and N(Mc) for several years before the Loma Prieta earthquake of 1989. The cross-correlation function between them is shown for the period 1984-1989, 5-year period preceding the Loma Prieta earthuake. The simultaneous correlation shown in Figure 2.4 is disturbed by a 1-year delay of the coda Q^{-1} relative to N(Mc). [Reproduced from Jin et al., 2003].

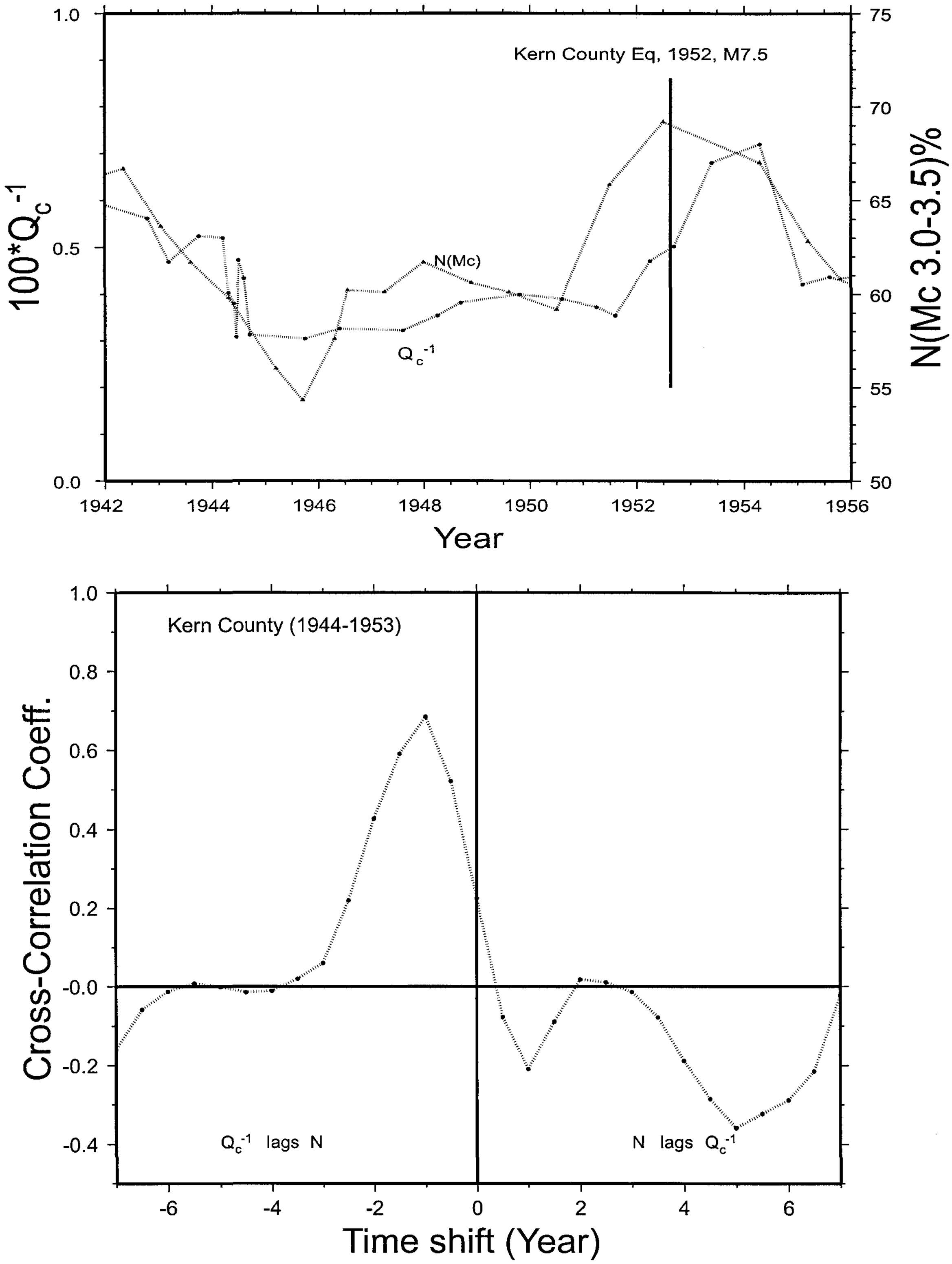

Figure 2.7. A close look at the relation between coda Q^{-1} and N(Mc) for several years before the Kern County earthquake of 1952. The cross-correlation function between them is shown for the period 1944-1953, 10-year period including the Kern County earthquake.The simultaneous correlation shown in Figure 2.5 is disturbed by a 1-year delay of the coda Q^{-1} relative to N(Mc). [Reproduced from Jin et al.,2003].

Part 3. An Introduction to Seismology for Earthquake Prediction

Preface

Most of conclusions presented in Part 1 and 2 were obtained by a solely seismological approach in mid-2002 and described in a preprint of a book with the same title as this part of my lecture note. I submitted the preprint to a publisher, who decided not to publish it because my idea was too controversial. I accepted the decision and tried to firm up my idea by getting additional supporting data as well as some help from Tectonophysics, Geodynamics and Non-linear Dynamics as described in Part 1 and 2.

In this part of lecture note, I shall use the unpublished book in order to show how my idea was developed. This is a long story, but hopefully convinces the reader that my idea is rooted in the knowledge accumulated by seismological studies about earthquakes, volcanoes and the earth's lithosphere in the past several decades. I must apologize in advance that I could not avoid an autobiographical tone in telling this story.

When I was a student at the Geophysical Institute of the Tokyo University, I decided that my lifetime goal should be predicting the occurrence of an earthquake. My first paper in English published in 1954 was about a quantitative prediction of the earthquake occurrence based on the earthquake catalog data using the method described by Norbert Wiener (1948). I soon realized that the information contained in the catalog was not sufficient for my purpose. Thus I proposed the monitoring of micro-earthquakes with their enormous information contents as an important element of the earthquake prediction research, in meetings of the working group organized by Kiyoo Wadati, Chuji Tsuboi and Takahiro Hagiwara for preparing the so-called blue print of Japanese program for earthquake prediction in the beginning of the 1960's.

The funding of Japanese national program for earthquake prediction was started in 1965. It was a giant step forward in the science of natural disaster, but I felt that I was not ready to produce anything meaningful for the society in the foreseeable future. That was one reason why I moved in 1966 from the Earthquake Research Institute of the Tokyo University to join Frank Press who had become the chairman of Department of Earth and Planetary Sciences at MIT and who enlightened me earlier during my visit to the Seismological Laboratory at Caltech with possibilities toward the deterministic quantitative approach in Earthquake Seismology.

The deterministic approach in Earthquake Seismology started in the 1960's from the long period end of the seismic spectrum, where the small-scale heterogeneities in both earth structures and earthquake processes can be safely neglected and simple mathematical models of the Earth and earthquakes can be used for interpreting observed seismograms. The first important product from this approach is the seismic moment, namely, the earthquake size measured at the longest period end of spectrum generated by an earthquake. It was expressed simply in terms of the fault area and the slip averaged over the area and offered a common physical basis for various disciplines working on the earthquake problem, and has been used as a unifying concept for integrating observations on earthquakes from geology, geodesy, historic seismology and instrumental seismology.

With the progress in the knowledge of the earth structures, it has become possible to study greater details about the earthquake rupture processes. It is now a common practice after a major earthquake to compare observed seismograms with those computed using mathematical models of earthquake rupture up to a frequency as high as 1 Hz or even higher. Such comparisons have revealed various parameters of an earthquake fault playing important roles in the rupture process. These are, in the increasing order of scale length, the fault gouge zone, the rupture nucleation zone, asperities and barriers, fault segmentation, the total length ruptured in an earthquake and the plate boundary zone to which the fault belongs. For a major earthquake, their length ranges from the order of 100 meters to that of 1000 km.

Figure 3.0.1 summarizes various conventional and unconventional methods currently used to study the seismogenic structures and earthquake processes covering the above broad range of scale lengths. So far, the seismological method of studying the fault zone at the finest scale relies on the guided waves trapped in the fault zone. Seismic scattering and attenuation give information on small-scale structure, and the power spectra of ground motion give information on the high frequency radiation from the rupture process. Their study requires stochastic modeling of both earth structures and earthquake processes, but enabled us to go beyond the upper limit of the frequency range imposed by the deterministic approach.

The community of scientists working on earthquakes in a region has the responsibility to inform the population in the region about their hazards. Such information should come not only from the above seismological studies on earth structures and earthquake processes in the region, but also from the studies such as in historic seismology, earthquake geology and geodesy. The current practice in integrating such information and transmitting it to the public is essentially based on the empirical statistical relation like the magnitude-frequency formula originated by Gutenberg and Richter (1954), although, at some earthquake centers, the seismic moment has been adopted as a common parameter to be estimated from available seismological, geologic and geodetic data in an attempt to inject an element of physics in the integration process.

The medical sciences in the mid-19th century were apparently struggling for a similar integration of various branches (such as the branch dealing with a normal organ of a human body, that with a defective organ, and practice for curing a disease), which had been developing more or less independently. There has been a proposal to put statistical empirical laws at the foundation of the integration base, but was opposed by Claude Bernard, a scientific giant of his time and a pioneer of the experimental medicine, who asserted that statistical relations are useful for an ensemble of human beings, but not for diagnosing and curing the disease of an individual. Instead, we should put the universally accepted laws of physics and chemistry at the foundation of the integration basis, by constructing models for each study case to which we can apply these laws. I see parallel to this assertion in problems of earthquake and volcano hazards.

The most effective information transfer to the public regarding the earthquake and volcano hazards is the prediction of the times of their occurrences. The goal of earthquake prediction has emerged in the community of earthquake scientists in the 1960's and some national programs, in particular in Japan, have survived the formative decades of hopes and despairs to accumulate monitoring data with increasing quantity and improving quality. In the past, the emphasis in these programs has been placed primarily on searching for empirical relations from the accumulated data to be used as the basis for prediction.

Empirical relations obtained from past monitoring data may not be useful for predicting the occurrence of an earthquake or the eruption of a volcano, because their physical system likely changes with time. On the other hand, a model effectively constrained by monitored data will have a predictive potential. The importance of both modeling and monitoring for putting the earthquake prediction research on a solid foundation of Physical Science has been recognized in Japan, and a group of new leaders along this direction is emerging, as evidenced by presentations in various recent national and international meetings. For example, A physical model specifically constructed for earthquake prediction was discussed intensively in the International Symposium titled "Flow and Slip Processes in and beneath the Inland Seismogenic Regions" at Sendai, Japan in November, 2001. In the concluding session of the symposium, the specific model proposed by the organizers was approved as a viable physical model to which the laws of physics and chemistry may be applicable, but it was also recognized that we need many such models to prepare for a variety of future courses of earthquake processes. Another relevant meeting was a special session titled "Integration of Earth Science Information for Earthquake Prediction" subtitled "Relating Seismogenic Structures and Earthquake Processes" convened during the annual meeting of the Seismological Society of Japan at Kagoshima in October, 2001. where possibilities of physical models for earthquake prediction were discussed by the present author using Figure 3.0.1.

I recognized, while attending these meetings, a major bottleneck in the current effort in modeling for earthquake prediction from the perspective of Figure 3.0.1. Most modelers attempt to solve a big problem at the scale of plate tectonics using parameters estimated at an extremely small scale of laboratory experiment. On the other hand, the existing monitoring data reflect the phenomena occurring in the intermediate scales between the two extremes. That appears to be the major obstacle preventing productive interplay between monitoring and modeling in earthquake prediction research.

In this part of my lecture note, I propose a physical model for earthquake prediction that can be effectively constrained by the currently monitored seismological data. I had various materials needed for constructing this model before coming to La Reunion in 1995 for an on-site study of an active volcano, but did not know how to interpret them for the purpose of earthquake prediction until I gained a perspective of various precursory phenomena associated with the eruption history of the Piton de la Fournaise.

Chapter 1 of this part describes a historical development of earthquake studies after the wide acceptance of their fault origin with emphasis on the building blocks of my new model for earthquake prediction. Chapter 2 will be focused on the key elements of the seismogenic structure needed for understanding the model. Chapter 3 will describe lessons learned from the Piton de la Fournaise that enabled me to resolve inconsistencies among various precursory observations on earthquakes. Chapter 4 presents a new concrete procedure for an intermediate-term (a few years) prediction that seems to work well with all cases in which necessary data are available. The examples presented are mostly from the inland seismic regions within the major plate boundary zones. We shall discuss possibilities of extending the model to earthquakes in subduction zones and in regions far away from major plate boundaries.

Some of my ideas described in Chapter 1 have been subjects of controversy among seismologists, such as the interpretation of the maximum cut-off frequency in the strong motion spectrum, the departure from the self-similarity in both the scaling law of seismic spectrum and the frequency-magnitude relation, and the reality of temporal changes in the so called "coda Q". Most criticisms of my interpretation, however, have been that it was not unique and alternative interpretations were possible. I found that showing the uniqueness of my interpretation was difficult and time-consuming in many cases and would never allow me a good grasp of the whole earthquake phenomena that is needed for earthquake prediction. This is the main reason why I needed a book to describe my view rather than journal papers addressing particular cases.

Chapter 1. Introduction

1.1. Fault-specific study of individual earthquakes

In the early 1960's, seismologists experienced a new understanding of an earthquake when they finally resolved the controversy called "single-couple or double couple". Most seismologists in North America, who believed in Reid's elastic-rebound theory, thought that the origin of an earthquake was a slip on a geologic fault, therefore, it must be equivalent to a single couple with the force in the direction of slip and the arm directed normal to the fault plane. On the other hand, Honda(1962) from Japan showed convincing evidence that the observed radiation pattern for S waves required an additional couple orthogonal to the initial one with the moment of identical magnitude but opposite sign. This model was called a "double couple", and Honda attributed its physical basis to a catastrophic process in which a volume of the Earth originally under shear stress suddenly collapses due to the vanishing of rigidity. This controversy was resolved by the consistent support of the double couple source from observations and by the mathematical proof that the point force system equivalent to a fault slip must be a double couple. The proof was given for a special case of homogeneous isotropic body by Maruyama (1963) and for a general case by Burridge and Knopoff (1964).

The consensus finally reached among seismologists about the fault origin of an earthquake had a profound and far reaching impact. It gave seismologists a mathematical procedure, which relates the observed seismograms with the dynamic process at the earthquake source and the structure of the Earth. This procedure, together with the advent of digital computers and the availability of data from the Worldwide Standardized Seismograph Station Network (WWSSN) and later global networks of digital seismographs, led to the new era of quantitative seismology.

There is only one physical parameter in the point source equivalent to an earthquake fault, namely, the magnitude of moment of the component of the double couple. This parameter is now called seismic moment, and is equal to the product of rigidity, fault area and the fault slip averaged over the fault plane. This parameter is proportional to the seismic spectrum of the earthquake motion at its lowest end of frequency and can be measured by the use of waves with wavelength much longer than the fault length. I measured its amount for the Niigata earthquake of 1964 using the WWSSN data of long-period Love waves (called G waves), for which the propagation characteristics had been well known by that time from the works of Ewing, Press and their colleagues. The value of moment obtained (Aki, 1966) agreed well with the slip and fault area determined from near-field data such as the geodetic data on deformation, the tsunami source area and the aftershock area, supporting the fault model of earthquake quantitatively.

The importance of seismic moment in Earthquake Seismology was quickly and widely recognized by the seismological community. Kanamori (1971) demonstrated that it was a crucial parameter for understanding the behavior of great earthquakes throughout the world. The cumulative seismic moment of earthquakes that occurred in a fault zone was translated to the cumulative slip across the zone by Brune (1968), and that occurred in a seismic area to the cumulative strain in the area by Kostrov (1974).

It is interesting to note that the beginning of plate tectonics came after the consensus among seismologists was reached about the fault origin of earthquakes. In other words, seismologists were ready to accept earthquakes as a slip along plate boundaries, when Isacks et al. (1968) made a comprehensive survey of seismological evidence supporting plate tectonics. Thus, applying the method of determining the fault-plane solution developed by Byerly (1938) to records of mid-ocean ridge earthquakes from the WWSSN, Sykes (1967) was able to turn many seismologists into accepting the plate-tectonic theory by proving Wilson's (1965) idea of transform fault. The success of plate tectonics in turn conclusively supported the fault origin of earthquakes. Slip vectors obtained from fault-plane solutions of numerous earthquakes became one of the basic data set for determining the present-day plate motion by Minster and Jordan (1978). The discovery of the high Q region along the Wadati-Benioff zone by Oliver and Isacks (1967) and Utsu (1967) was another major contribution to plate tectonics from Earthquake Seismology.

Another important event predated the beginning of plate tectonics is the so called "gap theory" proposed by Fedotov (1965), who found that the aftershock areas of great earthquakes along the circum Pacific seismic belt do not overlap in space and show some regularity in their occurrence in time. His idea was further developed by Sykes and his colleagues (e.g., Nishenko and McCann and several other papers in Simpson and Richards, 1981) and Mogi (1982) for the specific purpose of the long-term earthquake prediction. The gap theory is consistent with the steady rigid motion of the tectonic plate, and offered a basis for estimating recurrence times of great earthquakes from historic and geologic data. It was a surprise to me because the theory implies a departure of the earthquake process from the Poissonian with the probability of occurrence increasing with the time from the last event while the earthquake catalog data invariably indicated the departure in the opposite sense, namely, the probability decreasing with the time from the last event (e.g., Aki, 1956).

The success of plate tectonics in explaining the cause of earthquakes encouraged me to propose a new direction for seismic hazard estimation by predicting the strong ground motion using the fault model and its parameters estimated from plate tectonics (Aki, 1970). At that time, I was already convinced that the fault model could be used to simulate the short-period strong ground motion from my work on the Parkfield, California, earthquake of June, 1966 which occurred a few months before my move from the University of Tokyo to the MIT in Boston. This earthquake offered unprecedented wealth of the near-field data, including detailed mapping of surface breaks, accurate determination of aftershock hypocenters and a record of ground motion obtained at an accelerograph station located only 80 meters from the fault trace. Housner and Trifunac (1967) studied the observed accelerogram and showed that the horizontal displacement perpendicular to the fault trace is a simple impulsive motion directed to the northeast. The simplicity of the observed record and the extremely short distance between the fault and the observation point encouraged me to apply the formula of Maruyama (1963) obtained for a fault model embedded in a homogeneous media to this case. I found that the observed simple displacement is precisely what should be expected for a right-lateral strike slip propagated from north to south along the surface trace of the fault (Aki, 1968). The same conclusion was obtained by Haskell (1969) who had been modeling the earthquake rupture with a spatially-uniform ramp-function slip propagating at a constant speed from the nucleation point to the end of the fault. This model characterized by only 5 parameters; fault length, fault width, final slip, rupture speed and rise time, is called the Haskell model as described in detail in Chapter 10 of Aki and Richards (2002) and was used successfully for the interpretation of numerous seismograms recorded at short epicentral distances in the first decade of the quantitative seismology. It was simple, but captured the essence of kinematics of fault rupture.

The slip function assumed in the Haskell model, however, is physically unrealizable. For example, the stress on the slipping part of the fault plane neither vanishes nor drops to the dynamic friction, but becomes infinite near the crack tip inside the crack. In order to remedy the situation, it was necessary to study the dynamics of the rupture propagation over a fault with a specified fracture criterion under a given initial stress. Chapter 11 of Aki and Richards (2002) was devoted to early results from these studies including Kostrov (1966), Burridge and Halliday (1971), Ida (1972), Madariaga (1976), and Das and Aki (1977).

These works on the dynamics of the rupture led to an intriguing dilemma that the kinematic model with the uniform slip function can explain observation much better than the physically realizable dynamic model of crack propagation. Let us take the study of the San Fernando, California earthquake of 1971 as an example. First Bouchon and Aki (1977) showed that the Haskell model of uniform slip function can explain the observed accelerogram at Pacoima dam reasonably well. Then Bouchon (1978) found that the dynamic model of crack propagation with uniform stress drop generates too smooth ground motion compared to the observed. To resolve this dilemma, he considered a slip function corresponding to a chain of small cracks on which slip motion is successively triggered. Such a chain of cracks generates seismic motion rich in high frequency contents like the uniform slip-function model as schematically demonstrated by snap-shots of slip-function for the above three models shown in ***Figure 1.1.1***. The model corresponding to a chain of cracks is named "barrier model", because the physical realizability of such a model was verified by numerical experiments of Das and Aki (1977) on rupture propagation over the fault plane with distributed barriers.

The slip-function as shown in Figure 3.1.1.1 can be studied using relatively long-period seismic waves recorded at long distances as was done by Kanamori and Stewart (1978). The latter authors, however, attributed the variation of slip along the fault to "asperities" rather than "barriers". These two concepts are illustrated in ***Figure 3.1.1.2***. which compares the state of a fault plane before and after an earthquake. The shaded region is stressed, and the blank region is slipped. The completely shaded fault plane at the upper left corner corresponds to a uniformly stressed fault, while the completely blank one at the lower right corner represents a smoothly slipped fault without any unbroken patches. On the upper right of this figure we show the fault plane containing unbroken patches remaining after an earthquake. These strong patches are barriers and may cause aftershocks by local stress concentration. On the lower left we show the fault plane containing strong patches under stress surrounded by a region where stress has already been released by pre-slip and foreshocks. These strong patches are asperities. The breaking of asperities results in an earthquake and makes the fault plane free of stress. This model represents the mainshock as a stress-smoothing process in contrast to the barrier model in which the mainshock is considered as a stress-roughening process. Since both aftershocks and foreshocks exist, we expect that some of the strong patches on a fault plane behave as barriers and others as asperities.

Thus these new concepts opened possibilities for relating the temporal behavior of seismicity before and after an earthquake with the rupture process during the mainshock

The progress in Paleoseismology (Wallace,1981; Sieh,1981), encouraged seismologists to assimilate geologic data into earthquake modeling. For example, Aki (1984) interpreted the idea of "characteristic earthquake" proposed by Schwartz and Coppersmith (1984) in terms of the stability of asperities and barriers on faults and presented the new approach for strong ground motion prediction based on geologic data on fault segmentation. An important parameter emerging from these works is the length scale corresponding to the size of asperities and the interval of consecutive barriers distributed over the fault plane. When there is no need for distinguishing between barriers and asperities, the asperity size or barrier interval is called "sub-event size".

The specific barrier model of Papageorgiou and Aki (1983) consists of circular cracks of equal diameter **d** filling up a rectangular fault with length L and width **W**. In this model the stress drop in the circular crack is called "local stress drop", and is distinguished from the "global stress drop" determined from the average slip and the total fault area. As the rupture front sweeps the fault plane with a speed **v**, a stress drop takes place in each crack starting from its center and spreading with a fixed speed. The slip stops suddenly and is frozen over the whole crack as soon as the crack diameter reaches its final size **d**. The maximum final slip **Dm** on the crack is determined from the given stress drop (local stress drop) inside the crack. The seismic far-field waveform radiated from such a circular crack was given by Sato and Hirasawa (1973) in a compact form and has essential features of the waveform calculated for more realistic models studied by Madariaga (1976). After the passage of the rupture front, the region between neighboring cracks is left unbroken constituting a barrier. The ruptures of individual cracks are assumed to take place statistically independently. Thus this model has 5 parameters; **L, W, v, d** and **Dm**, and allows to calculate the power spectra of far-field acceleration.

Papageorgiou and Aki (1983) chose California earthquakes for which all the above parameters except the sub-event size **d** are already known from geologic and seismological studies other than the strong motion. From a comparison of observed and calculated spectra, they determined the value of **d**, and found a systematic increase of **d** with increasing magnitude. This systematic magnitude dependence was later confirmed to be a global rule by a similar stochastic modeling of strong motion records by Beresnev and Atkinson (2002) as well as deterministic modeling of the low frequency part of the records by various authors. ***Figure 3.1.1.3*** reproduced from Beresnev and Atkinson (2002) compares the sub-event size estimated by them with those by Aki (1992) who corrected the original estimates of barrier intervals by Papageorgiou and Aki (1983) for the average recording site effect and the deterministically estimated asperity sizes summarized by Somerville et al. (1999). The sub-event sizes estimated by the three independent methods agree well except that the data points from Papageorgiou and Aki lie on a steeper line than others. We shall come back to this point in the discussion of the seismogenic structure of the San Andreas fault zone in Section 2.1.

In comparing the observed acceleration spectra with those predicted for the specific barrier model, Papageorgiou and Aki (1983) had to introduce a sixth parameter to their model defining a cutoff frequency, called "f_{max}" by Hanks (1982), beyond which the acceleration spectrum decays sharply with increasing frequency. In the model of Beresinev and Atkinson (2002), f_{max} is not a free parameter but was fixed by the so-called "**κ**- effect" introduced by Anderson and Hough (1984) with a constant **κ** independent of earthquakes for a given region.

The observed f_{max} was interpreted by Papageorgiou and Aki (1983) in terms of the

slip weakening model of fracture mechanics introduced to seismology by Ida (1973). The slip-weakening model has been explained in the context of elastic shear crack pertinent to earthquake rupture by Freund (1979), Rice (1980) and Aki and Richards (1980, 2002). It may be characterized by the average cohesive stress σ_c and the critical slip-weakening displacement **D** as illustrated in ***Figure 3.1.1.4***. The upper part of Figure 3.1.1.4 shows the distribution of shear stress and slip as a function of distance along a fault plane in the direction of rupture propagation. The stress at the infinity is σ_0, and it drops to the dynamic frictional stress σ_f inside the crack. The stress rises to σ_u ahead of the crack tip where non-zero slip is occurring over the cohesive zone of length d, and the stress in the cohesive zone drops to σ_f when the slip reaches the critical slip-weakening distance **D**. The lower part of Figure 3.1.1.4 shows the constitutive relation between the slip and stress for the cohesive zone. The area of the shaded region gives the apparent Griffith energy **g**; the energy needed to create a unit area of the ruptured fault plane. As explained in Chapter 11 of Aki and Richards (1980), **g** can be expressed in terms of σ_c and **d**, or σ_c and D. For a given σ_c, **d** is proportional to **D**.
As can be seen from the sketch of the slip function in Figure 3.1.1.4, the cohesive zone acts as a low pass or high cut filter with the time constant d/v where v is the rupture velocity, which was considered to be about the reciprocal of the observed f_{max} by Papageorgiou and Aki (1983). The constitutive law governing the stress and displacement across slipping fault is fundamental for characterizing the seismogenic structure. Our interpretation of f_{max} in terms of the coehsive zone size allowed inferring the law for actual faults from the observed seismogram, and the result will be used in Section 2.1 as a building block for defining the ***brittle-ductile transition complex***, a key concept of the idea to be developed in this book. There have been considerable progress made for determining the constitutive law deterministically from seismograms obtained during the earthquake (e.g., Ide and Takeo, 1997), but most approaches are limited to the frequency range lower than 1 Hz offering a too coarse resolution to observed effects of complex geometry other than major fault segmentation as discussed by Madariaga and Olsen (2000).
The constitutive law of rock failure has been studied by laboratory experiments for a long time and there have been several attempts to extrapolating the laboratory results to field observations on earthquakes. Recent works by Ohnaka and his colleagues (e.g., Ohnaka et al., 1997) considered the heterogeneities of the fault zone explicitly and is most relevant to us. They recognized that the slip-dependence rather than the rate- and state- dependence formulated by Dieterich (1979) and Ruina (1983) is more fundamental and uniformly applies to both the friction on a pre-existing fault and the fracture in an intact rock, and developed scaling relations among the parameters of constitutive law from laboratory experiments. They found that these relations may be extrapolated to cover the results obtained by Papagiorgiou and Aki (1983) from the observed strong motion spectra as well as those obtained by Ellsworth and Beroza (1995) from seismic data relevant to the nucleation phase.
So far we mentioned about inferring the elements of the seismogenic structure such as the asperities, barriers and the cohesive zone from the seismograms recorded during an individual earthquake. They can be studied from other seismological investigations. For example, some asperities and barriers have been identified as velocity anomalies in the subsurface image obtained by seismic tomography. The seismic tomography invented by Aki et al. (1977) was a natural consequence of the development of seismic arrays for the purpose of detecting

distant underground explosions and the inverse theory of Backus and Gilbert (1968) who prepared seismologists for data analysis using an earth model with a large number of parameters. It was not introduced from the medical technology as the name might imply. The use of local earthquake data (Aki and Lee, 1976) was particularly unique to Seismology, which required the separation of source locations before determining the tomographic image of the Earth (Pavlis and Booker, 1980). The tomographic images obtained from the existing monitoring network are in general of poor resolution for defining the fault zone heterogeneity, although encouraging results begin to appear with the improvement in the network quality and increasing amount of data (e.g., Zhao et al. 2001,). Another tomographic approach for identifying asperities is mapping the sources of seismic scattering. For example, Nishigami (2000) found strong scatterers along the fault zones of Central California, which appear to correlate with the fault segmentation.
At present the study of the fault-zone trapped mode offers much higher resolution than these tomographic studies. The most effective method for determining the fault width is the use of the guided waves trapped in the fault zone, as demonstrated by Li et al. (1994) for the 1992 Landers earthquake, who also showed that the fault depth as well as the segmentation can be studied using the trapped mode. If the cohesive zone is more or less equi-dimensional, we may infer its size from the fault zone width.
Let us now move to the study of earthquakes occurring in a region as a whole. We shall first give a broader view of such studies with special reference to earthquake prediction and then seek for links that may connect the regional study with the fault-specific study of individual earthquakes reviewed in the present section.

1.2. Regional study of earthquakes

In 1984, I moved from MIT to the University of Southern California and experienced an upheaval of seismicity in Southern California, starting with the Whitier-Narrows earthquake of 1987, going through the Landers and Big Bear Lake sequence of earthquakes in 1992, and culminating with the Northridge earthquake of 1994, the most costly earthquake in the history of the U.S.
"If I were a brilliant scientist, I would be working on earthquake prediction". This is a statement from a Los Angeles radio talk show I heard just after the Northridge earthquake. Five weeks later, at a monthly meeting of the Southern California Earthquake Center (SCEC) where more than two hundred scientists and engineers gathered to exchange notes on the earthquake, a visiting French geologist who works on earthquake faults in China envied me for working now in Southern California, comparing it to North China 20 years earlier, when the high seismicity and research activities led to the successful prediction of the Heicheng earthquake of 1975 with magnitude 7.3. A difficult question still haunting us (Aki, 1989) is whether the Haicheng prediction was founded on the physical reality of precursory phenomena or on the wishful thinking of observers subjected to the political pressure which encouraged precursor reporting. It is, however, true that a successful life-saving prediction like the Haicheng prediction can only be carried out by the well coordinated effort of decision makers and physical scientists.
Earthquake prediction research in the U.S. has become stagnant after the early optimism regarding precursory phenomena was dissipated by negative observations. By the time of the Northridge earthquake, however, we saw a revival of interest in the prediction research at several fronts in a more subdued manner but rooted on a more solid scientific ground.
First, sufficient data began to accumulate for testing the validity of certain prediction methods and hypotheses underlying them. For example, the seismic gap theory mentioned in Section 1.1 was tested by Kagan and Jackson (1991).

Likewise, the method of intermediate-term prediction developed by Keilis-Borok and his colleagues (e.g. Keilis-Borok et al., 1988) in the former Soviet Union using the earthquake catalog data is being tested by researchers in the U.S. (e.g. Healy et al. (1992), and Minster and Williams (1993)). Furthermore, the IASPEI (International Association for Seismology and Physics of Earth's Interior) sub-commission on Earthquake Prediction evaluated claims of earthquake precursors (Wyss, 1991). It is essential for a healthy development of earthquake prediction research to formulate the prediction method testable by others.

Another trend is the increasing use of probabilities in communicating earthquake information to the public. Instead of predicting the time, place and magnitude of a future earthquake, public-policy documents began to estimate an earthquake probability in a given window of time, space and magnitude. Examples are the reports of Working Group on California Earthquake Probabilities (WGCEP, 1988, 1990) based on the recurrence data of "characteristic earthquake" on major fault segments in California. Along a similar line of approach, SCEC (for which I served as the founding Science Director) characterized earthquake sources in Southern California by integrating the geologic data on faults, catalog data on historic earthquakes and GPS (Global Positioning System) data on crustal strain (WGCEP, 1995). Through this work we found that the method of probabilistic seismic hazard analysis (Cornell, 1968) was useful not only as a means for integrated transmission of multidisciplinary earth science data to the user community, but also for promoting interactions among the different disciplines and identifying critical issues that can be resolved only by a multidisciplinary cooperative work.

Probability is a relatively new concept in human history. The origin of the theory of probability goes back to as late as the 17th century, when B. Pascal and P. de Fermat exchanged letters on dice throwing (Encyclopedic Dictionary of Mathematics, 1980). The concept appears to be useful in dealing with difficult problems in human society. In recent years, several earthquake predictions made officially by the U.S. Geological Survey were in terms of probabilities. For example, the 1988 and 1990 working group mentioned above evaluated the probability of fault rupture in the following 30 years, and the so called Parkfield prediction project issued the short-term alert on the basis of the 72-hour probability.

In addition to the above new trends, namely, the hypothesis testing and the use of probabilities, there was a more fundamentally important new trend to simulate the complex space-time-magnitude behavior of earthquake occurrence by physical modeling. A central issue in these attempts is whether the complex behavior of seismicity is caused by the non-linear dynamics inherent to physics of earthquake rupture or by the interaction of rupture with geologic heterogeneities of fault zone structure.

The gap theory, which hypothesizes that an earthquake is more probable over the segment of a given plate boundary where last rupture occurred earlier, may be a natural consequence of the steady plate motion, and its rejection by Kagan and Jackson (1993) on the basis of clustering found in the earthquake catalog was probably a news for most people. For me, the gap theory proposed by Fedotov (1965) was a surprise, because almost all the statistical studies on earthquake catalogs indicated that earthquakes cluster in time and space at all levels of magnitudes as mentioned in Section 1.1.

The gap theory modified by Kelleher et al. (1973), McCann et al. (1979), Sykes and Nishenko (1984), and Nishenko (1991) assumes that a "characteristic earthquake" can be identified for a given segment of plate boundary. This concept of characteristic earthquake was generalized by Schwartz and Coppersmith (1984) to all faults including those in the mid-plate. A great merit of this concept has been to offer a link among multidisciplinary observations. For example, seismological observations on asperities and barriers that control the rupture process of the characteristic earthquake have become related to geological and geophysical observations on fault segmentation and fault zone structures as mentioned in Section 1.1.

Once a characteristic earthquake is identified for a given fault segment, it becomes an individual like a human being to which life expectancy at a certain age can be evaluated and used for determining the premium for life insurance. The long-term prediction based on the gap theory gives the conditional probability of occurrence of characteristic earthquake given the time from the last one (corresponding to the age of a human being). The probability is small immediately after the earthquake as opposed to the clustering tendency of earthquake occurrences revealed from statistical analysis of catalog data. These two opposite trends are not logically conflicting because one is for the whole catalog of earthquakes, and the other is for its subset, namely, characteristic earthquakes. Both are also physically reasonable because the fault slip in an earthquake generates stress concentration wherever the slip is non-uniform, while stress is generally relieved in the scale of the whole fault plane.

The idea of characteristic earthquake in the strict sense may be simplistic reflecting to some degree the wishful thinking of hazard analysts. For example, according to Segall and Du (1993), the rupture of the Parkfield segment (considered to be an ideal case of characteristic earthquake) apparently stopped at the right step in fault trace in the Cholame Valley in 1934, but went through it in 1966, although the starting point and total seismic moment were indistinguishable between the two events. There is a need for modifying the characteristic earthquake concept to allow for some variations like this, but it would be a mistake to abandon the concept entirely and give up identifying a geophysically meaningful subset of earthquakes in the earthquake catalog. For example, detailed analysis of nearly identical seismograms of eighteen small earthquakes occurred on the Calaveras fault over a period of 11 years by Vidale et al. (1994) yielded a systematic dependence of duration on the time since the previous earthquake, offering in-situ data relevant to the fault zone healing.

As mentioned earlier, several public policy documents have been published on earthquake predictions in terms of probabilities. For example, the Working Group on California Earthquake Probabilities (WGCEP, 1988) estimated the long-term (up to 30 year) probability for each segment of the San Andreas and San Jacinto fault. The probabilities were revised for segments in the San Francisco Bay area after the 1989 Loma Prieta earthquake by WGCEP (1990). The short-term (up to 72 hours) probabilities are also estimated for the Parkfield and other characteristic earthquakes as described below.

In order to arrive at a probability estimate for public use, consensus must be reached on the method of calculating the probability as well as on the input data. This is a very difficult time-consuming process, and some scientists view this process as a waste of time and manpower. It is certainly not a scientifically creative process, but is important for the users of earthquake information such as the government officials responsible for emergency preparedness and land use, and may be essential for the survival of the community of earthquake researchers. Several years ago NSF recognized the need for returning the product of science to the society and initiated the Science and Technology Center program. SCEC is one of these centers, and the transmission of earth science information on seismic hazard in Southern California to the public is one of its major tasks.

SCEC was officially started on February 1, 1991, and the Landers earthquake (M7.3) occurred during its second year. Two weeks after the earthquake, SCEC organized a one-day workshop to discuss the implications of the event and SCEC's response. The workshop decided to produce two documents. The first document (Phase I) to address (1) recent seismicity in Southern California, (2) effects of the Landers-Big Bear sequence on nearby faults, and (3) the potential for future ground shaking in southern California. The second document (Phase II) should address the long-term seismic hazard broadly over the whole of southern California revising the 1988 Working Group report by improving the methodology and updating the data. The Phase I report was published in November 1992 (Ad-hoc Working Group on the Probabilities of Future Large Earthquakes in Southern California, 1992). Phase II report was published in the April, 1995 issue of the Bulletin of the Seismological Society of America (WGCEP, 1995).

The Phase II report went beyond the report of WGCEP (1988) in several aspects. It addresses the whole southern California by dividing it into 65 source zones. The earthquake potential for each zone is estimated not only from the paleoseismological data on ruptures on fault segments, but also the historic earthquake data spatially smoothed by the method of Kagan and Jackson (1994), as well as the GPS data by translating the observed strain rate into earthquake frequency by the procedure of Ward (1994). In addition to characteristic earthquakes, the Phase II report consider the contribution of distributed earthquakes. The model for the characteristic earthquake allowed for ruptures over neighboring multiple segments (Wesnousky, 1986) and is called "Cascade". The consensus geologic parameters used to characterize each source zone was developed by a group of geologists under the leadership of David. Schwartz. The resultant earthquake source model can be used to estimate probabilities of ground shaking at any point in southern California, and as an example, Phase II report shows a map of probability that any point experiences the peak ground acceleration greater than 20% of gravitational acceleration in the next 30 years. The report also documents the uncertainty in input data as well as the range of alternative models. The probabilistic estimate of seismic hazard can also be used as the cost-benefit study of mitigation efforts. The benefit is the reduction of damage or loss expected from future earthquakes, and may be estimated from probabilities of seismic hazard. An objective decision can be made by comparing the expected benefit with the mitigation cost.

Probabilities have been used also for several official short-term earthquake predictions. For example, five alert levels A, B, C. D and E were introduced for different ranges of the conditional probability of the occurrence of the target earthquake, based on foreshocks, fault creep and continuous strain monitored at Parkfield by an extensive instrumentation (Bakun and Lindh, 1985; Bakun et al., 1987). The alert level A (USGS issuing geologic hazard warning) corresponds to the 72-hour probability greater than 37%, and alert B (alerting the USGS director and California State Geologist) corresponds to the 72-hour probability in the range 11 to 37%. Alert C, D and E correspond to probabilities lower than 11%, and directed to scientists involved in the experiment.

According to a recent review of the Parkfield experiment by a working group (B. Hager, Chair) of the National Earthquake Prediction Evaluation Council (1993), the experiment has brought scientists together with state and local officials, emergency managers, and the news media, in a productive, mutually beneficial relationship. The State established the first scientifically-based emergency management protocol for a specific predicted earthquake. The first A-level alert was issued on Oct. 22, 1992. The USGS notified California Office of Emergency Service (OES) of the A-level alert triggered by the M=4.7 earthquake at Middle Mountain. Eight minutes later, OES broadcast the alert to State agencies and local governments over the California Warning System. Kern County was the first county to activate its Emergency Operation Center, 47 minutes after the OES alert. OES completed its alert of local government and response officials in less than one hour following the earthquake. It was a complete success in transmitting earth science information to the public. The working group concluded that Parkfield remains the best identified location to trap an earthquake, and the experiment should be continued both for its geophysical and its public response benefits.

Turning to more scientific aspects of regional earthquake studies, we saw in late 1980's the beginning of involvement of physicists in modeling earthquake phenomena since Bak and Tang (1989) proposed that the Gutenberg-Richter frequency magnitude relation may be attributed to a process described as "self-organized criticality". It reminded me of theGoishi model of Otsuka (1972) and the branching model of Vere-Jones (1976). The Goishi (stone of the game of go; a Japanese game played with stones on a board marked into 361 squares) model describes a probabilistic growth of an earthquake fault in the manner similar to the percolation theory. Saito et al. (1973) and Maruyama (1978) demonstrated analytically that the frequency-size distribution becomes a power law similar to the Gutenberg-Richter relation at a critical transition probability. I was reluctant (Aki, 1981) to accept these models because elastodynamics of rupture propagation along a fault with velocity comparable to shear waves are essential to earthquake source but missing in these models.

More recent works on seismicity simulation by a group of physicists, however, include the elastodynamic effect based on the block-spring model of Burridge and Knopoff (1967). Most of these works (e.g. Carlson and Langer, 1989, Langer, 1992) are published in Physical Review, while a clear concise description of the model is given by Pepke et al. (1994), who used it to develop effective prediction algorithms. The model includes the velocity weakening friction law and generates complex seismicity from the self-organization of repeated ruptures.

Rice (1993) has raised a serious concern regarding whether the self-organizing explanation can give rise to complexity on a spatially uniform fault. His analysis is based on three-dimensional vertical strike-slip fault with a rate- and state-dependent friction law (Dieterich, 1979; Ruina, 1983). The law includes a characteristic slip distance L for evolution of surface state and slip weakening. He solves the governing equations of elasticity and frictional slip by discretizing with the cell size h. He found an important result that the simulated slip shows spatio-temporal complexity when h is greater than a critical size h* called "nucleation size" which scales with L. When h is less than h*, the complexity disappears in favor of simple periodically repeated large earthquakes like the characteristic earthquake discussed earlier.

His concern about the self-organizing explanation of complexity using the Burridge-Knopoff model is that L and h* are zero in the velocity weakening friction law adopted in these models, thus having no well-defined continuum limit as h diminishes. He also points out significance of failure of these models (restricted to the nearest neighbor interaction) to scale the stress concentration at the edge of a slipping zone with the size of that zone, as required by elasticity theory. This effect makes a dynamic fracture unstoppable once it grows larger on a spatially uniform fault, and appears to lead to the idea that complexity of seismicity comes from fault heterogeneities of multiple scales.

The formulation of Rice (1993) does not include the inertia term, and include elastodynamic effects only approximately through radiation damping or allowance for dynamic overshoot. Thus, the possibility exists that the proper elastodynamics solutions of uniform fault models with a well defined continuum limit would lead to complex seismicity, as discussed by Madariaga and Cochard (1992) and Cochard and Madariaga (1994). Shaw (1994) also responds to the criticism of Rice

(1993) by introducing a viscous damping term into the equation for the Burridge-Knopoff model to make the continuum limit well defined, and demonstrated that complex seismicity can be generated for a uniform fault even when the discretization is made within the continuum limit. A recent article by Shaw and Rice (2000) reveals that the question of complex seismicity or characteristic cyclic earthquake occurrence for a uniform fault is still open awaiting for a more complete treatment of dimensionality, friction law and dynamics of the problem.

Now I am ready to focus on seismological observations from regional studies of earthquakes directly relevant to our physical model for earthquake prediction. I shall present the evidence supporting the existence of unique heterogeneities in the seismogenic structure whether they were originated from the non-linear dynamics of repeated earthquake ruptures or the inherent geologic structure of a fault zone. If there is any structural heterogeneity controlling the earthquake process in a region, it should show up as a departure from the self-similarity among earthquakes of different sizes. There are two independent data sets showing such a departure, namely, the frequency-magnitude relation and the scaling law of the seismic spectra.

If the Gutenberg-Richter formula, log N = a – b M, applies to the frequency magnitude relation of earthquakes in a given region without any upper bound in magnitude M, there will be no earthquake cycle and no hope for a deterministic earthquake prediction. The gap theory developed for a plate boundary and the idea of the characteristic earthquake specific to a geologic fault justified the introduction of the upper bound, namely the maximum magnitude for a given seismic region, which is an important parameter characterizing the regional model of earthquakes such as the one constructed by the SCEC described earlier (WGCEP, 1995). The laws of physics and chemistry governing the maximum-magnitude earthquake necessarily involve the cohesive zone or the transition zone between the elastic region surrounding the fault zone and the freely slipping fault plane. Then there should be the minimum earthquake that can occur on such a fault, because the size of the cohesive zone must be smaller than the final fault length by definition, and there must be a departure of the frequency-magnitude relation from the Gutenberg-Richter formula for earthquakes associated with a particular fault zone at the magnitude corresponding to the minimum earthquake. Such a departure was found by Aki (1987) from the records obtained at a borehole seismograph station located within the fault zone of the Newport-Inglewood fault that caused the Long Beach, California earthquake of 1933. For this study, I developed a formula to estimate the moment magnitude using the amplitude of coda waves and carefully examining the detection limits for different magnitudes, found that the observed frequency-magnitude relation deviates from the Gutenberg-Richter formula as shown in ***Figure 3.1.2.1***. The minimum magnitude there was about 3, which corresponds to a size of a few hundred meters comparable to the cohesive zone size estimated from the f_{max} discussed in Section 1.1. A similar departure of the frequency-magnitude relation from the Gutenberg-Richter formula at M=3.5 was reported by Dysert et al. (1988) for the Matsushiro region, Japan, the area of a major earthquake swarm in the mid-1960's. In most cases of regional study, however, such a departure has not been detected, possibly because of the mixing of faults of different cohesive zone size, and in some cases because of the systematic error in assigning the magnitude. It is customary to estimte magnitude for small local earthquakes using the total duration since Tsumura (1967) used it for local earthquakes in the Wakayama, Japan, area. The physical basis of the duration magnitude is the existence of the common decay curve in the coda of local earthquakes as described in Section 1.3. On this basis, the duration must be measured from the origin time of earthquake and not from

the arrival time of P waves as commonly done. The wrong choice of duration may introduce a serious bias in magnitude determination as discussed by Aki (1987) and may affect the observed frequency-magnitude relation at small magnitude.
Let us now move to the departure of the scaling law of seismic spectrum from the self-similar relation. The ω-squared scaling law of seismic spectra introduced by Aki (1967) is based on the fault model characterized by a single parameter, namely, the fault length. The assumption of self-similarity under the condition of constant stress drop explained the source spectral ratios between large and small earthquakes estimated by Berckhemer (1962) and resolve the inconsistencies among the different magnitude scales developed by Gutenberg and Richter. The applicability of the constant stress drop has been shown for earthquakes in a broad range of magnitude by many workers using the source model of Brune (1970).
It was then natural to extend the study of the scaling law for various seismic regions to find any systematic regional difference in stress drop. For this purpose we used the method based on the coda waves (Aki and Chouet, 1975; Chouet et al.,1978), and found very often that the corner frequency does not follow the ω-squared scaling law, but stays constant over a considerable range (2 to 3 orders of magnitude) of seismic moment, violating the self-similarity. Rautian and Khalturin (1978) have studied the same problem using the same approach independently in the former Soviet Union and discovered the same phenomena. Both studies were based on the empirically established separability of the source effects from other effects on the power spectra of coda waves as explained in Section 1.3.
The departure of the scaling law of seismic spectrum from the self-similarity may be expressed in terms of the relation between the seismic moment and fault length or the corner frequency. ***Figure 3.1.2.2*** shows an example for the Matsushiro area obtained by Dysart et al (1988), showing a constant fault length at about 500 m for the range of moment magnitude from 1.5 to 3.5. This is consistent with the departure of the frequency-magnitude relation for the same area mentioned above. A similar result can be seen for other areas of Japan as summarized by Jin et al. (2000) in ***Figure 3.1.2.3***, which shows a change of stress drop from about 100 bar to 1 bar as the moment magnitude decreases from 3.5 to 1.5, supporting the existence of a unique scale length of the order of a few hundred meters controlling the earthquake process in these areas.
The departure from the self-similarity was also found by Gusev (1983) on a global scale using empirical relations among various magnitude scales and spectral amplitude data. The family of spectral curves constructed by Aki (1967) had to be modified in such a way that a bump appears for frequencies from 0.1 to 10 Hz as shown in ***Figure 3.1.2.4*** for acceleration spectra. This is consistent with the clearly recognized difference in stress drop of more than a factor of 100 between Aki's model applicable to the frequencies lower than about 0.1 Hz and the ω-squared model developed by Hanks (1979), McGuire and Hanks (1980), and Hanks and McGuire (1981) for higher frequencies. The Gusev scaling law implies that the fault length is not the only parameter controlling the earthquake phenomena and I suspected that the cause of Gusev's bump may be the heterogeneities of fault plane which was described as barriers and asperities in the study of individual earthquakes described in Section 1.1.

1.3. Unifying the fault-specific earthquake study with the regional study

We shall unify the fault-specific earthquake study described in Section 1.1 with the regional study described in Section 1.2 through the study of seismogenic structures relying heavily on the coda waves of local earthquakes. We shall first describe the frequency dependence of S wave attenuation determined by the coda normalization method for the seismically active lithosphere. We shall find that the fault zone heterogeneities revealed from the individual earthquake study as well as the departure of the scaling law and frequency-magnitude relation from the self-similarity found from the regional study are reflected in the frequency dependence of seismic attenuation.

More important for our model of earthquakes is the discovery of a strong temporal correlation between the coda Q and the frequency of occurrence of earthquakes with a certain magnitude designated as Mc characteristic to the region by Jin and Aki (1989, 1993). As shown in Chapter 4, the relation between the coda Q and the frequency of with magnitude Mc depends on the phase of the regional earthquake cycle, offering an important observable to monitor for earthquake prediction. We shall reconsider some of the estimates of Mc made by Jin and Aki (1993) and maintain that the value of Mc is nearly a universal constant, 3 to 4, slightly dependent on regions. The size of an earthquake with these values of Mc is close to the cohesive zone size obtained for individual earthquakes as well as the fault length corresponding to the characteristic corner frequency at which the scaling law of the seimic spectrum shows a departure from the self-similarity. We believe that the above closeness in scale length implies some causal relationship among them, thus unifying the individual earthquake study with the regional study for a practical purpose of earthquake prediction.

Let us first review the frequency dependence of attenuation of S waves. The lithosphere in a seismic region containing earthquake faults may scatter and absorb seismic waves propagating through it, and the frequency dependence of the seismic attenuation may reveal the nature of the heterogeneity related to the fault. The first clear indication of the strong attenuation of seismic waves in a tectonically active region was found by Molnar and Oliver (1969) from a global study of S waves propagated along the top of the mantle called Sn. They found that Sn was missing for the propagation path through tectonically active regions.

A strong contrast observed in the temporal decay of the coda of local earthquakes between active and stable regions was attributed to the difference in S wave attenuation by Aki and Chouet (1975) as described later in this section. The coda decay in California and Japan was more than ten times as rapid as those in stable areas such as the central United States and Scandinavia and it was also found that the inferred Q factor of attenuation in tectonically active regions increases nearly proportionally with frequency in the range from 1 to 10 Hz.

The frequency dependence of seismic attenuation is a difficult subject to study for the same reason that the f_{max} mentioned in Section 1.1 is a difficult one. An observed seismogram represents intricately combined results of the source radiation effect, the propagation path effect and the recording site effect, and it is not easy to separate one effect from the others particularly for high frequency records of local earthquakes. Most of the studies on the frequency dependence of seismic attenuation at frequencies higher than 1 Hz have been unsatisfactory because the spectral shapes of either the source or the site effect are more or less arbitrarily assumed, until Aki (1980) found a method isolating the propagation path effect on S waves by the use of coda waves which share the same source and path effects as S waves. The method is called " the coda normalization method" by Sato and Fehler (1998) who summarized the results obtained from various seismic regions of the world, confirming the above proportionality for Q in the frequency range from 1 to 10 Hz. This proportionality, however, cannot be extended to frequencies lower than 1 Hz, because we know that the Q is very high at the period around 20 seconds obtained from the global measurements on surface waves (See Mitchel and Romanovicz (1998) for the latest review on Q of the Earth).

For this reason Aki (1980) proposed that there must be a peak in the coda Q^{-1} at a frequency a little below 1 Hz. A clear evidence for such a peak at around 0.8 Hz was demonstrated by Kinoshita (1994) for shear waves in the crust of the southern Kanto area, Japan. The Q^{-1} of Lg waves in Columbia determined by Ojeda and Ottemoller (2002) also show a definite peak at around 1 Hz. But, in general, the well known high seismic background noise in the frequency range from 0.1 to 1 Hz, where also the current boundary between the deterministic and stochastic approaches in seismogram analysis lies, has made difficult a definitive conclusion about the peak frequency.

Recent studies of Q for frequencies higher than 10 Hz using borehole data are bringing some new insight to the frequecy dependence of Q. Both Adams and Abercrombie (1998) and Yoshimoto et al. (1998) found that the Q of S waves obtained from the borehole recordings of local earthquakes, respectively, in Southern California and Central Japan tends to become constant for frequencies above 10 Hz.

Combining the above three pieces of observations, namely, (1) the near proportionality of Q from 1 to 10 Hz, (2) the high Q below 0.1 Hz and (3) the nearly constant Q above 10 Hz, we see a broad peak in the Q^{-1} of S waves in the lithosphere of seismically active regions at frequencies between 0.1 and 10 Hz as shown in ***Figure 3.1.3.1***. The corresponding range of wave length of S waves would be from a few tens of km to a few hundreds of meters. This range agrees with the range of the heterogeneity scale length of the fault plane discussed in earlier sections. The upper bound corresponds to the size of sub-events for the largest earthquakes and the lower bound to the size of the cohesive zone discussed in Section 1.1 and the size of earthquakes marking the departure from the self-similarity discussed in Section 1.2.

The coda wave of local earthquakes has been attractive to me for many reasons. The common decay curve independent of the locations of the earthquake or the receiver within a seismic region supported empirically a simple separation of the effects of the source, propagation path and the recording site effect on their spectrum. This simplicity is symbolized by the coda Q which is a single number for a given region, for a fixed window of lapse time (time measured from the earthquake origin time) and for a given frequency. This regional parameter can be easily obtained from the seismograms of small earthquakes recorded by the usual seismic monitoring networks. The coda Q, therefore, is an average property of the lithosphere in a given region obtained by the averaging made not by man but by nature. We may say that the coda Q is a product of purely passive approach to the study of Earth's structure.

When I moved to MIT from Tokyo University in 1966, I was hoping to use the excellent engineering capabilities of MIT to develop artificial seismic sources for measuring the seismic velocity accurately and continuously over a large region for the purpose of earthquake prediction. After several attempts along this line as described in DeFazio et al. (1973) and Reasenberg band Aki (1974) including a field experiment in the San Jacinto fault zone in California (Aki et al.,1970), I realized that our active experiment for measuring a geophysically meaningful quantity such as the regional tectonic stress requires too much time and effort to contribute significantly to the goal of earthquake prediction in my life time. I also felt that the need for placing the seismic source on or close to the Earth's surface may pose a severe limitation on the depth range of penetration for monitoring. The discovery of the common decay in the coda of aftershocks of the Parkfield earthquake of 1966 encouraged me to switch from the active approach to the passive approach for earthquake prediction.

As will become apparent in this section, most of our knowledge about the small-scale heterogeneity of the lithosphere come from the study of coda waves. If we did not discover coda waves, the enormous difficulty in deciphering numerous factors affecting primary waves prevented us from even recognizing the existence of small-scale heterogeneity related to the seismogenic structure. There was, however, a drawback to this passive approach. It was difficult to convince students to work on the coda Q, because it gives an average property of a large region when the rest of the seismological community is making progress toward imaging finer details of Earth's structure. It was much easier to talk students into working on the seismic tomography of a seismic region and the rupture process of a single earthquake. The study of coda Q nevertheless attracted seismologists in various parts of the world, and the progress made in the past two decades was thoroughly described in a book by Sato and Fehler (1998) mentioned earlier. Here we shall summarize the properties of coda waves needed for the purpose of this book.
When an earthquake or an underground explosion occurs in the earth, seismic waves are propagated away from the source. After P waves, S waves and various surface waves are gone, the area around the seismic source is still vibrating. The amplitude of vibration is nearly uniform in space, except for the local site effect, which tends to amplify the motion at soft soil sites as compared to hard rock sites. This residual vibration is called seismic coda waves, and decays very slowly with time. The rate of decay is independent of the locations of seismic source and recording station, as long as they are in a given region.
The closest phenomenon to this coda wave is the residual sound in a room, first studied by W. C. Sabine in 1922. If you shoot a gun in a room, the sound energy remains for a long time due to incoherent multiple reflections. This residual sound has a very stable, robust nature similar to seismic coda waves, independent of the locations where you shoot the gun or where you record the sound in the room. The residual sound remains in the room because of multiple reflections at rigid wall, ceiling and floor of the room. Since we cannot hypothesize any room-like structure in the earth, we attribute seismic coda waves to back-scattering from numerous heterogeneities in the Earth.
The seismic coda waves from a local earthquake are best described by the time-dependent power spectrum $P(\omega | t)$, where ω is the angular frequency and t is the time measured from the origin time of the earthquake. $P(\omega | t)$ can be measured from the squared output of a band-pass filter centered at a frequencyω, or from the squared Fourier amplitude obtained from a time window centered at t. The most important property of $P(\omega | t)$ is the simple separability of the effects of seismic source, propagation path and recording site response, expressed by the following equation. The coda power spectrum $P_{ij}(\omega | t)$ observed at the i-th station due to the j-th earthquake can be written as

$$P_{ij}(\omega|t) = S_j(\omega)\, R_i(\omega)\, C(\omega | t) \qquad (1.3.1)$$

for t greater than about $2t_\beta$, where t_β is the travel time of S waves from the jth earthquake to the ith station. Equation (1.3.1) means that $P_{ij}(\omega | t)$ can be written as a product of a term which depends only on the earthquake source, a term which depends only on the recording site and a term common to all the earthquakes and recording sites in a given region.
The above property of coda waves expressed by Equation (1.3.1) was first recognized by Aki (1969). The condition that Equation (1.3.1) holds for t greater than about $2t\beta$ was found by the extensive study of coda waves in central Asia by Rautian and Khalturin (1978). Numerous investigators demonstrated the validity of Equation (1.3.1) for earthquakes around the world, as summarized in a review article by Herraiz and Espinosa (1987). In general, Equation (1.3.1) holds more

accurately for a greater lapse time t and for higher frequencies (e.g. Su et al., 1991). Equation 3.1.1 has been used for a variety of practical applications, including the mapping of frequency-dependent site amplification factor (e.g. Su et al., 1992), discrimination of quarry blasts from earthquakes (Su et al., 1991), single station method for determining frequency-dependent attenuation coefficients (Aki, 1980), and normalizing the regional seismic network data to a common source and recording site condition (Mayeda et al., 1992). The source factor $S_j(\omega)$ was used to study the scaling law of seismic spectrum for earthquakes in a given region.

There are, however, some exceptions to the rule given in Equation (1.3.1), when there exist slow waves trapped in a low velocity structure near a recording station. An important example is the coda waves of local earthquakes in La Reunion which show the dependence of $C(\omega|t)$ on the distance between the earthquake source and the summit of the volcano, Piton de la Fournaise, the subject of Chapter 3. The slow wave in this case is associated with the magma body, and we use the observed $P(\omega|t)$ corrected for the recording site factor (estimated using distant earthquakes from the summit area) for mapping the magma location.

The coda Q was introduced by Aki and Chouet (1975) to characterize $C(\omega|t)$ in the framework of single-scattering theory under the following assumptions.

(1) Both primary and scattered waves are S waves.

(2) Multiple scatterings are neglected.

(3) Scatterers are distributed randomly with a uniform density.

(4) Background elastic medium is uniform and unbounded.

The assumption (1) has been supported by various observations, such as the common site amplification (Tsujiura, 1978) and the common attenuation (Aki, 1980) between S waves and coda waves. It is also supported theoretically because the S to P conversion scattering due to a localized heterogeneity is an order of magnitude smaller than the P to S scattering as shown by Aki (1992) using the reciprocal theorem. Zeng (1993) has shown that the above difference in conversion scattering between P to S and S to P leads to the dominance of S waves in the coda.

Since the observed $P(\omega|t)$ is independent of the distance between the source and receiver, we can simplify the problem further by co-locating the source and receiver. Then, we find

$$P(\omega|t) = \beta/2\, g(\pi)\, |\phi_0(\omega|\beta t/2)|^2 \qquad (1.3.2)$$

where β is the shear wave velocity, $g(\theta)$ is the directional scattering coefficient, and $\phi_0(\omega|r)$ is the Fourier transform of the primary waves at a distance r from the source. $g(\theta)$ is defined as 4π times the fractional loss of energy by scattering per unit travel distance of primary waves and per unit solid angle at the radiation direction θ measured from the direction of primary wave propagation.

Aki and Chouet (1975) adopted the following form for $|\phi_0(\omega|r)|$.

$$|\phi_0(\omega|r)| = |S(\omega)|\, r^{-1} \exp(-\omega r/(2\beta Q_c)), \qquad (1.3.3)$$

where $|S(\omega)|$ is the source spectrum, r^{-1} represents the geometrical spreading, and Q_c is introduced to express the attenuation. Combining (1.3.2) and (1.3.3), and including the attenuation of scattered waves, we have

$$P(\omega|t) = \frac{2g(\pi)\,|S(\omega)|^2}{\beta t^2} \exp(-\omega t/Q_c) \qquad (1.3.4)$$

Q_c is called "coda Q", and Q_c^{-1} is called "coda Q inverse ".

The measurement of coda Q according to Equation (1.3.4) is very simple. Coda Q^{-1} is the slope of straight line fitting the measured $\ln(t^2 P(\omega | t))$ vs. ωt. Since there is a weak but sometimes significant dependence of the slope on the time window for which the fit is made, it has become a necessary routine to specify the time window for each measured coda Q^{-1}.

The physical meaning of coda Q^{-1} has been debated for a long time. Within the context of the single scattering theory, coda Q^{-1} appears to represent an effective attenuation including both absorption and scattering loss. This idea prevailed for some time after Aki (1980) found a close agreement between coda Q^{-1} and Q^{-1} of S waves measured in the Kanto region, Japan. On the other hand, numerical experiments by Frankel and Clayton (1986), laboratory experiments by Matsunami (1991), and theoretical studies including multiple scattering effects (e.g. Shang and Gao, 1988) concluded that the coda Q^{-1} measured from the time window later than the mean free time (mean free path divided by wave velocity) should correspond only to the intrinsic absorption, and should not include the effect of scattering loss. The debates concerning this issue were summarized by Aki (1991).

In order to resolve the above issue, attempts have been made to separately determine the scattering loss and the intrinsic loss in regions where coda Q^{-1} has been measured. For this purpose, it is necessary to include multiple scattering in the theoretical model, either by the radiative energy transfer approach (Wu, 1985) or by the inclusion of several multiple-path contributions to the single-scattering model (Gao et al., 1983). Zeng et al. (1991) demonstrated that all these approaches can be derived as approximate solutions of the following integral equation for the seismic energy density $E(\underline{x}, t)$ per unit volume at a location $\underline{x}$ and at time t due to an impulsive point source applied at χ_o at t=0.

$$E(\underline{x},t) = E_0\left(t - \frac{|x-x_o|}{\beta}\right)\frac{e^{-\eta |x-x_0|}}{4\pi |x-x_o|^2} + \int_V \eta_s E\left(\xi, t - \frac{|\xi - x|}{\beta}\right)\frac{e^{-\eta |\xi-x|}}{4\pi|\xi - x|^2} dV(\xi) \quad (1.3.5)$$

where symbols are defined as follows:

$E(\underline{x},t)$: seismic energy per unit volume at $\underline{x}$ and t

β: velocity of wave propagation

η: total attenuation coefficient: $\eta=\eta_s+\eta_i$ (energy decays with distance $|\underline{x}|$ as $\exp[-\eta|\underline{x}|]$)

η_i: intrinsic absorption coefficient

η_s: scattering attenuation coefficient

$Q_s^{-1} = \frac{\eta_s \beta}{\omega}$: scattering Q^{-1}

$Q_i^{-1} = \frac{\eta_i \beta}{\omega}$: absorption Q^{-1}

$B = \frac{\eta_s}{\eta}$: seismic albedo

$L_e = \frac{1}{\eta}$: extinction distance

$L = \dfrac{1}{\eta_s}$: mean free path

$\beta E_0(t)$: rate of energy radiated from a point source at x_0 at t.

The assumptions underlying Equation (1.3.5) are less restrictive and more explicit than the assumptions used in deriving Equations (1.3.2) and (1.3.4). The background medium is still uniform and unbounded, but scattering coefficients and absorption coefficients are explicitly specified, and all the multiple scatterings are included, although scattering is assumed to be isotropic. Equation (1.3.5) gives the seismic energy density as a function of distance and time in contrast to Equations (1.3.2) and (1.3.4) which depend on time only. By comparing the predicted energy density in space and time with the observed, we can uniquely determine the scattering loss and the intrinsic absorption, separately.

An effective method using the Monte-Carlo solution of Equation (1.3.5) was developed by Hoshiba et al (1991) and Fehler et al. (1992) who calculated seismic energy integrated over several consecutive time-windows (e.g. 0 to 15, 15 to 30, 30 to 45 sec from the S arrival time) and plotted them against distance from the source. The method has been applied to the various parts of Japan (Hoshiba, 1993), Hawaii, Long Valley, California, central California (Mayeda et al., 1992), and southern California (Jin et al., 1994). ***Figure 3.1.3.2*** shows typical examples of comparison between the predicted energy density and the observed. The observed energy density data come from many small earthquakes recorded at a single station, and are normalized to a common source by the coda normalization method mentioned earlier. In spite of the simplified assumptions made in the prediction, the comparison with the observed is quite good, giving us some confidence in the estimated scattering and absorption coefficients. ***Figure 3.1.3.3*** reproduced from Jin et al.(1994) compares seismic albedo B_0, total attenuation coefficient η(= 1/Le) in km^{-1}, scattering coefficient η_s and intrinsic absorption η_i among Long Valley, central California, southern California, Hawaii, and Japan. Except for 1.5 and 3 Hz in Hawaii, we found the following consistent result. First, η_s tend to decrease with increasing frequency. This corresponds to the decrease of Q_s^{-1} faster than f^{-1} with increasing frequency f. In terms of the random medium model, this implies that the auto-correlation function (ACF) may be more like Gaussian rather than exponential. The Gaussian type medium shows much smoother variation than the exponential type at scale-lengths below the correlation distance. Figure 3.1.3.3 also show that the intrinsic absorption η_i shows a slight increase with increasing frequency. Because of the opposite trend in frequency dependence of η_s and η_i, the intrinsic absorption dominates the scattering at higher frequencies. In order to answer the question whether the coda Q corresponds to the intrinsic absorption or the total absorption including the scattering loss, we show in ***Figure 3.1.3.4*** Q_i^{-1}, Q_s^{-1} and Q_t^{-1} as a function of coda Q^{-1} determined for the lapse time interval 20 to 45s for southern California, 30 to 60s for Long Valley, Hawaii and central California, and 20 to 60s for Japan. In general, coda Q^{-1} lies between Q_i^{-1} and Q_t^{-1}. It is closer to Q_i^{-1} for Japan, and closer to Q_t^{-1} for all other regions. According to Gao and Aki (1994), who made numerical study of the departure of coda Q^{-1} from Q_i^{-1} for models of a scattering layer with a finite thickness, the above results may indicate that the thickness of scattering layer is greater than the mean free path under Japan, but comparable or smaller than the mean free path for the other regions.

Although, for a more complete understanding of coda Q, we need further studies on models with non-uniform scattering and absorption coefficients, Figure 3.1.3.4 assures us empirically that coda Q^{-1} are in general bounded between intrinsic Q_i^{-1} and total Q_t^{-1}. With this understanding of coda Q^{-1}, we proceed to the discussion of its spatial variation, temporal variation and frequency dependence.
The coda Q shows a strong geographic variation. For example, the coda in the frequency band around 4 Hz last for 200 seconds (800 oscillations) in Norway, an old stable region. The example from Norway, an old stable region. On the other hand, the coda decays much more quickly in young active regions, such as Japan and California. For example, Singh and Herrmann (1983) found a systematic variation of coda Q at 1 Hz in the conterminous U.S.; more than 1000 in the central part decaying gradually to less than 200 in the western U.S. The spatial resolution of the map of coda Q obtained by Singh and Herrmann (1983) was rather poor, because they had to use distant earthquakes to cover regions of low seismicity. As mentioned earlier, Equation (1.3.1) holds for the lapse time t greater than about twice the travel time for S waves. For a more distant earthquake, the coda part governed by Equation (1.3.1) starts later, making the region traveled by waves composing the coda greater and consequently losing the spatial resolution.
Peng (1989) made a systematic study of the spatial resolution of coda Q mapping as a function of the lapse time window selected for measuring coda Q. He used the digital data from the Southern California Seismic Network operated by Caltech and USGS, and calculated spatial auto-correlation function of coda Q^{-1} by the following procedure. Southern California is divided into meshes of size 0.2° (longitude) by 0.2° (latitude), and the average of coda Q^{-1} is calculated for each mesh using seismograms which have the mid-point of epicenter and station in the mesh. The average value for the ith mesh is designated as X_i. Then two circles of radius r and r + 20 km are drawn with the center at the ith mesh, and the mean of coda Q^{-1} at mid-points located in the ring between the two circles is calculated and designated as y_i (r). The auto-correlation coefficientρ(r) is computed by the following formula,

$$\rho(r) = \frac{\sum_{i=1}^{M}(\chi_i - \bar{x})(y_i(r) - \bar{y}(r))}{\sqrt{\sum_{i=1}^{M}(\chi_i - \bar{x})^2}\sqrt{\sum_{i=1}^{M}(y_i(r) - \bar{y}(r))^2}}$$

where, M is the total number of meshes, $\bar{\chi}$ is the mean of X_i, and $\bar{y}(r)$ is the mean of $y_i(r)$. ρ(r) is calculated for coda Q^{-1} at four different frequencies (1.5, 3, 6 and 12 Hz) and three different lapse time windows, namely, 15-30 sec, 20 to 45 sec and 30 to 60 sec measured from the origin time. As shown in ***Figure 3.1.3.5*** through ***3.1.3.7***, the auto-correlation functions are similar among different frequencies, but depend clearly on the selected time window. The longer and later time window gives the slower decay in the auto-correlation with the distance separation. If we define the distance at which the correlation first comes close to zero as the "coherence distance", the average coherence distance is about 135 km for time window 30-60 sec, 90 km for the window 20-45 sec, and 45 km for the window 15-30 sec.
The above observation offers a strong support to the assumption that coda waves in these windows are primarily composed of S to S back-scattering waves,

because the distance traveled by S waves with a typical crustal S wave velocity of 3.5 km/s in half the lapse time 60, 45 and 30 sec are, respectively, 105, 79 and 53 km, which are close to the corresponding coherence distance, namely, 135, 90 and 45 km. In other words, the coda Q^{-1} measured from a time window represents the seismic attenuation property of the earth's crust averaged over the volume traversed by the single-back-scattering S waves.

Jin and Aki (1988) were able to construct a map of coda Q at 1 Hz for the mainland China with a high spatial resolution using earthquakes at short distances from each station as shown in ***Figure 3.1.3.8.*** The variation in coda Q at individual stations estimated for the time window from 2 $t\beta$ to 100 sec. is smooth enough to draw contours of equal coda Q. The contour map of coda Q is compared with epicenters of major earthquakes with M>7 in ***Figure 3.1.3.9.*** A strong correlation was found between the coda Q and seismicity. Seismically active regions, such as Tibet, western Yunnan and North China, corresponds to low coda Q regions, and stable regions such as Ordos plateau, middle-eastern China, and the desert in Southern Xinjiang have very high coda Q. The difference between the highest coda Q value and the lowest amounts to more than a factor of 20. It is interesting to note here that a significant spatial correlation of coda Q with seismicity within a relatively stable region was also found by Woodgold (1994) for the Charlevoix, Quebec, region, where larger earthquakes occurred in areas of lower coda Q.

In Figure 3.1.3.9, two different symbols are used to distinguish earthquakes that occurred before 1700 from those that occurred after 1700. There has been a migration of epicenters from west to east during the past 300 years in North China, and the coda Q value for the region active before 1700 is about twice as high as that for the region currently active. Jin and Aki (1988) suggested that the low coda Q region might also have migrated together with the high seismicity, citing the low Q values estimated by Chen and Nuttli (1984) from intensity maps for past major earthquakes in the region

Chouet (1979) was the first to observe a significant temporal change in coda Q over a 1-year period from the summer of 1973 at Stone Canyon, California, which could not be attributed to changes in instrument response, or in the epicenter locations, focal depths, or magnitudes of earthquakes used for the measurement. The change was associated with neither the rainfall in the area nor with the occurrence of any particular earthquake, but showed a weak negative correlation with the temporal change in a seismicity parameter called "b-value" (Aki, 1985). The b-value is defined in the Gutenberg-Richter formula $\log N = a - bM$, where N is the frequency of earthquakes with magnitude greater than M.

Numerous studies made since (see Sato (1988) for a critical review of early works on temporal changes in coda Q^{-1}) revealed that the temporal correlation between coda Q^{-1} and seismicity is not as simple as the spatial correlation described above. In a number of cases (Gusev and Lemzikow, 1984; Novelo-Casanova et al., 1985; Jin and Aki, 1986; Sato, 1986; Faulkner, 1988; Su and Aki, 1990), the coda Q^{-1} showed a peak during a period of 1-3 years before the occurrence of a major earthquake. A similar precursory pattern can also be recognized in ***Figure 3.1.3.10*** reproduced from Jin and Aki (1993) before the 1989 Loma Prieta earthquake in central California, and the Landers earthquake in southern California. They concluded, however, that the coda Q^{-1} precursor is not reliable, because the characteristic pattern preceding some earthquakes does not occur before others, and a similar pattern was not followed by a major earthquake.

This judgment of the reliability of the coda Q precursor was based on the preconception that the physical system governing the precursor phenomena should be stationary in time. In Chapter 3, we shall learn from the behavior of certain precursors of eruptions that this preconception is not valid, and in Chapter 4 we shall give a new look at earthquake precursors without it. In order to prepare for these later chapters, it is necessary to discuss various observations pertinent to the cause of the temporal change in coda Q. First, we noticed a rather surprisingly consistent observation that coda Q^{-1} tends to take a minimum value during the period of high aftershock activity (Gusev and Lemzikov, 1984, Novelo-Casanova et al., 1987, Faulkner, 1988). Furthermore, Tsukuda (1988) found in the epicentral area of the 1983 Misasa earthquake that a period of high coda Q^{-1} from 1977 to 1980 corresponds to a low rate of seismicity (quiescence). The period of the high coda Q^{-1} before the Tangshan earthquake from 1973 to 1976 observed by Jin and Aki (1986) also coincides with the period of quiescence in the epicentral area, and surprisingly, the aftershocks showed a value of coda Q^{-1} 20 % lower than that estimated from earthquakes occurring before 1973. These observations suggest that the temporal change in coda Q^{-1} may be related primarily to fractures in the ductile part of lithosphere or in the transition zone from the brittle part to the ductile part, but not to the fractures in the brittle part where the aftershocks are occurring.

The above suggestion, in fact, gives a satisfactory answer to the question raised by Sato (1988) in his review of studies on the coda Q precursor. Referring to the western Nagano earthquake of 1984 and the Tangshan earthquake of 1976 for which the temporal change in both coda Q and Q of P wave had been measured (Sato (1987), Ohtake (1987), Jin and Aki (1986) and Zhu et al. (1977)), he asked why the coda Q increased after the mainshock while the Q of P waves decreased as expected from the fractures produced by the mainshock and aftershocks. He suggested that the increase in coda Q might be due to the increase of scattering intensity in the crust by the mainshock that elongated the coda duration. This hypothesis, however, can explain neither the increase in coda Q occurring before the occurrence of the mainshock observed for several cases, nor the significant temporal variation during the period without any major earthquakes. We believe that the temporal change in the seismic attenuation in the ductile part or the transition zone between the ductile and brittle part is much stronger than in the brittle part because of the higher mobility due to higher temperature and increased involvement of fluid, thus dominating the observed temporal change in the coda Q.

Coming back to the relation between coda Q and seismicity, several convincing cases have been made for the temporal correlation between coda Q^{-1} and b-value. The result was at first puzzling because the correlation was negative in some cases (Aki, 1985, Jin and Aki, 1986, Robinson, 1987) and positive in other cases (Tsukuda, 1988, Jin and Aki, 1989). To resolve this puzzle, Jin and Aki (1989) proposed the creep model, in which creep fractures in the ductile part of the lithosphere are assumed to have a characteristic size in a given seismic region. The increased creep activity would then increase the seismic attenuation and at the same time produce stress concentration in the adjacent brittle part favoring the occurrence of earthquakes with magnitude M_c corresponding to the characteristic size of the creep fracture. Then, if M_c is in the lower end of the magnitude range from which the b-value is evaluated the b-value would show a positive correlation with coda Q^{-1}, while if M_c is in the upper end, the correlation would be negative. The creep model is consistent with the observed behaviors of

coda Q^{-1} during the periods of aftershocks mentioned above.
If the creep model is correct, the strongest correlation should be found between coda Q^{-1} and the seismicity of earthquakes with M_C, and the correlation should always be positive. Indeed, Jin and Aki (1993) found a remarkable positive correlation between coda Q^{-1} and the fraction of earthquakes in the magnitude range $M_C<M<M_C+0.5$ for both Central and Southern California ***Figure 3.1.3.11*** shows the result for Central California where the appropriate choice of M_C is 4.0. The correlation is highest (0.84) for the zero time lag and decays symmetrically with the time shift as shown in ***Figure 3.1.3.12.*** A very similar result is obtained for Southern California as shown in ***Figure 3.1.3.13*** for which the appropriate choice of M_C is 3.0. The correlation is again the highest (0.81) at the zero time lag as shown in ***Figure 3.1.3.14.***
Jin and Aki (1993) extended the idea of the creep model to other cases in which both the coda Q^{-1} and the b-value were determined by then, and inferred that Mc was 3 to 4 for most areas except for the Misasa area, western Japan, studied by Tsukuda (1988) for which Mc was found less than 2. As discussed in Chapter 4, the strong positive correlation between the coda Q^{-1} and the relative frequency of earthquakes with magnitude Mc may be disturbed before the occurrence of a major earthquake. This will not only offer a basis for a new precursor, but relax the Mc assigned for the Misasa area toward a larger value allowing it nearly a universal constant. The nearly universal value of Mc may be related to another nearly universal value of f_{max} coming from the fault-specific study of earthquakes as well as that of the characteristic corner frequency fc marking the departure from the self-similarity obtained from the regional study of earthquakes. Thus we shall have an earthquake precursor broadly and deeply rooted in the studies of individual earthquakes and regional studies made in the past several decades.

Chapter 2. Seismogenic structures and the brittle-ductile transition complex

In Chapter 1 we introduced earthquakes as displacements across geologic faults originating from the plate motion. From the perspective of physics, earthquakes are a dissipative process of a non-equilibrium system. The first physical models of the Earth developed by Pratt and Airy from geodetic and gravitational observation were rather static, consisting of the crust approximately 100 km in thickness in "isostatic" equilibrium. The material below that depth was considered as highly plastic and would not be subject to rupture, fracture or fissuring. Therefore the maximum depth of earthquakes must be about 100 km. This harmonious view of the Earth was seriously disrupted by the discovery of deep focus earthquakes at depths of several hundred km conclusively established by Wadati in 1928. It took 40 years to reestablish a new harmony by the plate tectonics, which explained both shallow and deep earthquakes as a part of a global dissipative process of a non-equilibrium system.
In Chapter 1, I followed the development of earthquake studies in the past several decades more or less chronologically. I shall focus now on the seismogenic structures in the framework of plate tectonics. We find that the data needed for our purpose are most complete for the area where the plate boundary lies on land and where enough scientific manpower is available, such as California. The subduction zone involving the sinking of the oceanic plate has been more difficult

to access by the monitoring network, but we find that the inland region of the subduction zone such as the western Honshu, Japan, offers valuable information needed for constructing our model of seismogenic structure. Limited observations pertinent to our model for the region directly involving the sinking oceanic plate and for seismic regions far away from major plate boundaries will be discussed briefly in Section 2.3.

2.1 Two selected inland seismic regions

We shall start with a region well covered by a high quality seismic network where a known change in tectonic stress has occurred recently. This is the Tamba region in the western Honshu, Japan, located immediately in the northeast of the epicentral area of the Hyogo-ken Nanbu earthquake of 1995. The well investigated distribution of fault slip for this earthquake enabled a reliable estimation of stress change in the surrounding area. A thorough and careful study of the effect of this stress change by Hiramatsu et al. (2000) on seismic data from the monitoring network offered a valuable insight to the physical meaning of the temporal changes in the monitored observables, in particular, the coda Q.

The Tamba region is characterized by numerous active faults and high seismicity as shown in ***Figure 3.2.1.1***. This figure, reproduced from Hiramatsu et al. (2000), shows epicenters of earthquakes shallower than 20 km for the period from 1987 to 1996 in the Tamba region and its surrounding area, including the aftershocks of the Hyogo-ken Nanbu earthquake of 1995. The seismicity of the Tamba region and its surrounding area until 1987 has been studied by Ito (1990) with special attention to the depth of the brittle-ductile transition zone inferred from the maximum focal depth. He relocated more than 8000 earthquakes in the magnitude range from 1.8 to 5.3 and found that the frequency of occurrence of hypocenters per unit focal depth increases with depth down to about 10 km and sharply drops beyond about 12 km as shown in ***Figure 3.2.1.2***. He draws attention to a remarkable similarity between the observed distribution and the theoretical distribution of the shear resistance (Sibson, 1982) as shown in ***Figure 3.2.1.3*** based on Byerlee's law (Byerlee, 1978) for the brittle part and the dislocation creep law for the ductile part.

Interestingly, Iio (1996) found a systematic depth dependence of focal mechanism in this region. Earthquakes with focal depths shallower than 12 km include both strike-slip and reverse-dip slip sharing the common P-axis in EW direction, but those deeper than 12 km become dominantly strike-slip. He interprets this observation as the decrease in the minimum tectonic stress (relative to the vertical) below 12 km, and calls the depth range from 12 km to the maximum focal depth of about 15 km as the semibrittle zone.

Ito (1990) made a contour map, shown in ***Figure 3.2.1.4***, of the depth of brittle-ductile transition in this region based on the observed map of epicenters of earthquakes with a fixed range of focal depth. The resultant map was found to be similar to the map of the Curie point derived from aeromagnetic surveys by Okubo et al. (1989). The comparison with the Curie point depth as well as the heat flow data gave estimate of the temperature at which the brittle-ductile transition occurs. In the Tamba region, the brittle ductile transition occurs at depths of 14-16 km corresponding to a temperature around 350 degree C.

The Hyogo-ken Nanbu earthquake (M7.2), on January 17, 1995 produced a significant change in the tectonic stress in the Tamba region. The Coulomb failure function due to the earthquake was calculated by Hashimoto (1996, 1997) who attributed the sudden increase in the seismicty in the Tamba region after the earthquake to the increase in the Coulomb failure function by about 0.04 MPa.

Hiramatsu et al (2000) also calculated the change in shear stress at the depth of 10 km, close to the depth of brittle-ductile transition zone, on the vertical plane trending N45E as shown in ***Figure 3.2.1.5***. The average increase in the shear stress over the study area was estimated to be about 0.02 MPa. The focal mechanism study by Katao et al. (1997) found, however, no change in the geometry of stress field in the Tamba region due to the Hyogo-ken Nanbu earthquake.

The sudden increase in seismicity after the Hyogo-ken Nanbu earthquake is clearly shown in the space-time plot of earthquakes for the 10 year period 1987 through 1996 in ***Figure 3.2.1.6*** reproduced also from Hiramatsu et al. (2000). The coda Q was determined for events selected after a careful check on the data quality and is plotted as a function of the event time in ***Figure 3.2.1.7*** for the two frequency bands centered at 3 and 4 Hz, at which the temporal change associated with the occurrence of the Hyogo-ken Nanbu earthquake is the most significant. The change in coda Q^{-1} is about 20% in terms of the difference in mean of the coda Q^{-1} at 3 and 4 Hz for the 2-year period before and after the Hyogo-ken Nanbu earthquake. Its statistical significance is confirmed by the Student's t test with a confidence level of 99 %.

The coda Q may change due to the change in the epicenter locations, focal depth distributions, and focal mechanisms of the earthquakes used for the analyses, and their effects were carefully examined and all rejected by Hiramatsu et al. (2000). A consistent complaint from some seismologists about the temporal change in coda Q has been that they must recognize the difference in the time domain records to believe its reality. That is impossible in most cases because the change is much smaller than the fluctuation of the individual measurements. Others have insisted that we must compare seismograms of so called doublets or repeating events before and after the occurrence of the presumed change. If we follow their advice in the study of the Tamba region, we must throw away all the records used in the analysis because there was no such doublet in the data set. In fact the doublet approach works only if there was no change in the medium property because as long as we find the difference between two seismograms we can attribute it to the difference in the seismic source used for the analysis. Thus it can prove that there were no change in a particular case, and argue to extend the conclusion to all other cases.

If we follow this line of critical view of the coda Q change, repeated active experiments using a controlled source may become imperative. Any seismic source in an active experiment, however, must be placed at or near the Earth's surface, and the seismic signals received also at or near the surface. Seismic waves from a surface source to a surface receiver may not penetrate effectively into the region inside the Earth where any physical change is taking place. Active experiments are not necessarily better than passive experiments for our purpose. For example, in her thesis work on Piton de la Fournaise, Rouseau (1999) found that seismic signals from repeated rock falls within a well known cavity near the summit of the volcano did not show any significant change in their characteristics as the volcano followed its eruptive cycle, although the cyclic change in the structure of magma system was successfully detected by passive experiments using naturally occurring seismic sources in the volcano as described in Chapter 3.

Coming back to the result of Hiramatsu et al. (2000), the change in coda Q^{-1} due to the Hyogo-ken Nanbu earthquake gives the stress-sensitivity of about 10% change per 0.01 MPa (0.1 bar). If we apply this sensitivity to the observed coda Q^{-1} for Central and Southern California shown in Figure 3.1.3.11, we find that the fluctuation over the 50-year period corresponds to the change in stress on the order of 0.1 MPa (1 bar).

The frequency dependence of the change in coda Q^{-1} found by Hiramatsu et al. (2000) may be attributed to scattering attenuation by fractures. According to Yomogida and Benites (1995), for example, the scattering of seismic waves by a fracture is most effective when the wave length is comparable to twice the characteristic length of the fracture. The wave length of S waves for which the change in coda Q^{-1} was most significant is around 1 km corresponding to the characteristic size of the fracture around 500 m, which agrees well with the characteristic magnitude Mc discussed in Section 1.3.

In fact, Hiramatsu et al. (2000) reported temporal changes in the frequency of earthquakes in different magnitude ranges and the b value as shown in ***Figure 3.2.1.8***, and suggested that the observed changes are consistent with the creep model of Jin and Aki (1989, 1993). A closer look at Figure 3.2.1.8, however, reveals that although the frequency of earthquakes in the magnitude range in 2.6-3.0 showed a greater rate of increase than smaller earthquakes after the Hyogo-ken Nanbu earthquake, that in the magnitude range 3.0-3.5 did not. Rather we get impression from the figure that we cannot reject the uniform increase of the seismicity independent of magnitude. The uniform increase may be more reasonable in this case, because the loading is done elastically through the whole lithosphere and not through the brittle-ductile transition zone as implied in the creep model. In other words, if we accept the uniform increase in seismicity in this case, we must accept a loading process different from the elastic stress transfer through the entire lithosphere for cases in which we observe the strong positive correlation between coda Q^{-1} and N(Mc). I propose to refer to this process as *the loading of tectonic stress (called more specifically as loading of plate-driving forces in Part 2) through the brittle-ductile transition complex.*

The strength-depth relation shown in Figure 3.2.1.3 suggests that a major earthquake may occur once the strongest point at the brittle-ductile boundary is broken. Sibson (1982) noted that most of moderate to large earthquakes are initiated near the base of aftershock zone which closely coincides the seismic-aseismic boundary of background seismicity. Ito (1990) presents the case of the western Nagano, Japan, earthquake of 1984 studied by Ooida et al. (1990) as an example in which the nucleation point of a major earthquake occurs where the boundary depth is changing laterally. The nucleation point of a major earthquake naturally draws attention of seismologists as the site for an intensive monitoring for prediction. The best example is the Parkfield, California, earthquake which has been repeated with the widely accepted nucleation point under the Middle Mountain (Bakun and McEvilly, 1984). The fault trace shows a slight bend of about 4 degree at this point which is at an end of the boundary zone between the creeping segment and the blocked segment of the San Andreas fault. The steady aseismic slip called "creep" occurring along the San Andreas fault to the north of this point accumulates stress for a Parkfield earthquake. Repeated Parkfield earthquakes in turn accumulates the stress concentration near Cholame to cause the great earthquake of California along the segment slipped in 1857 as schematically illustrated in ***Figure 3.2.1.9*** reproduced from Sieh (1978).

The similarity between the above figure and the diagram of slip function given in Figure 3.1.1.4 is intriguing, suggesting some link between laboratory studies of rock failure and geologic studies of active faults. It suggests that the cohesive zone may correspond to the area of offsets in fault traces depicted in Figure 3.2.1.9. A more quantitative discussion was made by Aki (1992) using the specific barrier model of Papageorgiou and Aki (1983) introduced in Section 1.1. The model parameters determined for major California earthquakes are shown as a function of magnitude in ***Figure 3.2.1.10*** after a correction for the recording site effect by Aki and Papageorgiou (1989). The parameters for the Loma Prieta earthquake were added by Chin and Aki (1991). They are shown from top to bottom in the order of the cohesive stress σ_c, the local stress drop $\Delta\sigma$, the sub-event diameter $2\rho_0$, Griffith's fracture energy G, the critical weakening slip D, the size d of thecohesive zone, and the reciprocal of f_{max}. The source parameters show a remarkably systematic dependence on magnitude. The universal constancy of the local stress drop needed for explaining observed strong motion acceleration has been known since Hanks and McGuire (1981). The strong dependence of the sub-event size on magnitude is necessary to keep the local stress drop constant while the average slip changes with magnitude. As noted earlier in Figure 3.1.1.3 reproduced from Beresnev and Atkinson (2002), the sub-event size attributed to Aki (1992) shows a stronger dependence of the sub-event size on magnitude than the global average. This is because of the stronger dependence of the average slip on magnitude for major California earthquakes due to the fixed width of their fault planes by the brittle zone thickness as discussed in detail by Aki (1992). If we extrapolate the constancy of local stress drop to the maximum or characteristic earthquake in the creeping zone, which is about 5, we get its sub-event size of a few hundred meters. The corresponding cohesive zone size should be much smaller than that.

Chouet (1979) found a significant temporal change in coda Q from the records of a spectral analyzing seismograph operated at Stone Canyon in the creeping zone as mentioned in Section 1.3. The coda Q decreased during the 1-year period from July, 1973 by about 40 % for the frequency band centered at 1.5 Hz and 80 % for that at 24 Hz. (The greater change at higher frequency may be attributed to the smaller fracture size in the ductile part as discussed in Part 1, which is consistent with the smaller cohesive zone inferred above. In my memo to Keilis-Borok dated May 15, 2003 given in Part 1, I identified the creeping zone as an exhumed, scaled-down brittle-ductile transition zone.) If we apply the stress sensitivity estimated for the Tamba region by Hiramatsu et al. (2000), the 40-80 % change in coda Q corresponds to the change in tectonic stress of 0.04-0.08 MPa (0.4-0.8 bar). There was no major earthquakes in the creeping zone during the period.

So far in this chapter we focused our attention to the Tamba region in the in-land Japan and the segment of the San Andreas fault connecting the creeping segment with the blocked segment in Central California. In the San Andreas fault zone, we saw that the fault slip in the creeping brittle zone is loading the nucleation point for the Parkfield characteristic earthquake, and the slip accumulated by repeated Parkfield earthquakes is in turn loading the nucleation point for the 1857 type great California earthquake. Thus we can trace the origin of the great earthquake to the region where both the brittle fracture and ductile slip is taking place. There exists some physical process in this region that is manifested as a temporal change in coda Q. We inferred from the observed magnitude dependence of the earthquake model parameters that the process involves fractures of linear dimension of a few hundred meters both in the brittle and ductile part in the Tamba region, and those of smaller dimension in the creeping zone of the San Andreas fault. We shall call this region where both brittle and ductile processes are taking place interactively the brittle-ductile transition complex. The coda Q will be the crucial observable pertinent to the structure and process of this region.

From the change in seismicity and coda Q in the Tamba region due to the Hyogo-ken Nanbu earthquake, we recognized a detectable difference between the elastic stress transfer through the entire lithosphere and a loading process of tectonic stress (called plate-driving forces in Part 1 and 2) through the brittle-ductile transition complex.

2.2 The brittle-ductile transition complex and a new analysis of coda waves

The classical earth model constructed from standard regional seismic studies such as the refraction survey using explosion generated P waves and the phase velocity dispersion study of earthquake generated surface waves were often characterized by the following 5 homogeneous layers; (1) upper crust, (2) lower crust, (3) mantle lid, (4) mantle low-velocity layer, and (5) lower mantle. It was generally found that the difference between the seismically active region such as Japan and California and the stable region such as the Canadian shield in the seismic structure does not appear in the crust but most strongly in the mantle lid, namely, the mantle part of the lithosphere. For example, both the P velocity found by refraction studies and S velocity found from Rayleigh waves at the top of the mantle under Japan were found as low as those in the global low-velocity layer in the upper mantle suggesting that the lid is absent and the low-velocity layer is directly touching the bottom of the crust under Japan (e.g., Aki, 1961). The absence of the lid under tectonically active region was also supported by the absence of S waves propagating along the top of the mantle under active regions due to strong attenuation (Molnar and Oliver, 1969).

It has been customary to associate the upper crust with the brittle layer, the lower crust with the ductile layer, and the Conrad discontinuity with the brittle-ductile transition (e.g., Hashizume and Matsui, 1979). Ito (1990), however, found in the Kinki region of the western Japan that the Conrad discontinuity is deeper than the maximum depth of crustal seismicity by 3-5 km.

Another interesting result from seismic structural studies relevant to the brittle-ductile transition comes from the reflective lower crust universally observed from large-scale reflection studies such as COCORP (Consortium for Continental Reflection Profiling; e.g., Oliver et al., 1976). For example, Klemperer (1987) found that the top of the reflective crust is shallower in the area of high terrestrial heat flow. From the correlation between the maximum focal depth and the heat flow in the Kinki area, Ito (1990) argues for a causal relation between the high reflectivity and the ductility of the lower crust, supporting the hypothesis that the high reflectivity is created by the ductile flow in the lower crust (Pavlenkova, 1984; Meissnerand Wever, 1986; Mooney and Brochier, 1987). If the high reflectivity of the lower crust implies horizontal lense-like structures, it can also explain the transverse isotropy universally observed from the dispersion of Love and Rayleigh waves since Aki and Kaminuma (1963). I have been tempted to associate the origin of the coda Q to the high reflective layer because of the increasing evidence that temporal change in coda Q may be originated primarily in the lower crust. Although the apparent global existence of the reflective layer and the strong difference in coda Q between active and stable regions prevented me from connecting the two directly, the mechanism for creating the reflector by ductile flow could create scatterers and absorbers for the coda waves.

There are other lines of evidence supporting the lower-crust origin of the temporal change in coda Q. The sharp increase in coda Q^{-1} in 1986-87 in Southern California shown in Figure 3.1.3.11 was concurrent with the increase in electrical conductivity in the lower crust of the same region detected by Madden et al. (1993). A high conductivity anomaly in the lower crust was found by Utada (1987) under the zone of strain concentration in the in-land Japan revealed by the GPS measurement. A similar zone of high strain concentration was found also in Southern California from the lateral distribution of the uplift rate by Castle and Gilmore (1992) where several recent earthquakes of moderate size occurred. In an effort for finding any relation between the coda Q and the zone of strain concentration, Ouyang and Aki (1994) constructed maps of coda Q using the enormous amount of high quality data from the Southern California Seismic Network. The resultant maps showed significant anomalies in coda Q, some of which can be associated with the Castle-Gilmore high strain zone and the P velocity anomalies at a depth of 20 km mapped by Hu et al. (1994), but could not give a conclusive result regarding the origin of the coda Q anomaly.

Traditionally, the coda wave analysis was done first at a single station to measure the coda Q, and then its spatial distribution was studied combining the single-station results obtained at different stations. We realized that this procedure is not taking advantage of the spatial smoothness inherent to the coda amplitude as a diffusive process. We revised the procedure by first studying the spatial distribution of coda wave characteristics for a single event and then synthesizing results from many events. Our new method takes advantage of the spatial smoothness inherent to the distribution of scattered energy, which obeys a diffusion type equation similar to temperature and is physically guaranteed to be smooth in space. The new analysis method of coda wave describe below is an outcome of my study of Piton de la Fournaise in La Reunion where I used coda waves of the volcano-tectonic events for tracing the magma movement as described in Chapter 3. In the course of the study, I realized that mapping the coda Q in space for a given event corresponds to taking the derivative of the distribution of scattered energy with respect to the lapse time. It is not the primary quantity corresponding to the energy distribution, but a secondary quantity, namely, its time derivative. We should expect an erratic behavior for them, because they may be strongly affected by the process of interaction between the primary source waves and the heterogeneity in the earth, flow of energy into or away from a given area, and heterogeneity in absorption strength of the medium than the distribution of scattered energy itself.

In the following, I shall first describe the problem encountered at La Reunion and then look at the California data. I measured the coda amplitude for about 40 volcano-tectonic events in La Reunion occurred in 1991-97. The largest magnitude was 3.3. I selected records of 9 earthquakes with epicentral distance to the summit greater than 20 km and computed the site amplification factor for each station of our network. Then I selected 11 events occurred in the caldera called Enclos Fouque (hereaftrer we refer to it the Enclos caldera, see Figure 3.3.1.0) for which the signal to noise ratio is sufficient for the coda analysis at the lapse time of 15 sec and 5 events at the lapse time of 30 sec. The coda amplitude corrected for the recording site effect are smoothly varying throughout the network area as expected for diffusive waves and is nicely peaked in the summit area for all cases. This localization of scattered energy is attributed to slow waves trapped in the fluid-solid 2-phase system of the magma body in Chapter 3.

I then looked at the spatial distribution of the ratio between the amplitudes at the two lapse times, 15 and 30 sec., which would correspond to mapping the coda Q. I found that the distributions of amplitude ratios are no longer smooth and strongly dependent on the location of earthquake used for the analysis. Only in the case of earthquake located directly beneath the central cone of the volcano, we obtained a concentric distribution of higher amplitude at 30 sec relative to that at 15 sec with the center at the summit area. This corresponds to a high coda Q at the summit area surrounded by a low coda Q as expected for a strong localization of coda amplitude in the area. Such a pattern of the ratio disappears and is replaced by an entirely different one for earthquakes located a few km away from the central cone, offering an explanation for the long-standing puzzle among those who studied the coda Q; why it shows a large variation and a strong erratic behavior (e.g., Aster et al., 1996).

With this insight gained at La Reunion I analyzed the data from Southern California prepared by Anshu Jin (personal communication) using the following procedure. (1) A single earthquake is used to map the coda ratio between two time windows. (2) The two time windows selected for the ratio are 50 to 60 and 80 to 90 seconds measured from the origin time. Only those stations for which the above time windows fall later than twice the S arrival time are used. (3) The amplitude ratio is calculated as the square root of energy at the 50-60 s window divided by that at the 80-90 s window, separately for the three frequency bands; 1.0 to 2.0, 2.0 to 4.0, and 4.0 to 8.0 Hz. (4) The ratio is normalized to the mean over all available stations, and plotted on the map.

I drew contours of equal ratio at an interval of 0.1 by trying smoothly interpolating the data points. I was able to draw them for all the maps, but I was overwhelmed by the great variability, erratic behavior and strong sensitivity to epicenter location as well as to frequency band. A small difference in the epicentral location produced a large change in the coda ratio map. This is consistent with the result of Ouyang and Aki (1994) who studied the difference in coda Q between two events, and found that the variance of the difference did not decrease with the decreasing distance between their hypocentral locations. By mapping the coda ratio in space for a single event, I was able to capture the cause of variability as a physical process. It appears that time derivative of the scattered energy is very sensitive to the radiation pattern of primary waves and to the relative locations of the scatterers, in other words, it depends strongly on how these scatterers are illuminated.

In view of the large variability and strong erratic behavior, many of the apparent anomalies in coda ratio may not be directly related to significant scatterers in the earth. Considering the physical process involved in the interaction between the primary waves and the scatterers, I adopted the following 3 criteria for a significant anomaly.

(1) The anomaly must be close to the epicenter of the earthquake used for the mapping. Preferably the epicenter is located within the anomaly, and must be located within 10 km from the anomaly. (2) The anomaly must appear consistently for different events and frequency bands. (3) The maximum value of the ratio associated with the anomaly must be at least 1.5.

The first criterion that the significant anomaly must be close to the primary source of seismic energy is consistent with Green's function involved in the phenomena, which decays inversely proportional to the squared distance (Equation 1.3.5). Using the above criteria, we identified 5 high coda ratio (low coda Q) anomalies in the study area. They are Salton Sea geothermal area, Sierra-Madre-Banning fault, San Cayetano-Santa Susana fault, White Wolf fault, and Coso geothermal area. It is remarkable that all of these areas fall precisely in the zone of steep gradient in vertical displacement change between 1959 and 1975 as revealed by Castle and Gilmore (1992), who hypothesized a localized creep below the zone of steep gradient along the detachment surface between the brittle and ductile part of lithosphere. This is again in harmony with the creep model of Jin and Aki (1989, 1993) introduced in Section 1.3.

As demonstrated for La Reunion, a low coda ratio (high coda Q) anomaly may be related to a structure that can trap scattered energy. I used the same criteria as used for a high coda ratio anomaly for identifying a significant low coda ratio anomaly, except that the ratio must be at most 0.6, instead of at least 1.5. We found only two areas that meet our criteria. One was in the middle of Sierra Nevada, and the other was a zone trending in the north-east near the junction of the San Andreas and San Jacinto fault. The latter area may correspond to the Transverse Range subduction zone which was found by Revenaugh (1995) to be a scattering source contributing to coda waves in Southern California. The anomaly in Sierra Nevada is expected to be of low coda ratio, because of the hard rock composing the body. We may expect a strong heterogeneity associated with the batholith structure and it is reasonable that the body stands out as one of the two strong low coda ratio anomalies in Southern California.

2.3 Seismogenic structures in regions involving the subducting plate

Most of the earthquakes to be discussed in Section 4.1 about their precursory observations will be from the inland seismic regions not directly involving the subducting oceanic plate, and Part 3 will be complete as an Introduction to Seismology for Earthquake Prediction without discussions on the seismogenic structures in other regions. In the future when we broaden our idea to include earthquakes in other regions, however, we shall need to extend the concept of the brittle-ductile transition complex to be applicable to them. As well known, this complex will occupy regions sandwiched between the near-surface brittle zone and the deep brittle zone of sinking plate for a great thrust earthquake in the subduction zone.

As mentioned in Section 2.1 referring to my memo to Keilis-Borok dated May 15, 2003 given in Part 1, we now identify the creeping zone of the San Andreas fault as an exhumed scaled-down brittle-ductile transition zone. From this viewpoint, the above sandwiched region in the subduction zone is very similar to the creeping zone of the San Andreas fault, and we may expect a similar interaction between the brittle part and ductile part also in the subduction zone. In fact, an example of the positive simultaneous correlation between the coda Q^{-1} and N(Mc) similar to the one described in Section 1.3 for California has been observed for the Wellington, New Zealand, area as discussed in Section 4.1

The mode of occurrence of great earthquakes in the subduction zone varies from place to place depending on the tectonic setting as classified by Kanamori (1977) according to the degree of coupling between the subducting plate and the over-riding one. An example of the region of the strongest coupling is Southern Chile where the largest earthquake of the world occurs, and that of the weakest is Mariana where the great earthquake is absent. Lay and Kanamori (1981) hypothesized the size of the asperity distributed over their fault plane according to the classification. The pattern of asperity distributions for subduction-zone earthquakes has been the main target of teleseismic study by Kikuchi and his colleagues (e.g., Kikuchi, 1997). Some of the asperities have been attributed to the surface topography of the subducting plate such as sea mounts in the Pacific ocean off shore Northeast Japan.

There have also been numerous attempts to define the characteristic earthquakes in the subduction zone from historic, geologic and geophysical observations. Very little, however, has been done regarding the fine-scale behavior as described for inland earthquakes in Section 2.1. A rare example is the Wellington, New Zealand, area which will be included as an applicable region of our new precursor in Section 4.1. The systematic geographic variation of coda Q across the subduction zone in the British Columbia-Washington State region found by Zelt et al. (1999) and Havskov et al. (1989) confirms the tectonic significance of coda Q, but the period of the study of its temporal variation may be too short for detecting any significant temporal change.

Highly relevant for characterizing the small-scale seismogenic structure, Obara and Sato (1995) found a systematic variation of the parameters of the random medium (used for interpretation of high-frequency seismic scattering) across the subduction zone, with the result which showing a rougher medium on the inland side of the volcanic front than the outside. It is interesting to study how this roughness may be related to the fractures responsible for the temporal variation in coda Q.

Kinoshita (1992) found from the analysis of records obtained at deep bore-hole seismographs in the Kanto region that the source-controlled f_{max}, for earthquakes in the magnitude range from 3.6 to 6.0, varies considerably depending on the earthquake location relative to the Pacific, Eurasia and Philippine Sea plates, suggesting a strong spatial variation in Mc in the region involving three plates, another promising study area for delineating the interaction between the brittle and ductile part.

The newly discovered zone of deep low-frequency tremors under the western Japan (Obara, 2002) may be relevant to the condition of the brittle-ductile transition complex in the subduction zone, in addition to pre-slips and silent earthquakes of which the relevance to the earthquake prediction has been well recognized. The deep low-frequency events are located at depths between the upper and lower brittle zones, and have seismic spectra broadly peaked around a few Hz like typical long-period events widely found in active volcanoes. The occurrence of the events with the nearly identical characteristic spectra throughout the subduction zone in western Japan indicates the existence of another nearly universal scale length associated with the seismogenic structure. In fact the source size corresponding to the dominant frequency of a few Hz can be attributed to the same scale length as those corresponding to Mc, f_{max} and the critical corner frequency discussed earlier for the inland seismic region, suggesting a causal relationship among them. They may be simply produced by adding water or magma to the fractures responsible for the temporal variation of coda Q.

According to Obara (2002), a swarm of the deep low-frequency earthquake can be started by a nearby tectonic earthquake or stopped by it. This is similar to the behavior of the long-period events during the declining period of the activity at Piton de la Fournaise discussed in Section 3.3. The state of the brittle-ductile transition complex may change with the regional cycle of earthquake process, and may be reflected in the manner how the occurrence of low-frequency earthquake respond to external forces. It will be interesting to see the effect of tidal loading on their occurrence, for example, in the manner proposed by Yin et al. (2000).

Chapter 3. Lessons learned from an active volcano for prediction science

I used to think that volcanoes are more complicated than earthquakes, because they involve gas and liquid in addition to solid that was the only earth medium needed for understanding the ground shaking caused by the rupture of an earthquake fault. The structure of a volcano is also complicated with its much stronger heterogeneity and anisotropy than that of a fault zone. Working with earthquakes in Southern California for a decade or so, however, I realized that volcanoes are simpler than earthquakes in a very fundamental way. An individual volcano exists before and after an eruption, while we can clearly identify an individual earthquake only after its occurrence. Before its occurrence we must consider a system of fault segments in a large area interacting each other. This interaction had become a main target of research by the SCEC (see Section 1.2) Earthquake Physics group led by Leon Knopoff. An individual earthquake is a small part of a large system and cannot be defined separately from the surrounding. In this aspect, a volcano is less complicated than an earthquake. I decided to switch from the earthquake study to the volcano study with the hope for learning some basics of the prediction science, and moved in 1995 from the University of Southern California to the Observatoire Volcanologique du Piton de la Fournaise at the Reunion island in the Indian ocean. It turned out that I chose a right volcano for my purpose as explained in this chapter.

Piton de la Fournaise, as shown in ***Figure 3.3.1.0***, is a basaltic island volcano like Kilauea, Hawaii. Both are intra-plate volcanoes on an oceanic lithosphere with a supply of magma from hot spot in the mantle. The rate of erupted magma is not much different between the two volcanoes. An estimate for Kilauea by Dzurisin et al. (1984) for the period from 1956 to 1983 is 30 M cubic meters per year, while Lénat and Bachèlery (1988) gives 10 M cubic meters per year for the Piton de la Fournaise during the period from 1930 to 1985. Since Dzurrisin et al. (1984) estimate that 65 percent of the magma supplied from the upper mantle remains in the rift zone under Kilauea, while there is no evidence for such a steady accumulation of magma in the rift zone of Piton de la Fournaise, the difference in magma supply from the upper mantle may be about a factor of 10 between the two volcanoes. The rift zone clearly exists in Piton de la Fournaise, as demonstrated by eruptions along the northeast rift zone outside the Enclos caldera (labeled Enclos Fouque in Figure 3.3.10) in April, 1977, and a series of fissure eruptions extending from the summit to the southeast in March 1986. It is also clear that the rift zone is not developed here as well as in the Hawaiian volcanoes. From a sea beam bathymetry survey, Lenat et al. (1989a) found that the active rift zones of Piton de la Fournaise quickly widen down slope unlike typical Hawaiian rift zones which form narrow ridges extending tens of kilometers offshore.

Nakamura (1980) was the first to ask why long rift zones develop in Hawaiian volcanoes. Comparing with the Galapagos islands, another intraplate basaltic volcano lacking a rift zone and located on a young lithosphere, he suggested that the rift zone intrusion in Hawaii is sustained by repeated Kalapana-type earthquakes caused by a slip along the top of the oceanic crust which may have anomalously low friction due to a thick sediment and a high pore pressure (Hubbert and Rubey, 1959). This idea has been supported by more recent works(e.g. Dieterich, 1988; Thurber and Gripp, 1988).

Piton de la Fournaise is located on an old oceanic lithosphere with a flexural rigidity (Walcott, 1970; Bonneville et al., 1988) comparable to the Hawaiian lithosphere, and the oceanic crust upon which the volcano was built must have had a thick sediment cover. There is, however, a major difference in the speed of lithosphere relative to the mantle under these two volcanoes. In Hawaii, the old oceanic crust is always present in front of the youngest volcano due to the high speed of the Pacific plate, and the Kalapana-type earthquake occurs along the weak plane formed by the deep sea sediment, sustaining the intrusion into the rift zone. On the other hand, the African plate, on which Piton de la Fournaise is located, moves so slowly that a fluctuation in the path of magma ascent in the crust can move the volcano back and forth. The remains of proto Fournaise volcano between the ocean and the present summit, as evidenced from the old magma chamber encountered by deep drilling (Rancon et al., 1989) as well as the gravity highs deviating from the current summit area (Rousset et al., 1989) support such a fluctuation which prevented a full development of rift zone. Thus it is more difficult for magma to intrude into the rift zone here than in Hawaii, and that explains why Piton de la Fournaise has a remarkable central cone as high as 400m from the floor of the Enclos caldera due to repeated summit eruptions,

which is absent in the Kilauea volcano.
From the above geologic and geodynamical setting, we expect that the eruption at the summit of the central cone and that at the rift zone may have distinctly different seismic signatures. In fact, we found a systematic relation between the elevation of an eruption site and the duration of the swarm of volcano-tectonic events under the summit area preceding the eruption. We also found that the so-called long-period (LP) events occur during the precursory swarm for the rift-zone eruption, but not for the summit eruption. The duration of precursory swarms at this volcano are extremely short in comparison with other volcanoes. While, according to Benoit and McNutt (1996), the duration for 191 precursory swarms of world's volcanoes range from 0.04 to 300 days, with a mean of 8 days, those at this volcano ranges from 17 minutes to about 36 hours.

3.1 Construction of an initial model before the 1998 eruption.

When I arrived at La Reunion in 1995, the volcano was in one of the longest quiet period in recent decades, and gave me time for constructing an initial model using the data accumulated at the observatory since the early 1980's. The initial model was based primarily on the long-period (LP) events and the newly discovered phenomenon called "coda localization", and was completed just before the largest eruption since 1930's occurred on March 9, 1998. The detailed description of the model construction was given in Aki and Ferrazzini (2000), and here we shall highlight the main result.
Seismological investigations of eruptions at Piton de la Fournaise since the establishment of the observatory by the Institut de Physique du Globe de Paris were described in journal papers by individual scientists (Bachèlery et al., 1982; Lépine, 1987; Lénat et al., 1989b, 1989c; Delorme at al, 1989; Hirn et al., 1991; Grasso and Bachèlery, 1995; Nercessian et al., 1996; Sapin et al., 1996) as well as in the annual report of the world volcanic eruptions in Bulletin of Volcanology contributed by the observatory personnel. It was found that almost all the eruptions were preceded by the so-called "seismic crisis" which is a swarm of volcano-tectonic earthquakes occurring beneath the central cone at about sea level. The seismic signature of the eruption itself is marked by steady continuous tremors originating from the eruption site. In addition there have been occasional mention of "low-frequency events", but they have not received much attention partly because their occurrences are not simply related to eruptions, and partly because of the difficulty in discriminating them from other seismic events such as numerous rock falls along the steep valleys of the island and P, S and T phases from earthquakes along active mid-ocean ridges in the Indian ocean.
Active volcanoes generate the so called "low-frequency events" or " long-period (LP) events" (see Chouet, 1996, for a recent review) in addition to the volcano-tectonic (VT) earthquakes similar to those of tectonic origin found elsewhere. They are distinguished from the latter by an emergent onset, a lack of clear S phase, and a lack of the high frequency part of the spectrum expected for a tectonic earthquake of a similar size. In order to discriminate the LP events originating from the volcano, we developed a location method based on the spatial distribution of their amplitude across the network, since the classical method for locating tectonic earthquakes is not applicable to them because of the lack of clear onset for P and S waves. For this purpose it is essential to eliminate the local effect of recording site from the observed amplitude. Koyanagi et al (1995) have demonstrated that the coda amplification factor described in Section 1.3 can be effectively used to smooth the amplitude distribution of T phase recorded by the seismic network of Hawaii. We found that the coda method works well at La Réunion, for T phases, seismic waves from rock falls and long-period events as shown by Aki and Ferrazzini (2000).

In order to obtain the station amplification factor by the coda method, we need a volcano tectonic event (seismic event indistinguishable from the usual tectonic earthquake, hereafter called VT) which gives a good signal to noise ratio at a lapse time late enough for applying Equation 1.3.1. As described in Section 1.3, the choice of lapse time twice the S wave arrival time has been found adequate for most part of the world. We found, however, that La Réunion is a special place where the station site factor depends on the distance from the event location to the summit area. To avoid this effect we initially used an event far away from the volcano with coda of high signal to noise ratio at a long lapse time, namely, an M=3 event occurred offshore near the northern end of the island, from which we estimated the coda site factor using the peak-to-peak amplitude averaged over the lapse time window of 60 to 70 seconds. It varied by a factor of 4 from station to station with no systematic geographic pattern. We confirmed later when we accumulated records of many events located at distances from the summit greater than about 20 km, that the average site factor was very close to the one obtained from the single M=3 event.
We tested the coda amplification factor using seismic data from a known source, namely, rock falls in the Bras de Mahavel occurred in June-July, 1995. Rock falls are very common sources of seismic signals on this island, partly because of heavy rainfall (annual average around 10 meters) and partly because of steep cliffs and deep valleys originated from caldera formations. The dominant frequency of seismic waves from the rock fall was around 3 Hz at all stations. The variation of the amplitude corrected for the station site effect is smooth enough for drawing iso-amplitude contours at intervals of a factor of 2. The center of contours agrees well with the site of the rock fall. The decrease of amplitude with distance can be fitted with the formula for surface waves with the attenuation specified by the Q factor of 40 to 60. This range of Q agrees well with the value obtained by Koyanagi et al. (1995) for the summit area and rift zones of Kilauea, Hawaii from the amplitude decay of T phase. We also tested the site factor using the T phase with satisfactory results showing amplitude decreasing smoothly from the coast to inland.
After confirming the existence of LP events under Piton de la Fournaise, we studied their occurrence in relation to the eruption history of the volcano as described in Aki and Ferrazzini (2000). For this purpose, we made a catalog of LP events, listing the time of occurrence, the maximum amplitude at station BOR (Figure 3.3.1.0), the duration of the event and its dominant frequency. The identification of LP events is primarily based on visible records at 8 selected stations by the Sefram ink recorder. The criteria for the identification of LP events are (1) the dominant frequency less than about 3 Hz, (2) the coherency of waveform at the three crater-rim stations BOR, SFR, and DSR shown in Figure 3.3.1.0, (3) the amplitude is maximum in the summit area, and negligible at stations farther than 10 km from the summit. The Sefram record includes necessary information for the above criteria, except for small events to which the criterion (3) is difficult to apply due to noise at stations far away from the summit and closer to the ocean.
Our catalog of LP events starts with the seismic crisis of 5 August, 1985. The seismological characteristics of 13 LP events during this crisis are very similar to those of the December, 1991 crisis described in detail in Aki and Ferrazzini (2000). Our catalog lists the time of occurrence, peak amplitude and duration at station BOR, and dominant frequency for about 900 LP events since August, 1985. The most outstanding trend found in our catalog is the systematic disappearance of LP events after the eruption of August, 1992. LP events with the lowest frequency disappeared first. No events with a dominant frequency of 1 Hz

occurred since 1993 until 5 hours before the March, 1998 eruption. Those with dominant frequencies around 2 Hz become most frequent in 1993, decreasing gradually, practically vanished in 1996 and reappeared on June 4, 1997. The observed disappearance of 1 Hz LP events preceding that of 2 Hz LP events during the period of declining volcanic activity and its reappearance with its revival after that of the 2 Hz source suggests that the source of 1 Hz LP events is separate from that of 2 Hz LP events, the latter being located below the former.
A cursory look at the occurrence of LP events in relation to the eruption history led to initial disappointment from a simplistic view of the precursor, because they seem to occur more often following an eruption rather than preceding one. A break-through in recognizing their relation came when I noticed different behaviors of precursory LP events depending on the elevation of eruption site, which is related systematically on the duration of the seismic crisis as shown in the table below and Figure 3.3.1.1.

Table 3.1.1 Table of seismic crises at the Piton de la Fournaise for 1985-1996.

Number	Date	Precursory time	Elevation of the eruption site
1	14-06-85	less than hour	2500 m
2	10-07-85	no eruption	
3	05-08-85	2 hour 37 min.	2100-2000
4	01-12-85	17 min.	2500-2100
5	18-03-86	9 hour 24 min.	1750-1720
6	02-06-87	no eruption	
7	19-07-87	2 hour 13 min.	2050-2000
8	07-02-88	2 hour 5 min.	2000
9	18-05-88	31 min.	2300-2000
10	31-08-88	2 hour 25 min.	2250-2100
11	14-12-88	4 hour 31 min.	2100-2000
12	18-01-90	47 min.	2500
13	18-04-90	6 hour 45 min.	1800
14	18-07-91	52 min.	2510-2400
15	07-12-91	no eruption	
16	27-08-92	57 min.	2500-2100
17	26-11-96	no eruption	

From the above table we found the following:
(1) All the 17 crises start with a swarm of VT events located beneath the central cone at about the sea level, with only one exception, the crisis No.2, in which they are located on the east side of the central cone at deeper depths. This crisis No. 2 shows no apparent relation with any eruption, but plays an important role in Section 3.3 for understanding the cyclic behavior of the activity of this volcano.
(2) Of the remaining 16 crises, three eruptions were not followed by eruption.
(3) For all the 13 crises that preceded an eruption, we can find the precursory time between the onset of the crisis and the beginning of the eruption estimated from the records of seismic tremors originating from the eruption site. The precursory time ranges from 17 minutes to 9 hour 24 min. There is a strong correlation between the precursory time and the elevation of the highest point of each eruption site listed in the same table. The precursory time is less than 1 hour for eruptions near the summit, and more than 6 hours for eruption sites with an elevation lower than 1800 m as shown in Figure 3.3.1.1. Briole et al. (1998) recognized a similar correlation between the duration of geodetic

disturbance associated with a seismic crisis and the distance of the eruption site from the summit, which increases with the decreasing elevation.

(4) For four eruptions (No.3, 5, 11 and 13) which occurred near the rim of the Enclos caldera, seismic records during the crisis show a swarm of LP events originated beneath the central cone. LP events are completely missing in the precursory crises of all other eruptions in the list.

The above observations suggest two distinct paths of magma to the eruption site under this volcano, namely, the summit path and the rift-zone path. The eruption through the summit path starts at elevation higher than about 2100m on fissures which extend downward. The precursory seismic swarm lasts for less than about 2 hours, and does not include LP events. The LP events may occur, however, during or immediately after the summit path eruption as in September, 1985, December, 1985, February, 1987, and September, 1992. On the other hand, the eruption through the rift-zone path occurs at elevation lower than about 2100 m on fissures which sometimes extend upward as in December, 1988. The precursor seismic swarm lasts longer than about 2 hours, and includes the LP event. Thus the LP event generator is located on the rift-zone path but not on the summit path. The reason why some summit eruptions accompany LP events near the end may be the diversion of magma flow from the summit path to the rift-zone path. In some cases such a diversion may stop a summit eruption.

Thus the second element of our model is the two separate paths to eruption site, namely the summit path and the rift-zone path. Both 1 Hz and 2 Hz LP generator introduced as the first element are part of the rift-zone path as shown schematically in ***Figure 3.3.1.2***. Let us now proceed to the third element of our model, namely, magma reservoirs located deeper than the LP generators introduced from the spatial and temporal variation of coda localization observed after 1996.

The first seismic crisis (swarm of VT events) since the eruption of August, 1992 occurred on November 26, 1996 as listed in Table 3.1.1. This crisis involved 138 earthquakes located at about the sea level beneath the central cone. The largest magnitude was 2.4 and the duration of crisis was 104 minutes. We shall refer to this crisis as Crisis I to distinguish it from a minor crisis, which is referred to as Crisis II and consisted of 21 events with maximum magnitude 2.1, occurred later on August 23, 1997. After Crisis II, the shallow seismicity beneath the summit maintained the high rate comparable to 1992 until the precursory crisis to the eruption on March 9,1998.

As described in detail in Aki and Ferrazzini (2000), the coda of VT events occurred between Crisis I and the 1998 eruption showed a strong concentration of amplitude in the summit area with the peak amplitude about 5 times that of stations away from the summit. The amplitude decays to a half of the peak value at about 5 km from the location of the peak. This is an extraordinary concentration of scattered wave energy. If we consider, as usual, that coda are composed of S waves with velocity around 3 km/s, the observed half decay distance of 5 km would lead us to conclude that the wave length (about 1 km) is longer than the mean free path (a few hundred meters), putting the phenomenon into the regime of the Anderson localization (Anderson, 1958), which was predicted theoretically, but has never been observed in nature or laboratory.

We prefer an alternative explanation that the observed coda localization is due to very slow waves that can exist in the fluid-solid 2-phase system. The existence of waves slower than the acoustic waves in the fluid has been known for a fluid filled crack (Chouet, 1986; Ferrazzini and Aki, 1987), lamination of fluid and solid (Schoenberg, 1984) and porous media (Biot, 1956). For example, Ferrazzini and Aki (1987) showed that both the phase velocity and group velocity tends to zero as the wave length increases to infinity for a fundamental symmetric mode in a fluid layer sandwiched between solid. Recently Yamamura (1997) explained these slow waves by a common mechanism in which the pressure change in the fluid due to acoustic wave is relaxed by the coupled deformation in the solid. If the wave velocity is reduced by a certain factor, the wave length will be shortened, and the mean free path will increase by the same factor, putting the observed coda localization into the diffusion regime. The consistency of the spatial-temporal pattern of the peak of coda localization with the magma process described below supports this explanation.

The peak location of coda localization found for the VT events between Crisis I and the 1998 eruption made a systematic migration with time. The peak for the earliest event was located in the NW direction from the summit in agreement with the path of magma inferred from the locations of clusters of deep VT events occurred in September, 1996. The event during Crisis I shows the peak location precisely in the summit area. Magma must have reached beneath the summit at this time, but instead of erupting to the summit, it moved toward SE (to station NTR shown in Figure 3.3.1.0) as indicated by the peak area of coda localization for the event occurred one month before Crisis II. By the time of Crisis II, magma stopped spreading to SE, and at Crisis II it moved to NE of the summit toward FLR and then NCR as indicated by the peak locations for the event during Crisis II and the later one. We envision the process of magma movement into two reservoirs associated with the two crises as marked by arrows in Figure 3.3.1.2.

We then noticed that there is a relatively flat area in the Enclos caldera seemingly bounded by the local caldera wall with a small radius of curvature near both NCR and NTR that was interpreted by Bachèlery(1981) as collapsed blocks. We associate these surface features with our two reservoirs, and call them NCR and NTR reservoirs. Since the average elevation is higher for the NCR reservoir than the NTR, it is natural to put the former at a higher level than the latter. Then it is also natural for the latter to be filled before the former by the ascending magma. In terms of the model depicted in Figure 3.3.1.2, this means that a summit eruption may occur when the NCR reservoir is filled completely. The NTR reservoir was filled during 9 months between Crisis I and Crisis II. If the two reservoirs have a similar size, the filling of the NCR reservoir may take about the same time. We then expect a seismic crisis in May, 1998 which will precede an eruption according to the model shown in Figure 3.3.1.2.

The above prediction of the May eruption was written on March 4, 1998 (the eruption occurred on March 9) as a part of manuscript for the observatory's Seismology Annual Report for 1997. It was based on the assumption that Crisis II marked the beginning of filling the NCR reservoir. The cumulative moment curve for the VT events (Ferrazzini, personal communication), however, indicates that the high seismicity rate started about a month earlier than the time of Crisis II. This revision would predict the March eruption more precisely.

In this section, we began to construct our initial model by distinguishing the summit path to eruption from the rift-zone path, and introduced 1 Hz and 2 Hz LP generators as part of the rift-zone path. From the above results on the coda localization, we added the NTR and NCR reservoirs located below these LP generators to the schematic view of the model shown in Figure 3.3.1.2. In this figure, we distinguished coherent and incoherent LP sources. The coherent source means that the waveforms are the same among the three crater-rim stations, BOR, SFR and DSR shown in Figure 3.3.1.0. All the LP events observed before September 1993 showed such coherence. After that we began to observe LP events which lost this coherence, and all the LP events after January 1994 until January 2000 showed incoherent wave forms among the crater-rim stations. We placed the

source of incoherent LP events deeper than those of coherent ones, because they disappeared last after the 1992 eruption.
The last LP event during the disappearing phase after the 1992 eruption occurred on April 1, 1995. Its dominant frequency was 2.6 Hz and the waveforms are incoherent among the three crater-rim stations. The first LP events since then confirmed to originate from beneath the summit area occurred on June 4, 1997. The dominant period of this event was 2 Hz and the waveforms are incoherent among the three crater-rim stations. Thus, the last disappearing is similar to the first reappearing, supporting the validity of the model depicted in Figure 3.3.1.2. The time of the appearance is near the end of the presumed filling of the NTR reservoir and the beginning of filling the NCR reservoir, suggesting the proximity of the incoherent 2 Hz LP source to theses reservoirs. The depths of these reservoirs will be estimated from the hypocenters of VT events occurred immediately before the March 9, 1998 eruption in Section 3.2.
The seismicity of VT earthquakes at all depths was extremely quiet for several months after Crisis I. During this period, however, the coda localization was intensified and spread to the southern part of the Enclos caldera. Either the magma transfer was smooth or the structure involved was detached from the source of VT earthquakes. Now we are ready to examine how this initial model functioned immediately before and during the March-September, 1998 eruption.

3.2 Performance of the initial model during the 1998 eruption and its revision afterward

For the first time since the establishment of the monitoring network, the eruption of March, 1998 was preceded by an upward migration of VT events from a depth of about 5 km as reported by Staudacher et al. (1998). The eruption started when the migrating hypocenters reached the surface after an ascent for 1 1/2 days. This migration not only confirmed our model sketched in Figure 3.3.1.2, but also gave the reliable estimate of the depth of the NTR/NCR reservoir at about 5 km below sea level. This is close to the depth of the bottom of the volcanic edifice lying above the pre-existing oceanic crust according to the seismic surveys by Hirn and his coworkers (e.g., Driad, 1997). Thus we find that the whole magma system introduced in Section 3.1 is contained within the volcanic edifice.
This eruption differed from the earlier ones also regarding the relation between the duration of precursory VT swarm and the elevation of the eruption site shown in Figure 3.3.1.1. The observed duration of the precursory seismic crisis, 1 1/2 days, will predict a wrong result. The eruption site predicted by the empirical relation is at a very low elevation, but the actual eruption started from the summit path. This demonstrates that an empirical relation from past data alone may not be useful for a prediction of future, simply because the physical system under a volcano changes with time.
In fact, such a change was reflected in the observed characteristic of LP event. Although the first 1 Hz LP event recorded 5 hours before the eruption is consistent with the shallowness of the 1 Hz LP source in our model as depicted in Figure 3.3.1.2, the waveform of this event did not show the coherency among the three crater-rim stations. As discussed earlier, this lack of coherency indicates that the source of the revived LP event no longer had the horizontally extended geometry beneath the summit as did in 1980's.
We now know that the horizontally extended LP source reappeared in January 2000, and the observed duration of the precursory seismic crisis for the eruptions

after the reappearance agrees well with the prediction by the empirical relation shown in Figure 3.3.1.1. For example, the duration for the January 2002 eruption, 6 hours, predicts an elevation of 1900 m in an excellent agreement with the actual one. Thus, the empirical relation can be useful when the physical system is in the applicable condition. If we had only the empirical relation given in Figure 3.3.1.1 alone without our model, we must have made a wrong prediction in 1998 by insisting on its applicability (which might have had a serious social impact because of the proximity of predicted eruption site to populated areas), and another wrong prediction in 2002 by discarding it because of the failure in 1998. The model allows the flexibility and quick adjustment that lack in the empirical prediction based only on past data.

Our initial model allowed us to interpret the observation during the early days of the 1998 eruption as follows: The ascending magma tried to find the way to erupt through both the summit path and the rift-zone path. The former path must have had relatively low resistance and it broke through first. The eruption started with a lava flow from a fissure near the summit of the central cone, and extended downward in en-echelon segments. The curtain of lava fountains was formed along the fissures, but the one along the near-summit slope disappeared in about 10 hours, and the eruptive activity became concentrated at two centers, named "Piton Kapor" and "Maurice and Katia Krafft" crater, as shown in ***Figure 3.3.2.1***, at an altitude, 2150 m and 2080 m, respectively, in the depth range intermediate between the summit path and the rift-zone path as classified in Figure 3.3.1.1.

Figure 3.3.2.2 shows the tremor amplitude observed at station Phr averaged over 10 seconds, plotted against the time of measurement. The amplitude can be safely considered as the intensity of the tremor source because of the stability of the propagation path effect on this relatively distant station (6 km from the Piton Kapor). At any time during the eruption episode, the iso-amplitude contour at distances greater than 5 km became roughly circular with the center close to Piton Kapor and M. and K. Krafft craters. The decay of amplitude is similar to that of seismic waves generated by rock falls mentioned in Section 3.1. They fit well with the theoretical decay for surface waves with a Q factor of 40 to 60, which again agrees well with the Q factor determined by Koyanagi et al. (1995) for the summit area of Kilauea, Hawaii. We also observed at TCR a phase difference of 90 degrees between the vertical and horizontal component, corresponding to a retrograde motion for waves propagating from east, suggesting that they are the fundamental mode Rayleigh waves. An isolated eruption site named "Fred Hudson" southwest of the central cone (Figure 3.3.2.1) opened on March 12 had a negligible effect on the tremor amplitude.

The tremor amplitude shown in Figure 3.3.2.2 indicates a sharp rise and quick decay within about 10 hours after the commencement of the eruption. This corresponds to the vigorous fountaining from fissures opened successively downward starting from the one near the summit mentioned above. There are two steep rises beginning on March 13 and 17, which do not appear to correspond to any changes in morphology of the eruption sites. We interpret them as the opening connection to a magma reservoir through the rift-zone path, because the peak zone of the amplitude distribution during this phase extended to the summit area, as shown in Aki and Ferrazzini (2000), suggesting magma movement through the rift-zone path activating the LP tremor sources beneath the summit.

The tremor amplitude reaches a peak on March 18 and decays gradually to the end of March, by which time venting was restricted to Piton Kapor. Then the amplitude suddenly increases by a factor of 5 on March 31 followed by a quick decay. We attributed this to a change in the near-surface condition at Piton Kapor, because the vent was closed before the sudden increase in tremor amplitude, and vigorous fountaining followed it. The closure of the vent must have increased the pressure in gas filled lava and caused subsequent active fountaining and tremor amplitude increase. A similar sharp rise and quick decay observed on April 5 may also be attributed to the near-surface condition at the eruption site.

After about 2 months of ups and downs, the amplitude of the tremor originating from the eruption site became nearly constant as shown in Figure 3.3.2.2. We interpreted this to an opening of a channel between the eruption site and a reservoir with a large capacity, because in order to maintain a constant pressure gradient through the channel despite the withdrawal of magma, the reservoir must have an infinite capacity. As described below, this temporal behavior of the tremor was synchronous with the change in the chemical composition of erupted lava and will lead us to a significant revision of our model. In this revision, the isolated eruption site named "Fred Hudson" mentioned earlier plays an important role. We did not recognize its importance at the time of eruption partly because it had negligible effect on the observed tremor, and partly because it was not compatible with our initial model. This underlines the importance of having many models or a model of many attributes to accommodate a variety of scenarios in prediction science.

Lenat and Bachelery (1988, 1990) proposed a model of magma system under Piton de la Fournaise based on a variety of observations covering petrology, geochemistry, geodesy and seismology. Their model is radically different from our initial model. It consists of numerous small magma reservoirs located at a few hundred meters below sea level or shallower depths beneath the summit area as shown in ***Figure 3.3.2.3*** reproduced from their 1990 paper. They are assumed to have been filled with magma in 1977 or earlier and supplied lava for all eruptions after 1977 without any additional supply from below.

The geochemical data from the 1998 eruption analysed by Semet and coworkers (1999) revealed that the chemical composition of erupted magma showed a large variation during the first two months of eruption followed by a smoothly varying trend in a manner similar to the variation of the tremor amplitude as shown in Figure 3.3.2.2. Bachelery (1999) interpreted the geochemical result in the following way. The lava erupted in the first two months can be considered as that of the old magma remaining since 1977, and the lava erupted afterward as the result of gradual mixing between the old magma and the newly arrived magma represented by the lava erupted at the Fred Hudson site.

The unified model is constructed by merging our initial model with the Lenat-Bachelery model as sketched in ***Figure 3.3.2.4***. It now contains a few small magma reservoirs remaining since 1977 in addition to the elements in our initial model. When the new magma came close to these reservoirs of old magma, they were stimulated to higher pressure and erupted through the summit path and later through the rift-zone path. During the first two months the new magma could not enter the reservoir occupied by the old magma, but a small part of it found a way out to the surface erupting at the Fred Hudson site. Two months after the beginning of the eruption, the new magma finally became in contact with the old magma marking the beginning of their mixing. This time must coincide with the opening of the hydro-dynamical connection between the eruption site and the reservoir of large capacity as inferred from the temporal variation of the tremor amplitude shown in Figure 3.3.2.2.

We naturally identify this large capacity reservoir with the NTR/NCR reservoir of our initial model. In other words, the observed synchronous temporal variation in the lava geochemistry and the seismic tremor amplitude requires a large deep reservoir under Piton de la Fournaise that was detected earlier by the coda localization observed during the 15 month period from the seismic crisis of

November 26, 1996 to the beginning of eruption on March 9, 1998. Thus we need not only to develop a model that can synthesize data from different disciplines, but also to monitor data that can constrain the model effectively.

Near the end of the 1998 eruption, we had an opportunity to confirm the validity of our magma location method. On July 28, an M=2.0 earthquake occurred at 04:19 GMT, off shore to the south of the summit, allowing the mapping of coda localization. It was the only useful earthquake for the coda study during the eruption, but the result rendered a strong support to our association of coda localization with the presence of magma. As shown in Figure 24 of Aki and Ferrazzini (2000) (please note that the correct figure is in Figure 14 by an editing error), we found the peak zone centered about the main eruption site, Piton Kapor. The peak zone is elongated in the northeast direction roughly coincident with the rift zone in this area.

The 1998 eruption lasted for more than 6 months with the output of lava amounting to 60 million cubic meters covering the area shown in Figure 3.3.2.1. The large lava output is consistent with the large capacity of deep reservoirs included in our initial model. The depth and the stored amount of magma roughly meets the constraint imposed by the space geodesy result of Sigmundsson et al. (1999).

3.3 Recognition of cycles in the eruptive history and a further revision of the model based on observations during more recent eruptions

After the 1998 eruption, Piton de la Fournaise continued to be active with 8 eruptions during the following 3 years and 4 months. They occurred in July 99, Sept. 99, Feb. 00, June, 00, Oct. 00, March 01, June 01 and Jan. 02. Their duration ranges from 8 to 37 days with the mean of 22 days and the total amount of lava output was estimated to be about 50 million cubic meters (Staudacher et al., 2002). During this period, the character of LP events occurring beneath the summit changed. As mentioned earlier, the coherency of the LP waveforms consistently observed in 1980's and early 1990's was lost around 1994. When LP events reappeared in 1997, the waveforms were incoherent among the crater-rim stations. The incoherency persisted throughout the 1998 eruption and later until January, 2000, suggesting that the horizontally extended LP source was not existing at the time of the 1998 eruption, and took about 2 years to develop under the summit after the arrival of new magma. The first LP events showing the coherency since 1994 appeared on January 14, 2000 with the dominant frequency of 4 Hz, indicating probably a smaller source. The first 1 Hz coherent LP event since 1992 appeared on August 16, 2000. The waveforms were very similar to those observed in the 1980's. By this time the shallow, horizontally extended, reservoir beneath the summit must have been well reestablished.

With this change in the structure of the magma system, the style of eruption also changed. The four eruptions (July 99, Sept. 99, Feb. 00 and June 00) before that time showed a gradual decay in tremor amplitude near the end of eruption (which suggests stopping due to emptied reservoir) with no associated LP events, while the three eruptions (Oct 00, March 01 and June 01) after that time ended abruptly followed by a swarm of 1 Hz LP events. We attributed such LP events following the stopping of a summit eruption to the diversion of magma from the summit path to the rift-zone path in Section 3.1. We recognized two summit eruptions with a similar stopping style prior to the rift-zone eruption outside Enclos in 1986. The October-November, 2000 eruption was different from earlier ones in 1999 and 2000 also in the temporal behavior of the eruption tremor. The amplitude decayed quickly after the beginning of the eruption as usual, but later gradually increased with accelerating rate to a high steady value, suggesting an involvement of new magma supply coming from depth.

The January 2002 eruption occurred when we were concerned about the possibility of another eruption in the rift-zone outside Enclos because of the above similarity in the eruption style to the 1986 episode. Fortunately, it did not go out of Enclos although the lava flow reached the ocean and an evacuation order was issued to a nearby village. A preliminary look at the petrology of the lava suggested that this eruption might have involved newly arrived magma. Looking for some other unusual marks before the January 2002 eruption, we found that the site of the 14 February, 2000 eruption was located away from the others occurred since 1999. Remembering the peculiar location of the Fred Hudson vent in relation to the main site of the 1998 eruption, we looked at two other periods in which one might expect the arrival of new magma. One such period is just after the 6-year inactivity period ended in 1972 and the other is before the major oceanite eruption of 1977. We found that the site of the June 9, 1972 eruption, the first eruption after the 6-year inactivity period, was close to the Fred Hudson vent, and the site of the November 2, 1976 immediately preceding the 1977 eruption was close to that of the February 14, 2000.

Stimulated by the above discovery, we mapped the sites of all 47 eruptions since 1972 following Benard and Krafft (1986) and various observatory reports. There are 13 eruptions located on the west side of the N 15 E trending line passing through the summit of Bory. This area, which we shall call "Bory west", is shown in ***Figure 3.3.3.1 (Figure 2.1 of Part 2)*** together with the NE and SE rift-zones and the area we shall call "Dolomieu east". In addition to the four eruptions mentioned above, the Bory west area contains the eruption site of the June 14, 1985 eruption preceding the 1986 eruption outside Enclos and that of the June 11, 1987 eruption preceding a sharp increase in erupted volume at Piton de la Fournaise as shown in ***Figure 3.3.3.2 (Figure 2.3 of Part 2)***. It is natural to divide the whole period into three cycles of 13-year duration, each starting with an eruption in the Bory west area. In each cycle, there is a second eruption in the Bory west area marking the second phase of high activity. The first eruption sites are near the southern end of the area, and the second ones near its northern end.

The remaining eruptions in the Bory west area, as shown in ***Table 3.3.1***, includes a sequence of 5 eruptions between July 13, 1979 and January 18, 1984 with the total lava output of 24 M cubic meters, during which there was no eruption in the other three areas except one with an output of 5 M cubic meters in the NE rift-zone. This sequence is followed by the June 14, 1985 eruption identified as the beginning of Cycle II, and then by an exceptional seismic crisis called "east flank crisis" on July 10-11, 1985. This crisis was not followed by an eruption as listed in Table 3.1.1 and did not occur below the central cone as usual. It was unusual also in the range of their focal depths covering from 1 km b.s.l. down to 6 km b.s.l. Lenat et al. (1989c) attributed this crisis to the stress induced by intrusion of magma into the fracture system associated with the preceding series of eruptions in the Bory west area. A similar explanation was given by Zlotnicki et al. (1990) for the displacement vectors obtained by photogrammetric areal surveys made in 1981 and 1983. The deep origin of the seismic crisis suggests that the source of magma for these eruptions are not supplied from the shallow magma patches hypothesized by Lenat and Bachelery (1990). The upward migration of the eruption sites of the sequence after December, 1983 also appears to favor the deeper source of magma supply. We shall come back to this sequence later in the prediction of the future activity (as of April, 2002). (The explanation of the remaining two eruptions, the September 9, 1972 and August 31, 1988 is given in the appendix of Part 2 of this lecture note.)

One may question why these new arrivals of magma associated with the eruption in the Bory west area have never given rise to the upward migration of the precursory seismic events as observed in 1998. The answer is that the fluid flow through a smooth channel without barriers to flow is usually aseismic. Many years ago, I participated in the so called "Hot Dry Rock Project" at the Los Alamos National Laboratory, in which a fracture is formed in a hot rock to extract thermal energy by circulating water through it. After numerous controlled experiments, a consensus was developed among seismologists that the fluid flow is usually aseismic, and generate seismic signals only when it encounters some barriers to overcome.

Our model of the magma system in Piton de la Fournaise now requires a 3-D presentation. Our initial model shown in Figure 3.3.1.2 is still valid for the N-S vertical cross-section through the summit of the central cone, if we replace the label "summit path" by "Dolomieu east" and add small reservoirs of Lenat and Bachelery. The corresponding E-W cross-section passing the summit will not have the rift-zone paths. Instead the magma path from the depth is inclined to the west, and separates into two eruption paths. One goes straight to the eruption sites in the "Dolomieu east" area, and the other goes vertically to the Bory west area defining a dike-like structure trending at about N15E, and branching from the main path at some point deeper than the elevation of the horizontally extended LP source. The main magma path inclined to the west is clearly recognizable in recent 3-D images from seismic tomography by Hirn and his coworkers as a high velocity body. It is of high seismic velocity, because the fluid magma fills cracks and joints of the volcanic edifice and solidify them. The magma conduits must be harder than the surrounding, and we may visualize a system of several such channels connected at a junction below the summit. Such a system of channels will cause stress concentration at their junction wherever the fluid flow meets barriers to overcome. That seems to be the reason why we observe a swarm of VT events (called seismic crisis) wherever the fluid moves in the system. A sketch of the above 3-D structure of the magma system is given in ***Figure 3.3.3.3*** (***Figure 2.2 of Part 2***).

Now we like to address the question about the future (as of April, 2002). First, we are in Phase 2 of Cycle III, with lava output of already 110 M cubic meters since the beginning of the present cycle. The total output from Cycle I and II are 101.7 and 118.7 M, respectively. If the total amount should be roughly the same for each cycle, we are in the declining period of Cycle III. Second, if the fundamental period of 13 years is stably fixed by the magma supply process in the mantle, the next new arrival of magma will be in 2011. From the viewpoint of physical state of the magma system, at present we observe LP events originating from beneath the summit, indicating that the horizontally extended LP source exists now. As of April, 2002, we observe a very high steady activity of LP events, highest in Cycle III so far and comparable to the activity in 1989 which marked the beginning of the declining phase of Cycle II. (More detailed chronological description of the eruption history since 1972 and the prediction as of June, 2003 is given in the appendix of Part 2.)

If, however, something unusual happen at the magma supply process deep in the crust-mantle and a new magma arrives unexpectedly from depth, we shall observe its first indication in the Bory west area. Looking at ***Table 3.3.1*** more carefully, we notice that the Bory west eruptions in Cycle III show much longer duration than those at the beginning of each phase in Cycles I and II. Their durations are comparable to those of the sequence of 5 eruptions between July, 1979 and January, 1984, which was associated with the deep seismic crisis of July 10-11, 1985. Phase 2 of Cycle I which included the above sequence started with the July 13, 1979 eruption. Since this eruption site is close to that of the February 14, 2000, the first eruption of Phase 2 of Cycle III, a similar sequence may happen in the present phase. Thus at present, both the declining and reviving scenarios seem to be possible. We can perhaps tell which is right by closely watching the level of the LP seismicity beneath the summit and eruptions in the Bory west area.

Table 3.3.1 List of eruptions in the Bory west area during the period from 1966 to 2002.

	Start date	Duration in days	Erupted lava in M cubic m	Remarks	Cumulative Lava erupted in the whole area
1	1972/6/9	2	0.1	beginning of Cycle I	0.1
2	1972/9/9	19	5		8.1
3	1976/11/2	2	0.3	beginning of Phase 2 of Cycle I	24.4
4	1979/7/13	1	0.3		72.7
5	1981/2/3	18	3		75.7
6	1981/2/26	32	4		79.7
7	1983/12/4	46	8		92.7
8	1984/1/18	32	9		101.7
9	1985/6/14	1	1	beginning of Cycle II	102.7
10	1987/11/6	3	1.6	beginning of Phase 2 of Cycle II	165.6
11	1988/8/31	57	7		205.6
12	1998/3/12	21	1	beginning of Cycle III	291.4
13	2000/2/14	19	4	beginning of Phase 2 of Cycle III	298.7

The 3-D view of the structure of the magma system in Figure 3.3.3.3 and the temporal regularity in the eruption history in Figure 3.3.3.2 together represent our current (as of April 2002) perspective on the working of Piton de la Fournaise. We like to emphasize that cycles identified on the curve of the lava output in Figure 3.3.3.2 was not based on the characteristics of the curve itself, but on the internal physical process inferred from our model of the magma system sketched in Figure 3.3.3.3. If cycles were identified only from the observed curve, it will be rigid and inflexible as the empirical relation between the precursory crisis duration and the elevation of the eruption site discussed earlier. If the condition of the magma system changes, it will make a wrong prediction, and will be discarded as useless; a double mistake. The earthquake prediction research may be full of these double mistakes. We can avoid these mistakes by developing a model that can accommodate the changing condition through the monitored data. We see here again the importance of close interplay between modeling and monitoring for the prediction research.

We may summarize the lessons learned from Piton de la Fournaise for prediction science as follows:

(1) *We need a physical model to which we can ask about the current condition and the future course of the magma system.* In the case of the 1998 eruption, the model allowed an estimation of the time of eruption from the time of filling the NCR reservoir, and also allowed a quick adjustment of scenario when the observation contradicted the empirical relation between the eruption site and the precursory swarm duration.

(2) *We need to monitor observables which constrain the model effectively.* In our case, they are VT events, eruption tremors, LP events, and coda localization. The first two are commonly used for the short term prediction and monitoring of active volcanoes. The third has begun to be monitored at some volcanoes, but the last one is new and was most effective for the long-term prediction of the 1998 eruption. The scientific community must be broad-minded to permit applications of new methods for the purpose of prediction.

(3) *We need to assume the initial condition of the study system when we start the process of monitoring and modeling and must be prepared for its revision in the course of the process.* We were fortunate to start our process when the volcano was in an unusually quiet period allowing a simpler assumption than otherwise and were able to correct it later by including the old patches of magma remaining at shallow depths.

(4) *We need to be prepared for a possible change in the system structure with time.* We found that the coherency of LP events among the three crater-rim stations, which was attributed to the existence of a horizontally extended source beneath the summit, disappears and reappears as the magma system changes due to a cyclic supply from the mantle. An empirical relation developed during the period of its existence did not apply to eruptions in the period of its non-existence.

(5) *In order to cope with the diversity of the process possible in the future, it is important to generate many scenarios by considering all available models.* In the case of the 1998 eruption, we had both our initial model and the Lenat-Bachelery model before the eruption, but could not conceive the unified model presented in Section 3.2 until 1 year after the eruption partly because of our narrow-mindedness regarding models generated from other disciplines.

(6) *A daily contact with the monitored data and a frame of mind prepared by the model construction are both essential for detecting subtle precursory phenomena.* We started the on-site search for LP events in August, 1995 during the quietest period of activity in recent decades and found no LP events large enough for a conclusive identification for nearly two years. When we observed the first LP event definitely originating from beneath the summit area on June 4, 1997, we were convinced immediately that the magma was coming back to the volcanic edifice. If we had been doing the same work remotely without a daily contact to the monitored data, we might have missed the recognition of its importance.

Chapter 4. Application of lessons learned from Piton de la Fournaise to earthquakes

The lessons learned from Piton de la Fournaise impacted my thinking about earthquake prediction in general and about precursors in particular in a fundamental and far-reaching way. First, I recognized that I myself made the double mistake mentioned in the concluding remark of Chapter 3 regarding the coda Q precursor. Section 4.1 will describe how all the inconsistencies surrounding the coda Q and N(Mc) discussed in Section 1.3 are resolved and unified to support a new practical procedure which will enable us to tell whether a given seismic region is approaching a major earthquakes in several years or not.

4.1. Reinterpretation of the observed correlation between coda Q^{-1} and N(Mc)

At the time of my move to the Reunion island, I was discouraged by the observations about coda Q as expressed in Aki (1996), quoting the work of Jin and Aki(1993), that the coda Q precursor was not reliable because the characteristic pattern observed before some major earthquakes was not observed before others, and in some cases a similar pattern was not followed by any major earthquakes. Examples can be found in Figure 3.1.3.10 showing the temporal variation of coda Q in Southern California and Central California for about 50 year period. The characteristic precursory peaks in coda Q^{-1} were observed before the Loma Prieta earthquake (M7.1) of 1989 and the Landers earthquake (M7.3) of 1992, but not before the Kern County earthquake (7.5) of 1952. It also shows several strong peaks not followed by any major earthquakes.

We had some understanding of the temporal variation in coda Q as discussed in Section 1.3, from its strong positive simultaneous correlation with the frequency of earthquakes in a specified range of magnitude, the lower bound of which is called Mc. The correlation was found in California by Jin and Aki (1989, 1993)), in Japan by Tsukuda (1988) and Hiramatsu et al. (2000), in New Zealand by Robinson (1987) and in China by Jin and Aki (1986). The observed correlation was explained by Jin and Aki (1989, 1993) by the existence of creep fractures in the brittle-ductile transition zone with a size characteristic to a given seismic region. The increased creep activity in the ductile part would increase the seismic attenuation (coda Q^{-1}) and at the same time produce stress concentration in the brittle part stimulating the occurrence of earthquakes with a characteristic magnitude Mc corresponding to the characteristic size of the creep fracture. The value of Mc inferred from the correlation was 3 to for most regions, with the notable exception (Mc<2) of the case of the Misasa earthquake studied by Tsukuda. This exception was very convincing and troubled me, because otherwise I could assert that the value of Mc is nearly universal and corresponds well to the two other nearly universal constants, namely, the source-controlled f_{max} and the corner frequency at which the departure from the self-similarity occurs described, respectively, in Sections 1.1 and 1.2. The universality of these constants would offer a basis for constructing quantitative models of seismogenic structure. Furthermore, I did not know how the creep model can be related to the occurrence of major earthquakes. It was only explaining the relation between the coda Q^{-1} and the occurrence of small earthquakes, and their simultaneous correlation in time appeared to be useless as a precursor.

After recognizing a cycle in the eruptive activity of Piton de la Founaise and considering the particularly erratic behavior of the LP events as a precursor as explained in Chapter 3, it occurred to me that the period in which the strong correlation exists between coda Q and the frequency of earthquake with magnitude Mc may correspond to a particular phase in the regional earthquake cycle which does not involve the occurrence of large earthquakes, because there is a suggestion of the departure from perfect simultaneous correlation just before the Loma Prieta and Landers earthquakes as shown in 3.s 1.3.11 and 3.1.3.13, respectively.

With regard to the peaks in coda Q^{-1} not followed by earthquakes conspicuous in Central California, I recall the evasive character of the LP seismicity at Piton de la Fournaise. As explained in Section 3.3, the LP swarm was found during the precursory seismic crisis of eruptions through the rift-zone path, but not for those through the summit path. They occur, however, near the end or immediately after some of the summit eruptions. Furthermore the LP seismicity is in general higher during the declining phase than the height of activity in the eruption cycle. If we tried to use the observed LP seismicity for predicting eruptions without understanding through our model of magma system we must have been baffled by the apparent inconsistencies. It may be that the large variation of coda Q^{-1} without any associated major earthquakes, as observed prominently in Central California during the 50 year period from 1940, may reflect the low level of tectonic stress in the earliest phase of regional cycle probably started after the 1906 San Francisco earthquake.

The coda Q is the only observable related to the seismogenic structure that have been measured long enough for covering a significant portion of an earthquake cycle of a seismic region. A series of work by Li and his coworkers, using the fault-zone trapped waves, successfully confirmed the temporal change in velocity and attenuation within a fault zone related to the healing after the occurrence of an earthquake (e.g., Li et al., 1998) and there are in general revived interest in monitoring seismic velocity particularly in Japan, but their time spans of monitoring are still too short to cover a significant portion of the regional earthquake cycle.

As a possible effect of the regional cycle on coda Q, we notice a trend of steady increase in coda Q^{-1} by a factor of about 3 from late 1950's to 1990 for Southern California. According to Jones (1992), the annual frequency of earthquakes with M>6 in Southern California increased from 0 to 0.6 during the same period. The Kern County earthquake occurred just before this period, and the Landers earthquake at its end. According to the earthquake catalog compiled by Ellsworth (1990) major earthquakes (M>6) in Southern California after the great earthquake of 1857 till the Long Beach earthquake of 1933 seem to have occurred on the faults subparallel to the San Andreas fault, but afterwards their activity has shifted to two separate zones transverse to the San Andreas system, one including the Kern County earthquake and the other the Landers earthquake.

There are numerous observations on seismicity that have been linked to different phases of the regional earthquake cycle. For example, Mogi (1981) defines five phases of the cycle for the giant earthquake along the Nankai trough in terms of the seismicity pattern including the so called "Mogi's donut". The "quiescence" at the center of the donut is probably the precusory seismicity pattern most often reported in literature with well established success stories such as the prediction of the Oaxaca earthquake of 1978 by Ohtake et al. (1977). Wyss and Habermann (1988) reported 17 significant cases of precursory quiescence for earthquakes in the subduction zone (11 cases), inland (4 cases) and volcano (2 cases).

A standard explanation of the quiescence (e.g., Kanamori (1981) and Mogi (1982)) has been to assume a finite number of asperities of small and medium sizes ready to break in a region where a large earthquake is expected. After these asperities are all broken as small and medium size earthquakes, the region ran out of the asperities except the one preparing for the large one. Habermann (1988) points out, after a thorough review of the observed quiescence, the difficulty of this explanation regarding the onset of the quiescence and change in the seismicity rate. Scholz (1988) reviewed various observations on the precursory quiescence and proposed that the explanation may be found in fault zone dilatancy hardening and/or slip weakening within a nucleation zone following a behavior known in rock mechanics as the Kaiser effect which requires only a very slight increase in strength to cause quiescence.

Here we come to the central idea for reinterpreting and unifying all available observations on the coda Q^{-1} and N(Mc). That is the idea that whatever causing the quiescence in the earthquake preparation zone in the brittle part of lithosphere may disturb the loading process of tectonic stress coming primarily through the underlying brittle-ductile transition complex introduced in Section 2.1. If we look back at the relation between the coda Q^{-1} and the relative frequency N(Mc) of earthquakes with the characteristic magnitude Mc=4 for Central California shown in Figure 3.1.3.11, we notice a sudden departure from the high correlation between the two at about two years before the Loma Prieta earthquake of 1989. We also recognize a similar departure for Southern California, with Mc=3, several years before the occurrence of the Landers earthquake of 1992 as shown in Figure 3.1.3.13. Apparently the strong positive correlation between the two time series represents the normal period of the tectonic stress loading process in the brittle-ductile transition complex and the precursory hardening or weakening of the brittle part disturbs the correlation.

Let us look more closely at the change in coda Q^{-1} and N(Mc) before and after the Loma Prieta earthquake as shown in ***Figure 3.4.1.1.*** The positive simultaneous correlation between the two time series clearly shown before 1987 is suddenly disrupted by the decrease in N(Mc) in 1988. The coda Q^{-1} keeps increasing at this time, but turn to a sharp decrease about 1 year later, at which time there is no simultaneous change in N(Mc). So the positive correlation between the two time series was lost during the 2 year period preceding the occurrence of the mainshock. The mainshock has no visible effect on the coda Q^{-1} because the temporal change in coda Q^{-1} is affected primarily by the fractures in the brittle-ductile transition complex rather than those in the brittle part as discussed in Section 1.3.

Unfortunately, at present, we do not have the complete data before and after the Landers earthquake, but it is clear from Figure 3.1.3.13 that the sharp rise in coda Q^{-1} started at 1986 was not accompanied by a similar increase in N(Mc), indicating the beginning of a disruption of the positive correlation about 6 years before the Landers earthquake,. A quiescence in the epicentral region of the Landers earthquake started in January, 1988, 4 1/2 years before and lasting up to the earthquake according to Wiener and Wyss (1994).

Next, we looked at the 10 year period before and after the Kern County earthquake of 1952, the largest in Southern California since 1857 as shown in ***Figure 3.4.1.2.*** We see again the disruption of the positive correlation between coda Q^{-1} and N(Mc) beginning in 1948, 4 years before the mainshock, at which time N(Mc) shows sudden decrease but the coda Q^{-1} continue to increase in the same manner as in the case of the Loma Prieta earthquake.

When we look again at the result on coda Q^{-1} and N(Mc) obtained for the Tamba region by Hiramatsu et al. (2000) with this new idea, we find a remarkable thing. The authors might have noticed it without mentioning, but there was a clear precursory change both in coda Q and N(Mc) before the Hyogo-ken Nanbu earthquake as shown in Figures 3.2.1.7 and 3.2.1.8. The authors divided the period of study into five consecutive 2-year segments in such a way that the time of the mainshock corresponds to the boundary between the fourth (IV) and the fifth (V). In periods I, II and III, coda Q^{-1} decreases while N(Mc), for both Mc=2.5 and Mc=3, also decreases. In period IV, however, N(Mc) for Mc=3 starts increasing while the coda Q^{-1} continues to decrease. In other words, the correlation between the two time series was positive in I, II and III, and became negative for 2 years or so before the earthquake.

I mentioned earlier about the study of coda Q and seismicity precursory to the Miasasa earthquake (M=6.2) of 1983 by Tsukuda (1988), which troubled me because of the low value of Mc obtained under the assumption of the positive correlation between coda Q^{-1} and N(Mc). The observed temporal change in both seismicity and coda Q are shown in ***Figure 3.4.1.3***. The seismicity change is rather complicated with a clear quiescence in 1978-79 followed by a sharp rise in 1980 and return to another quiescence immediately before the occurrence of the earthquake. The change in coda Q was also complicated with double peaks in the coda Q^{-1}, but the correlation between the coda Q^{-1} and the frequency of earthquake is definitely negative for almost 10 years before the earthquake. Our new interpretation of Tsukuda's observation, as indicating the disruption of the normal period characterized by the positive simultaneous correlation. leaves us free from our earlier conclusion about the value of Mc less than 2, and allows us to raise the value of Mc closer to the nearly universal value of 3 to 4.

We can probably add the case of the North Palm Springs earthquake (M=5.6) of 1986 studied by Su and Aki (1990) to our list of test cases, but the limited data on earthquake frequency given in the paper does not allow us to find conclusively about the nature of correlation between coda Q^{-1} and N(Mc). Likewise for other studies of coda Q precursor mentioned in Section 1.3, the data are not complete yet to find whether the positive simultaneous correlation was disrupted or not before the occurrence of earthquake.

On the other hand, we have the case of Wellington, New Zealand studied by Robinson(1987)) in addition to Southern and Central California to support the positive simultaneous correlation for the normal period. He combined the data on the duration magnitude Md and the amplitude magnitude M of local earthquakes in the subduction zone under the Wellington region to estimate the temporal change in coda Q, and found a significant change during the period 1978-85 with a similar time constant of fluctuation as found for California. He found a clear negative correlation between the coda Q (expressed by the cumulative monthly mean of Md-M) and the cumulative monthly rate of local earthquakes with magnitudes greater than 3.0 as shown in ***Figure 3.4.1.4*** indicating that Mc=3 (the earlier estimate of 5 by Jin and Aki (1993) is revised here to conform the definition of Mc as the lower bound magnitude as given in Section 1.3) in this region. There was no major earthquake during the period of this study.

(The case of Stone Canyon studied by Chouet (1979) is interpreted, in Section 2.1 and my May 15, 2003 memo to Keilis-Borok in Part 1 of this lecture note, as an exhumed scaled-down loading process of plate-driving forces at the brittle-ductile transition zone with Mc smaller than other cases.)

Summarizing the results of applying our new interpretation of the coda Q^{-1} -N(Mc) relation to all the cases in which both data are available, we find that the correlation is positive during the normal period and that the positive correlation is disrupted several years before a major earthquake. The value of Mc is nearly a universal constant of 3 to 4 (except for the creeping zone of the San Andreas fault) corresponding to the other nearly universal constants associated with the seismogenic structure, namely f_{max} and the corner frequency at which the self-similarity between large and small earthquakes breaks down. The temporal change in coda Q^{-1} reflects the state of fractures in the ductile part of the lithosphere and that of N(Mc) reflects the state of fractures in the brittle part. The tectonic stress loading on the brittle part from plate motion is done primarily through the interaction of the two parts, and the correlation between coda Q^{-1} and N(Mc) is positive and simultaneous during its normal mode of working. The simultaneous correlation is disrupted by the preparation for a major earthquake in the brittle part, such as dilatancy hardening and/or slip-weakening. (In Part 2, we find that the disruption of the correlation is caused by the delay of coda Q^{-1} relative to N(Mc) by 1 to 4 years for all known cases, in agreement with the idea that it is caused by some change in the brittle part, and suggest that the strain energy accumulated in the brittle part may start flowing back to the ductile part after having reached a saturation limit before a major earthquake.)

The normal period of the loading process may correspond to the stationary state in irreversible thermodynamics of a dissipative system in which the entropy production is minimized (De Groot, 1952; Prigogine, 1967) under the external constraint imposed by the plate-loading forces. Progogine's book suggests explicitly a possible approach for a macroscopic physical modeling of earthquake processes in the framework of the irreversible thermodynamics. A fundamental theorem in the irreversible thermodynamics is the Onsager reciprocity relation describing the cross-coupling between two irreversible processes involved in a dissipative phenomenon. In Chapter IV of the book it is derived under the assumption of linearity between the generalized flow and force starting with the microscopic reversibility of component processes expressed by equation 4.46 of the book. This equation shows that the fluctuations in the component processes have cross-correlation functions which are even-functions with respect to the time shift. This is exactly observed for the temporal variations in the coda Q^{-1} and N(Mc) for the normal period and may express the microscopic reversibility for the process in the brittle part and that in the ductile part of the brittle-ductile complex. Chapter VI of Prigogine's book shows how the Onsager relation leads to the principle of minimum entropy production for a steady state under an external constraint, and Chapter VII and VIII discuss the possible emergence of structures in a dissipative system, like the Benard's convection cell, if the linearity relation between the force and flow breaks down. Our finding of nearly universal value of Mc may be attributed to a formation of such structures in the brittle-ductile complex. It may be that, in the normal period of the earthquake loading process, the microscopic reversibility holds to ensure the steady state characterized by the minimum entropy production, and that such a reversibility may be disturbed when the brittle part approaches to a major earthquake.

Such a steady state may not be found in the case of man-made earthquakes generated by the construction of large high dam or extensive deep mining. The evidence for triggering earthquakes by underground nuclear explosions in the Nevada test sites (e. g., Aki and Tsai, 1972) suggests that such a steady state can be destroyed by man. With land development needed for increasing population in the future, such a destruction of natural steady state may become important. In this sense we may say that an earthquake is an endangered species like some dangerous wild animals.

In addition to the region of man-made earthquakes, there may be particular conditions in which no significant changes in coda Q may occur, for example, due to a poorly developed brittle-ductile complex region. The coda Q in some seismic regions show no temporal change in the normal period as in the case of the Charlevoix, Quebec, region between 1980 and 1991 as reported by Woodgold (1994), for Anza, California between 1982 to 1992 by Aster et al. (1996) and for Parkfield, California between 1987 and 1995 by Antolik et al. (1996). If it is a permanent feature of a certain area, the coda Q^{-1} -N(Mc) precursor cannot be applied to these regions. We then must look for other indicators of the condition of the loading process. On the other hand, we may expect greater applicability of our precursor to a region involving ample fluid supply in the brittle ductile complex. The Long Valley, California with its geothermal activities may be such a region as a significant temporal change in coda Q^{-1} was observed associated with the nearby Round Valley earthquake (M=5.7) of November 23, 1984 (Peng et al., 1987).

The immediate foreshocks and other short-term precursors are probably phenomena occurring within the brittle domain only, and correspond to the swarm of VT events preceding the eruption called the seismic crisis in the case of Piton de la Fournaise as described in Section 3.1. These VT events always occur beneath the summit at about the sea level, wherever the magma intrudes or erupts, and they are essential as a practical means for the short-term prediction of eruption time in the time scale of hours.

My experience with the volcano taught me that we can predict certain things but not everything even with our latest model. For example, the model tells at present (April, 2002) that the volcano is in the declining phase of activity as mentioned in Section 3.3. The next eruption will be in the Dolomieu east or one of the two rift zones unless new magma arrivals are signaled by an eruption at the Bory west area. It cannot, however, tell when and in which of these areas it will erupt. We must wait until the time when the precursory seismic crisis occurs, then we can tell the eruption site by examining the presence or absence of LP events and tracing the migration of its source to the eruption site. This division of short-term and long-term prediction has been well recognized in the practical strategy of the earthquake prediction as in the case of Parkfield experiment mentioned in Section 1.2 and the Tokai, Japan, experiment. We see here again the need for a close interplay between modeling and monitoring for prediction.

4.2. Similarities between earthquake and volcano modeling

Several comparisons made above between the volcanic and earthquake processes suggest that they may be similar not only from the point of prediction strategy but also from the point of physical modeling. The quantitative model used by Aki and Ferrazzini (2001) for a computer simulation of volcanic eruption histories may be helpful to illustrate the similarity from the physical point of view. The model consists of several "reservoirs" that are connected by "channels" to each other. The capacity of the reservoir is defined as the rate of pressure increase per unit net flow coming into the reservoir. The resistance of a channel is defined as ratio of the pressure difference between two ends of the channel to the flow rate. The channel opens when a critical pressure is exceeded, and closes when the flow becomes less than the minimum (critical freezing) flow. Origins of this type of modeling for volcanoes may be traced to electric-circuit analog of Shimozuru (1981) and Decker (1968, 1987).

This type of modeling is not new in earthquake studies. If we replace the mass of magma by the seismic moment of earthquake, it may be considered as a generalization of Shimazaki and Nakata (1980) for modeling earthquake cycles. The slip-predictable model, for example, can be represented by a single reservoir system with a constant minimum flow and a varying critical pressure, and the time-

predictable model by that with a constant critical pressure and a varying minimum flow. After all, an eruption history is an episodic outflow of magma supplied constantly from the mantle, while an earthquake history is an episodic outflow of seismic moment supplied constantly from the plate motion.
The earthquake model developed at the Southern California Earthquake Center described in Section 1.2 may be considered as a set of 65 reservoirs of seismic moment each with a constant rate of moment supply as estimated from geologic, geodetic, instrumental and historic seismological data with the constraint on the total moment flow from plate motion. Some of the reservoirs have their own cycles, but others are the stationary Poisson process. There is no regional cycle in this model.
The shallowest reservoir in the model of Aki and Ferrazzini (2001) is connected to eruption sites through a hierarchy of channels covering a large range of resistance corresponding to the observed variation in the amount of magma for individual eruptions. This hierarchy of channels may correspond to different earthquakes or seismic zones sharing the common source of moment supply.
The mantle reservoirs in the model of Aki and Ferrazzini (2001) receive a supply of magma at a constant rate. There are two of them in order to allow two phases in a cycle as shown in Figure 3.3.3.2. The assumption of the constant rate may correspond to that of a constant plate speed for the earthquake modeling. There is some seismological evidence supporting the constancy of rate of magma supply from the mantle. Aki and Koyanagi (1981) found that the rate of occurrence of deep tremors at depths around 30 km under Kilauea, Hawaii is nearly constant over the period in which the mode of eruption at the surface changes greatly. They interpreted the amplitude of tremor in terms of the magma flow rate, suggesting that the rate of magma supply from the mantle may be constant in spite of the episodic behavior of eruption history. The sources of deep tremor and deep LP events under Kilauea were conclusively identified with the magma path from the mantle hot spot by Wright and Klein (2003).
The characteristic earthquake with the permanent asperities and barriers presumed responsible for its existence introduced in Section 1.1, corresponds precisely to a reservoir in our volcano model. Some characteristic earthquake may change its character in time like a reservoir. As mentioned in Section 1.2, the characteristic Parkfield earthquake might have changed its character significantly in 1966, when the fault step at its southern end was broken as shown by Segall and Du (1993) from geodetic data and Aki(1968) and Bouchon (1979) from strong motion data.
The eruption in the Bory west area of the Piton de la Fournaise is not very significant in terms of amount of lava output, but extremely important as the indicator of the new arrival of magma from depth as discussed in Section 3.2. Its counter part in earthquake cycles may be found in several seismotectonic models proposed as guides for earthquake prediction research in Japan. Examples are the Odawara earthquake anticipated to trigger the great Tokyo Metropolitan earthquake as proposed by Ishibashi (1976, 1992), and the Miyagi-ken Oki earthquake of 1978 having triggered the Nihonkai Chubu earthquake of 1983 as proposed by Mogi (1998).
Sometimes a part of magma coming from the mantle stays within the volcanic edifice and never appears to the surface as well known in the case of intrusion into Kilauea's rift-zone. Likewise, some seismic moment is lost as aseismic fault creep in the brittle part of lithosphere.
A new insight may be gained by the inclusion of reservoirs of seismic moment in the brittle-ductile transition complex corresponding to the magma reservoir near the bottom of the volcanic edifice. By this inclusion, the seismic moment supply from

the plate motion to the brittle part can become episodic rather than constant, and may serve for a physical interpretation of various intriguing behaviors of earthquake occurrences in regions far from the plate boundaries such as long-term migrations of active regions and alternating activities between adjacent seismic regions. The coda Q, may help to quantify such processes, as Jin and Aki (1988) suggested that the low Q region inferred from the historical data on seismic intensity might have migrated with the high seismicity region in North China with a time constant around three hundred years.

The coexistence of old and new magma in the volcanic edifice was well demonstrated for Piton de la Fournaise in Section 3.2. Old magma can stay for a time well beyond the basic cycle period even in the shallow part of the edifice. On the other hand, geologic studies of active faults revealed nearby earthquake faults with very different recurrence intervals. If we can extend the analogy of old and new magma under a volcano to earthquake processes, we may postulate seismic moment reservoirs surviving for a long time, while the neighboring or overlapping areas can go through many cycles of moment release. We may even speculate a possibility that a region containing old seismic moment may be stimulated to release it by the approaching new batch of seismic moment as in the 1998 eruption of Piton de la Fournaise described in Section 3.2.

As mentioned in Chapter 3, when the horizontally extended LP source is well developed under the summit of Piton de la Fournaise, magma moves more freely in the shallow part of the volcanic edifice, reducing the pressure and consequently the eruptive activities. Apparently when the volcano is in such a condition, the magma system becomes sensitive to external effects. During the declining phase from 1989 to 1993, we observed a remarkable annual periodicity in the LP seismicity probably due to rainfall (annual rate of 10 meters) as well as a sudden termination of a very high LP activity by shaking due to a moderate-size earthquake in Madagascar 800 km away. We may find examples of their counter part in earthquakes such as the appearance and disappearance of correlation between the tidal stress and various earthquake related phenomena.

We summarize the above discussion by showing a list of corresponding elements used for modeling earthquakes and those for modeling volcanoes in ***Table 3.3.1*** (As we drew attention in Part 1 and Part 2, however, we now see a far more fundamental similarity between earthquake and volcano processes than listed here. Both are at the contact point of Geodynamics and Non-linear Dynamics, and the interaction between the ductile part and brittle part plays an important role in the precursory phenomena for both earthquake occurrence and volcanic eruption.)

Table 3.3.1. Comparison between earthquake and volcano modeling by a system of Reservoirs and channels

EARTHQUAKE	VOLCANO
Seismic moment	Mass of magma
Slip-predictable model	Single reservoir constant critical minimum flow
Time predictable model	Single reservoir with constant critical excess pressure
SCEC 1995 model for Southern California	65 reservoirs with independent constant magma supply rate
Episodic outflow of seismic moment	Episodic outflow of lava
Constant supply of moment from plate motion	Constant supply of magma from mantle
Characteristic earthquakes and asperities	Reservoirs of old and new magma
Regional cycle determined by the largest earthquake	Volcanic cycle determined by the periodic supply of magma from the mantle
Odawara earthquake preceding active period in the Tokyo metropolitan area	Bory west area eruption for Piton de la Fournaise

References for preface

Wiener, N., Cybernetics or Control and communication in the animal and the machine, 1948, John Wiley & sons, Inc., New York and Hermann et CIE, Paris.

Gutenberg, B., and C. F. Richter, 1954, Seismicity of the Earth (2nd edition), Princeton University Press.

References for chapter 1

Adams, D.A. and R.E. Abercrombie, 1998, Seismic attenuation above 10 Hz in California from coda waves recorded in the Cajon Path borehole, J. Geophys. Res., 103, 24, 257+

Ad-hoc Working Group on the Probabilities of Future Large Earthquakes in Southern California, 1992, Future seismic hazards in southern California, Phase I: Implications of the 1992 Landers earthquake sequence, 42p.

Aki, K., 1956, Some problems in statistical seismology, Zisin (Journal of Seismological Society of Japan), Ser II, 8, 205-227.

Aki, K., 1966, Generation and propagation of G waves from the Niigata earthquake of June 16, 1964, Part 2, Estimation of earthquake moment, released energy and stress-strain drop from the G wave spectrum, Bull. Earthq. Res. Inst., Tokyo Univ., 44, 73-88.

Aki, K., 1967, Scaling law of seismic spectrua, J. Geophys. Res., 72, 1217-1231.

Aki, K., 1968, Seismic displacements near a fault, J. Geophys. Res., 73, 5359-5376.

Aki, K., 1969, Analysis of the seismic coda of local earthquakes as scattered waves, J. Geophys. Res., 74, 615-631.

Aki, K., 1970, Geophysics, in Seismic design for nuclear power plants, ed. R. J. Hansen, The MIT Press, Cambridge, Mass., 1-113.

Aki, K., 1980, Attenuation of shear waves in the lithosphere for frequencies from 0.05 to 25 Hz, Phys. Earth Planet. Interiors, 21, 50-60.

Aki, K., 1981, A probabilistic synthesis of precursory phenomena, in D. W. Simpson and P. G. Richards, eds., Earthquake Prediction, an International Review, M. Ewing series, v. 4, Am. Geophys. Union, Washington, D. C., 680 pp.

Aki, K., 1984, Asperities, barriers, characteristic earthquakes, and strong motion prediction, J. Geophys. Res., 89, 5867-5872.

Aki, K., 1985, Theory of earthquake prediction with special reference to monitoring of the quality factor of lithosphere by the coda method, Earthq. Predict. Res., 3, 219-230.

Aki, K., 1987, Magnitude-frequency relation for small earthquakes; origin of f_{max} of large earthquakes, J. Geophys. Res., 92, 1349-1355.

Aki, K., 1989, Ideal probabilistic earthquake prediction, Tectonophysics, 169, 197-198.

Aki, K., 1991, Summary of discussions on coda waves at the Istanbul IASPEI meeting, Phys. Earth Planet. Inter., 67 (1991), 1-3.

Aki, K., 1992, Scattering conversions P to S versus S to P, Bull. Seis. Soc. Am., 82, 1969-1972.

Aki, K., T. DeFazio, P. Reasenberg, and A. Nur, 1970, An active experiment with earthquake fault for an estimation of the in situ stress, Bull. Seis. Soc. Am., 60, 1315-1336.

Aki, K. and Y. B. Tsai, 1972, Mechanism of Love-wave excitation by explosive sources, J. Geophys. Res., 77, 1452-1475.

Aki, K. and B. Chouet, 1975, Origin of coda waves: source, attenuation and scattering effects, J. Geophys. Res., 80, 3322-3342.

Aki, K. and W. H. K. Lee, 1976, Determination of three-dimensional velocity anomalies under a seismic array using first P arrival times from local earthquakes, 1. A homogeneous initial model, J. Geophys. Res., 81, 4381-4399.

Aki, K., A. Christoffersson, and E. S. Husebye, 1977, Determination of the three-dimensional seismic structure of the lithosphere, J. Geophys. Res., 82, 277-296.

Aki, K. and K. Kaminuma, 1963, Phase velocity of Love waves in Japan (Part 1): Love waves from the Aleutian shock of March, 1957, Bull. Earthq. Res. Inst., 41, 243-259.

Aki, K. and P. G. Richards, 1980, Quantitative Seismology, W.H.Freeman and Company, San Francisco, 932 pp. Second edition, 2002, University Science Books, Sausalito, California, 699 pp.

Anderson, J. G. and S. E. Hough, 1984, A model for the shape of the Fourier amplitude spectrum of acceleration at high frequencies, Bull. Seis. Soc. Am., 74, 1969-1994.

Backus, G., and F. Gilbert, 1968, The resolving power of gross earth data, Geophys. J. Roy. Astron. Soc.,16, 169-205.

Bak, P. and C. Tang, 1989, Earthquakes as self-organized critical phenomena, J. Geophys. Res., 94, 15635-15637.

Bakun, W. H. and A. G. Lindh, 1985, The Parkfield, California earthquake prediction experiment, Science, 229, 619-624.

Bakun, W. H., et al., 1987, Parkfield, California, earthquake prediction scenarios and response plans, U.S. Geol. Surv., Open-File Report 87-192.

Berckhemer, H., 1962, Die Ausdehnung der Bruchflache im Erdbebenherd und ihr Einfluss auf das seismische Wellenspektrum, Gerlands Beitr. Geophys., 71, 5-26.

Beresnev, I. A. and G. M. Atkinson, 2002, Source parameters of earthquakes in eastern and western North America based on finite-fault modeling, Bull. Seis. Soc. Am., 92, 695-710.

Bouchon, M. and K. Aki, 1977, Discrete wave-number representation of seismic-source wave fields, Bull. Seis. Soc. Am., 67, 259-277.

Bouchon, M., 1978, A dynamic crack model for the San Fernando earthquake, Bull. Seis. Soc. Am., 68, 1555-1576.

Brune, J. N., 1968, Seismic moment, seismicity, and rate of slip along major fault zones, J. Geophys, Res., 73, 777-784.

Brune, J. N., 1970, Tectonic stress and the spectra of seismic shear waves from earthquakes, J. geophys. Res., 75, 4997-5009.

Burridge, R. and L. Knopoff, 1964, Body force equivalents for seismic dislocations, Bull. Seis. Soc. Am., 54, 1875-1888.

Burridge, R. and L. Knopoff, 1967, Model and theoretical seismicity, Bull. Seis. Soc. Am., 57, 341-371.

Burridge, R. and G. S. Halliday, 1971, Dynamic shear cracks with friction as models for shallow focus earthquakes, Geophys. J. Roy. Astrono. Scc., 25 261-283.

Byerly, P., 1938, The earthquake of July 6, 1934: Amplitudes and first motion, Bull. Seis. Soc. Am., 28, 1-13.

Carlson, J. M. and J. S. Langer, 1989, Mechanical model of an earthquake, Physical Review, A40, 6470-6484.

Chen, P. and W. O. Nuttli, Estimates of magnitude and short-period wave attenuation of Chinese earthquakes from Modified Mercali intensity data, Bull. Seis. Soc. Am., 74 (1984) 957-968.

Chouet, B., 1979, Temporal variation in the attenuation of earthquake coda near

Stone Canyon, Calif., Geophys. Res. Lett., 6, 143-146.
Chouet, B., K. Aki and M. Tsujiura, 1978, Regioal variation of the scaling law of earthquake source spectra, Bull. Seis. Soc. Am., 68, 49-79.
Cochard, A. and R. Madariaga, 1994, Dynamic faulting under rate-dependent friction, PAGEOPH, 142, 419-445.
Cornell, C. A., 1968, Engineering seismic risk analysis, Bull. Seis. Soc. Am., 58, 1583-1606.
Das, S. and K. Aki, 1977, Fault planes with barriers: a versatile earthquake model, J. Geophys. Res., 82, 5648-5670.
DeFazio, T. L., K. Aki and J. Alba, 1973, Solid earth tide and observed change in the in situ seismic velocity, J. Geophys. Res., 78, 1319-1322.
Dieterich, J. H., 1979, Modeling of rock friction, 1. Experimental results and constitutive equations, J. Geophys. Res., 84, 2161-2168.
Dysart, P. S., J. A. Snoke, and I. S. Sacks, 1988, Source parameters and scaling relations for small earthquakes in the Matsushiro region, southwest Honshu, Japan, Bull. Seism. Soc. Am., 78, 571-589.
Ellsworth, W. L. and G. C. Beroza, 1995, Seismic evidence for an earthquake nucleation phase, Science, 268, 851-855.
Encyclopedic Dictionary of Mathematics, 1980, by the Mathematical Society of Japan,translation published by the MIT Press, Cambridge, MA.
Faulkner, J., 1988, Temporal variation of coda Q, MS Thesis, University of Southern California, Los Angeles.
Fedotov, S. A., 1965, Regularities of the distribution of strong earthquakes in Kamchatka, the Kurile Islands, and north-east Japan, Tr. Inst. Fiz. Zemli Akad. Nauk SSSR, 36, 66-93.
Fehler, M., M. Hoshiba, H. Sato and K. Obara, 1992, Separation of scattering and intrinsic attenuation for the Kanto-Tokai region, Japan, using measurements of S-wave energy versus hypocentral distance, Geophys. J. Int.,108, 787-800.
Frankel, A. and R. W. Clayton, 1986, Finite difference simulations of seismic scattering: implications for the propagation of short-period seismic waves in the crust and models of crust heterogeneity, J. Geophys. Res. 91, 6465-6489.
Freund, L. B., 1979, The mechanics of dynamic shear crack propagation, J. Geophys. Res.,84, 2199-2209.
Gao, L. S., N. N. Biswas, L. C. Lee and K. Aki, 1983, Effects of multiple scattering on coda wavesin three-dimensional medium, PAGEOPH, 121, 3-15.
Gao, L. S. and K. Aki, 1996, Effect of finite thickness of scattering layer on coda Q of local earthquakes, J. Geodynamics, 21, 191-213.
Gusev, A. A., 1983, Descriptive statistical model of earthquake source radiation and its application to an estimation of short period strong motion, Geophys. J. Roy. Astr. Soc., 74, 787-808.
Gusev, A. A. and V. K. Lemzikov, 1984, The anomalies of small earthquake coda wave characteristics before the three large earthquakes in the Kuril-Kamchatka zone (in Russian), Vulk. Seism., 4, 76-90.
Hanks, T. C., 1979, b-values and ω-γ seismic source models: Implications for tectonic stress variations along active crustal fault zones and the estimation of high frequency strong ground motion, J. Geophys. Res., 84, 2235-2242.
Hanks, T. C. and McGuire, 1981, The character of high-frequency strong ground motion, Bull. Seis. Soc. Am.,71, 2071-2096.
Hanks, T. C., 1982, f_{max}, Bull. Seis. Soc. Am., 72, part A, 1867-1880.
Haskell, N.A., 1969, Elastic displacements in the near-field of a propagating fault,

Bull. Seis. Soc. Am., 59, 865-908.
Healy, J. H., V. G. Kossobokov, and J. W. Dewey, 1992, A test to evaluate the earthquake prediction algorithm M8, U.S. Geol. Surv., Open File Rep., 92-401.
Herraiz, M. and A. F. Espinosa, 1987, Coda waves: a review, PAGEOPH, 125, 499-577.
Hiramatsu, Y., N. Hayashi, M. Furumoto and H. Katao, 2000, Temporal change in coda Q^{-1} and b value due to the static stress change associated with the 1995 Hyogo-ken Nanbu earthquake, J. Geophys. Res., 105, 6141-6151.
Honda, H., 1962, Earthquake mechanism and seismic waves, J. Phys. Earth, 10, 1-97.
Hoshiba, M., H. Sato, and M. Fehler, 1991, Numerical basis of the separation of scattering and intrinsic absorption from full seismogram envelope: A Monte-Carlo simulation of multiple isotropic scattering, Pap. Meterol. Geophys., 42, 65-91.
Hoshiba, M., 1993, Separation of scattering attenuation and intrinsic absorption in Japan with the multiple lapse time window analysis from full seismogram envelope, J. Geophys. Res., 98, 15809-15824.
Housner, A. W. and M. D. Trifunac, 1967, Analysis of accelerograms--Parkfield earthquake, Bull. Seis. Soc. Am., 57, 113-1220.
Ida, Y., 1972, Cohesive force across the tip of a longitudinal shear crack and Griffith's specific surface energy, J. Geophys. Res., 77, 3796-3805.
Ide, S. and M. Takeo, 1997, Determination of constitutive relations of fault slip based on seismic wave analysis, J. Geophys. Res., 102, 27379-27391.
Isacks, B., J. Oliver and L. R. Sykes, 1968, Seismicity and the new global tectonics, J. Geophys. Res., 73, 5855-5899.
Jin, A. and K. Aki, 1986, Temporal changes in coda Q before the Tangshan earthquake of 1976 and the Haicheng earthquake of 1975, J. Geophys. Res., 91, 665-673.
Jin, A. and K. Aki, 1988, Spatial and temporal correlation between coda Q and seismicity in China, Bull. Seis. Soc. Am., 78, 741-769.
Jin, A. and K. Aki, 1989, Spatial and temporal correlation between coda Q^{-1} and seismicity and its physical mechanism, J. Geophys. Res., 94, 14041-14059.
Jin, A. and K. Aki, 1993, Temporal correlation between coda Q^{-1} and seismicity - evidence for a structural unit in the brittle-ductile transition zone, J. Geodynamics, 17, 95-120.
Jin, A., K. Mayeda, D. Adams, and K. Aki, 1994, Separation of intrinsic and scattering attenuation in southern California using TERRAscope data, J. Geophys. Res., 99, 17835-17848.
Jin, A., C. A. Moya and M. Ando, 2000, Simultaneous determination of site responses and source parameters of some earthquakes along the Atotsugawa fault zone, Central Japan, Bull. Seis. Soc. Am., 90, 1430-1445.
Kagan, Y. Y. and D. D. Jackson, 1993, Seismic gap hypothesis: Ten years after, J. Geophys. Res., 98, 419-431.
Kagan, Y. Y. and D. D. Jackson, 1994, Long term probabilistic forecasting ofearthquakes, J. Geophys. Res., 99, 13685-13700.
Kanamori, H., 1971, Great earthquakes at island arcs and the lithosphere, Tectonophysics, 12, 187-198.
Kanamori, H., 1981, The nature of seismicity patterns before large earthquakes, in Earthquake Prediction, eds. D. W. Simpson and P. G. Richards, Maurice

Ewing Series 4, Am. Geophys. Union, Washington, D. C., 1-19.
Kanamori, H. and G. S. Stewart, 1978, Seismological aspects of the Guatemala earthquake of February 4, 1976, J. Geophys. Res., 83, 3427-3434.
Keilis-Borok, V. E., L, Knopoff, I. M. Rotwain, and CC. R. Allen, 1988, Intermediate-term prediction of occurrence times of strong earthquakes, Nature, 335, 690-694.
Kelleher, J. A., L. R. Sykes and J. Oliver, 1973, Possible criteria for predicting earthquake locations and their applications to major plate boundaries of the Pacific and Caribbean, J. Geophys. Res., 78, 2547-2585.
Kinoshita, S., 1994, Frequency-dependent attenuation of shear waves in the crust of the Southern Kanto area, Japan, Bull. Seis. Soc. Am., 84, 1387-1396.
Kostrov, B. V., 1974, Seismic moment and energy of earthquakes, and seismic flow of rock, Izv. Acad. Sci. USSR Phys. Solid Earth, 1, 23-40.
Kostrov, B. V., Unsteady propagation of longitudinal shear cracks, 1966, J. Appl. Math. Mech., 30, 1241-1248.
Langer, J. S., 1992, Models of crack propagation, Physical Review, A46, 3123-3131.
Li, Y. G., K. Aki, D. Adams, A. Hasemi and W. H. K. Lee, 1994, Seismic guided waves trapped in the fault zone of the Landers, California, earthquake of 1992, J. Geophys. Res., 99, 11,705-11,722.
McCann, W. R., S. P. Nishenko, L. R. Sykes and J. Krause, 1979, Seismic gaps and plate tectonics: Seismic potential for major boundaries, PAGEOPH, 217, 1082-1147.
McGuire, R. K. and T. C. Hanks, 1980, rms accelerations and spectral amplitudes of strong ground motion during the San Fernando, California, earthquake, Bull. Seis. Soc. Am., 70, 1907-1919.
Madariaga, R., 1976, Dynamics of an expanding circular fault, Bull. Seis. Soc. Am., 66, 639-666.
Madariaga, R. and A. Cochard, 1992, Heterogeneous faulting and friction, Proc. Int. Symp. on Earthq. Disaster Prevention, Mexico City, ed. R. Melli, v.1, CENAPRED, 103-118.
Madariaga, R. and K. B. Olsen, 2000, Criticality of rupture dynamics in 3-D, PAGEOPH, 157, 1981-2002.
Madden, T. R., G. A. LaTorraca and S.K. Park, 1993, Electrical conductivity variations around the Palmdale section of the San Andreas fault zone, J. Geophys. Res., 98, 795-808.
Maruyama, T., 1963, On the force equivalents of dynamic elastic dislocations with special reference to the earthquake mechanism, Bull. Earthq. Res. Inst., Tokyo Univ., 41, 467-486.
Maruyama, T., 1978, Frequency distribution of the size of fractures generated in the branching process—Elementary analysis, Bull. Earthq. Res. Inst., 53, 407-421.
Matsunami, K., 1991, Laboratory tests of excitation and attenuation of coda waves using 2-D models of scattering media, Phys. Earth Planet. Inter., 67, 104-114.
Mayeda, K., S. Koyanagi, M. Hoshiba, K. Aki and Y Zeng, 1992, A comparative study of scattering, intrinsic and coda Q^{-1} for Hawaii, Long Valley, and central California between 1.5 an 15 Hz, J. Geophys. Res., 97, 6643-6659.
Mitchell, B. J. and B. Romanowicz, 1998, edit. Q of the Earth, PAGEOPH, 153, 235-713.
Minster, J. B. and T. H. Jordan, 1978, Present-day plate motions, J. Geophys. Res., 83, 5331-5354.

Minster, B., and N. Williams, 1993, A systematic approach to assess intermediate-term earthquake prediction algorithms based on seismicity patterns, 1993 Annual Report, Southern California Earthquake Center, A29.

Mogi, K., 1982, Earthquake prediction in Japan, (in Japanese), Science-sha, Tokyo (translated into English by Academic Press, Tokyo in 1985).

Molnar, P. and J. Oliver, 1969, Lateral variations of attenuation in the upper mantle and discontinuities in the lithosphere, J. Geophys. Res., 74, 2648-82.

National Earthquake Prediction Evaluation Council Working Group to Evaluate the Parkfield Prediction Experiment, Earthquake Research at Parkfield -- 1993 and Beyond, 1993, U.S. Geological Survey Open-File Report 93-622.

Nishenko, S. P., 1991, Circum-Pacific seismic potential 1989-1999, PAGEOPH, 135, 169-259.

Nishenko, S., P. and W. R. McCann, 1981, Seismic potential for the world's major plate boundaries: 1981, in Simpson, D. W. and P. G. Richards, ed., Earthquake Prediction, Maurice Ewing series 4, Am. Geophys. Union, 20-28.

Nishigami, K., 2000, Deep crustal heterogeneity along and around the San Andreas fault system in central Californiaand its relation to segmentation, J. Geophys. Res., 105, 7983-7998.

Novelo-Casanova, D. A., E. Berg, Y. Hsu, and C. E. Helsley, 1985, Time-space variation seismic S-wave coda attenuation (Q^{-1}) and magnitude distribution (b-values) for the Petatlan earthquake, Geophys. Res. Lett., 12, 789-792.

Ohnaka, M., M. Akatsu, H. Mochizuki, A. Odera, F. Tagashira, and Y. Yamamoto, 1997, A constitutive law for the shear failure of rock under lithospheric conditions, Tectonophysics, **277**, 1-27.

Ohtake, M., 1987, Temporal change of Q_p in the focal area of the 1984 western Nagano, Japan earthquake as derived from the pulse width analysis, J. Geophys. Res., 92, 4846-4852.

Ojeda, A. and L. Ottemoller, Q_{Lg} tomography in Colombia, 2002, Phys. Earth Planet. Int., 130, 253-270.

Oliver, J. and B. Isacks, 1967, Deep earthquake zones, anomalous structures in the upper mantle, and the lithosphere, J. Geophys. Res., 72, 4259-4275.

Otsuka, M., 1972, A chain-reaction type source model as a tool to interpret the magnitude frequency relation of earthquakes, J. Phys. Earth, 20, 35-45.

Pavlis, G. L. and J. R. Booker, 1980, The mixed discrete continuous inverse problem: application to simultaneous determination of earthquake hypocenters and velocity structure, J. Geophys. Res., 85, 4801-4810.

Papageorgiou, A. S. and K. Aki, 1983, A specific barrier model for the quantitative description of inhomogeneous faulting and prediction of strong motion, Part 1. Description of the model, Bull. Seis. Soc. Am., 73, 693-722, Part 2. Applications of the model, Bull. Seis. Soc. Am., 73, 953-978.

Peng, J. Y., 1989, Spatial and temporal variation of coda Q^{-1} in California, Ph.D. thesis, University of Southern California, Los Angeles.

Pepke, S. L., J. M. Carlson, and B. E. Shaw, 1994, Prediction of large events on a dynamical model of a fault, J. Geophys. Res., 99, 6769-6788.

Rautian, T. G. and V. I. Khalturin, 1978, The use of coda for determination of the earthquake source spectrum, Bull. Seis. Soc. Am., 68, 923-948.

Reasenberg, P. and K. Aki, 1974, A precise, continuous measurement of seismic velocity for monitoring in situ stress, J. Geophys. Res., 79, 399-406.

Rice, J. R., 1980, The mechanics of earthquake rupture, Proc. Intern. School of

Physics N"Enrico Fermi", Italian Physical Society, Course LXXVIII on Physics of the Earth's interior, E. Boschi and A. M. Dziewonski, Editors, North-Holland Publishing Co., Amsterdam, 555-649.

Rice, J. R., 1993, Spatio-temporal complexity of slip on a fault, J. Geophys. Res., 98, 9885-9908.

Robinson, R., 1987, Temporal variation in coda duration of local earthquakes in the Wellington region, New Zealand, PAGEOPH, 125, 579-596.

Ruina, A. L., 1983, Slip instability and state variable friction laws, J. Geophys. Res., 88, 10359-10370.

Sabine, W. C., 1922, Collected Papers on Acoustics, Harvard University Press, Cambridge, Mass.

Saito, M., M. Kikuchi and K. Kudo, 1973, An analytic solution for Otsuka's Goishi model, Zisin (Journal of Seismological Society of Japan), Ser. II, 26, 19-25.

Sato, H., 1986, Temporal change in attenuation intensity before and after Eastern Yamanashi earthquake of 1983, in central Japan, J. Geophys. Res., 91, 2049-2061.

Sato, H., 1987, A precursor-like change in coda excitation before the western Nagano earthquake (Ms=6.8) of 1984 in central Japan, J. Geophys. Res.,92, 1356-1360.

Sato, H., 1988, Temporal change in scattering and attenuation associated with the earthquake occurrence - a review of recent studies on coda waves, PAGEOPH, 126, 465-498.

Sato, H. and M. Fehler, 1998, Seismic wave propagation and scattering in the heterogeneous earth, Springer-Verlag, New York, 308pp.

Sato, T. and T. Hirasawa, 1973, Body wave spectra from propagating shear cracks, J. Phys. Earth, 21, 415-431.

Schwartz, D. P. and K. J. Coppersmith, 1984, Fault behavior and characteristic earthquakes: Examples from the Wasatch and San Andreas fault zones, J. Geophys. Res., 89, 5681-5698.

Segall, P. and Y. Du, 1993, How similar were the 1934 and 1966 Parkfield earthquakes? J. Geophys. Res., 98, 4527-4538.

Shang, T. and L. S. Gao, 1988, Transportation theory of multiple scattering and its application to seismic coda waves of impulse source, Sci. Sinica, Series V, 31, 1503-1514.

Shaw, B. E., 1994, Complexity in a spatially uniform continuum fault model, preprint.

Shaw and Rice (2000), Existence of continuum complexity in the elastodynamics of repeated fault rupture, J. Geophys. Res., 105, 23791-23810.

Sieh, K. E., 1981, A review of geological evidence for recurrence times of large earthquakes, in Earthquake Prediction, Maurice Ewing Ser., 4, edited by D. W. Simpson and P. G. Richards, AGU, Washington, D. C., 181-207.

Singh, S. K. and R. B. Herrmann, 1983, Regionalization of crustal coda Q in the continental United States, J. Geophys. Res., 88, 527-538.

Somerville, P., K. Irikura, R. Graves, S. Sawada,D. Wald, N. Abrahmson, Y. Iwasaki, T. Kagawa,N. Smithand A. Kowada, 1999, Characterizing crustal earthquake slip models for the prediction of strong ground motion, Seis. Res Lett., 70, 59-80.

Su, F., and K. Aki, 1990, Spatial and temporal variation in coda Q^{-1} associated with the North Palm Springs earthquake of 1986, PAGEOPH, 133, 23-52.

Su, F., K. Aki and N. N. Biswas, 1991, Discriminating quarry blasts from earthquakes using coda waves, Bull. Seis. Soc. Am., 81, 162-178.

Su, F., K. Aki, T. Teng, Y. Zeng, S. Koyanagi, and K. Mayeda, 1992, The relation between site amplification factor and surficial geology in central

California, Bull. Seis. Soc. Am., 82, 580-602.
Sykes, L. R., 1967, Mechanism of earthquakes and nature of faulting on the mid-oceanic ridges, J. Geophys. Res., 72, 2131-2153.
Sykes, L. R. and S. P. Nishenko, 1984, Probabilities of occurrence of large plate rupturing earthquakes for the San Andreas, San Jacinto, and Imperial fault, California, 1983-2003, J. Geophys. Res., 89, 5905-5927.
Tsujiura, M., 1978, Spectral analysis of the coda waves from local earthquakes, Bull. Earthq. Res. Inst., Tokyo Univ., 53, 1-48.
Tsumura, K., 1967, Determination of earthquake magnitude from total duration of oscillation, Bull. Earthquake Res. Inst.,Tokyo Univ., 45, 7-18
Tsukuda, T., 1988, Coda Q before and after the 1983 Misasa earthquake of M6.2, Tottori Pref., Japan, 1988, PAGEOPH, 128, 261-280.
Utsu, T., 1966, Regional differences in absorption of seismic waves in the upper mantle as inferred from abnormal distribution of seismic intensities, J. Fac. Sci. Hokkaido Univ., Ser. 7, 2, 359-374.
Vere-Jones, D., A., 1976, Branching model for crack propagation, PAGEOPH, 114, 711-725.
Vidale, J. E., W. L. Ellsworth, A. Cole and C. Marone, 1994, Variations in rupture process with recurrence interval in a repeated small earthquake, Nature, 368, 624-626.
Wallace, R. E., 1981, Active faults, paleoseismology, and earthquake hazards in the western United States, in Earthquake Prediction, Maurice Ewing Ser., 4, edited by D. W. Simpson and P. G. Richards, AGU, Washington, D. C., 279-289.
Ward, S. N., 1994, A multidisciplinary approach to seismic hazard in southern California, Bull. Seis. Soc. Am., 84, 1293-1309.
Wesnousky, S. G., 1986, Earthquakes, Quaternary faults and seismic hazard in California, J. Geophys. Res., 91, 12587-12632.
Wiemer, S. and M. Wyss, 1994, Seismic quiescence before the Landers (M=7.5) and Big Bear (M=6.5) 1992 earthquakes, Bull. Seis. Soc. Am., 84, 900-916.
Woodgold, C.R.D., 1994, Coda Q in the Charlevoix, Quebec, region: Lapse time dependence and spatial and temporal comparisons, Bull. Seis. Soc. Am., 84, 1123-1131.
Wilson, J. T., 1965, A new class of faults and their bearing on continental drift, Nature, 207, 343-347.
Working Group on California Earthquake Probabilities (WGCEP), 1988, Probabilities of large earthquakes occurring in California on the San Andreas fault, U.S. Geological Survey Open-File Report 88-398, 62p.
WGCEP, 1990, Probabilities of large earthquakes in the San Francisco Bay region, California, U.S. Geological Survey Circular 1053, 61p.
Wu, R., 1985, Multiple scattering and energy transfer of seismic waves; separation of scattering effect from intrinsic attenuation, I. Theoretical modeling, Geophys. J. R. Astron. Soc., 82, 57-80.
Wyss, M., 1991, Evaluation of proposed earthquake precursors, Geophys. Monogr. Am. Geophys. Union, pp. 94. Washington, D.C.
Yoshimoto, K., H. Sato, Y. Ito, T. Ohminato and M. Ohtake, 1998, Frequency-dependent attenuation of high-frequency P and S waves in the upper crust in western Nagano, Japan, PAGEOPH, 153, 489-502.
Zhao, D., O. P. Mishra, R. Sanda, K. Obara, N. Umino and A. Hasegawa, 2001, Seismological evidence for the influence of fluids and magma on earthquakes, Bull. Earthq. Res. Inst. Univ. Tokyo, 76, 271-289.
Zhu, C., C. Fu, Z. Jung and S. Luo, 1977, Source parameters for small

earthquakes and the quality factorof the medium before and after the Haicheng earthquake, Acta Geophys. Sinica (in Chinese) 20, 222-231.

Zeng, Y., F. Su, and K. Aki, 1991, Scattering wave energy propagation in a medium with randomly distributed isotropic scatterers, 1.Theory, J. Geophys. Res., 96, 607-619.

Zeng, Y., 1993, Theory of scattered P and S waves energy in a random isotropic scattering medium, Bull. Seis. Soc. Am., 83, 1264-1277.

References for chapter 2

Aki, K., 1961, Crustal structure in Japan from the phase velocity of Rayleigh waves, Bull. Earthquake Res. Inst., Tokyo Univ., 39, 255-283.

Aki, K., 1992, Higher-order interrelations between seismogenic structures and earthquake processes, Tectonophysics, 211, 1-12.

Aki, K. and A. S. Papageorgiou, 1989, Separation of source and site effects in acceleration power spectra of major California earthquakes, Proc. 9th World Conf. Earthq. Engineering 8, 163-167.

Aster, R. C., G. Slad, J. Henton, and M. Antolik, 1996, Differential analysis of coda Q using similar microearthquakes in seismic gaps, Part 1: techniques and application to seismograms recrded in the Anza seismic gap, Bull. Seis. Soc. Am., 86, 868-889.

Bakun, W. H. and T. V. McEvilly, 1984, Recurrence models and Parkfield, California, earthquakes, J. Geophys., Res., 89, 3051-3058.

Beresnev, I. A. and G. M. Atkinson, 2002, Source parameters of earthquakes in eastern and western North America based on finite-fault modeling, Bull. Seis. Soc. Am., 92, 695-710.

Burford, R. O., 1988, Retardations in fault creep rates before local moderate earthquakes along the San Andreas fault system, central California, PAGEOPH, 126, 499-530.

Byerlee, J. D., 1978, Friction of rocks, PAGEOPH, 116, 615-626.

Castle, R. O. and T. D. Gilmore, 1992, A revised configuration of the southern California uplift, Geological Society of America Bulletin, v. 104, 1577-1591.

Chin, B. H. and K. Aki, 1991, Simultaneous study of the source, path and site effects on strong ground motion during the 1989 Loma Prieta earthquake; a preliminary result on pervasive non-linear site effects, Bull. Seis. Soc. Am., 81, 1859-1884.

Chouet, B., 1979, Temporal variation in the attenuation of earthquake coda near Stone Canyon, Calif., Geophys. Res. Lett., 6, 143-146.

Hashimoto, M., 1996, Static stress changes associated with the Kobe earthquake: Calculation of changes in Coulomb failure function and comparison with sesimicity change, J. Seis. Soc. Japan, 48, 521-530.

Hanks, T. C. and McGuire, 1981, The character of high-frequency strong ground motion, Bull. Seis. Soc. Am., 71, 2071-2096.

Hashizume, M. and Y. Matsui, 1979, Crustal structure of southwest Honshu, Japan, derived from explosion seismic waves, Geophys. J. R. Astron. Soc., 58, 181-200.

Havskov, J., S. Malone, D. McClurg and R. Crosson, 1989, Coda Q for the State of Washington, Bull. Seis. Soc. Am., 79, 1024-1038.

Hiramatsu, Y., N. Hayashi, M. Furumoto and H. Katao, 2000, Temporal change in coda Q^{-1} and b value due to the static stress change associated with the 1995 Hyogo-ken Nanbu earthquake, J. Geophys. Res., 105, 6141-6151.

Hu, G., W. Menke and C. Powell, 1994, J. Geophys. Res., 99, 15245-15256.

Iio, Y., 1996, Depth-dependent change in the focal mechanism of shallow earthquakes: Implications for brittle-plastic transition in a seismogenic region, J. Geophys. Res., 101, 11209-11216.

Ito, K., 1990, Regional variations of the cutoff depth of seismicity in the crust and their relation to heat flow and large inland-earthquakes, J. Phys. Earth, 38, 223-250.

Jin, A. and K. Aki, 1989, Spatial and temporal correlation between coda Q^{-1} and seismicity and its physical mechanism, J. Geophys. Res., 94, 14041-14059.

Jin, A. and K. Aki, 1993, Temporal correlation between coda Q^{-1} and seismicity - evidence for a structural unit in the brittle-ductile transition zone, J. Geodynamics, 17, 95-120

Kanamori, H., 1977, Seismic and aseismic slip along subduction zones and their tectonic implications, in M. Talwani and G. C. Pitman III, (eds.), Island arcs, deep sea trenches and back-arc basins, Maurice Ewing Series, I, 163-174, AGU, Washington, D. C.

Katao, H., N. Maeda, Y. Hiramatsu,Y. Iio and S. Nakao, 1997, Detailed mapping of focal mechanisms in/around the 1995 Hyogo-ken Nanbu earthquake rupture zone, J. Phys. Earth, 45, 105-119.

Kawasaki, I., 2003, Silent earthquakes occurring in a transition zone and its implication for earthquake prediction, presented at the Hagiwara symposium (JSS01), IUGG, Sapporo, July, 2003.

Kikuchi, M., 1997, Rupture process of the Kobe, Japan, earthquake of Jan. 17, 1995, determined from teleseismic body waves, T. Phys. Earth, 444, 429-436.

Kinoshita, S., 1992, Local characteristics of the f_{max} of bedrock motion in the Tokyo metropoliatan area, Japan, J. Phys. Earth, 40, 487-515.

Klemperer, S. L., 1987, A relation between continental heat flow and the seismic reflectivity of the lower crust, J. Geophys., 61, 1-11.

Lay, T. and H. Kanamori, 1981, An asperity model of large earthquake sequences, in D.W. Simpson and P. G. Richards, Earthquake prediction, Maurice Ewing Series, 4, 579-592, AGU, Washington, D. C.

Madden, T. R., G. A. LaTorraca and S. K. Park, 1993, J. Geophys. Res., 98, 795-808.

Meissner, R. and T. Wever, 1986, Intracontinental seismicity, strength of crustal units, and the seismic signature of fault zones, Philos. Trans. R. Soc. London, Ser. A, 317, 45-61.

Molnar, P. and J. Oliver, 1969, Lateral variations of attenuation in the upper mantle and discontinuities in the lithosphere, J. Geophys. Res., 74, 2648-82.

Mooney, W. and T. M. Brochier, 1987, Coincident seismic reflection/refraction studies of the continental lithosphere: a global review, Rev. Geophysics, 25, 723-742.

Obara, K., Science, **296**, 1,679-1,681 (2002).

Obara, K. and H. Sato, 1995, Regional differences of random inhomogeneities around the volcanic front in the Kanto-Tokai area, Japan, revealed from the broadening of S wave seismogram envelopes, J. Geophys. Res., 100, 2103-2121.

Okubo, Y., H. Tsu and K. Ogawa, 1989, Estimation of Curie point temperature and geothermalstructure of island arcs of Japan, Tectonophysics, 159, 279-290.

Oliver, J., M. Dobrin, S. Kaufman, R. Meyer and R. Phinney, 1976, Continuous seismic reflection profiling of the deep basement, Hardeman County, Texas, Geol. Soc. Am. Bull., 87, 1537-1546.

Ooida, T., F. Yamazaki, I. Fujii and H. Aoki, 1990, Aftershock activity of the 1984 western Nagano Prefecture earthquake, central Japan, and its relation to earthquake swarms, J. Phys. Earth, 37, 401-416.

Ouyang, H. and K. Aki, 1994, Eos, 75, 168 (abstract).

Papageorgiou, A. S. and K. Aki, 1983, A specific barrier model for the quantitative description of inhomogeneous faulting and prediction of strong motion, Part 1. Description of the model, Bull. Seis. Soc. Am., 73, 693-722, Part 2. Applications of the model, Bull. Seis. Soc. Am., 73, 953-978.

Pavlenkova, N. L., 1984, Crustal structure and distribution of earthquakes, Gerlands Beitr. Geophys., 93, 125-132.

Revenaugh, J., 1995, A scattered-wave image of subduction beneath the Transverse Ranges, California, Science, 268, 1888-1892.

Rouseau, N., 1999, PhD thesis, IPGP, Univ. Paris, Jussieu.

Sibson, R. H., 1982, Fault zone models, heat flow and depth distribution of earthquakes in the continental crust of the United States,Bull. Seis. Soc. Am., 72, 151-163.

Sieh, K. E., 1978, Central California foreshocks of the great 1857 earthquake, Bull. Seis. Soc. Am., 68, 1731-1749.

Tsukuda, T., 1988, Coda Q before and after the 1983 Misasa earthquake of M6.2, Tottori Pref., Japan, 1988, PAGEOPH, 128, 261-280.

Utada, Y. Hamano and J. Segawa, Contactivity anomaly around the Japanese islands, Geology and Geophysics of the Japan Sea (Japan-USSR Monograph Series, Vol. 1, 103-149.

Yin, X.C., Y.C. Wang, K.Y. Peng, Y.L. Bai, H.T. Wang and X.F. Yin, 2000, Development of a new approach to earthquake prediction: Load/unload response ratio (LURR) theory, PAGEOPH, 157, 2365-2383.

Yomogida, K. and R. Benites, 1995, Relation between direct wave Q and coda Q: A numerical approach, Geophys. J. Int., 123, 471-483.

Zelt, B. C., N. T. Dotzev, R. M. Ellis, and G. C. Rogers, 1999, Coda Q in Southwestern British Columbia, Canada, Bull. Seis. Soc. Am., 89, 1083-1093.

Zeng, Y., F. Su, and K. Aki, 1991, Scattering wave energy propagation in a medium with randomly distributed isotropic scatterers, 1.Theory, J. Geophys. Res., 96, 607-619.

Reference for chapter 3

Aki, K. and V. Ferrazzini, 2000, Seismic monitoring and modeling of an active volcano for prediction, J. Geophys. Res., 105, 16617-16640.

Anderson, P. W., 1958, Absence of diffusion in certain random lattices, Phys. Rev., 109, 1492-1505.

Bachèlery,P., 1981, Le Piton de la Fournaise (île de La Réunion). Etude volcanologique structurale, These de specialité, Clermont-Ferrand.

Bachelery, P., 1999, Le fonctionnement des Volcans-Boucliers, Memoire, Faculte des Sciences et Technologies, Universite de la Reunion, Saint-Denis, La Reunion, France.

Bachèlery, P., P.A. Blum, J.L. Cheminée, L. Chevallier, R. Gaulon, N. Girardin, C. Jaupart, X. Lalanne, J.L. LeMouel, J.C. Ruegg, and P.M. Vincent, 1982, Eruption at Piton de la Fournaise volcano on 3 February, 1981, Nature, 297, 395-397.

Benard, R. and M. Kraft, 1986, Au coeur de la Fournaise, Nourault-Benard ed., 220 pp

Benoit, J. P. and S. R. McNutt, 1996, Global volcanic earthquake swarm data base and preliminary analysis of volcanic earthquake swarm duration, Annali di Geofisica, 39, 221-230.

Biot, M. A., 1956, Theory of propagation of elastic waves in a fluid-saturated porous solid, I. low frequency range, J. Acoust. Soc. Am., 28, 179-196.

Bonneville, A., J.-P. Barriot and R. Bayer, 1988, Evidence from geoid data of a hotspot origin for the southern Mascarene plateau and Mascarene islands (Indian ocean), J. Geophys. Res., 93, 4199-4212.

Briole, P. P. Bachèlery,B. McGuire, J. Moss, J.C.Ruegg, and Ph. Sabourault, 1998, Deformation of Piton de la Fournaise: Evolution of the monitoring techniques and knowledge acquired in the last five years, Proceedings 2nd workshop on European Laboratory Volcanoes, Santrini, Greece, 1996, ed. R. Casale, M. Fytikas, G.sigvaldasson and G. Vougioukalakis, 467-474.

Chouet, B., 1986, Dynamics of a fluid driven crack in three dimensions by the finite difference method, J Geophys. Res., 91, 13,967-13,992.

Chouet, B., 1996, Long-period volcano seismicity: Its source and use in eruption forecasting, Nature, 380, 309-316.

Decker, R. W., 1968, Kilauea volcanic activity: an electrical analog model (abstract), Eos, Transactions American Geophysical Union, 49, 352-353.

Decker, R. W., 1987, Dynamics of Hawaiian volcanoes: an overview, in Volcanism in Hawaii, eds. R. W. Decker, T. L. Wright and P. H. Stauffer, U. S. Geological Survey Prof. Paper 1350, 997-1018.

Delorme, H., P. Bachèlery,P.A. Blum, J.L. Cheminée, J.F. Delarue, J.C. Delmond, A. Hirn, J.C. Lépine, P.M. Vincent, and J. Zlotnicki, 1989, March 1986 eruptive episodes at Piton de la Fournaise volcano (Reunion island), J. Volcanol. Geotherm. Res., 36, 199-208.

Deutsch, R., 1965, Estimation Theory, Prentice Hall, Englewood Cliffs, New Jersy.

Dieterich, J. H., 1988, Growth and persistence of Hawaiian rift zones, J. Geophys. Res., 93, 4258-4270.

Driad, L., 1997, Structure profonde de l'edifice volcanique de La Réunion (Ocean Indien) par sismique réfraction et grand angle, Ph. D. thesis, l'Université de Paris VII.

Dzurisin, D., R. Y. Koyanagi,and T. T. English, 1984, Magma supply and storage at Kilauea volcano, Hawaii, 1956-1983, J. Volcanol. Geotherm. Res., 21, 177-206.

Ferrazzini, V. and K. Aki, 1987, Slow waves trapped in a fluid-filled crack; implication for volcanic tremor, J. Geophys. Res., 92, 9215-9223.

Grasso, J.R. and P. Bachèlery, 1995, Hierarchical organization as a diagnostic approach to volcano mechanics: Validation on Piton de la Fournaise, Geophys. Res. Letters, 22, 2897-2900.

Hirn, A., J.C. Lépine, M. Sapin and H. Delorme, 1991, Episodes of pit-crater collapse documented by seismology at Piton de la Fournaise, J. Volcanol. Geotherm. Res., 47, 89-104.

Hubbert, M. K. and W. W. Rubey, 1959, Mechanics of fluid filled porous solids and its application to overthrust faulting, Geol. Soc. Amer. Bull., 70, 115-166.

Kato, K., K. Aki, and M. Takemura, 1995, Site amplification from coda waves: validation and application to S-wave site response, Bull. Seis. Soc. Am., 85, 467-477.

Koyanagi, R. Y., W. R. Tanigawa, and J. S. Nakata, 1988, Seismicity associated with the eruption, in "The Puu Oo eruption of Kilauea volcano, Hawaii: episode 1 through 20, January 3, 1983 through June 8, 1984", ed. E.W. Wolfe, 183-236, U. S. Geol. Surv. Prof. Paper 1463, 183-236.

Koyanagi, S., K. Aki, N. Biswas, and K. Mayeda, 1995, Infered attenuation from site-effect-corrected T phase recorded on the Island of Hawaii, PAGEOPH, 144, 1-16.

Lénat, J.-F. and P.Bachèlery, 1988, Dynamics of magma transfers at Piton de la Fournaise volcano (Réunion Island, Indian Ocean). In: C.-Y. King and R. Scarpa, ed., Fried. Vieweg und Sohn, Braunschweg/Wiesbaden, 57-72.

Lénat, J.-F., P. Vincent and P. Bachèlery, 1989a, The off-shore continuation of an active basaltic volcano: Piton de la Fournaise (Réunion Island, Indian Ocean); structural and geomorphologic interpretation from sea beam mapping, J. Volcanol. Geotherm. Res., 36, 1-36.

Lénat, J.F., P. Bachèlery,A. Bonneville, P. Tarits, J.L. Cheminee and H. Delorme, The December 4, 1983 to February 18, 1984 eruption of Piton de la Fournaise (La Réunion, Indian ocean): Description and interpretation, 1989b, J. Volcanol. Geotherm. Res., 36, 87-112.

Lénat, J.F., P. Bachèlery,A. Bonneville and A. Hirn, 1989c, The beginning of the 1985-1987 eruptive cycle at Piton de la Fournaise (La Réunion); New insights in the magmatic and volcano-tectonic systems, J. Volcanol. Geotherm. Res., 36, 209-232.

Lénat, J. F.,et P. Bachèlery, 1990, Structure et fonctionnement de la zone centrale du Piton de la Fournaise, in Le Volcanisme de La Réunion. -Monographie- ed. J. F. Lénat, Centre de Recherches Volcanologiques, Observatoire de Physique du Globe de Clermont-Universté Blaise Pascal and C. N. R. S., 257-296.

Lépine, J.C., 1987, Répartition de la sismicité dans la zone d'extension de Djibouti 1972-1986. Relations entre activité sismique et éruptions volcaniques au Piton de la Fournaise, Réunion, 1985-1986. Thése Université Paris VI, 285 pp.

Nakamura, K., 1980, Why do long rift zones develop in Hawaiian volcanoes - A possible role of thick oceanic sediments, Bull. Volcanol. Soc. Japan, Ser. 2, 25, 255-270.

Nercessian, A,, A. Hirn, J.C. Lépine, and M. Sapin, 1996, Internal structure of Piton de la Fournaise volcano from seismic wave propagation and earthquake distribution, J. Volcanol. Geotherm. Res., 70, 123-144.

Phillips, W. S. and K. Aki, 1986, site amplification of coda waves from local earthquakes in central California, Bull. Seis. Soc. Am., 76, 627-648.

Rancon, J.P., P. Lerebour and T. Auge, 1989, The Grand Brule exploration drilling: new data on the deep framework of the Piton de la Fournaise volcano, Part 1, J. Volcanol. Geotherm. Res., 36, 113-128.

Rodgers, C. D., 1976, Retrieval of atmospheric temperature and composition from remote measurements of thermal radiation, Rev. Geophys. Space Phys., 14, 609-624.

Rousset, D., A. Lesquer, A. Bonneville, J. F. Lenat, 1989, Complete gravity study of Piton de la Fournaise volcano, Réunion Island, J. Volcanol. Geotherm.Res., 36, 37-52.

Sapin, M., A. Hirn, J.C. Lepine, and A. Nercessian, 1996, Failure and fluid flow from earthquakes of eruptions at Piton de la Fournaise volcano, J. Volcanol. Geotherm. Res., 70, 145-168.

Sato, H. and M. Fehler, 1998, Seismic wave propagation and scattering in the heterogeneous earth, Springer-Verlag, N. Y., 308 pp, 1998.

Schoenberg, M.,1984, Wave propagation in alternating solid and fluid layers, Wave motion, 6, 303-320.

Semet and coworkers (1999), preprint.

Shimozuru, D., 1981, Magma reservoir systems infered from tilt patterns, Bull. Volcanologique, 44, 499-504.

Sigmundsson, F., Ph. Durand and D. Massonnet, 1999, Opening of an eruptive fissure and seaward displacement at Piton de la Fournaise volcano measured by RADARSAT satellite rader interferometry, Geophys. Res. Lett., *26*, 533-536.

Staudacher, T., P. Bachèlery, M. P. Semet, and J. L. Cheminée, 1998, Piton de la Fournaise, Bull. Global Volcanism Network, Smithsonian Institution, 23, No.3, 2-4.

Staudacher et al., 2002, preprint.

Su, F., K. Aki, T. L. Teng, Y. Zeng, S. Koyanagi, and K. Mayeda, 1992, The relation between site amplification factor and surfacial geology in central California, Bull. Seis. Soc. Am., 82, 580-602.

Tarantola, A., 1987, Inverse problem theory; Methods for data fitting and model parameter estimation, Elsvier, New York.

Thurber, C. H. and A. E. Gripp, 1988, Flexure and seismicity beneath the south flank of Kilauea volcano and tectonic implications, J. Geophys. Res., 93, 4271-4278.

Walcott, R. I., 1970, Flexure of the lithosphere at Hawaii, Tectonophysics, 9, 435-446.

Yamamura, K., 1997, Slow waves in the fluid-solid 2 phase system (in Japanese), M.S. Thesis, University of Tokyo.

Zeng, Y., 1991, Deterministic and stochastic modeling of the high frequency seismic wave generation and propagation in the lithosphere, Ph. D. Thesis, University of Southern California.

Zeng, Y., 1993, Theory of scattered P- and S-wave energy in a random isotropic scattering medium, Bull.Seis. Soc. Am., 83, 1264-1276.

Zlotnicki, J., J. C. Ruegg, P. Bachelery and P. A. Blum, 1990, Eruptive mechanism on Piton de la Fournaise volcano associated with the December 4, 1983, and January 18, 1984 eruptions from ground deformation monitoring and photogrammetric surveys, J. Volcan. Geotherm. Res., 40, 197-217.

Reference for chapter 4

Aki, K., 1968, Seismic displacements near a fault, J. Geophys. Res., 73, 5359-5376.

Aki, K., 1985, Theory of earthquake prediction with special reference to monitoring the quality factor of lithosphere by the coda method, Earthq. Predict. Res., 3, 219-230.

Aki, K., 1996, Scale dependence in earthquake phenomena and its relevance to earthquake prediction, Proc. Natl. Acad. Sci.USA, 93, 3740-3747.

Aki, K., and R. Koyanagi, 1981, Deep volcanic tremor and magma ascent mechanism under Kilauea, Hawaii, J. Geophys. Res., 86, 7095-7109.

Aki, K. and Y. B. Tsai, 1972, Mechanism of Love-wave excitation by explosive sources, 77, 1452-1475.

Aki, K. and V. Ferrazzini, 2001, Comparison of Mount Etna, Kilauea and Piton de la Fournaise by a quantitative modeling of their eruption histories, J. Geophys. Res., 105, 16617-16640.

Antolik, M., R. M. Nadeau, R. C. Aster, and T. V. McEvilly, 1996, Differential analysis of coda Q using similar microearthquakes in seismic gaps, Part 2: Application to seismograms recorded by the Parkfield high resolution seismic network, Bull. Seis. Soc. Am., 86, 890-910.

Aster, R.C., G. Slad, J. Henton, and M. Antolik, 1996, Differential analysis of coda Q using similar microearthquakes in seismic gaps, Part 1: techniques and application to seismograms recrded in the Anza seismic gap, Bull. Seis. Soc. Am., 86, 868-889.

Bouchon, M., 1979, Predictability of ground displacement and velocity at

proximity of an earthquake, An example: The Parkfield earthquake of 1966, J. Geophys. Res., 84, 6149-6156.
Burford, R. O., 1988, Retardations in fault creep rates before local moderate earthquakes along the San Andreas fault system, central California, PAGEOPH, 126, 499-530.
Chouet, B., 1979, Temporal variation in the attenuation of earthquake coda near Stone Canyon, Calif., Geophys. Res. Lett., 6, 143-146.
De Groot, S. R., 1952, Thermodynamics of irreversible processes, North-Holland Publishing Co. and Interscience Publ. Inc.
Decker, R. W., 1968, Kilauea volcanic activity: an electrical analog model (abstract), Eos, Transactions American Geophysical Union, *49*, 352-353.
Decker, R. W., 1987, Dynamics of Hawaiian volcanoes: an overview, in Volcanism in Hawaii, eds. R. W. Decker, T. L. Wright and P. H. Stauffer, U. S. Geological Survey Prof. Paper 1350, 997-1018.
Ellsworth, W. L., 1990, Earthquake history, 1769-1989, in The San Andreas Fault System, California, R. E. Wallace (editor), U. S. Geol. Surv. Profess. Pap. 1515.
Habermann, R.E., 1988, Precursory seismic quiescence: Past, present, and future, PAGEOPH, 126, 279-318.
Hiramatsu, Y., N. Hayashi, M. Furumoto and H. Katao, 2000, Temporal change in coda Q-1 and b value due to the static stress change associated with the 1995 Hyogo-ken Nanbu earthquake, J. Geophys. Res., 105, 6141-6151.
Ishibashi, K., 2003, Seismo-tectonic modeling of the repeating M7-class disastrous earthquakes near Odawara, Japan, due to the Izu collision, presented at the Hagiwara symposium (JSS1) at the IUGG meeting at Sapporo.
Jin, A. and K. Aki, 1986, Temporal changes in coda Q before the Tangshan earthquake of 1976 and the Haicheng earthquake of 1975, J. Geophys. Res., 91, 665-673.
Jin, A. and K. Aki, 1988, Spatial and temporal correlation between coda Q and seismicity in China, Bull. Seis. Soc. Am., 78, 741-769.
Jin, A. and K. Aki, 1989, Spatial and temporal correlation between coda Q^{-1} and seismicity and its physical mechanism, J. Geophys. Res., 94, 14041-14059.
Jin, A. and K. Aki, 1993, Temporal correlation between coda Q^{-1} and seismicity - evidence for a structural unit in the brittle-ductile transition zone, J. Geodynamics, 17, 95-120.
Jones, L., 1992, Phase I report of SCEC mentioned in Section 1.2; see Adhoc Working Group.
Kanamori, H., 1981, The nature of seismicity patterns before large earthquakes, in Earthquake Prediction, eds. D. W. Simpson and P. G. Richards, Maurice Ewing Series 4, Am. Geophys. Union, Washington, D. C., 1-19.
Li, Y.G., J.E. Vidale, K. Aki, F. Xu, and T. Burdette, 1998, Evidence of shallow fault zone strengthening after the 1992 M7.5 Landers, California earthquake, Science, 279, 217-219
Mogi, K., 1981, Seismicity in western Japan and long-term earthquake forecasting, in Earthquake Prediction, eds. D. W. Simpson and P. G. Richards, Maurice Ewing Ser. 4, AGU, Washington, D. C., 43-52.
Mogi, K., 1982, Earthquake prediction in Japan, (in Japanese), Science-sha, Tokyo (translated into English by Academic Press, Tokyo in 1985).
Mogi,K., 1998, Zisin yochi wo kangaeru (in Japanese), Iwanami shoten.
Ohtake, M., T. Matumoto and G. V. Latham, 1977, Seismicity gap near Oaxaca,

southern Mexicoas a probable precursor to a large earthquake, PAGEOPH, 115, 375-385.

Peng, J.Y., K. Aki, B. Chouet, P. Johnson, W.H.K. Lee, S. Marks, J.T.Newberry, A.S. Ryall, S.W. Stewart, and D.M. Tottingham, 1987, Temporal change in coda Q associated with the Round Valley, California, earthquake of November 23, 1984, J. Geophys. Res., 92, 3507-3526.

Prigogine, I., 1967, Introduction to thermodynamics of irreversible processes, third edition, Interscience Publishers, a division of John Wiley and Sons, New York-London-Sydney, 1967.

Robinson, R., 1987, Temporal variation in coda duration of local earthquakes in the Wellington region, New Zealand, PAGEOPH, 125, 579-596.

Scholz, C. H., 1988, Mechanisms of seismic quiescences, PAGEOPH, 126, 701-718.

Segall, P. and Y. Du, 1993, How similar were the 1934 and 1966 Parkfield earthquakes? J. Geophys. Res., 98, 4527-4538.

Shimazaki, K. and T. Nakata, 1980, Time-predictable recurrence model for large earthquakes, Geophys. Res. Lett., 7, 279-282.

Shimozuru, D., 1981, Magma reservoir systems infered from tilt patterns, Bull. Volcanologique, 44, 499-504.

Su, F., and K. Aki, 1990, Spatial and temporal variation in coda Q^{-1} associated with the North Palm Springs earthquake of 1986, PAGEOPH, 133, 23-52.

Tsukuda, T., 1988, Coda Q before and after the 1983 Misasa earthquake of M6.2, Tottori Pref., Japan, 1988, PAGEOPH, 128, 261-280.

Wiemer, S. and M. Wyss, 1994, Seismic quiescence before the Landers (M=7.5) and Big Bear (M=6.5) 1992 earthquakes, Bull. Seis. Soc. Am., 84, 900-916.

Woodgold, C.R.D., 1994, Coda Q in the Charlevoix, Quebec, region: Lapse time dependence and spatial and temporal comparisons, Bull. Seis. Soc. Am., 84, 1123-1131.

Wright and Klein (2002), preprint.

Wyss, M. and R. E. Habermann, 1988, Precursory seismic quiescence, PAGEOPH, 126, 319-332.

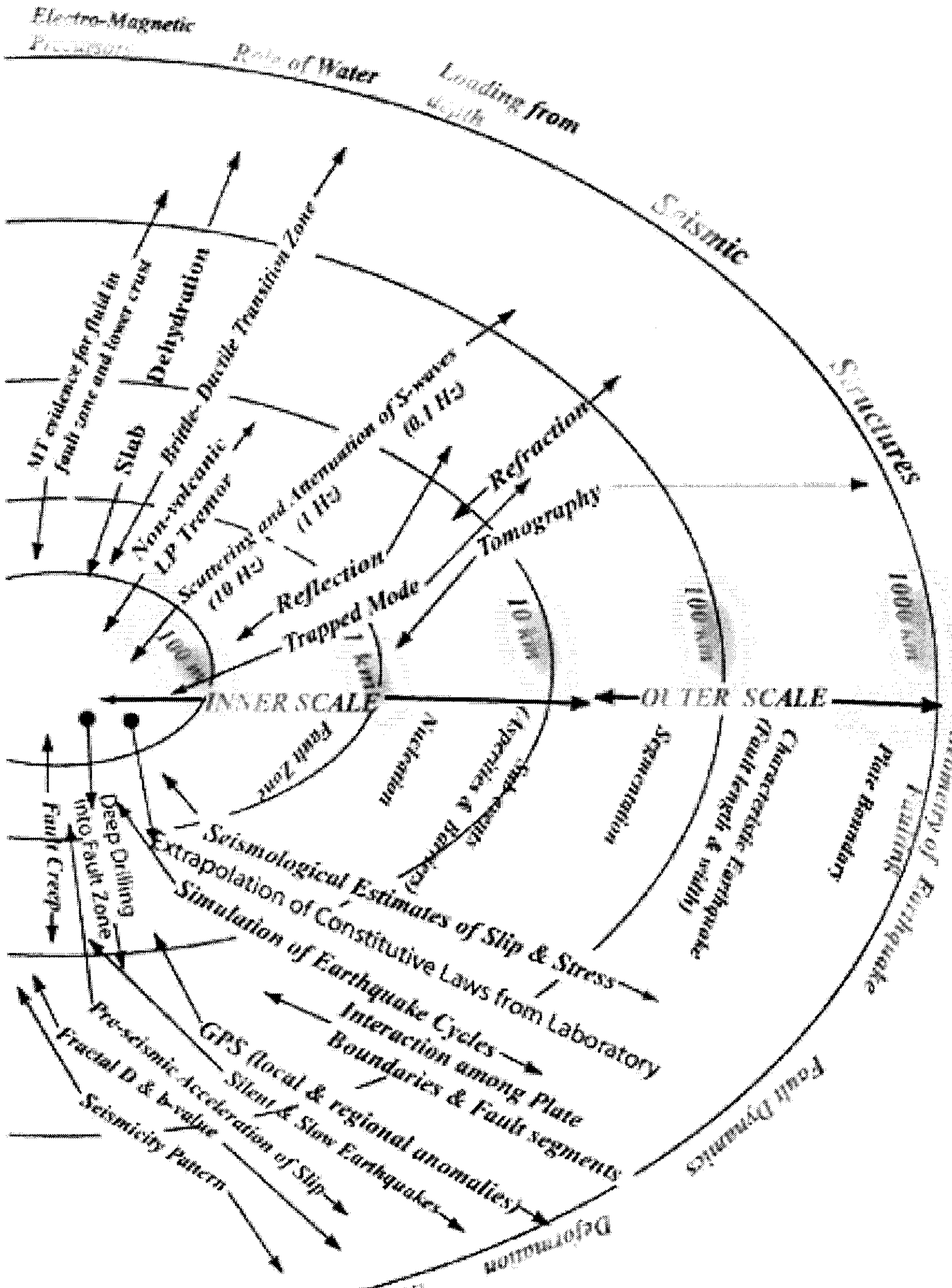

Figure 3.0.1. Classification of study areas on seismogenic structures and earthquake processes according to their scale length.

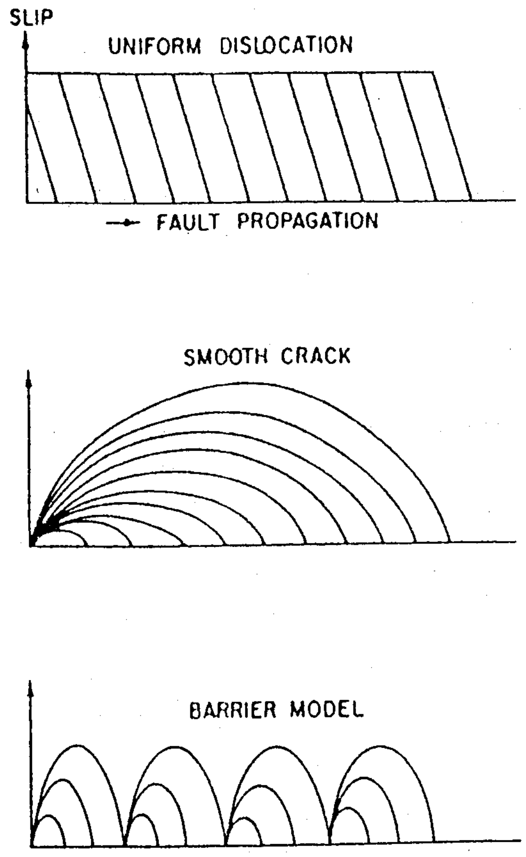

Figure 3.1.1.1. Schematic picture of snap shots of slip as a function of distance along the fault propagation, for an uniform slip-function model(top), a single smooth creak(middle), and a chain of creaks separated by unbroken barriers(bottom)[Reproduced from Aki,1979].

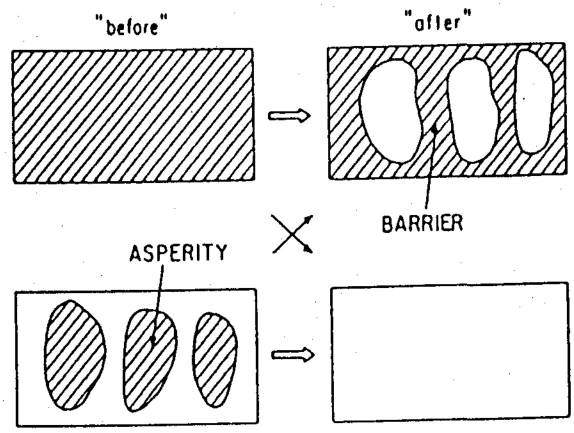

Figure 3.1.1.2. The barrier model and asperity model for the aftershock and foreshock processes, Respectively. [Reproduced from Aki,1992].

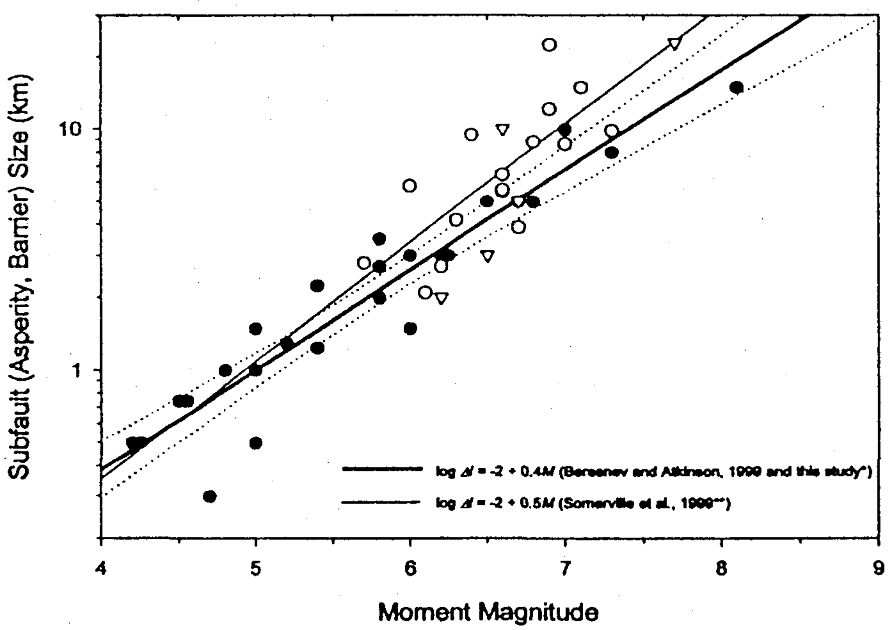

Figure 3.1.1.3. Empirically derived dependencies of the size of charateristic rupture zone(subfault) on an earthquake fault on earthquake magnitude.The results of three independent studies are shown:

- ● Beresnev and Atkinson, 1999, 2002. The thick solid line represents the regression line to data with exact equation as log Dl = -2.08 + 0.416 M.

.... 95% confidence interval.

- o Somerville et al.,1999. The thin solid line represents the regression to their data with exact equation as log Dl = -2.42 + 0.492 M.
- ∇ Aki (1992).

[Reproduced from Beresnev and Atkinson, 2002].

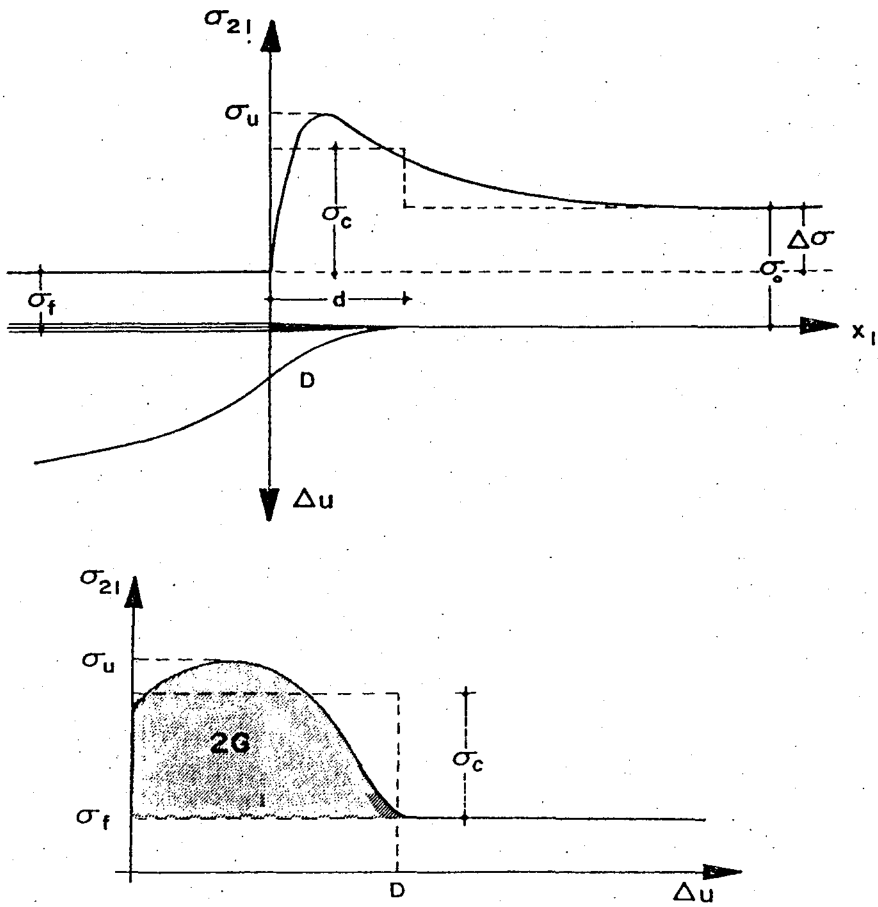

Figure 3.1.1.4. Smoothening of the stress singularity (top)due to the presence of the cohesive zone of length d which is assumed to exist just behind the creak tip. The slip necessary to break the bond of the cohesive zone completely is denoted by D. The average value of the cohesive stress,assuming the latter to be uniformly distributed over the cohesive zone, is denoted by σ_c . The bottom is a schematic representation of the constitutive law (cohesive force diagram) of the "slip weakening" model.
[Reproduced from Papageorgiou and Aki, 1983].

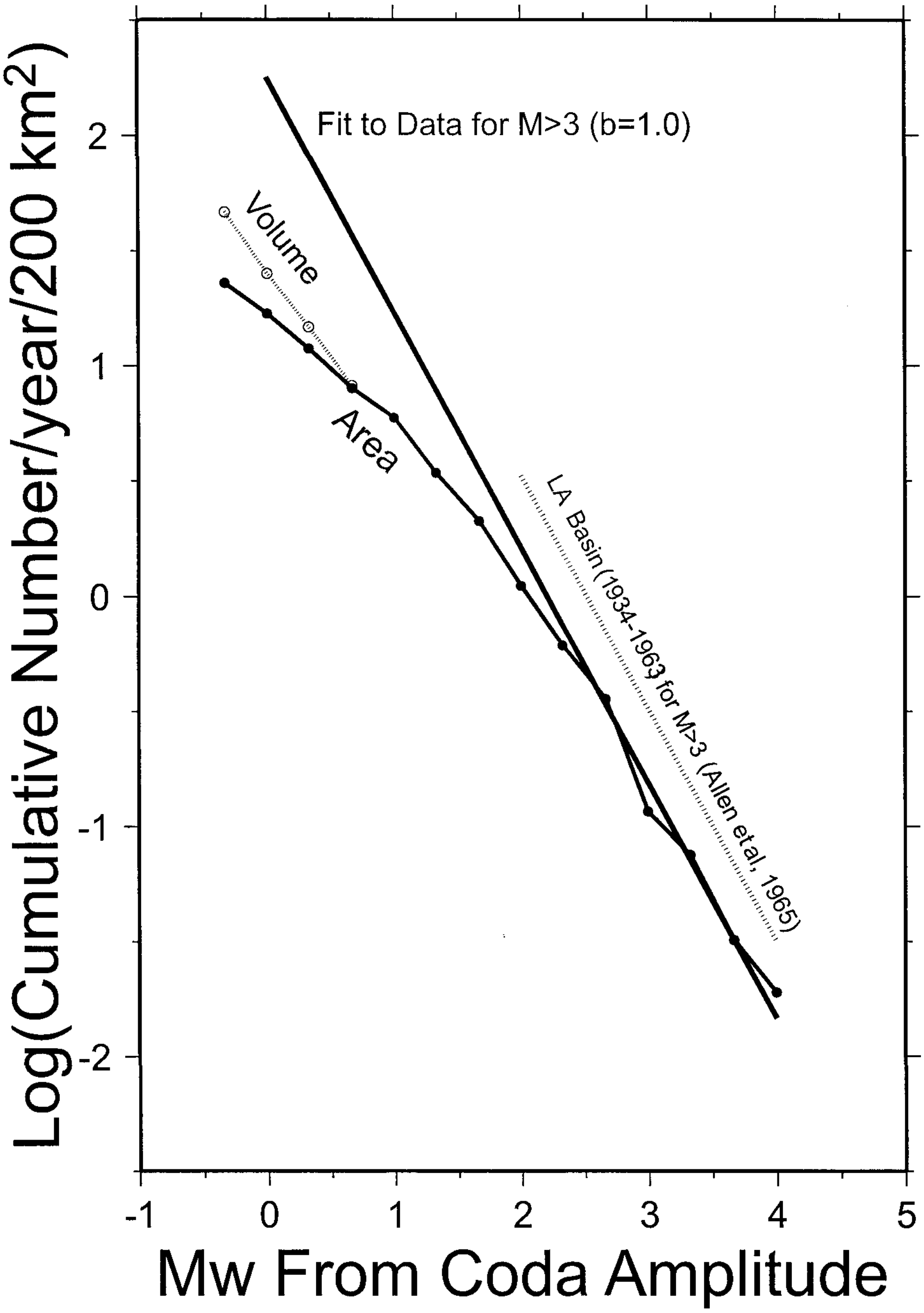

Figure 3.1.2.1. The frequency-magnitude relation deviates from the Gutenberg-Richter formula observed in Newport-Inglewood fault zone, California.[Reproduced from Aki, 1987].

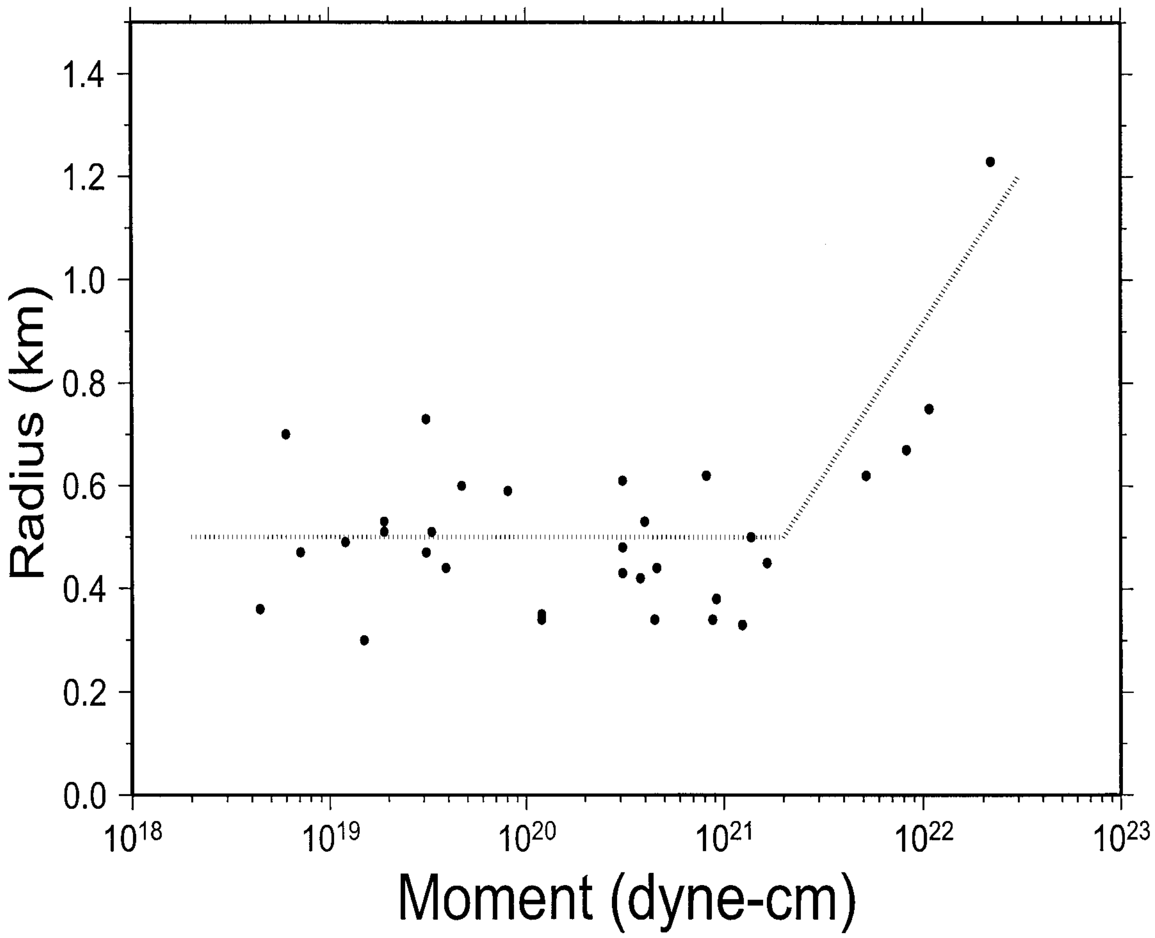

Figure 3.1.2.2. Fault length versus seismic moment determined from the analysis of small-magnitude events from Matsushiro region in Honshu, Japan (Dysart et al.,1988).

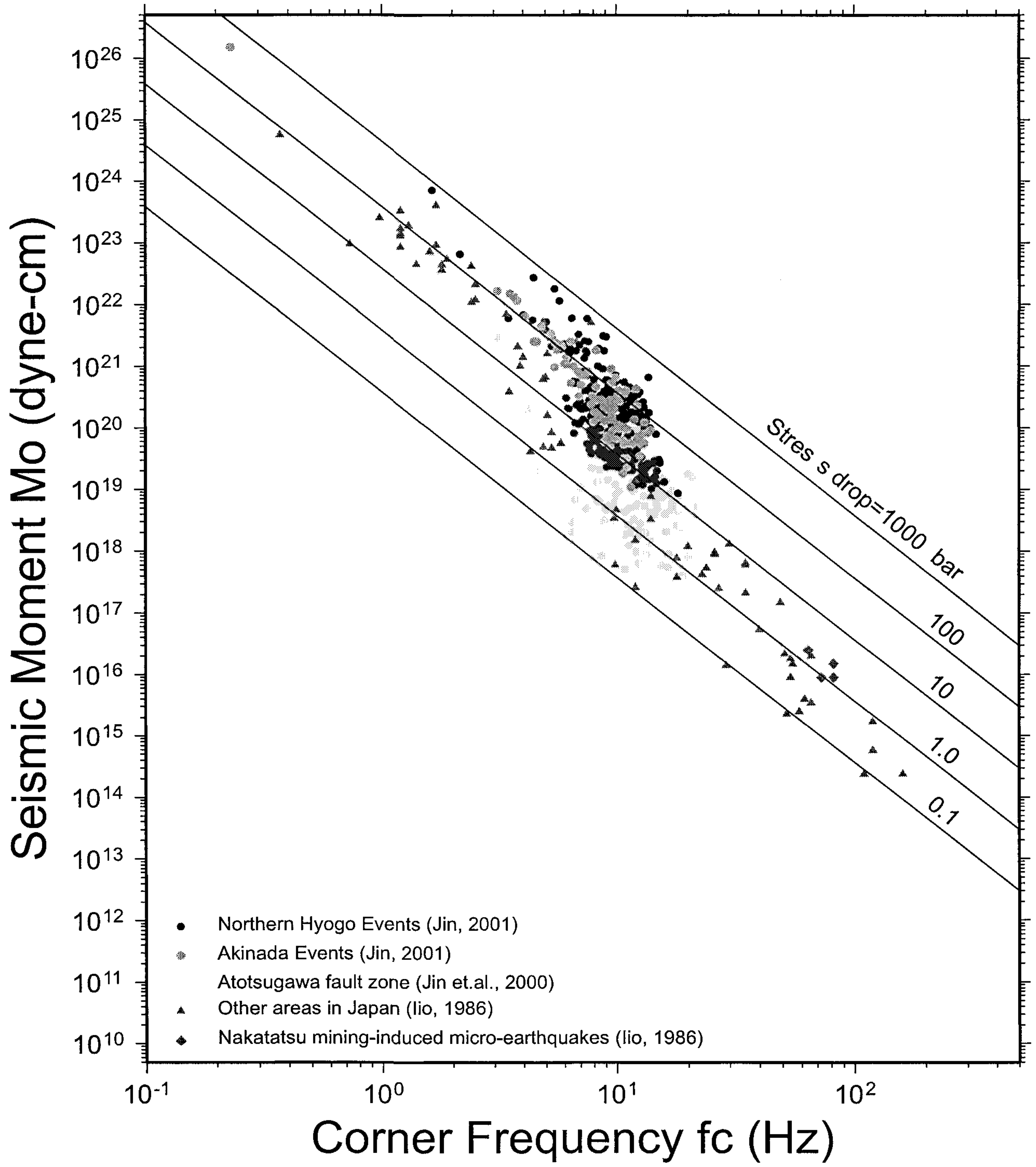

Figure 3.1.2.3. The frequency-moment relation deviates from the scaling law of earthquake spectra observed over Japan. Note the nearly verticall section for earthquakes with Mo ~ $5x10^{21}$- $5x10^{18}$ dyne-cm corresponding to corner frequency around 6-10 Hz. [Reproduced from Jin et al.,2000].

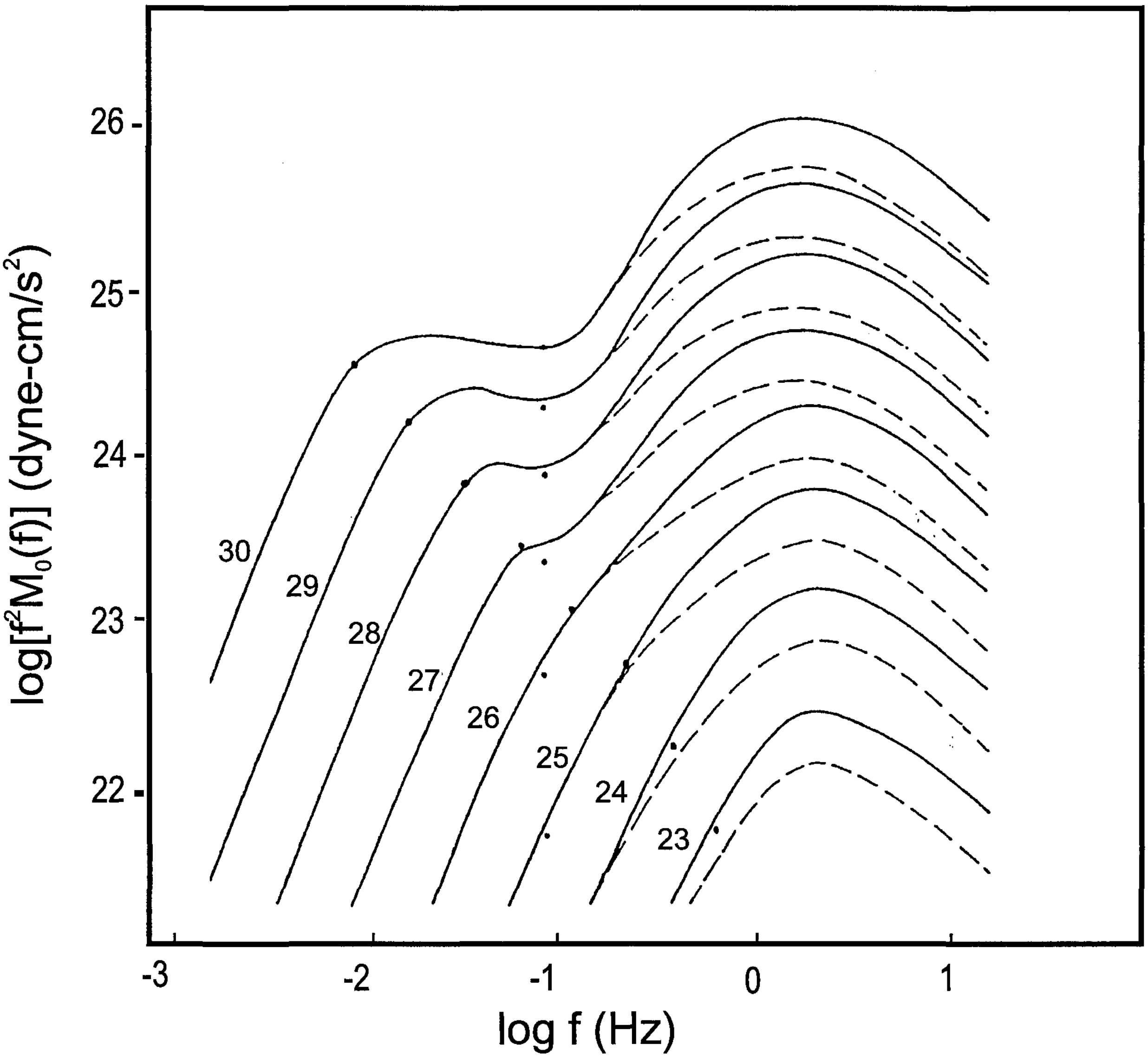

Figure 3.1.2.4. Scaling law of acceleration source spectra based on global data of various magnitude scales.The solid line corresponds to the observed spectra at the earth's surface while the broken line that reduced to the source.
Small dots lined up vertically indicate the spectral levels derived from ML $H(M_0)$ curves given by Gusev(1983) and points lined up along slanted line represent spectral levels at corner frequencies based on the model $M_0(f) = M_0[1+(f/f_0)g]^{-1}$. g is the constant from data fitting. [Reproduced from Gusev, 1983].

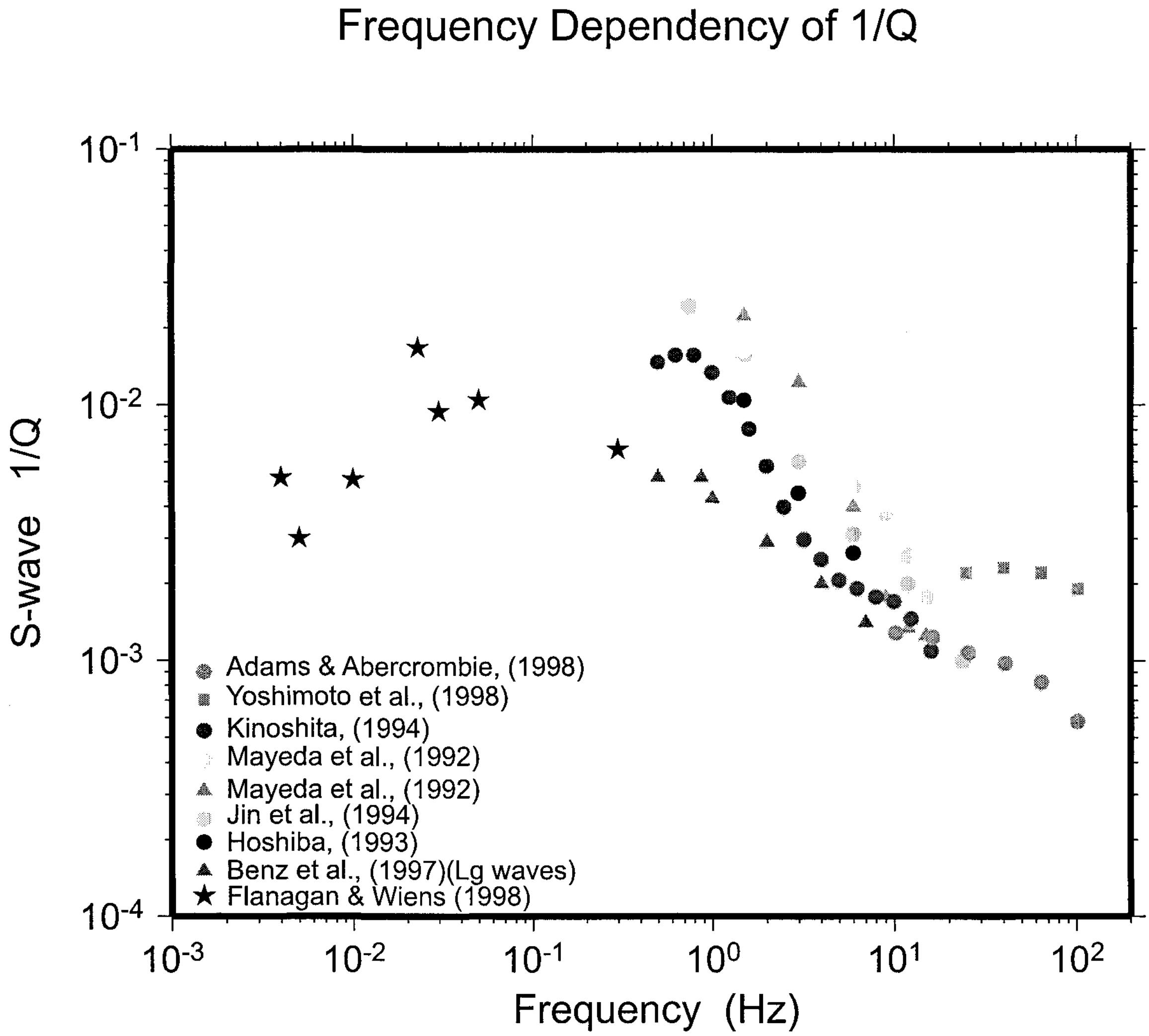

Figure 3.1.3.1. Frequency dependence of S-wave Q^{-1} based on the observations for seismic active regions around the earth. [Reproduced from Jin, 1999].

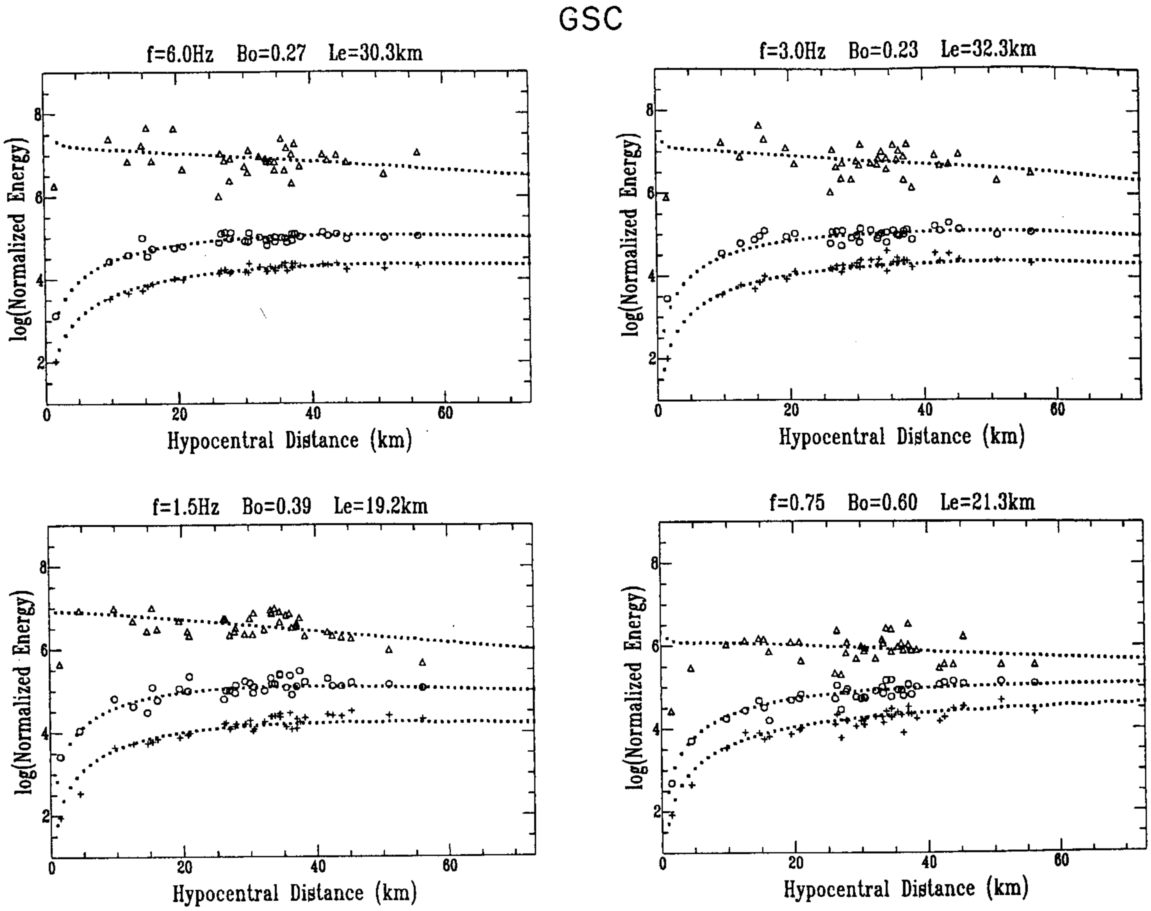

Figure 3.1.3.2. Plots of normalized energy corrected for geometrical spreading by $4\pi r^2$ vs. hypocentral distance for station GSC, southern California. Triangles,circles,and crosses represent energy integrated over time windows of 0-15s,15-30s,and 30-45s,after the S arrival, respectively. Dashed lines show the best fit model.The frequency and corresponding best fit model parameters Bo and Le are shown at the top of each panel, individually.[Reproduced from Jin et al.,1994].

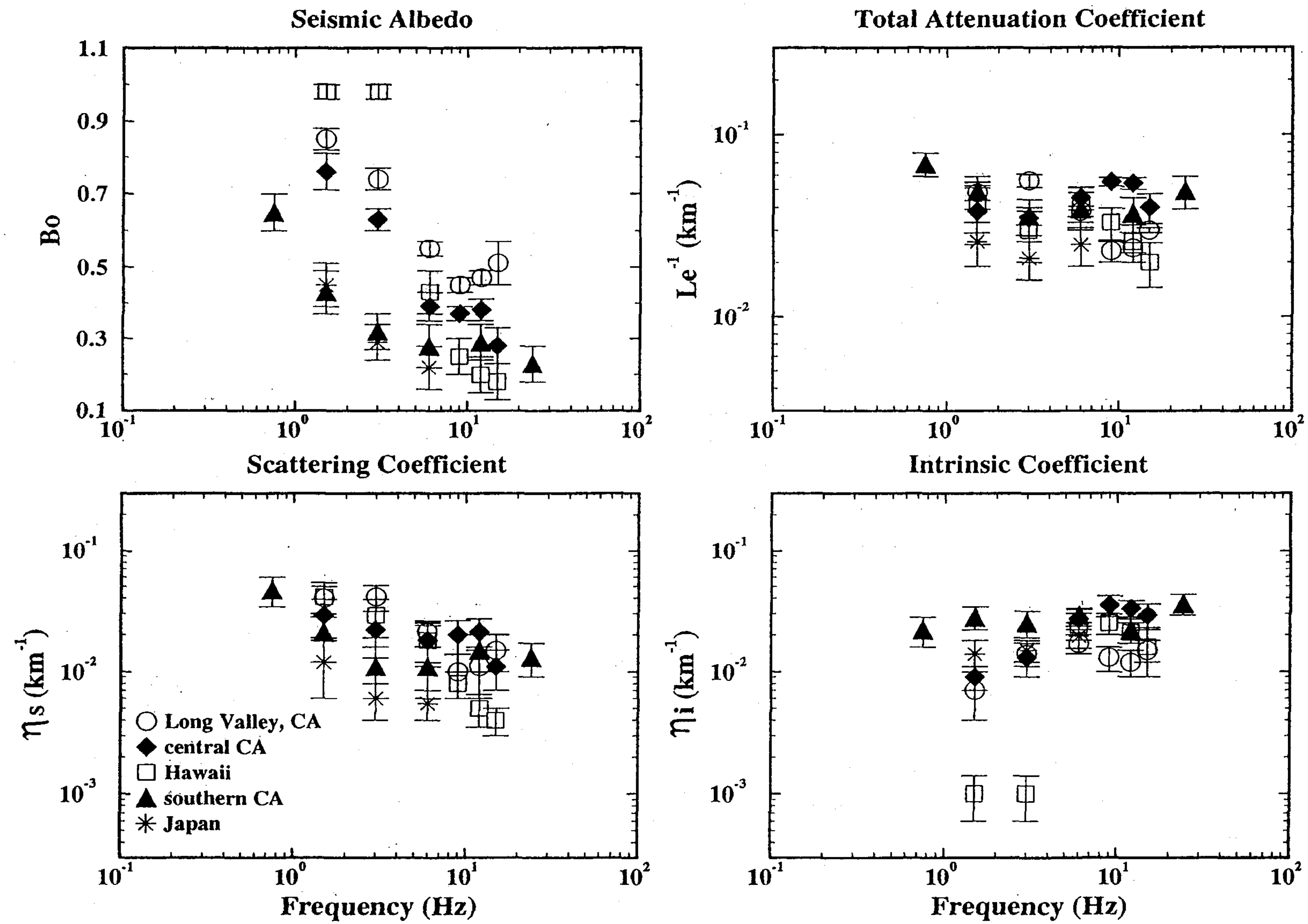

Figure 3.1.3.3. Comparison of seismic albedo and various attenuation coefficients for Japan(star),southern California(solid triangle), Hawaii(square), central California(solid diamond), and Long Valley,Californa (circle). All the errors were made at confidence level of 95% for southern California and 90% for the other regions. [Reproduced from Jin et al.,1994].

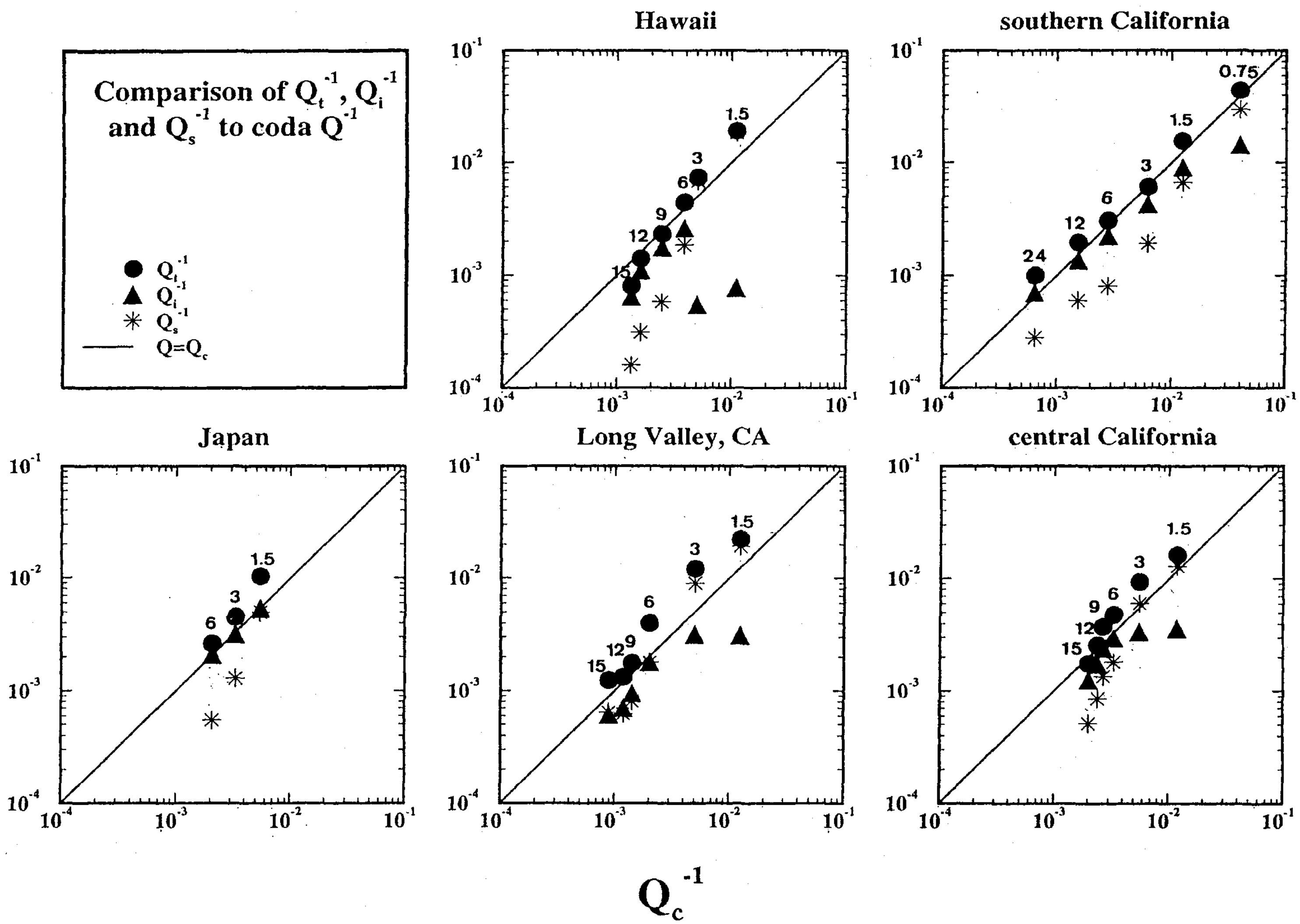

Figure 3.1.3.4. Plots of total attenuation, Q_t^{-1} (solid circle), intrinsic attenuation, Q_i^{-1} (solid triangle), and scattering attenuation, Q_s^{-1} (star) versus coda Q^{-1}, Q_c^{-1}, for various tectonic regions. The straight line represents where $Q = Q_c$, and the numbers indicate the corresponding frequency in Hz. [Reproduced from Jin et al., 1994].

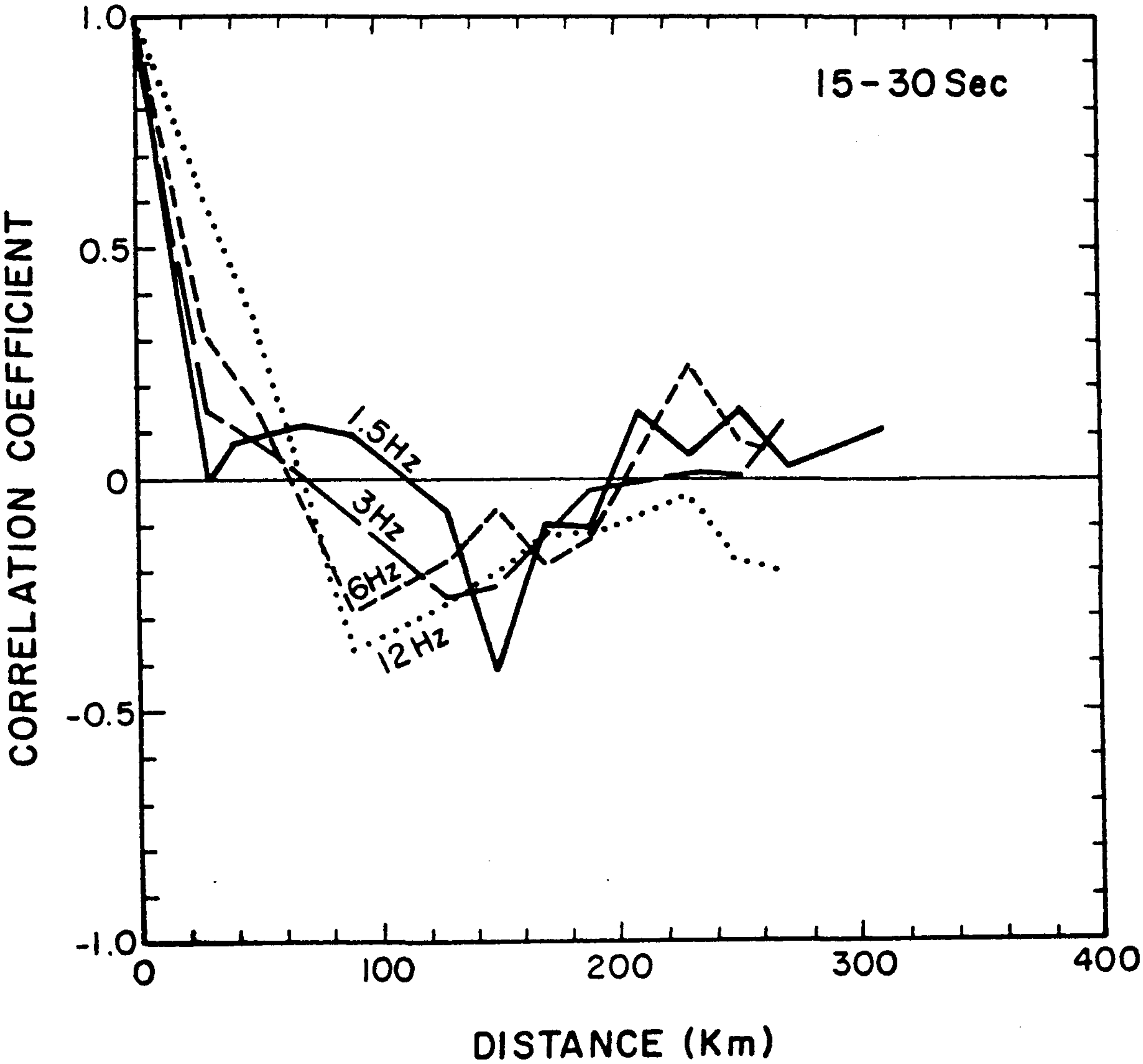

Figure 3.1.3.5. Spatial auto-correlation function of coda Q^{-1} at various frequencies measure from lapse time window 15-30 second in southern California obtained by Peng(1989).

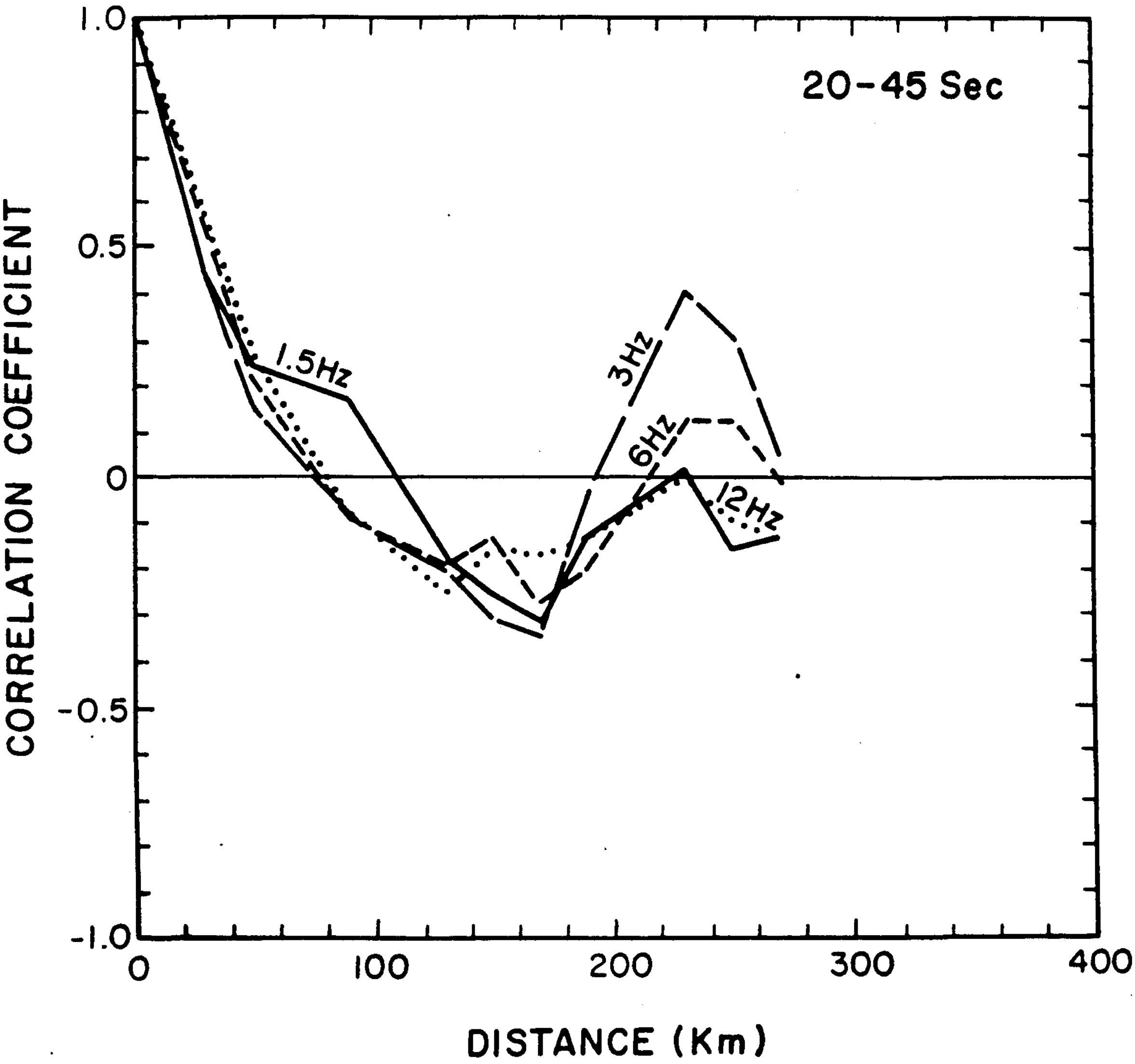

Figure 3.1.3.6. Spatial auto-correlation function of coda Q^{-1} at various frequencis measureed from lapse time window 20-45 second in southern California obtained by Peng(1989).

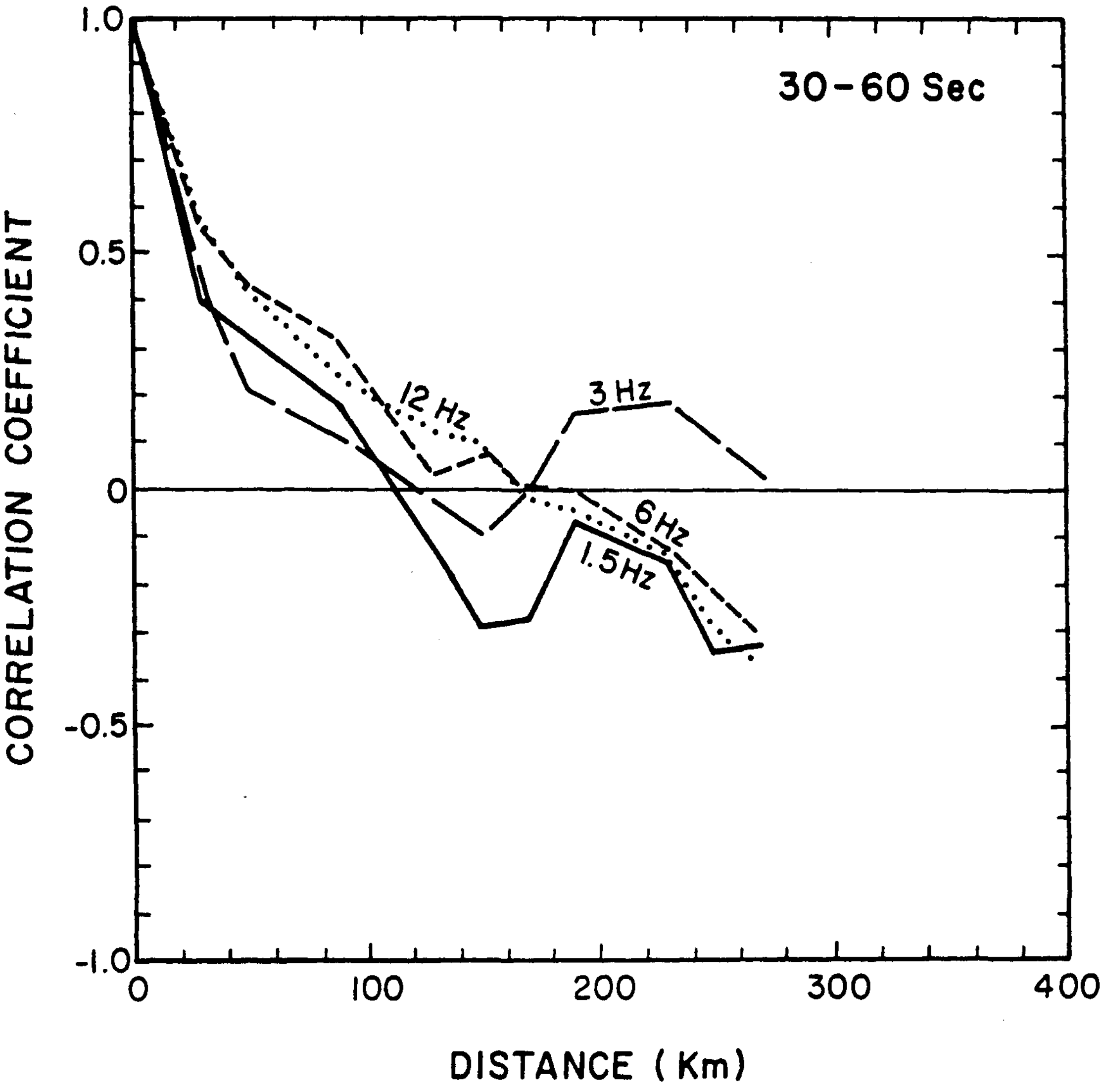

Figure 3.1.3.7. Spatial auto-correlation function of coda Q^{-1} at various frequencies measured from lapse time window 30-60 sec. in southern California obtained by Peng(1989).

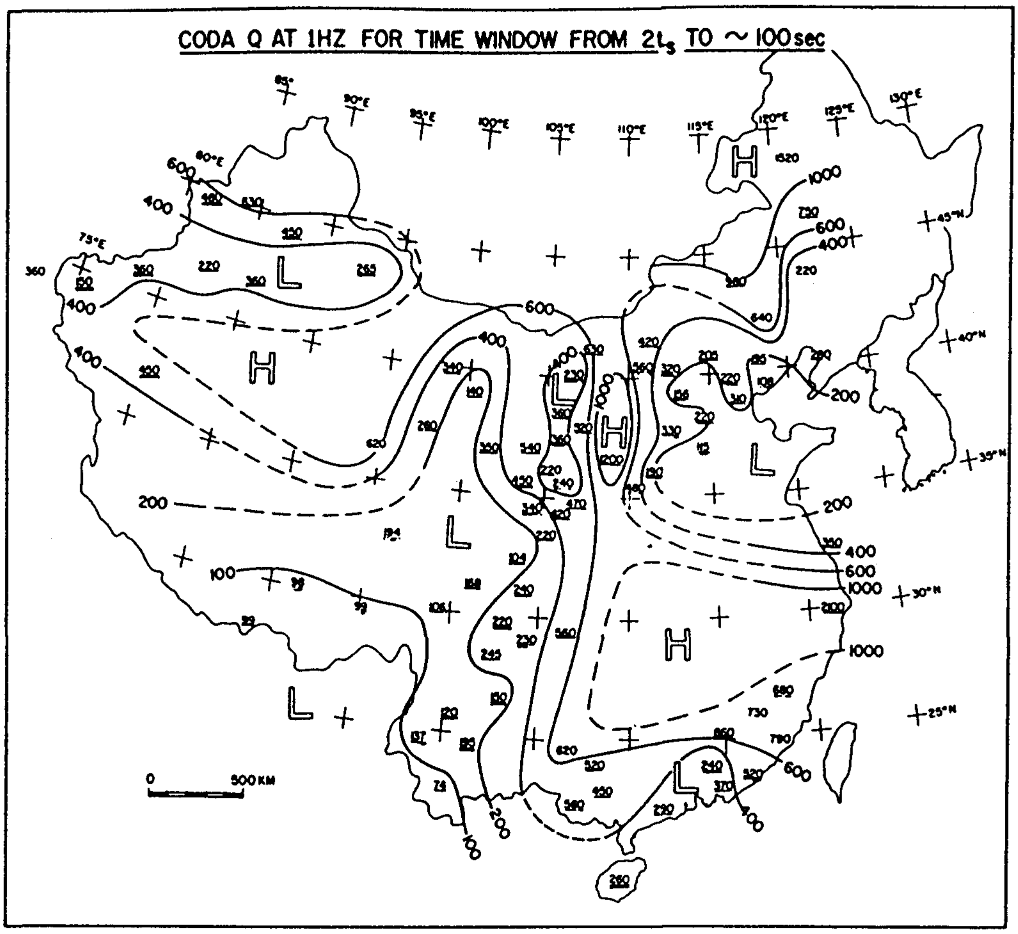

Figure 3.1.3.8. Measured coda Q values at 1 Hz within lapse time window from 2ts (ts:S-wave travel time) to 100 second and the iso-Q lines over the mainland of China. [Reproduced from Jin and Aki, 1988].

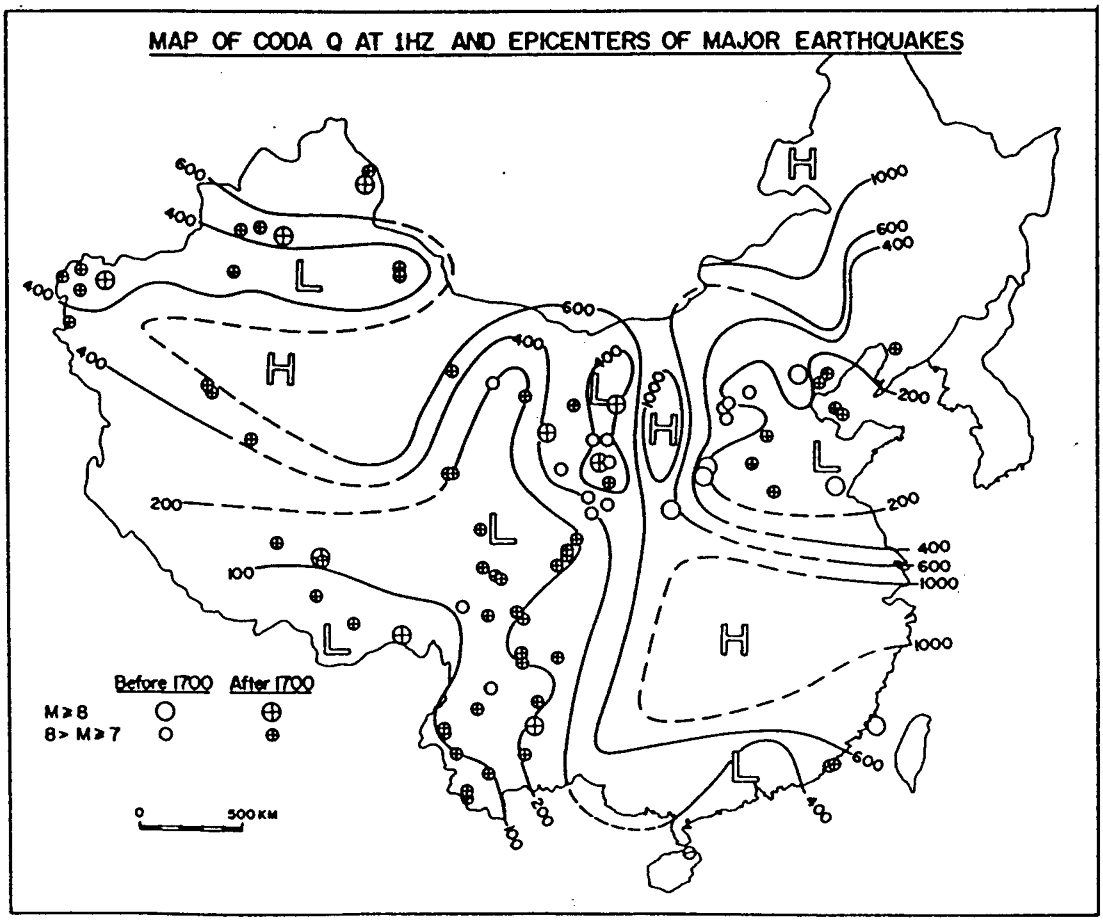

Figure 3.1.3.9. Map of coda Q at 1 Hz and epicenters of major earthquakes with M >= 7. Different symbols are used for M >= 8 and M < 8, and before and after 1700. [Reproduced from Jin and Aki, 1988].

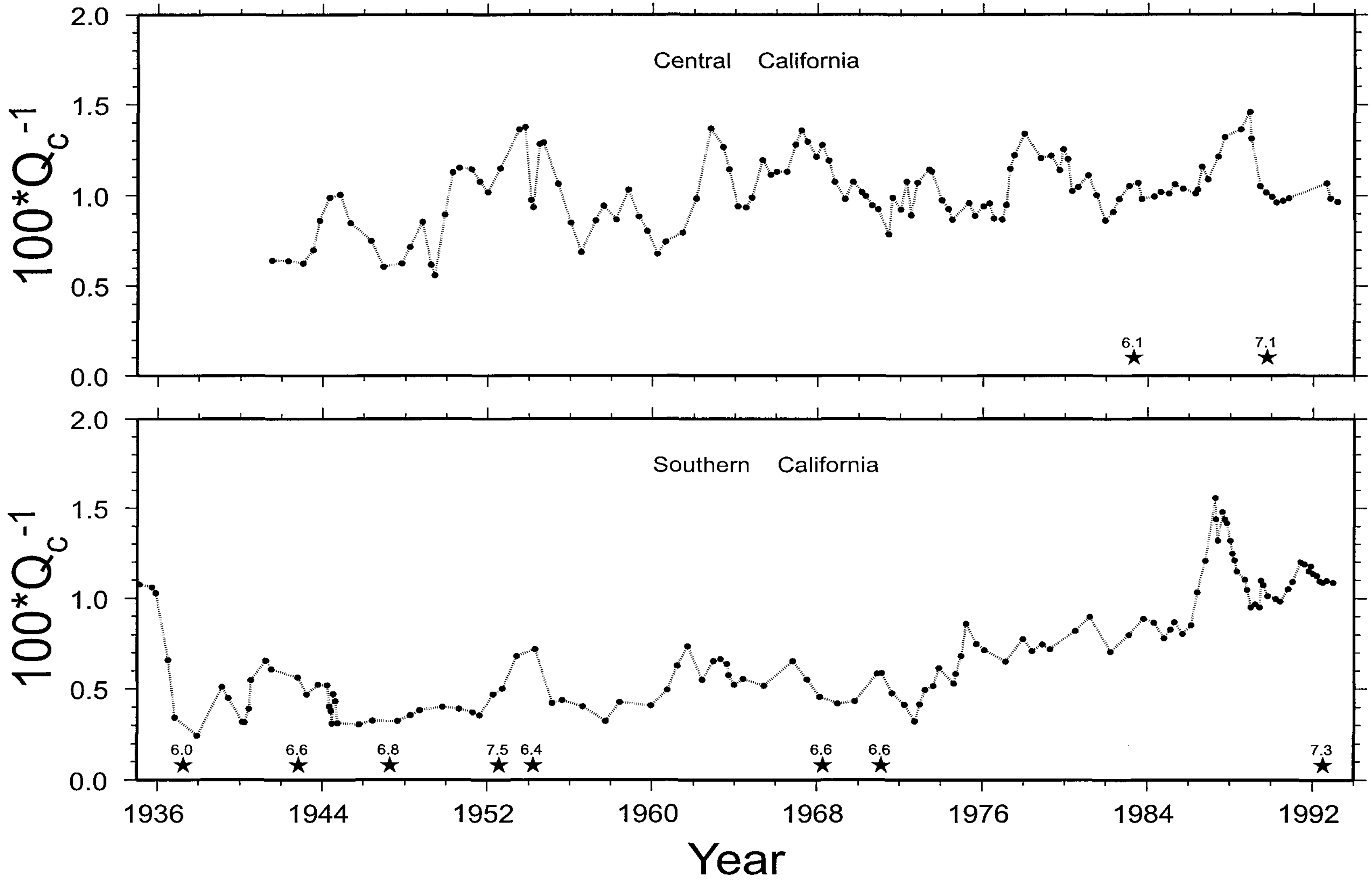

Figure 3.1.3.10. Coda Q^{-1} (at frequency around 2 Hz) as a function of time for central and southern California. Stars indicate major earthquakes occurred within each study area. The number above each star is the magnitude. [Reproduced from Jin and Aki,1993].

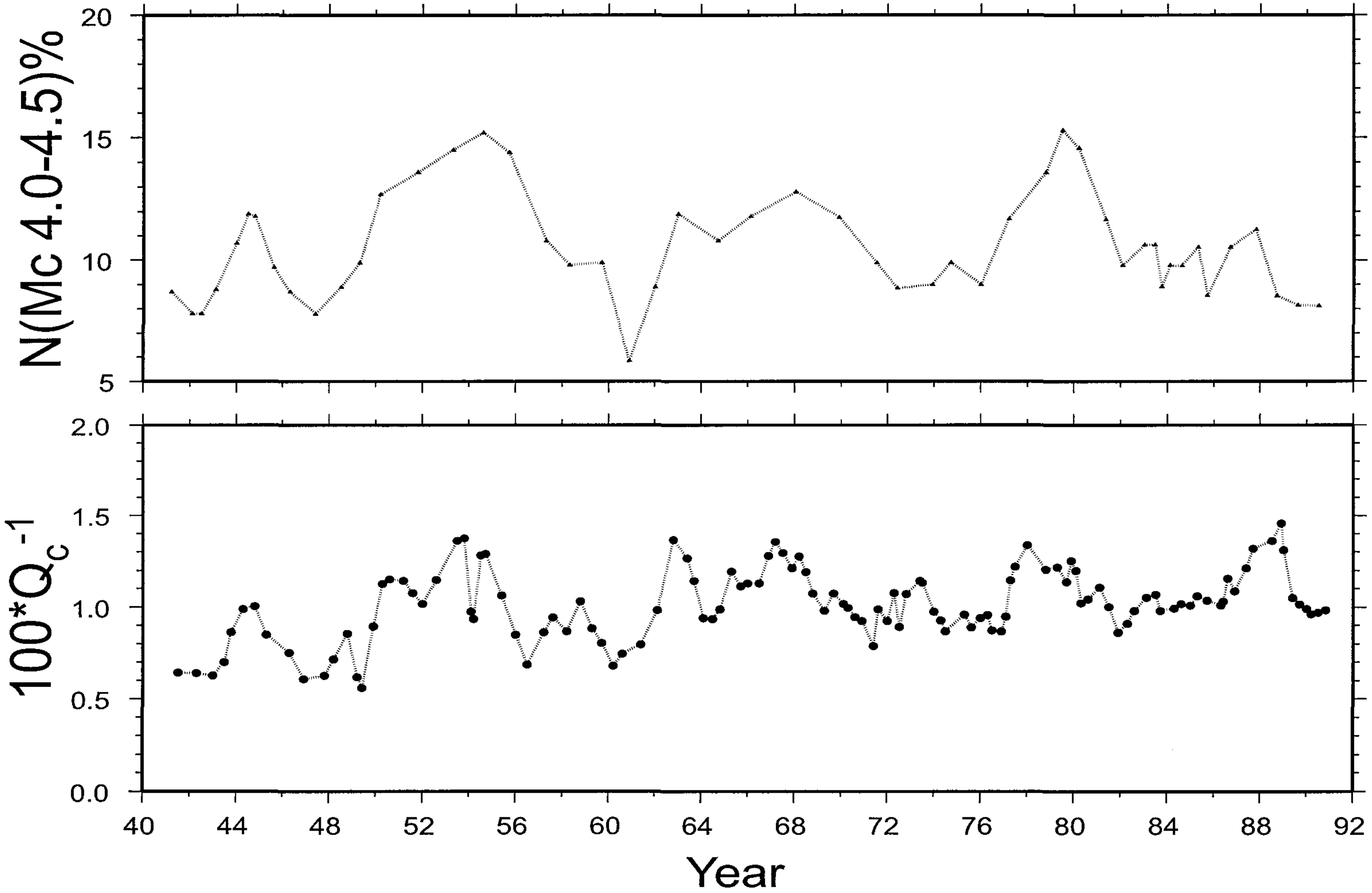

Figure 3.1.3.11. Comparison between temporal variation of coda Q^{-1} (at f about 2 Hz) and fractional frequency of earthquakes with magnitude 4.0 - 4.5, for central California. [Reproduced from Jin and Aki,1993].

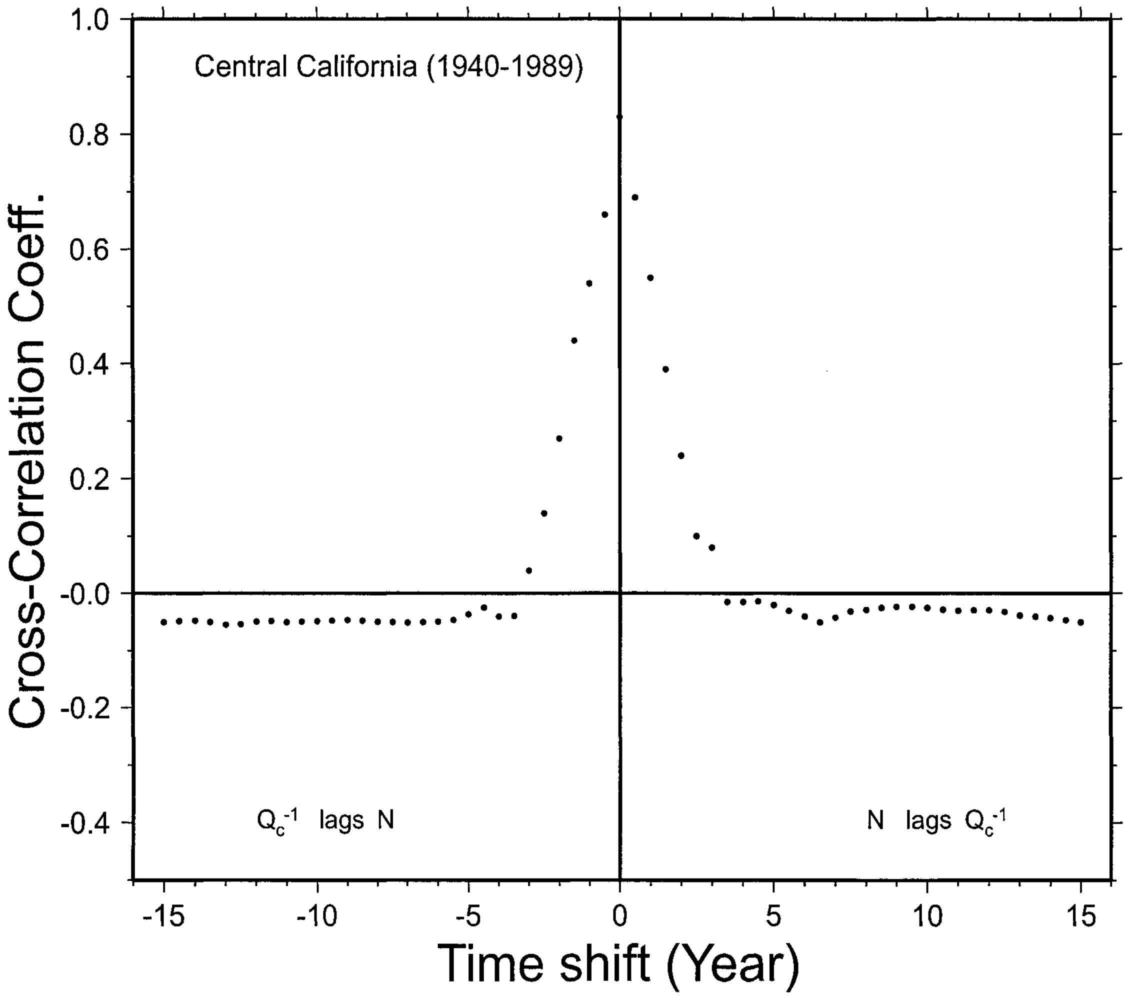

Figure 3.1.3.12. Cross-correlation function between the two time series shown in Figure 3.1.3.11. [Reproduced from Jin and Aki,1993].

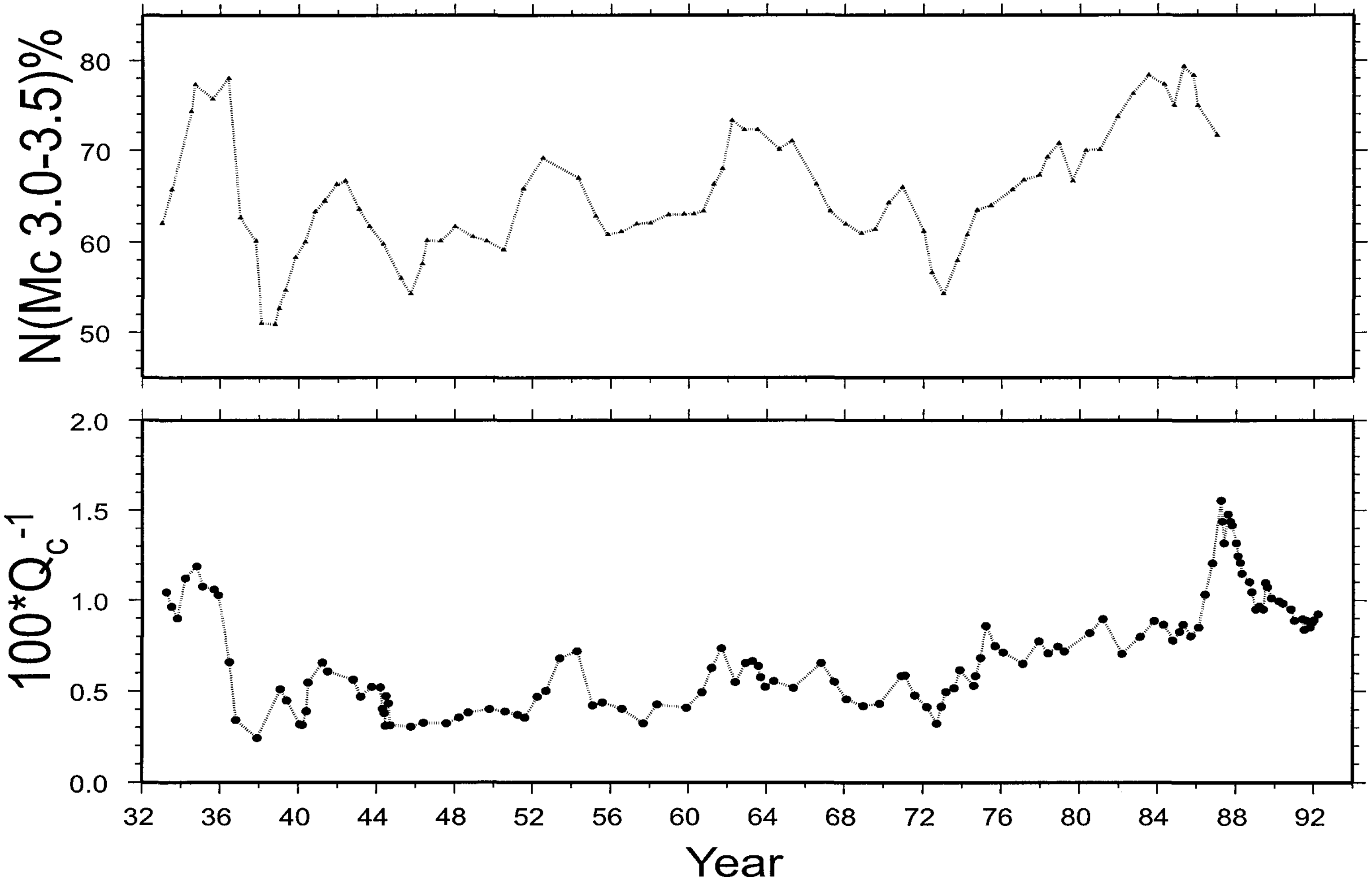

Figure 3.1.3.13. Comparison between temporal variation of coda Q^{-1} (f is about 2 Hz) and fractional frequency of earthquakes with magnitude of 3.0 - 3.5, for southern California. [Reproduced from Jin and Aki, 1989].

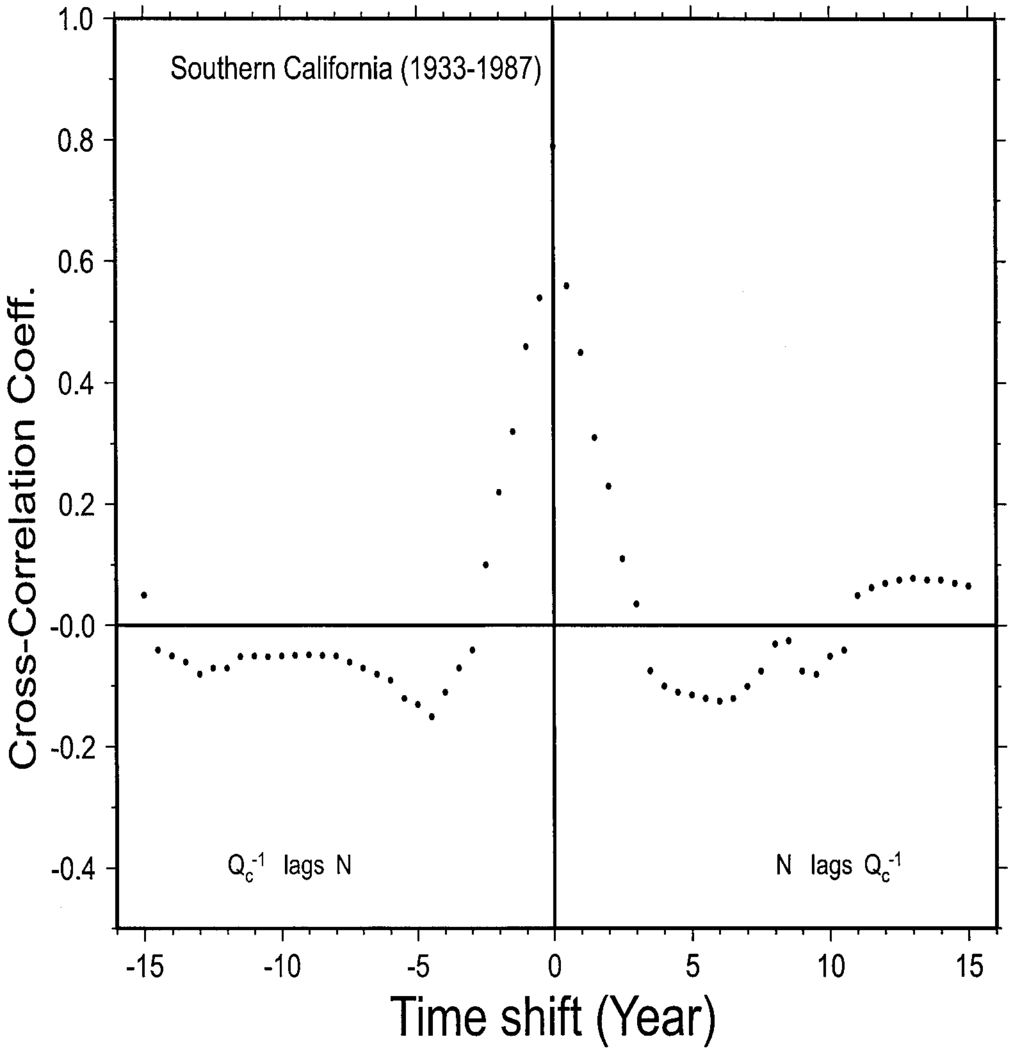

Figure 3.1.3.14. Cross-correlation function between the two time series shown in Figure 3.1.3.13. [Reproduced from Jin and Aki, 1989].

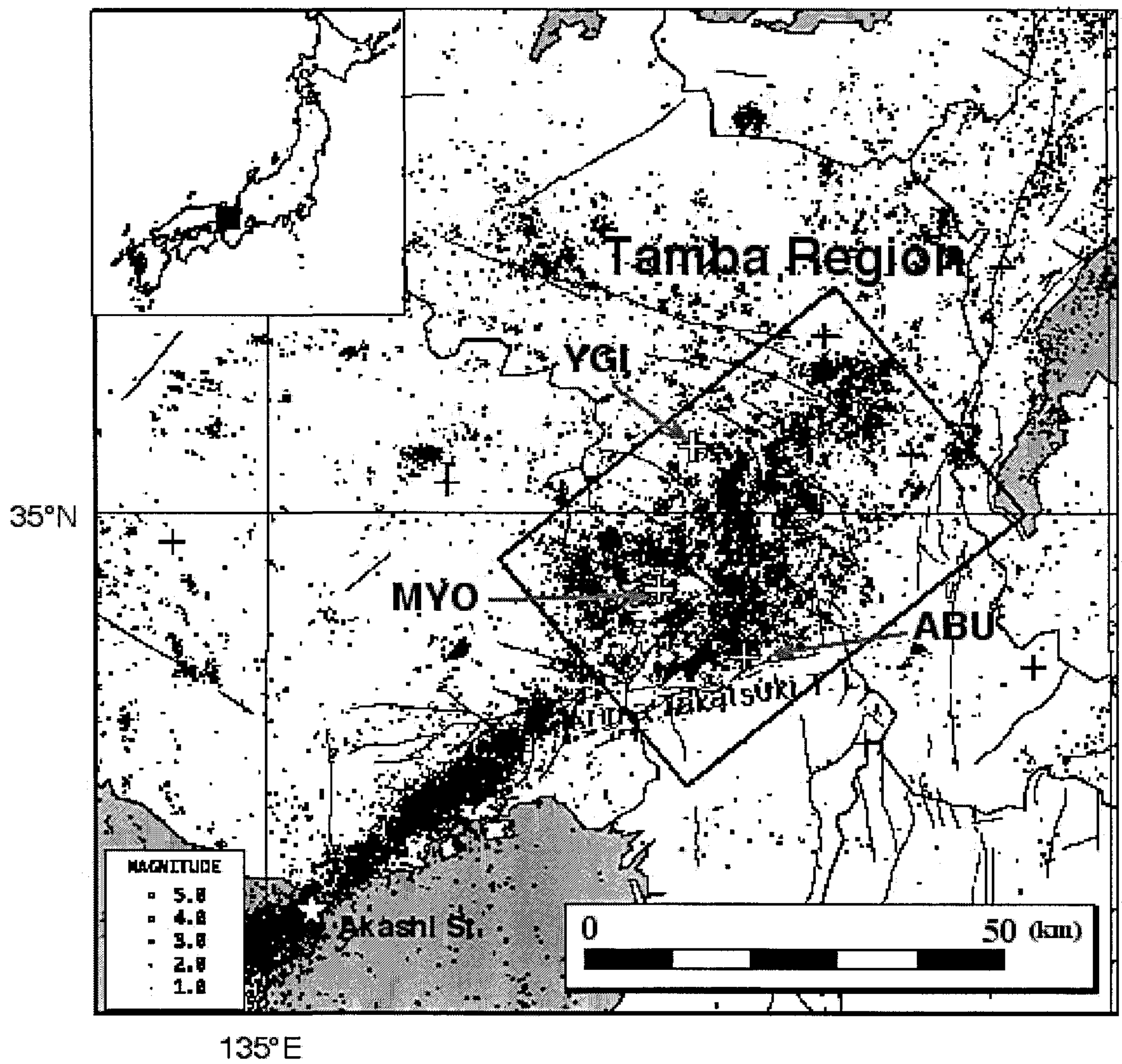

Figure 3.2.1.1. The distribution of epicenters in the depth range between 0 and 20 km (dots) and stations (crosses) from 1987 to 1996 in the Kinki district, central Honshu, Japan. The retangle shows the Tamba region where we analyzed Q_c^{-1}. Star shows the epicenter of the Hyogo -ken Nanbu earthquake. Thin lines are Quaternary active faults. Line A-B denotes a section of the spatial-temporal plot of seismicity in Figure 3.2.1.6.[Reproduced from Hiramatsu et al.,2000].

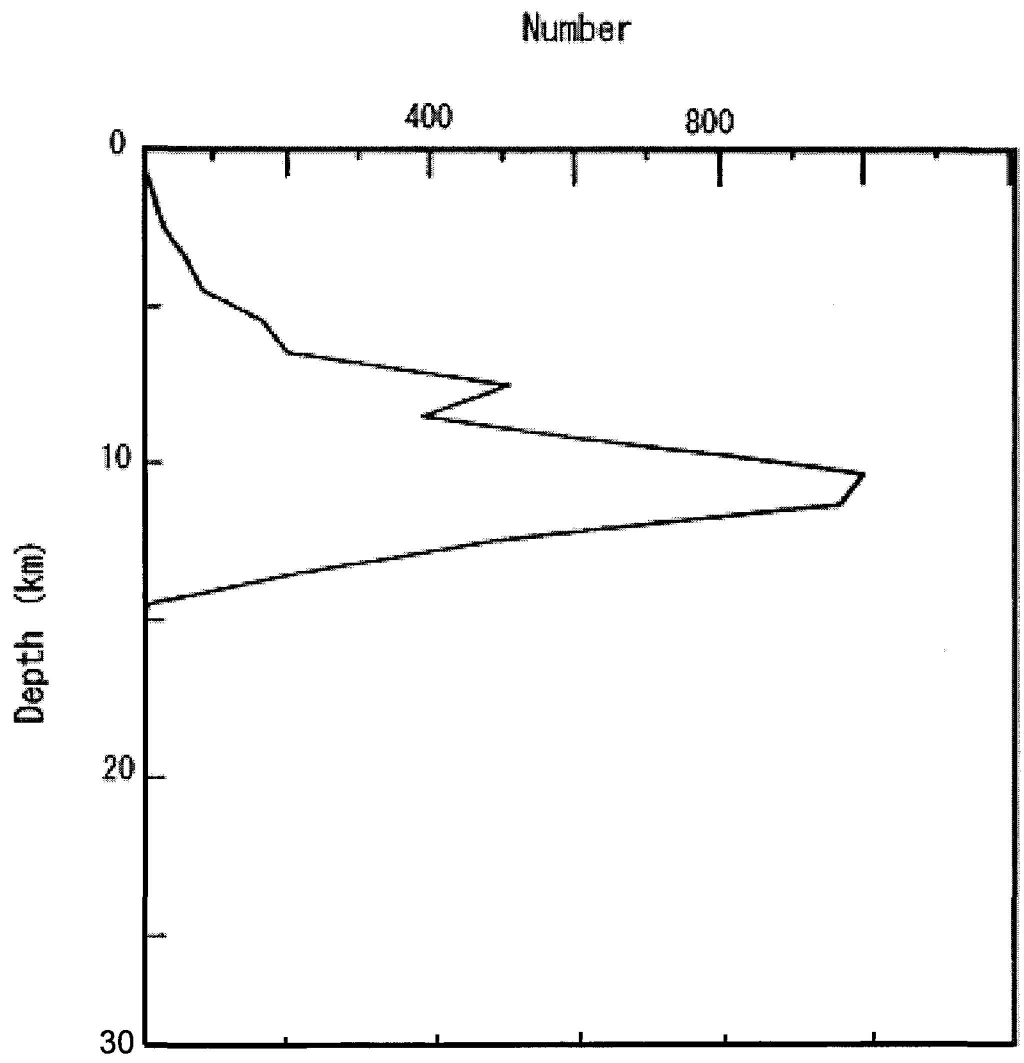

Figure 3.2.1.2. Depth-frequency distribution of earthquakes determined by the use of the master event location technique in the southern part of the study area [Reproduced from Ito, 1990].

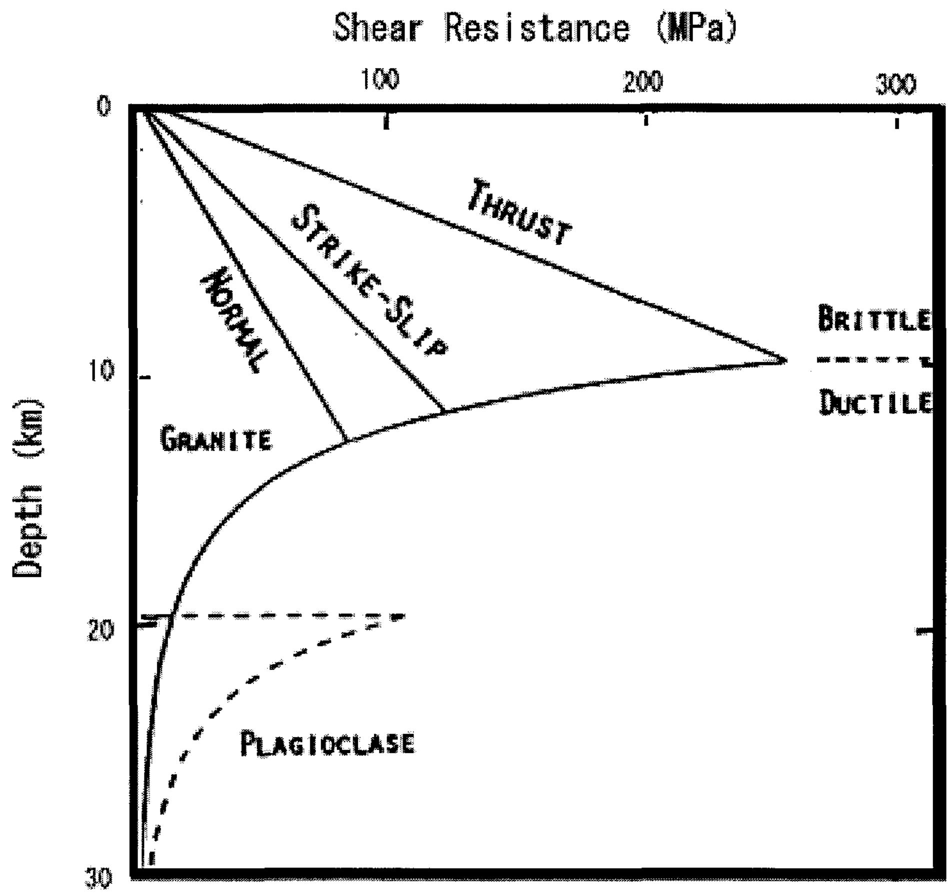

Figure 3.2.1.3. Shear resisitance with depth for a simple brittle-ductile transition model for granite (solid lines) and plagioclase(dashed lines)[Reproduced from Ito,1990].

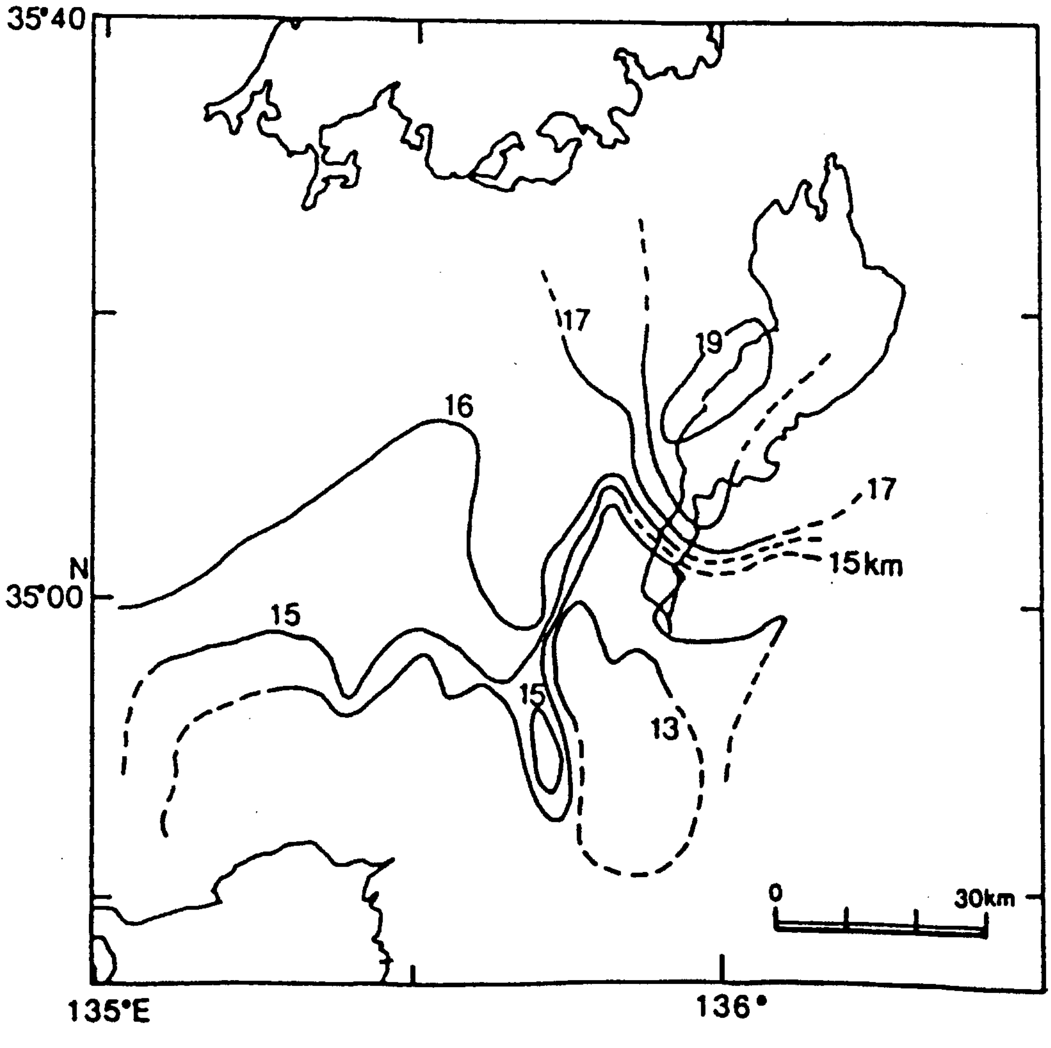

Figure 3.2.1.4. Contours of the seismic-aseismic boundary in the northern Kinki district, Japan [Reproduced from Ito,1990].

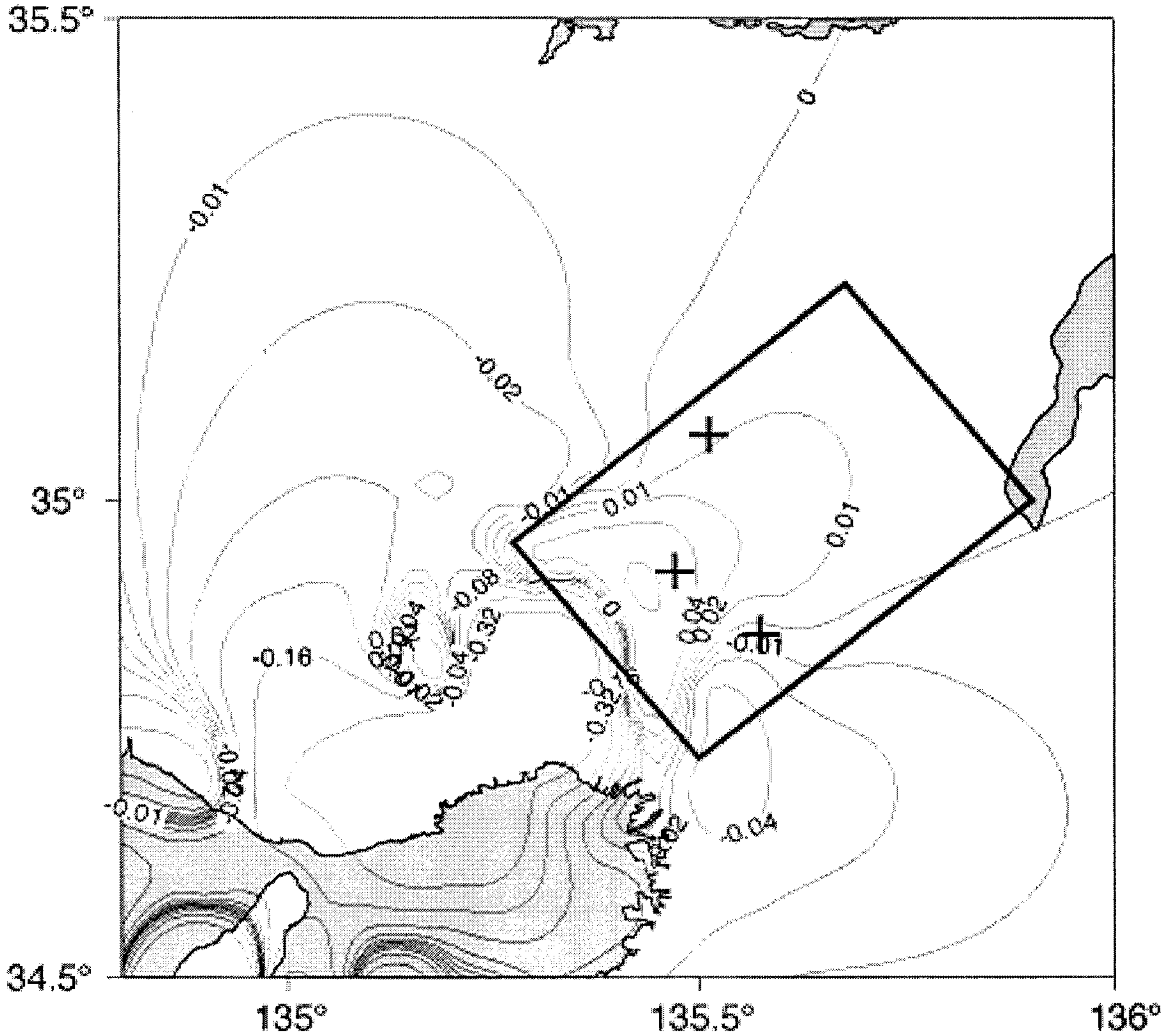

Figre 3.2.1.5. The change in the shear stress of the N 45° E component at the depth of 10 km due to the Kobe earthquake. Rectangle shows the analyzed area, and crosses show the stations for Q_c^{-1} measurement. The fault model, geometry, and slip distribution of the mainshock of Hashimoto et al.(1996) are used. Poisson's ratio and rigidity are 0.25 and 40 GPa, respectively. [Reproduced from Hiramatu et al.,2000].

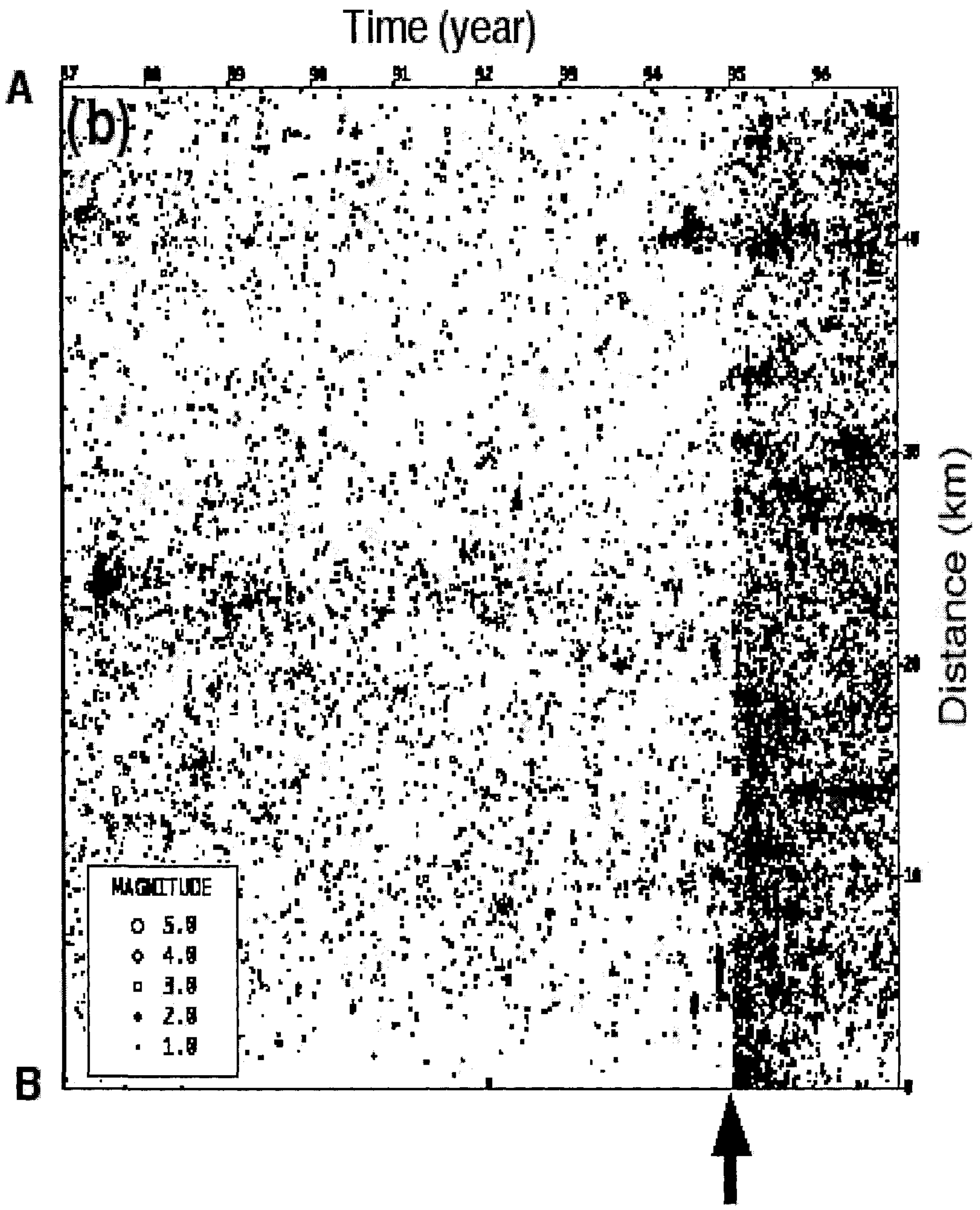

Figure 3.2.1.6. The spatial-temporal variation in seismicity in the analyzed area. Arrow shows the occurrence of the Hyogo-ken Nanbu (Kobe)earthquake. The change in seismicity associated with the Kobe earthquake is clearly shown as the increase of earthquake over the region. [Reproduced from Hiramatsu et al.,2000].

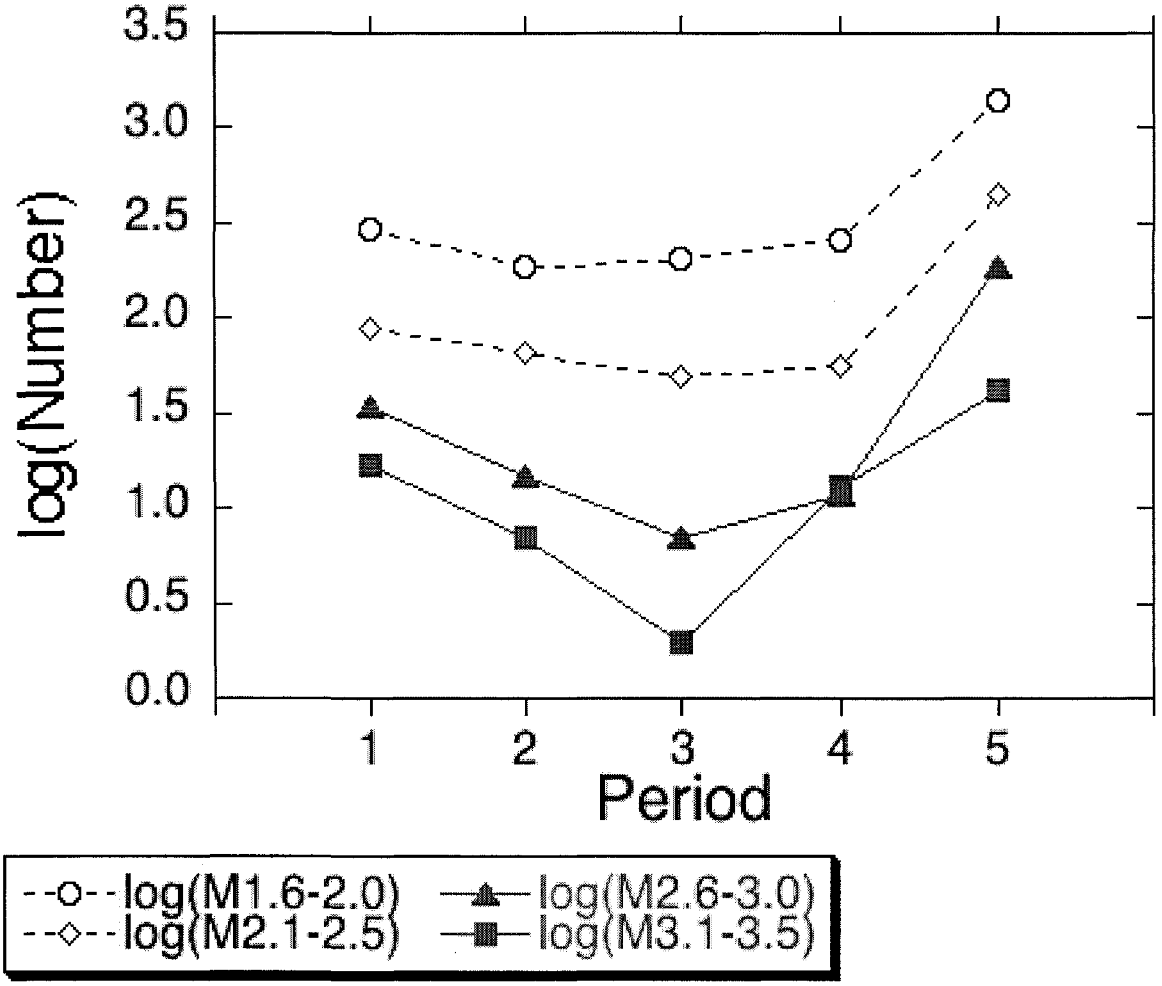

Figure 3.2.1.8. The temporal variation in the number of earthquakes of four magnitude ranges: 1.6-2.0 (open circles), 2.1-2.5 (diamonds), 2.6-3.0 (triangles), and 3.1-3.5 (squares).
[Reproduced from Hiramatsu et al., 2000].

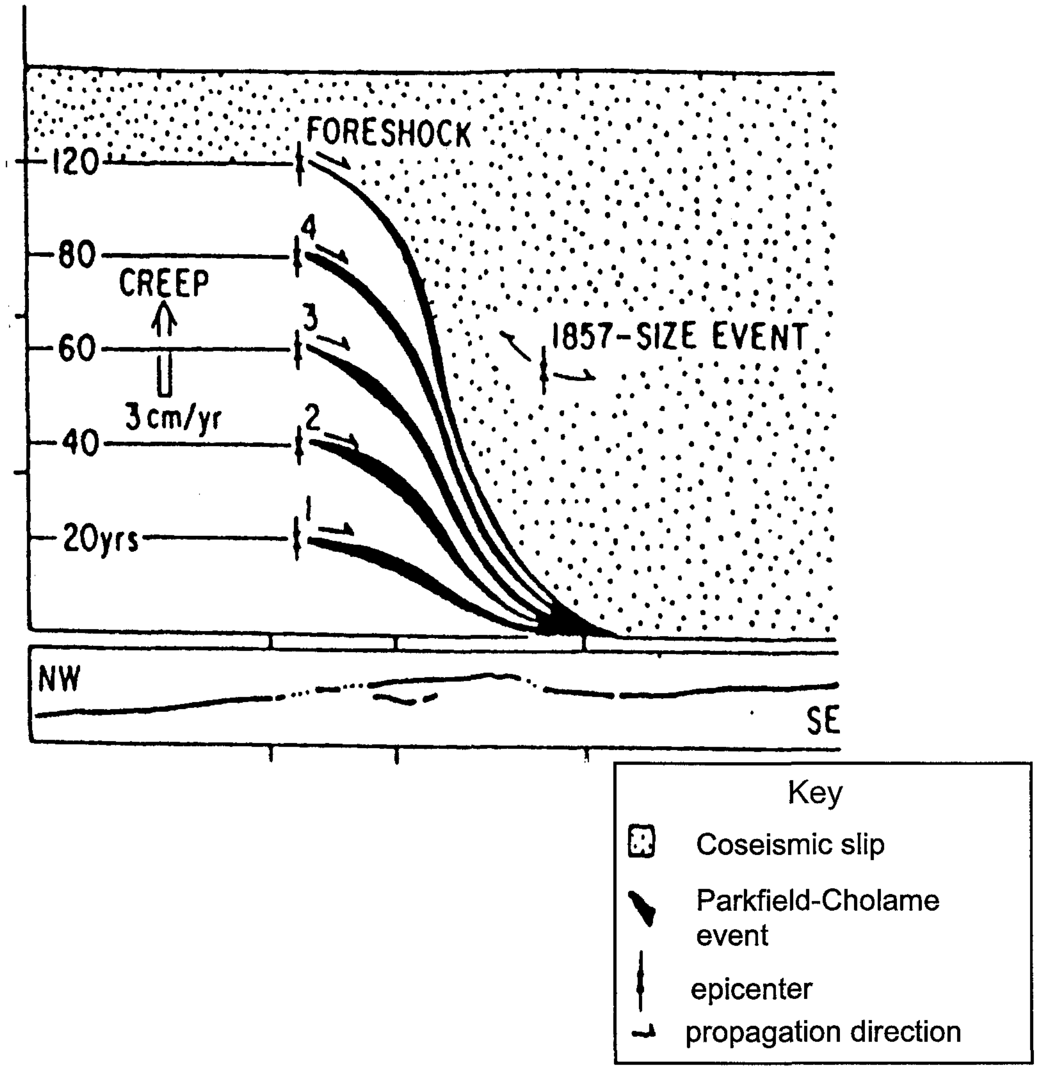

Figure 3.2.1.9. Hypothetical relationship of creep and moderate Parkfield -Cholame earthquakes to the initiation of great 1857-size earthquakes near Parkfield-Cholame. Relatively continuous right-lateral fault slip occurs along the creeping reach of the fault; creep punctuated about ever 20 years by a moderate-magnitude event occurs between Stone Canyon and Cholame; fault dormancy southeast of Cholame is broken every few hundred years by a great earthquake triggered by a moderate foreshock, such as occurred in 1857. The lower panel is a map view of the fault trace showing the segment which broke in 1966 (havy line) and a large bend in the fault near Cholame. [Reproduced from Sieh, 1978].

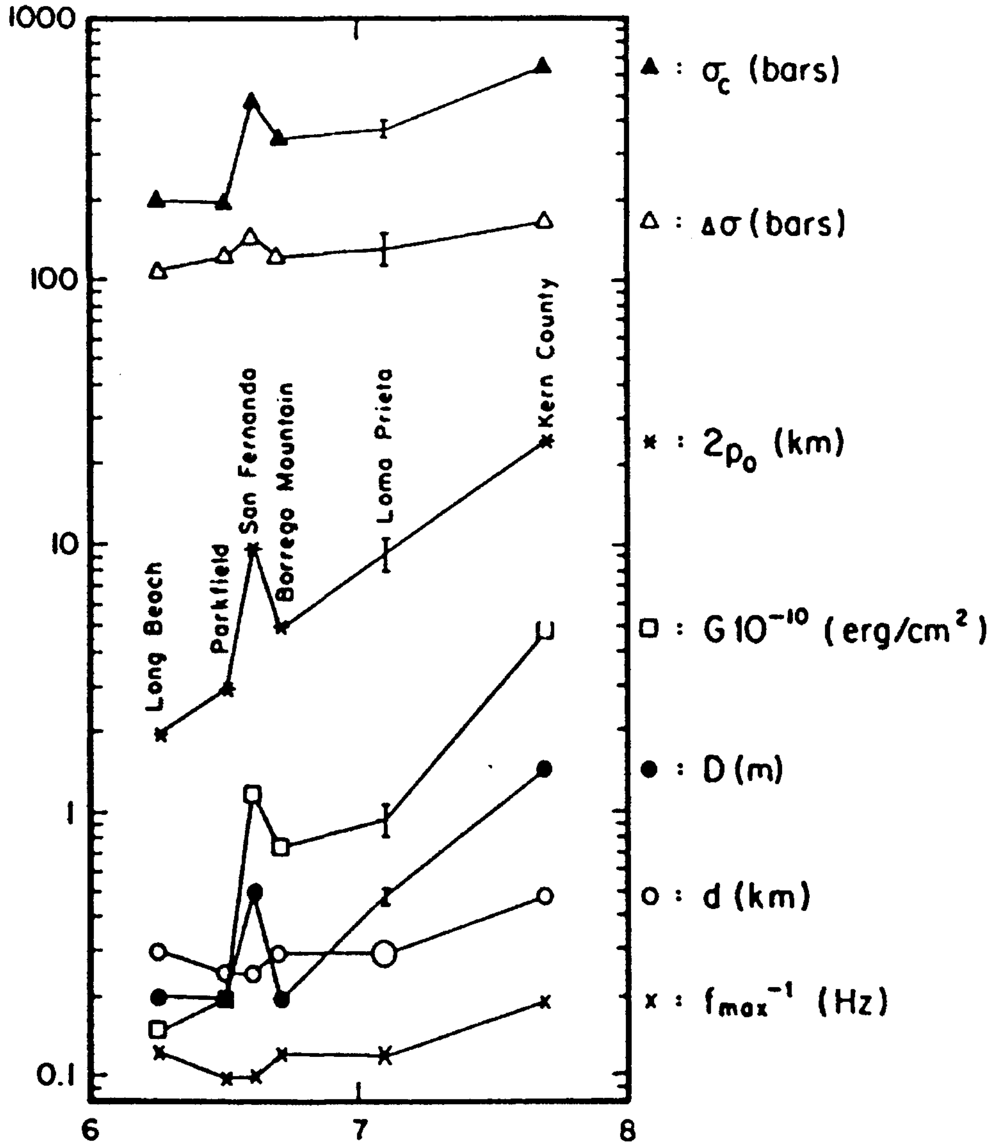

Figure 3.2.1.10. Source parameters of major California earthquakes determined by the application of the specific barrier model of Papageorgiou and Aki(1983) using the site amlification factor obtained by Phllips and Aki(1986).The parameters shown are, from top to bottom, the cohesive(breakdown) stress σ_c, the stress drop Ds in the circular creak(barrier interval),Griffith's specific fracture energy G, the critical weakening slip D, the size d of the cohesive(breakdown) zone, and the reciprocal of upper-limit frequency f_{max}. [Reproduced from Aki, 1992].

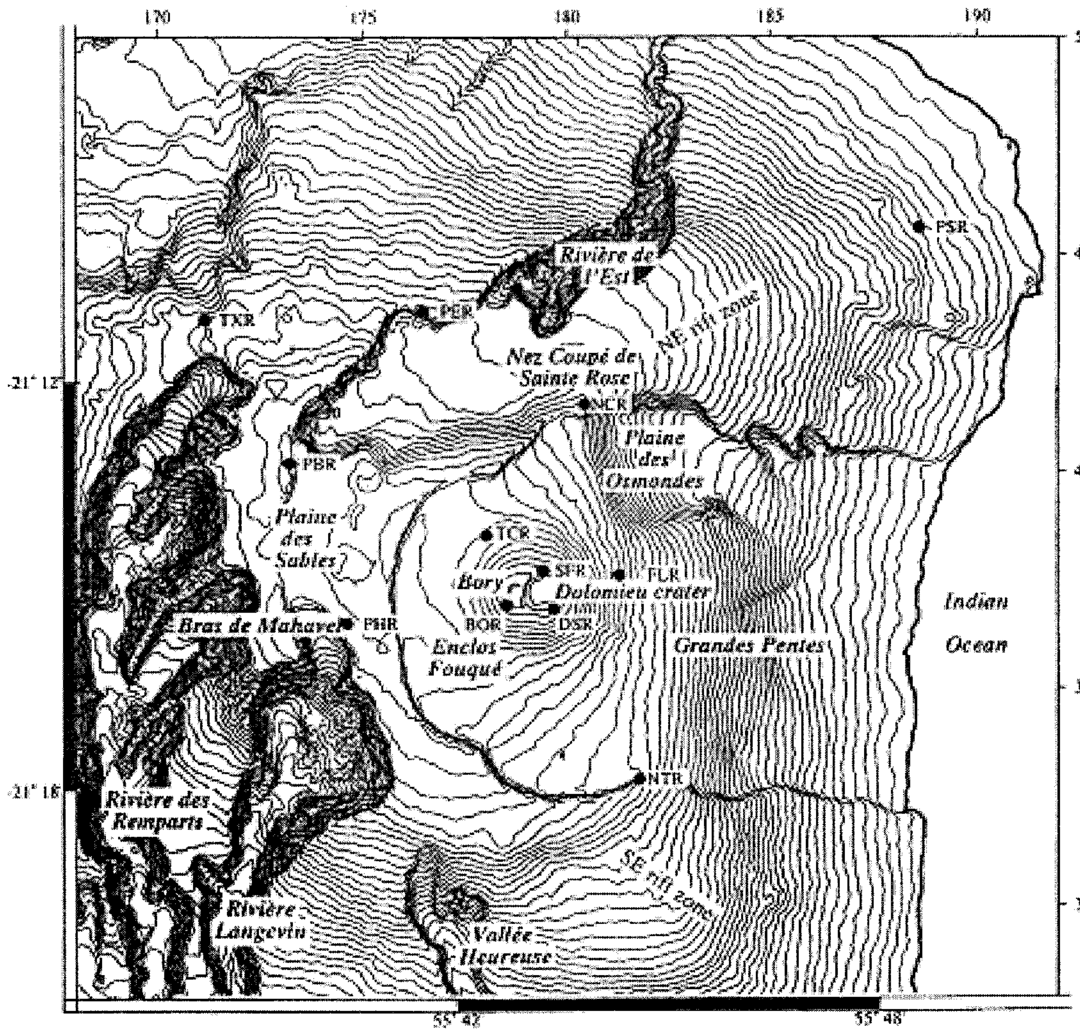

Figure 3.3.1.0. Topography map of the PdF, showing craters Bory and Dolomoeu at the summit of the central cone, the Enclos(Fouque) caldera, and the northeast and southeast rift zones. The locations of seismic stations within the map area are also marked. The numbers on the top and right sides of the map indicate, respectively, the eastward and northward co-ordinates in kilometers with the origin at (21.5°S, 54.0°E).

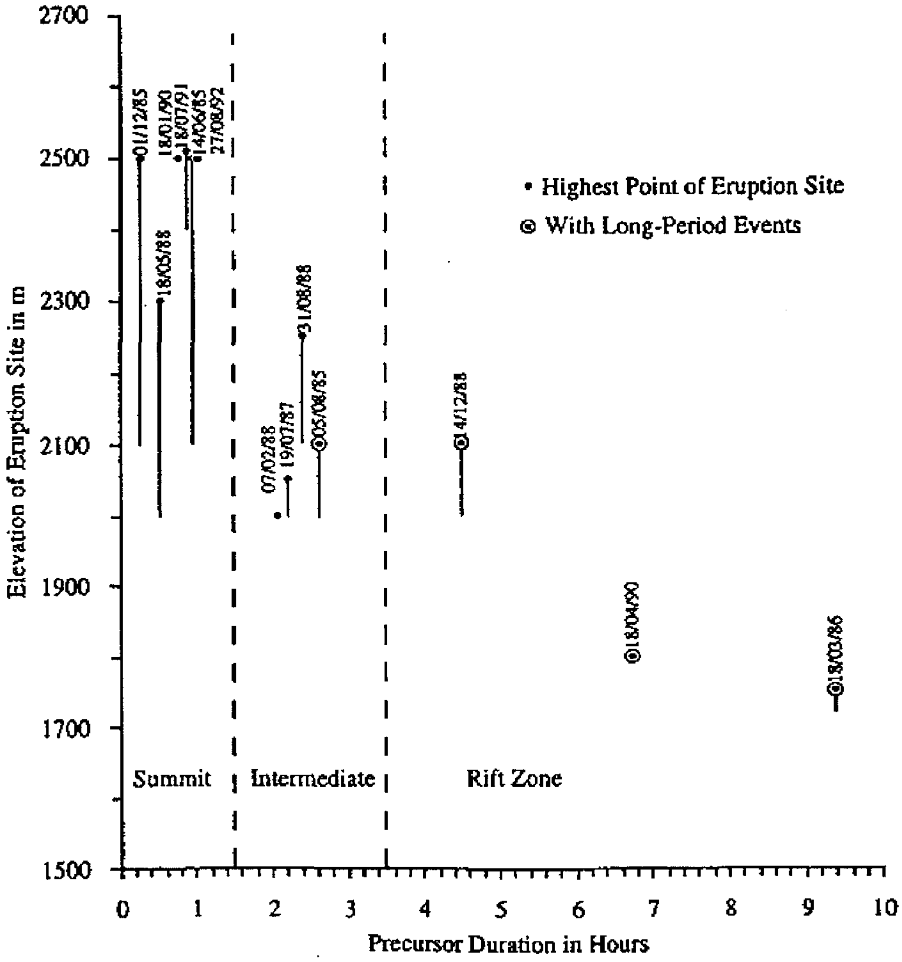

Figure 3.3.1.1. Relation between the precursor time of the seismic crisis and the elevation of the eruption site. Only those crises preceding the rift zone eruptions are accompanied by the occur--rence of LP events.

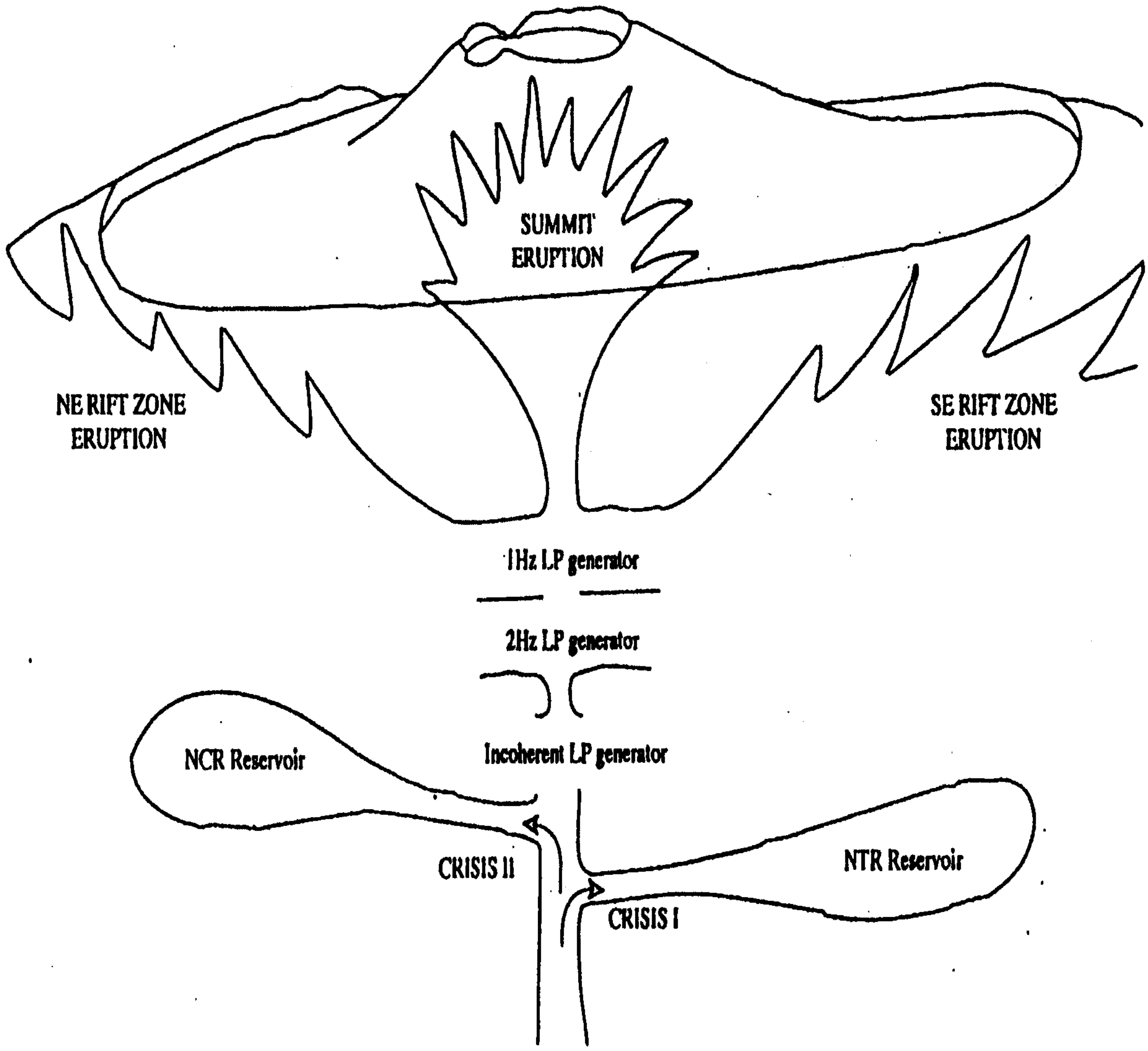

Figure 3.3.1.2. A schematic picture of the model drawn 4 days before the March 9,1998,eruption. The acture depth was unknow at that time, but estimated later from hypocenter migration during the precursory crisis.

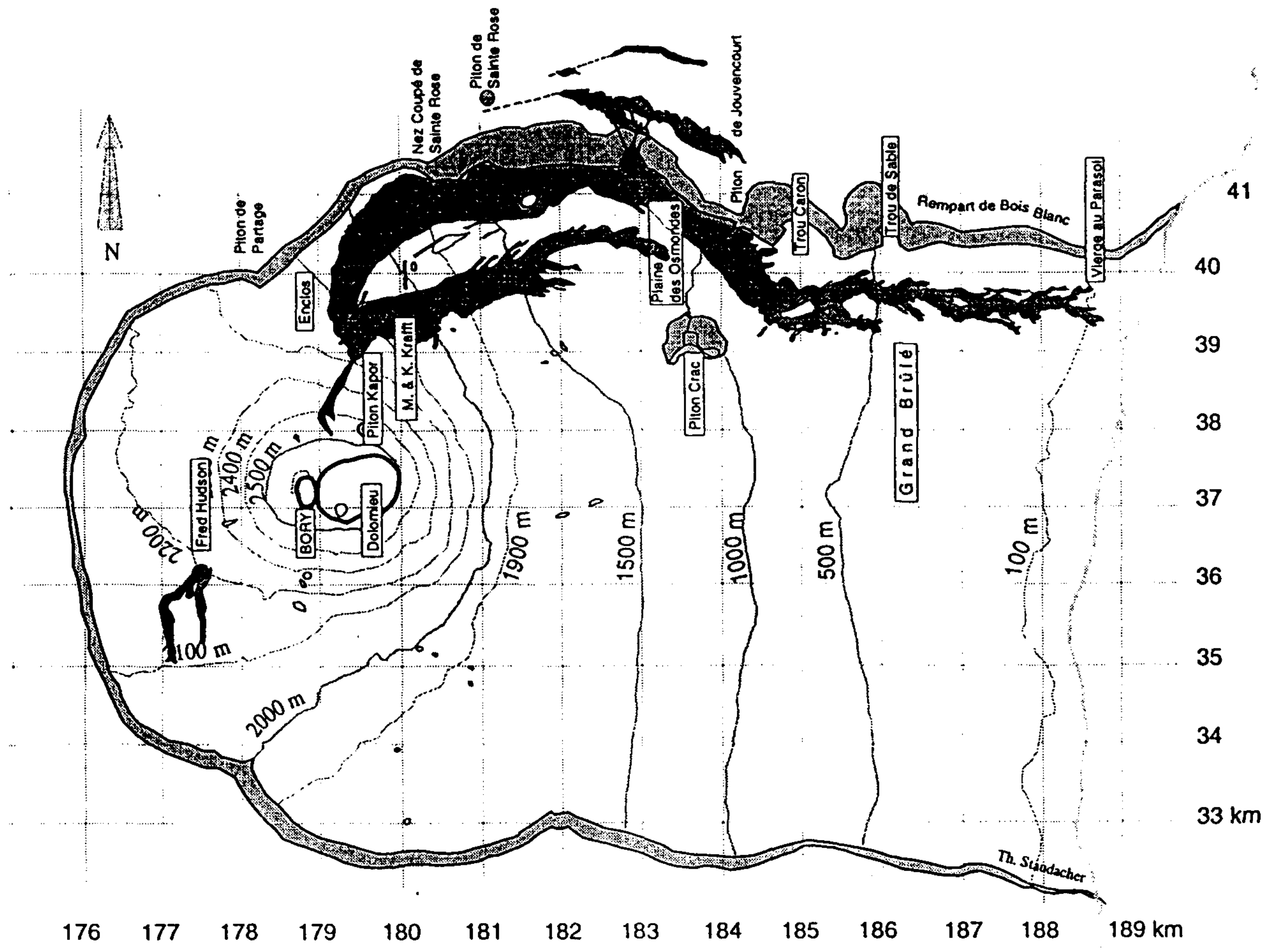

Figure 3.3.2.1. Three main vents of the March 1998 eruption are Piton Kapor, M. and K. Hudson. Eruption outside the Enclos caldera occurred in the last stage of the episode.

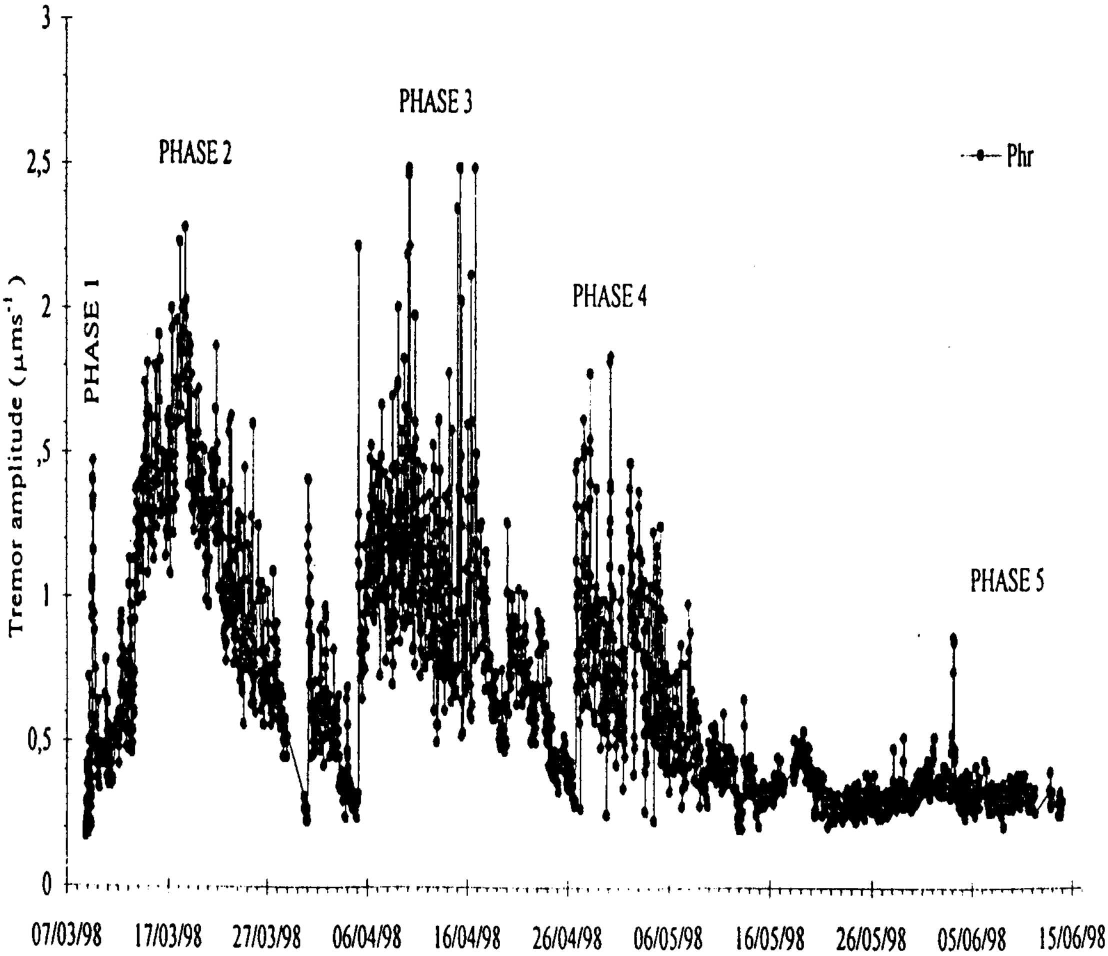

Figure 3.3.2.2. The amplitude of tremor at station PHR which is located at a distance of about 6 km W SW of the main eruption site. The amplitude is obtained by averaging the absolute value (in micrometers per second) over 10 s duration. (See Figure 3.3.1.0 for the location of the station).

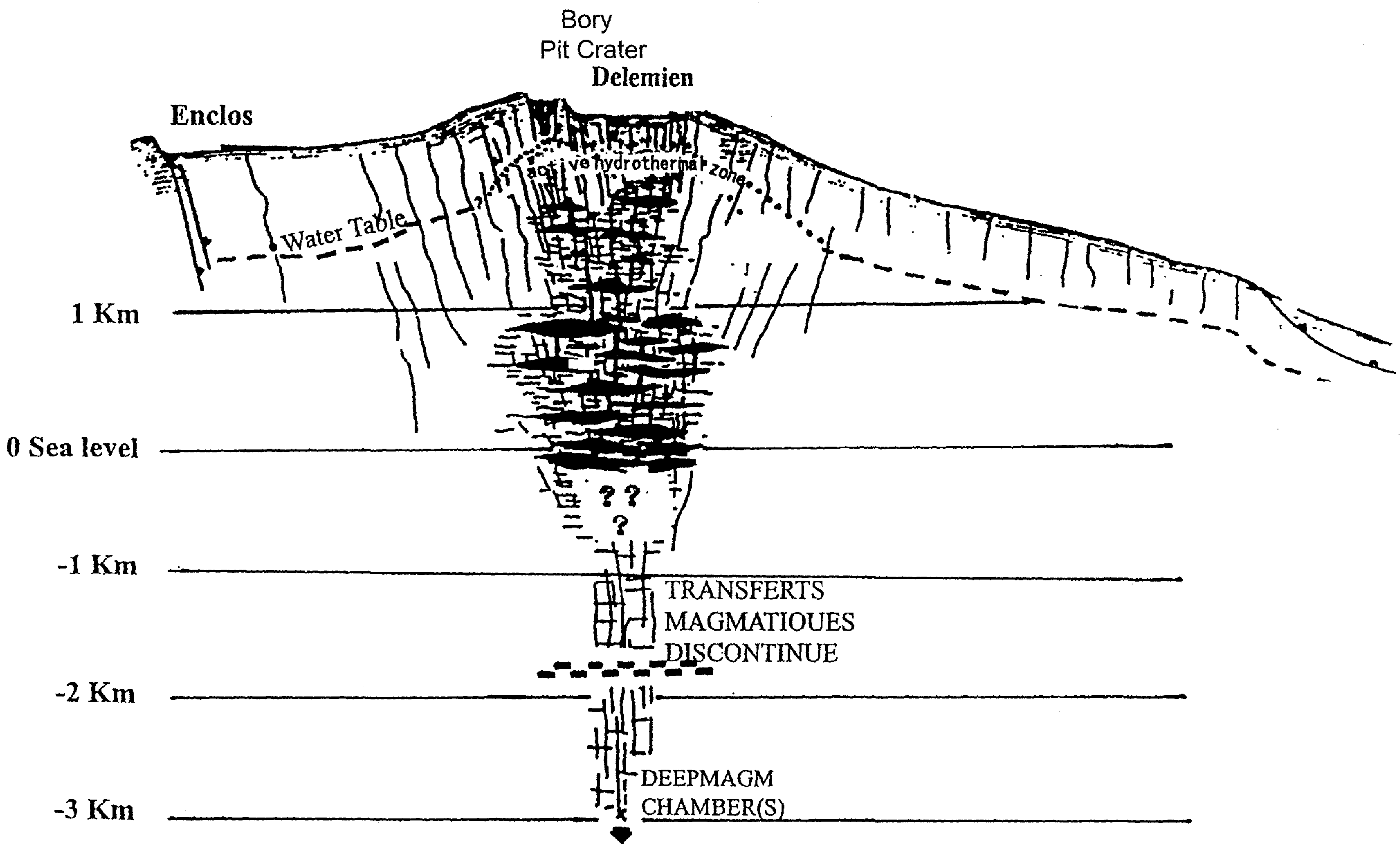

Figure 3.3.2.3. The model structure of The Piton de la Fournaise.[Reproduced from Lenat and Bachelery, 1990].

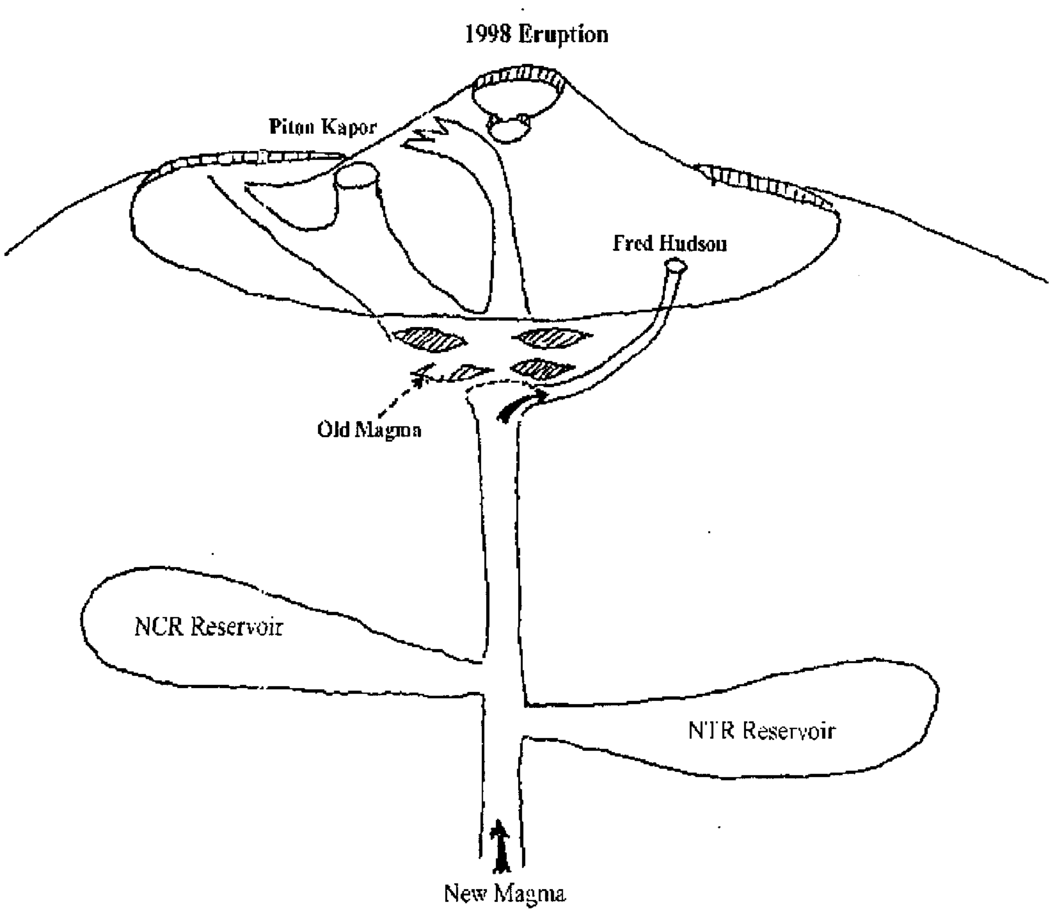

Figure 3.3.2.4. A schematic model of the magma path for the March, 1998 eruption.

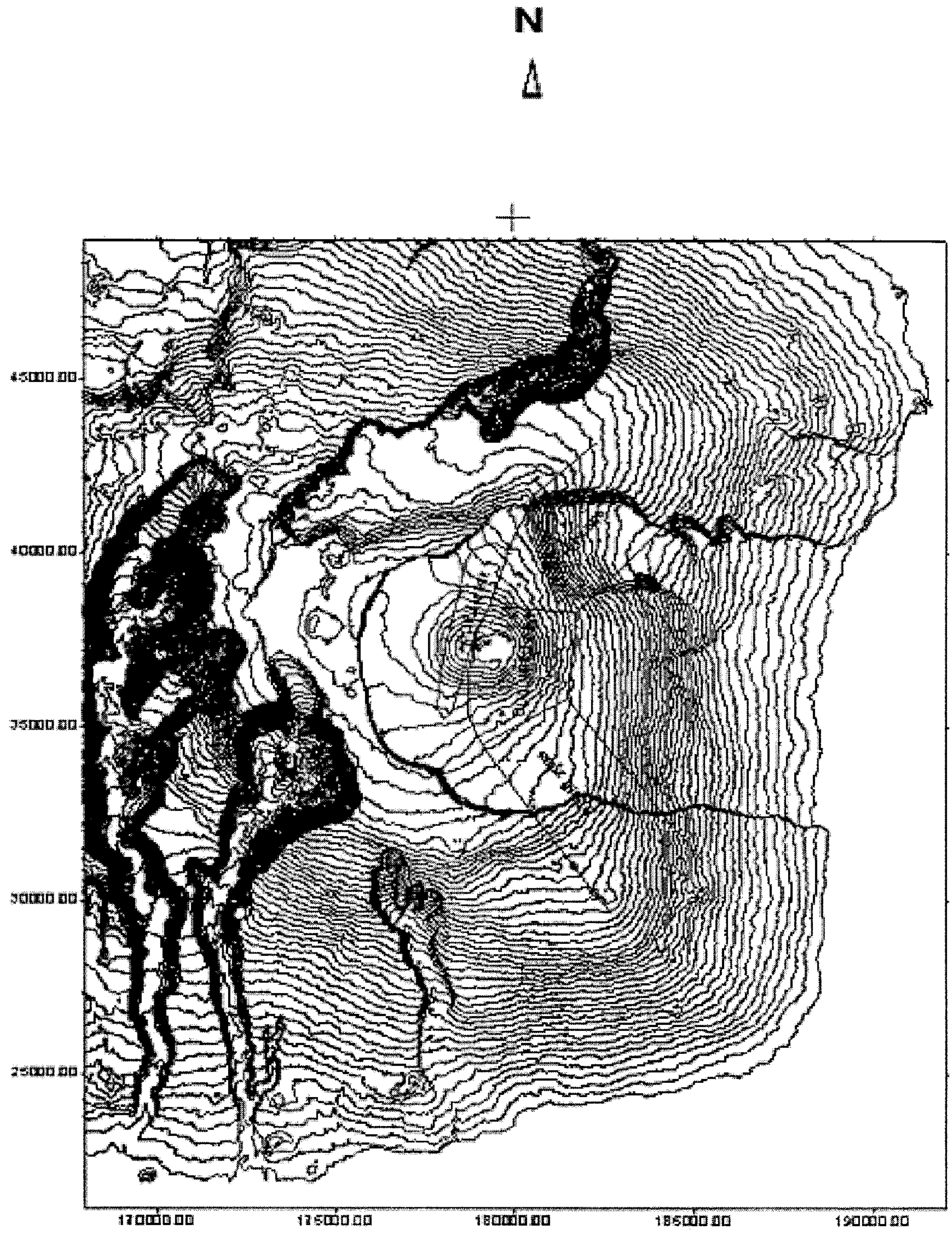

Figure 3.3.3.1. Boundaries of four areas of eruption sites at Piton de la Fournaise.

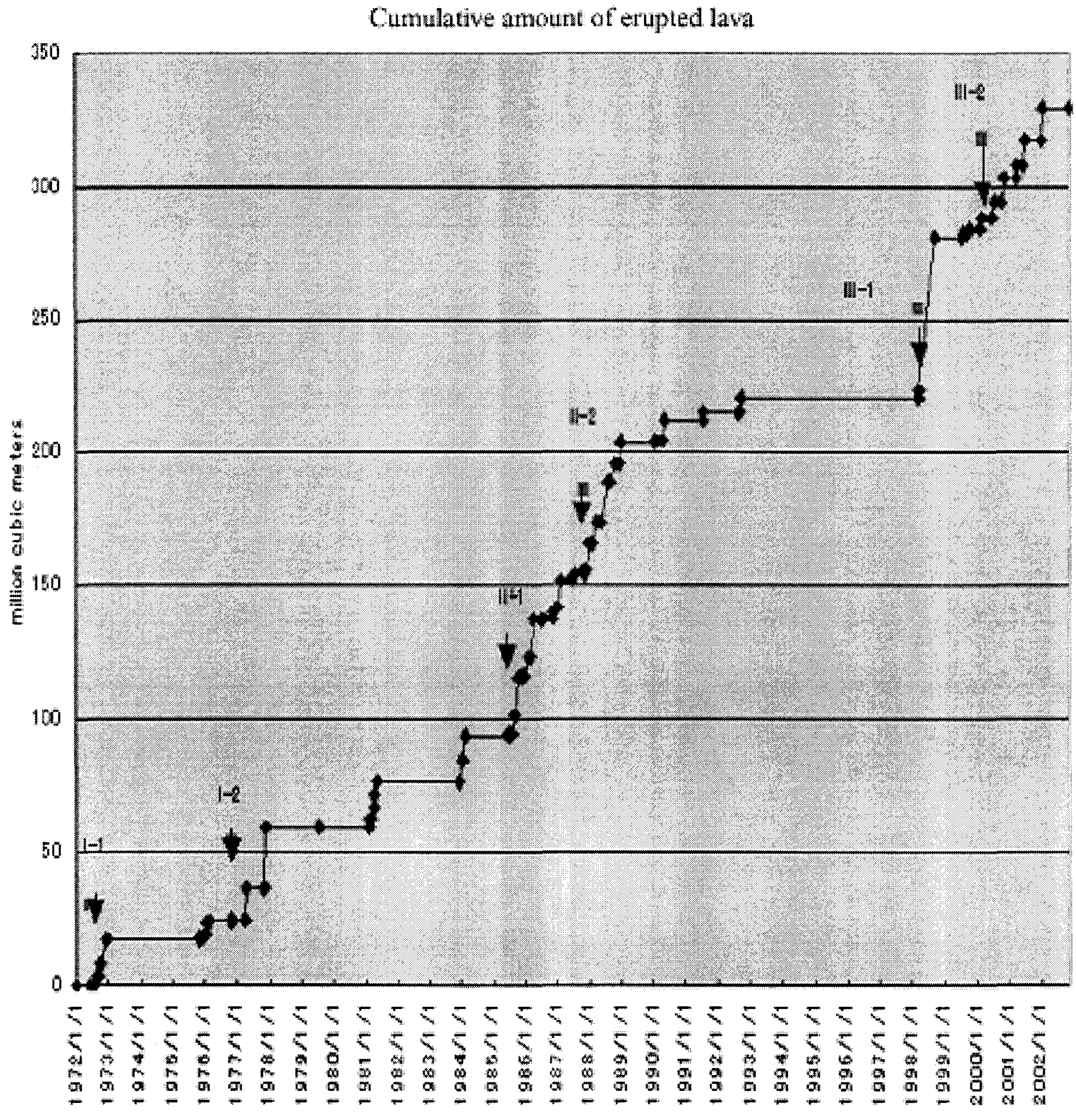

Figure 3.3.3.2. Cumulative lava output from Piton de la Fournaise in M (meter)^3. The starting dates of eruptions in the Bory west area indentified as the arrival of new magma are also indicated.

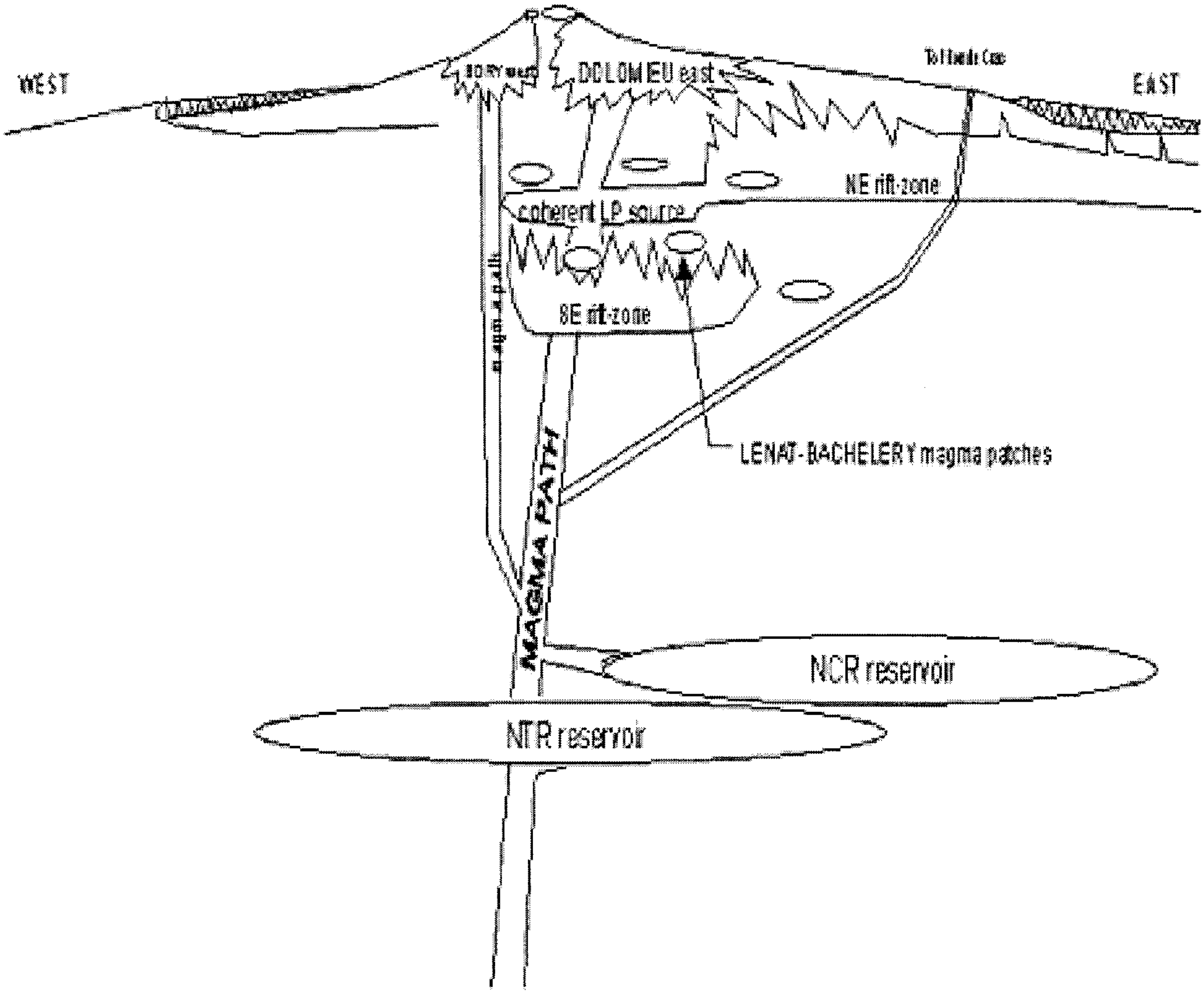

Figure 3.3.3.3. A model of magma system under Piton de la Fournaise.

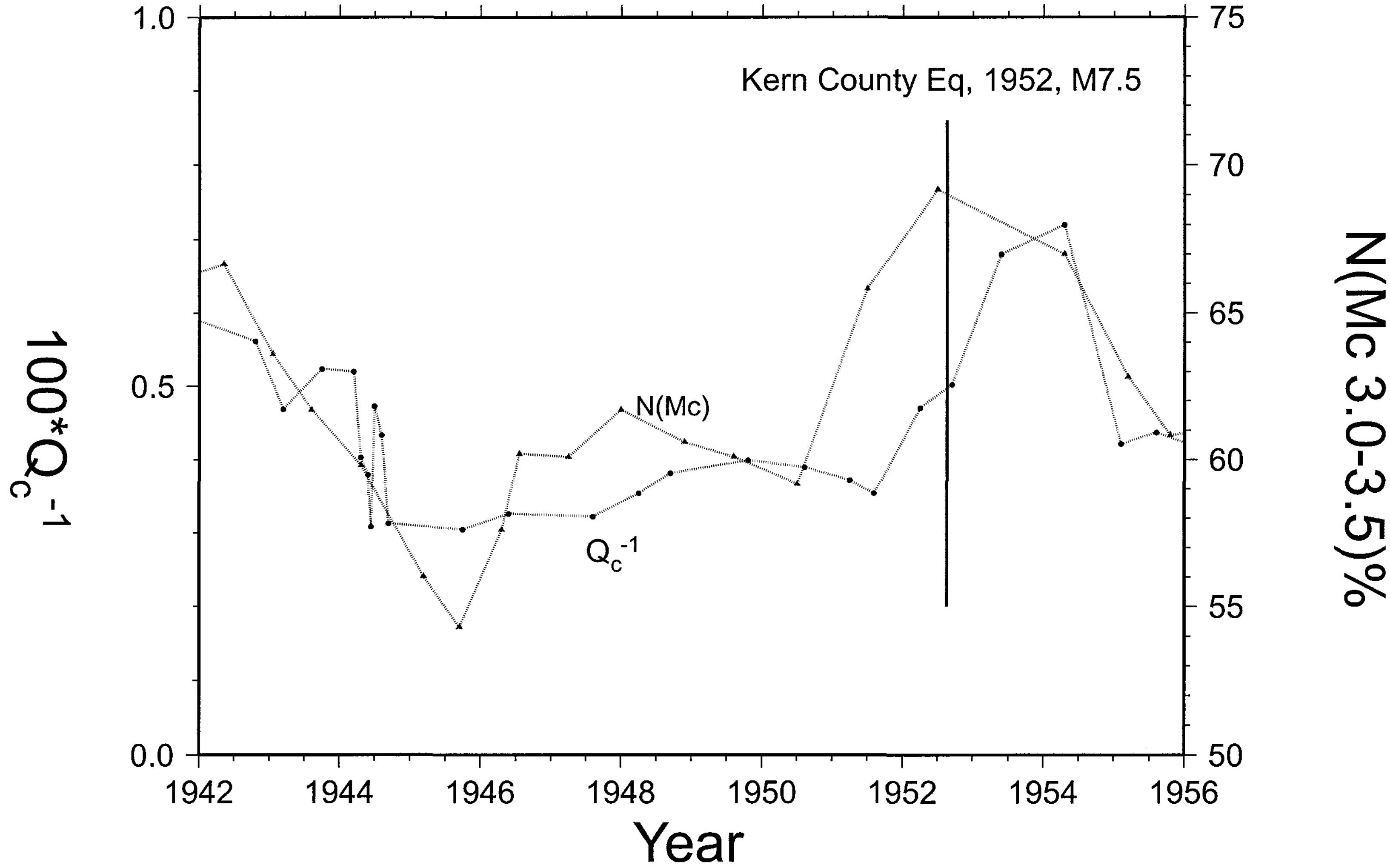

Figure 3.4.1.2. Close look at the temporal variation in coda Q^{-1} and N(Mc) in southern California before and after the Kern County earthquake, 1952.

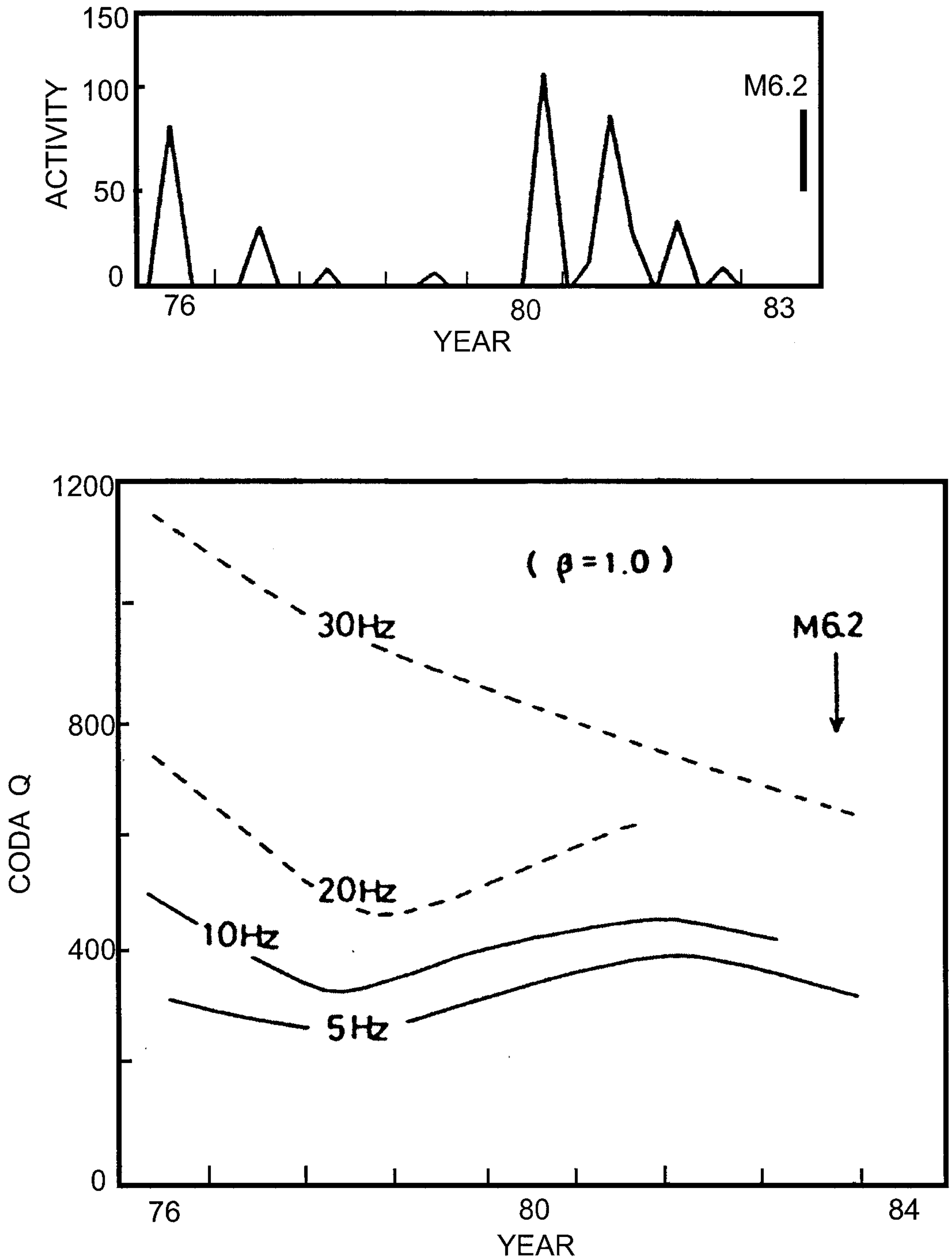

Figure 3.4.1.3. Summary of the coda Q variation at SNT before the Misasa earthquake assuming b=1.0.The curves with broken lines are of low quality with large dispersion.The top shows the activity in the Misasa region, a retangular area of 10km x 10km in the E-W and N-S directions centered at the foucs of the M6.2 event. The unit is Number/year/100 km2, the minimum b-value is 0.68. [Reproduced from Tsukuda, 1988].

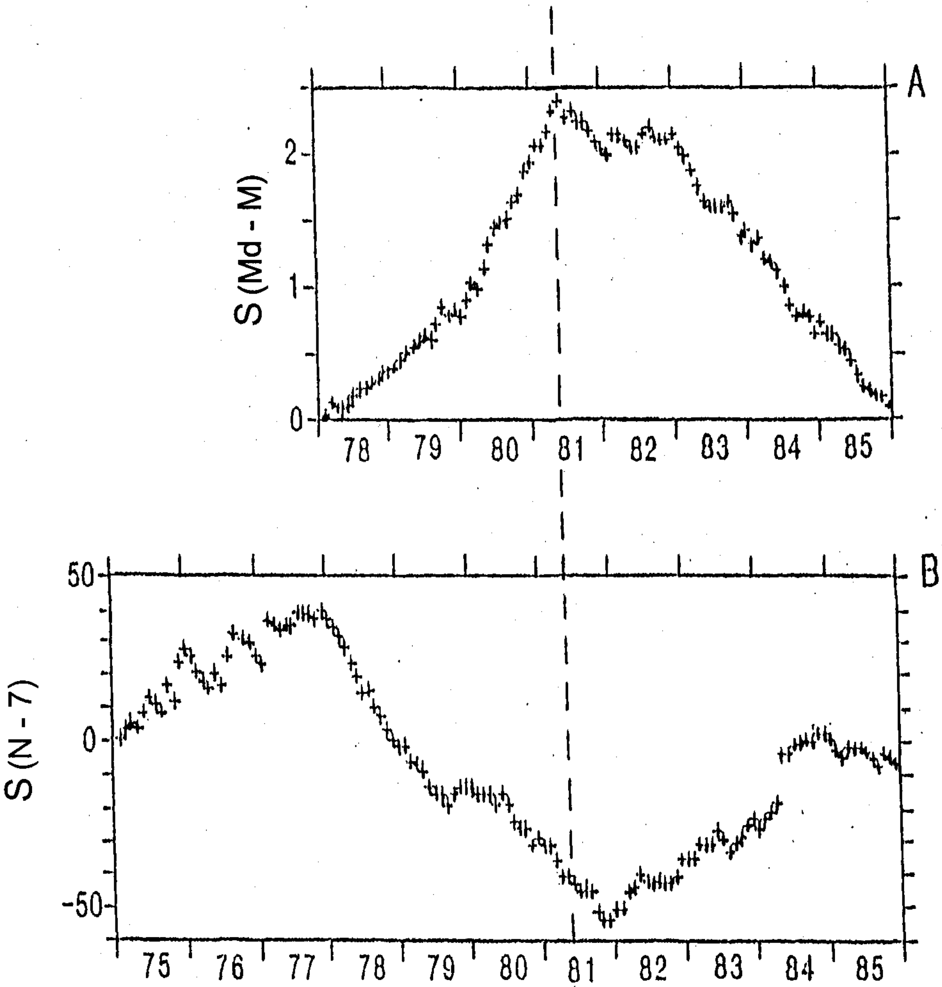

Figure 3.4.1.4. Comparison of (A)temporal changes in coda duration with monthly mean values of Md-M and monthly rate of activity as given by the number of events of M>=3.0 and S-P<= 12 s at W EL. [Reproduced from Robinson, 1987).